Environmental interpretation from Svalbard ice cores

Jefferson Cardia Simões

A dissertation submitted for the degree of Doctor of Philosophy in the University of Cambridge

Darwin College
Cambridge
January 1990

Frontispiece

Ice-core drilling at Skobreen, central Spitsbergen. The 1986 camp site and the assembled Rufli ice drill can be seen in the foreground. Bakaninbreen is in the background behind Paulabreen, which bisects the photograph from right to left.

In the bleak mid-winter
Frosty wind made moan,
Earth stood hard as iron,
Water like a stone;
Snow had fallen, snow on snow,
Snow on snow,
In the bleak mid-winter,
Long ago.

Mid-winter, Christina Rossetti

To Ingrid, Felipe and Carolina

Preface

The work presented in this dissertation was undertaken by the author at the Scott Polar Research Institute (SPRI) under the supervision of Dr. David J. Drewry. The dissertation does not exceed the regulation length and has not been submitted for a degree at any other university. The collection of radio echo-sounding data, the drilling and some chemical analyses of an ice core from Skobreen, central Spitsbergen, were a collaborative project involving a large number of individuals. The analyses and interpretation of the derived data presented here are, however, the result of my own work unless otherwise stated.

Acknowledgements

I would like to thank my supervisor, Dr. David J. Drewry, for his guidance and help throughout my training at the Scott Polar Research Institute. I am also grateful for discussions with Dr. J.L. Bamber, Dr. J.A. Dowdeswell, Mr. M.R. Gorman, and Dr. G. de Q. Robin at SPRI, and Dr. D.A. Peel at the British Antarctic Survey (BAS). I thank Mr. A.P.R. Cooper for advice on computing.

Some of the chemical analyses were carried out in European laboratories and I should like to thank: Prof. H. Oeschger, Physikalisches Institut, Universität Bern, for analysing tritium content and for the loan of the Rufli drill; Prof. W. Dansgaard, Geophysical Institute, University of Copenhagen, and Dr. J. Jouzel, Centre d'Études Nucléaires de Saclay, France, for stable-isotope analyses; Dr. D.A. Peel and the ice-chemistry group at the BAS, Cambridge, for chemical ionic analyses. I am also grateful to meteorologist Stein Kristiansen, of Norsk Meteorologisk Institutt, Oslo, for providing unpublished meteorological data from Svalbard.

The work towards this dissertation and my training as a glaciologist at the SPRI were generously funded by a grant contract from the Brazilian Antarctic Programme (PROANTAR) through the Interministerial Commission for the Resources of the Sea (CIRM), and the Brazilian National Research Council for Scientific and Technological Development (CNPq). I am grateful for support from PROANTAR during my time at the SPRI, and particularly to Drs. A.C. Rocha-Campos and C.O. Berbert.

I thank Miss Rosemary Graham for translating several papers from Russian and for kindly polishing the English in this dissertation.

I would like to express my gratitude to my wife, Ingrid, for her support and encouragement, and in particular for her infinite patience while this thesis was going through the final stage of completion. I am also grateful to my parents for help and encouragement.

Summary

The objective of this dissertation is to investigate some aspects of the environmental interpretation of ice cores from the glaciers and ice caps of Svalbard. It also attempts to derive time series for environmental changes, particularly for the anthropogenic impact on the composition of the snow and ice of Svalbard. The topics examined take into consideration three characteristics of the geographical area of study: its relatively mild climate with intense summer melting of the superficial snow pack, a record of abrupt climatic changes, and its proximity to Europe. Three main topics are examined.

First, a detailed examination of the variations in the stratigraphic, physical, and chemical properties of a core from a site subject to superficial summer melting is carried out. This aims to check if it is possible to obtain a reliable record of environmental change from a site with such characteristics. For this study a shallow ice core was recovered in 1986 from Skobreen, a valley glacier in central-eastern Spitsbergen. Data acquisition, the methodology used in the analysis, results, and problems encountered in dating and interpreting a core subject to melting and associated phenomena (i.e. percolation, refreezing, and flush-out) are discussed. When possible a methodology to circumvent the problems created by melting is also presented.

Second, the fractionation processes of the stable-isotope composition of the ice masses of Svalbard are investigated. These processes are complex because the Archipelago is situated in an area subject to frontal activity, and liquid precipitation occurs in summer. The long-term record derived from deep ice cores (>200 m) recovered from Svalbard by other authors are then reinterpreted. The regional representativeness of these records is tested by comparing them with other records from the Arctic North Atlantic. Particular attention was given to the period known as the Little Ice Age, as this is the climatic event best defined in the ice cores.

Third, the chemical composition of snow and ice is examined, both spatially and over time, to check atmospheric observations which indicate that Svalbard is an area greatly affected by anthropogenic pollution. The study uses the acidity profiles of the shallow Skobreen core and of a deep core drilled recently by Soviet scientists in Austfonna, Nordaustlandet, to extend the record of anthropogenic pollution back in time to the industrial revolution.

Table of Contents

List of Figures

List of Tables

List of Symbols

A	flow-law parameter
a_n	mean annual net accumulation rate
a_{ice}	ice-equivalent annual accumulation rate
b_n	net mass balance
b_s	summer balance
b_w	winter balance
d	deuterium excess
F	Nye's shape factor for the cross-section of glaciers
g	acceleration due to gravity
h	total ice thickness
I	Dawson's Integral
k	thermal diffusivity constant
n	flow-law constant
r	correlation coefficient
T	temperature
t	time of deposition of a layer
u_b, u_s	velocities at the base and surface
W	ratio of half-width to depth in a valley glacier
w_{so}	initial mixing ratio
y	vertical distance from the surface to a layer depth
y_b	vertical distance from bedrock
α	surface slope; also significance level of a linear regression
α_D, α_{18O}	isotopic fractionation factor for deuterium and ^{18}O
δD, $\delta^{18}O$	isotopic ratios
ρ	density
σ	electrolytic conductivity; also one standard deviation
τ_{xy}	basal shear stress
$(\partial T/\partial y)_b$	basal temperature gradient
$[SO_4^{2-}]^*$	excess sulphate

Superscripts

$\bar{}$	mean value

List of Abbreviations

BAS	British Antarctic Survey
BP	British Petroleum
B.P.	Before Present
CRREL	U.S. Army Cold Regions Research and Engineering Laboratory
EC	electrolytic conductivity
EGC	East Greenland Current
IAEA	International Atomic Energy Agency
IG (USSR)	Institute of Geography, USSR Academy of Sciences
LGGE	Laboratoire de Glaciologie et Géophysique de l'Environnement, Grenoble
LIA	Little Ice Age
MAAT	mean annual air temperature
NP	Norsk Polarinstitutt
NMI	Norsk Meteorologisk Institutt
NIPR	National Institute of Polar Research, Tokyo
PEG	Polar Exploration Group, Chesterfield
PWMAT	precipitation-weighted mean annual temperature
RES	radio echo-sounding
SIPRE	U.S. Army Snow, Ice and Permafrost Research Establishment (former name of CRREL)
SMOW	Standard Mean Ocean Water
SPRI	Scott Polar Research Institute
TU	tritium units
WSC	West Spitsbergen Current
w.eq.	water equivalent

CHAPTER 1

INTRODUCTION

"The worldwide temperature rise from 1920's to 50's reached its maximum in Svalbard"

Ahlmann, 1953

1.1- Aims and structure of the thesis

This dissertation uses data from ice cores and snow pits to investigate problems in the interpretation of variations in snow and ice properties as indicative of environmental changes. It also attempts to derive time series for environmental changes, particularly for the anthropogenic impact on the composition of the snow and ice of Svalbard. The geographical area of study, the archipelago of Svalbard, was chosen because it appears to be one of the most sensitive in the world to environmental changes (cf. Sections 1.3 and 1.4). The discussions in this dissertation are based mainly on the results obtained from a shallow ice core recovered by the author in Svalbard in 1986 and from deep cores recovered by Soviet scientists in the last 15 years; they are complemented by several snow-pit studies.

This dissertation has three main aims, which are summarized as follows:

(1) To examine the possibility of using the variations in the chemical and physical properties of an ice core from a site subjected to intense melting to derive a reliable time series of environmental variations. For this study a shallow ice core was recovered in 1986 from Skobreen, a valley glacier in central-eastern Spitsbergen. The main points investigated include: a) how the melting and associated phenomena have altered the composition of snow and ice since deposition; b) possible ways of circumventing the problems created by melting and associated phenomena (i.e. percolation, refreezing, and flush-out); c) a methodology which could provide a chronology for the core; and d) if possible, the use of the resulting time series to extend knowledge of environmental variations in central-eastern Spitsbergen this century.

(2) To examine the processes that control the stable-isotope composition of the ice masses in the Svalbard area. The fractionation processes are complex because the Archipelago is situated in an area subject to frontal activity, and liquid precipitation occurs in summer. Based on the results of this investigation, it also aims: a) to reinterpret the long-term record derived from deep ice cores (>200 m) recovered from Svalbard in the last 15 years, mainly by Soviet scientists (Kotlyakov, 1985; Punning, Vaykmyae and Tóugu, 1987); b) to test the regional representativeness of these records by comparison with other paleoclimatic records for the Arctic North Atlantic. In the examination of the long-term environmental variations emphasis is given to the cooling period known as the Little Ice Age (cf. Section 1.4), as it is the period defined best in the ice-core record.

(3) To examine the variations in the chemical composition of snow and ice, both spatially and over time. This examination aims to check atmospheric observations which indicate that Svalbard is one the areas most affected by anthropogenic pollution in the Arctic, although there are no significant local sources of pollution. From this examination it has proved possible to derive a record of anthropogenic pollution since the industrial revolution. This study is based mainly on the shallow Skobreen core and on my interpretation of the data from a deep core drilled to bedrock recently (1987) by Soviet scientists on Austfonna, Nordaustlandet (Zagorodnov and Arkhipov, in preparation).

Organization of this dissertation

In the first chapter the present climate of Svalbard and the record of environmental change and fluctuation are reviewed to provide the background for the rest of the dissertation. The discussions are restricted to the instrumental period (i.e. post-1911) and to the few paleoenvironmental records, which cover the last 700 years. There are two main reasons for this restriction: a) there are some continuous data (e.g. stable-isotope variations) for all the deep cores for this period; b) it includes the period which shows the best-defined climatic variation in recent times, the cooling known as the 'Little Ice Age' (cf. Section 1.4). The chapter is supplemented by Appendix 1, which describes the calculation of several climatic parameters relevant to the interpretation of glacio-environmental information. Chapter 2 discusses the glaciology of Svalbard. Glacio-environmental studies carried out in the Archipelago before this dissertation are reviewed. The chapter gives emphasis to parameters relevant to ice-core studies and discusses the advantages and disadvantages of drilling in glaciers and ice caps, which are frequently subject to strong melting of the superficial layers. It also attempts to define the best site for future ice-core investigations in the Archipelago. These discussions lead to an account of the glaciological survey carried out in 1985 and 1986 in central-eastern Spitsbergen by a team from the Scott Polar Research Institute (SPRI),

including the author of this dissertation. The chapter ends with a detailed glaciological examination of the site of the 1986 shallow-ice coring, Skobreen.

The next three chapters make up the main body of this dissertation. Chapter 3 is concerned with the analysis and interpretation of the Skobreen core. For each analysis carried out a brief introduction is given, which includes a discussion of the problems one might expect to encounter in a record from a core affected by melting, percolation, refreezing, and sometimes flush-out. This is followed by a discussion of the methodology used and the results. The chronology of the core is then examined. The chapter is supplemented by two appendices: Appendix 2 tables the data from the Skobreen core, and Appendix 3 details the ice-core drilling operations carried out on Skobreen in 1986. Chapter 4 examines the stable-isotope composition of Svalbard precipitation and tries to relate it to a simple model of fractionation. This is followed by a discussion of the 20th-century ice-core record, based on comparison with the instrumental climatic record in order to check the representativity of the cores. The chapter ends with the reinterpretation of the stable-isotope record of the deep cores and an assessment of its relationship to some environmental changes in other parts of the Arctic North Atlantic. The record of anthropogenic pollution in snow and ice is examined in Chapter 5. This study is based on a review of the knowledge of atmospheric pollution and followed by a detailed examination of the chemical composition of the snow and ice of Svalbard. Finally, Chapter 6 set outs the main conclusions of the dissertation and presents an extensive list of suggestions for future ice-core activities in Svalbard.

1.2- The geographical area of study

The studies described in this dissertation were carried out in the Archipelago of Svalbard. This group of islands is situated between latitudes 74° and 81°N and longitudes 10° and 35°E, at the northwestern edge of the Barents Sea. The total area of the Archipelago is 62,248 km^2 (Liestøl, in press, b), of which about 96% is formed by four islands: Spitsbergen (39,000 km^2), Nordaustlandet (15,000 km^2), Edgeøya (5,000 km^2), and Barentsøya (1,300 km^2). Other major islands include Kvitøya, Kong Karls Land, Prins Karls Forland, Hopen, and Bjørnøya. Fig. 1.1 shows the main islands and the location of Svalbard in the Northern Hemisphere. A small arrow marks the location of Bjørnøya, the southernmost island of the Archipelago, which is situated about 220 km from southern Spitsbergen. Ice covers about 59% of Svalbard (Liestøl, in press, b), but the proportion of the glacierized area varies from none at all, as on Hopen, to 99% on Kvitøya. Valley and cirque glaciers dominate in the west part of Spitsbergen and give way gradually to ice caps in the east. The largest European ice caps (Austfonna, 8,120 km^2, and Vestfonna, 2,511 km^2; Dowdeswell, 1984) are in Nordaustlandet.

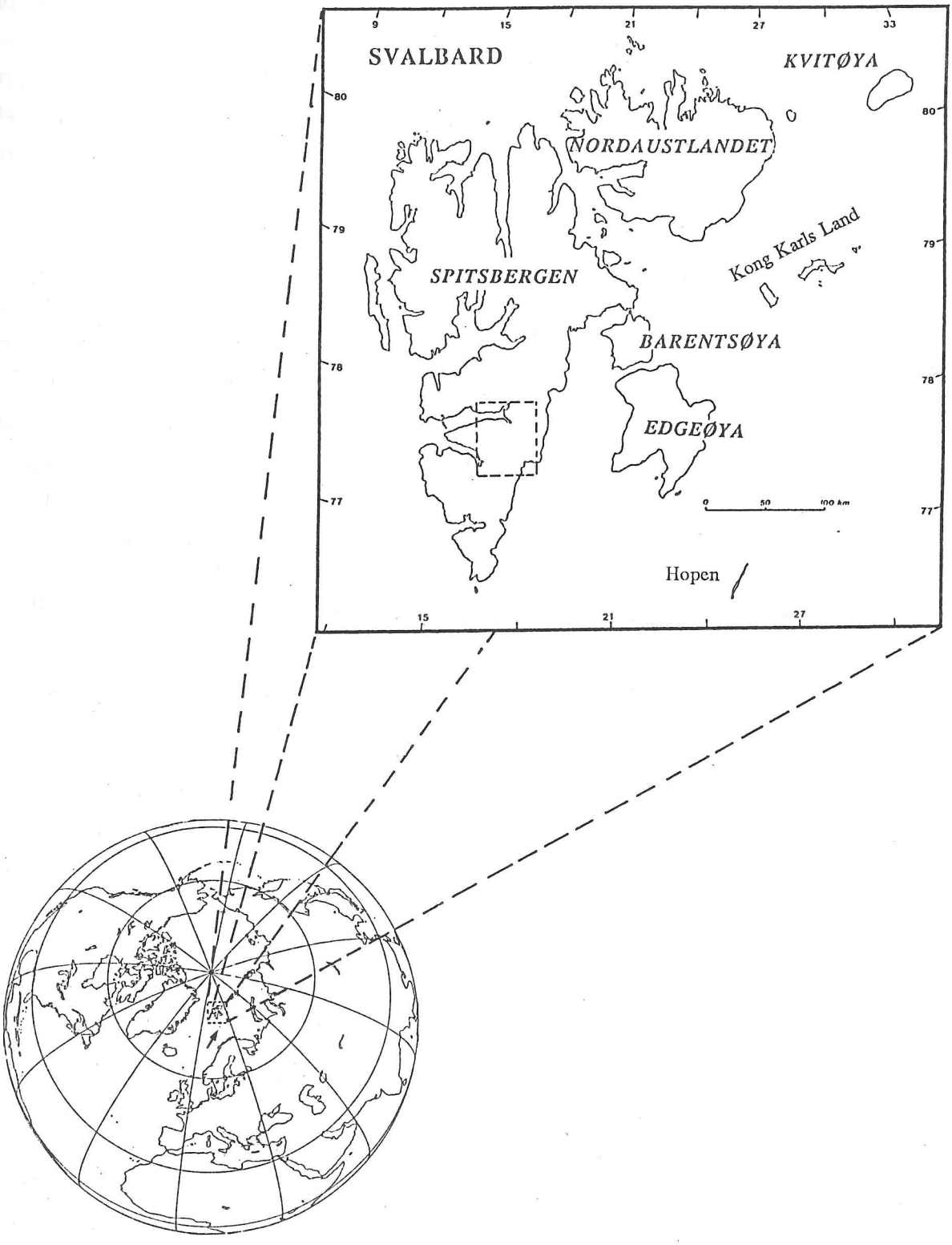

Figure 1.1- Map of Svalbard showing the major islands of the archipelago. The small globe locates Svalbard in the Northern Hemisphere. Stippled square in central-eastern Spitsbergen shows the area of studies in 1986 (Fig. 2.7).

Ice-coring activities, mainly by Soviet scientists, have all taken place in Spitsbergen and Nordaustlandet (except for a shallow core from Storøya, a small island off the northeast coast of Nordaustlandet), so the studies and discussions in this dissertation refer to the two largest islands. Place-names in the Archipelago are given in the Norwegian form (Orvin, 1942, 1958) and are taken from maps published by the Norsk Polarinstitutt (NP). Fig. 1.2 shows the main place-names and sites cited in this dissertation.

Spitsbergen is deeply cut by fjords and the two largest (Isfjorden and Wijdefjorden) extend for more than 100 km. The name of the island means 'pointed mountains' and gives a fair impression of the morphology of its west coast, which is characterized by jagged, alpine peaks of metamorphic and eruptive rocks. In contrast, central Spitsbergen was formed by plateaus of horizontal sedimentary rocks which are dissected by valley and cirque glaciers (Fig. 2.10). This area of the island has the least ice cover, mainly due to low accumulation and higher summer temperatures (i.e. a greater continentality). Some areas, such as Nordenskiöld Land, are relatively glacier-free. Farther to the northeast, small ice-cap covered plateaus have an altitude of more than 1000 m (e.g. Lomonosov, in Olav V Land). Major valley glaciers descend from these ice caps and frequently reach the sea, where some float (i.e. tide-water glaciers). The highest peaks of the Archipelago are found in northeastern Spitsbergen: Newtontoppen and Perriertoppen are 1,717 m a.s.l.. The extent of glacierization increases towards the northeast and 75% of Nordaustlandet is covered by ice caps, with its highest point on Austfonna (791 m a.s.l.; Dowdeswell, 1984).

In 1985 and 1986 it was possible to extend ice-core studies in Svalbard to central-eastern Spitsbergen, at the head of Van Mijenfjorden. Pit and trench studies were carried out in the Paulabreen system, which drains from Heer and Nathorst lands into Rindersbukta. These studies were carried out in association with a radio echo-sounding field campaign by the Scott Polar Research Institute (SPRI) and an experimental seismic survey undertaken by British Petroleum (BP). Figs. 2.8 and 2.11 show the location of the drilling and radio-echo studies in central-eastern Spitsbergen. The studies were carried out mainly in the trunk glacier, Paulabreen, and two of its tributaries, Bakaninbreen and Skobreen. The latter was the location for the drilling of a shallow core and for detailed glaciological examination (cf. Chapters 2 and 3).

Two characteristics of the Svalbard climate are of great importance for ice-core studies. First, the climate of Svalbard is relatively mild in relation to its latitude. The mean annual temperature was -4.9°C at Isfjord (78.1°N–13.6°E) from 1957 to 1975. Winter mean annual temperatures (-11.9°C from 1957 to 1975; Hisdal, 1985) can be more than 20°C warmer than those of sites at the same latitude in the Canadian Arctic islands and, although summer differences are not so great, the mean July temperature is still 1–3°C higher than at

Figure 1.2- Major place-names and other sites in Svalbard cited in this dissertation. Numbers above the two arrows locate Balderfonna (1) and Veteranen (2).

other stations in the Arctic (Hisdal, 1985). Temperatures are frequently above 0°C, even outside the summer period. The resulting melting, percolation, and flush-out of the superficial snow cover makes the environmental interpretation of ice cores from Svalbard complex. At different stages in this dissertation it has been necessary to create a methodology which circumvents the problems created by melting (e.g. the use of deuterium excess - *d* to identify the damped seasonal stable-isotope variations).

The other characteristic of the Svalbard climate is the great variability in its elements from year to year. For example, some of the short-period temperature variations have been some of the most abrupt in the world. It is not uncommon to have an increase or fall of 5–8°C in the mean annual atmospheric temperature (MAAT) over periods of 3–6 years (e.g. between 1915 and 1920 the MAAT increased by 8°C; Steffensen, 1982). This highly variable climate make the Svalbard region ideal for studies of climatic variations over short time-scales (i.e. less than 50 years). Furthermore, there is an instrumental record for the area over the past 78 years, allowing calibration of ice-core data. In the rest of this chapter the reasons for this mild and highly variable climate are examined in order to establish the environmental background for this work. The record of variations throughout the instrumental period is examined in detail to give a chronological frame of reference for the studies discussed in other chapters of this dissertation. This examination is then extended to the previous 700 years, albeit briefly, on the basis of information derived from other paleoclimatic studies, with the aim of providing independent information for comparison with the results of studies carried out in Chapter 4.

1.3- The environmental setting: the present Svalbard environment in the context of the Arctic North Atlantic

1.3.1- Introduction

The region between Greenland and Novaya Zemlya, and particularly Svalbard and Franz Josef Land, is known to be one of the most sensitive regions in the world, if not the most sensitive region, to climatic variations (Ahlmann, 1953; Lamb, 1977, 1982a, 1982b; Lamb and Mörth, 1978). Furthermore, during the instrumental period (i.e. since 1911 in Svalbard) it has shown some of the most sudden climatic variations. This great sensitivity is due to the geographical position of the area at the confluence of air masses and ocean currents with very different characteristics. Small changes in the strength or direction of either air mass or ocean current may result in a change to a different regime. Furthermore, the sensitivity of the area is increased because it lies on the main route of winds and ocean currents entering and leaving the Arctic. Finally, the sensitivity of the region is further enhanced by rapid changes in the sea-ice extent which are coupled with atmospheric and oceanic circulation. In the following paragraphs a brief review of the physical processes controlling the climate of this region is given in order to elucidate the climatic conditions in the Greenland-Norwegian-

Barents Sea† which may affect the Svalbard environment. The section describes the general atmospheric and oceanic circulation by which heat, moisture, and pollutants are transported to the North Atlantic sector of the Arctic, and ends with the description of present climatic conditions in Svalbard.

1.3.2- Atmospheric circulation and the Arctic Front

The upper atmosphere of the polar regions is dominated by the presence of a cold-core low which is observed at a height between 3 and 10 km (particularly between the 300 and 500 mbar pressure levels). These centres of low pressure result from the strongly negative energy balance of the polar regions. As a consequence, an intense pressure gradient exits between the Equator and the polar regions. The Coriolis force deflects the air from the direct path between high and low pressure and the air moves approximately in lines of equal pressure, resulting in a circumpolar vortex of upper westerly winds. The Northern Hemisphere vortex (in contrast to the Southern Hemisphere vortex) is not centred over the Pole and can have 2–3 centres and 2–5 waves. These waves appear to reflect the influence of the topography of the Northern Hemisphere and the inequalities of heating between continents and oceans (Lamb, 1972).

The north–south temperature gradient is far from regular, and is steeper in some areas than in others. It is represented at high altitudes (i.e. at about 10 km a.s.l.) by a maximum of the westerly winds. These atmospheric jet streams are associated with zones of intense baroclinicity (i.e. atmospheric fronts) at lower altitudes which represent the confluence of air masses with greatly differing characteristics. In the Atlantic region two frontal zones have been distinguished – one is known as the Atlantic Polar Front, marking the confluence of polar and tropical air in mid-latitudes, and oscillates from about latitudes 44° to 71°N over the year (Lamb and Mörth, 1978). The Atlantic Arctic Front, which is associated with the snow and ice margins of the high latitudes (Lamb and Mörth, 1978), is more relevant for this dissertation. It marks the confluence of the cold air mass of the Arctic Basin with the more maritime polar air which flows from the North Atlantic. During the winter the Arctic air mass expands, occupying a large fraction of the snow-covered continental land mass of North America and Eurasia (Barrie, 1986). The air masses acquire a more continental character and can be classified as cA (i.e. cold and dry Arctic air) according to the Køppen system. The thermal gradient between the air masses is increased and the frontal zone can be recognized in the latitudes between Svalbard and Iceland (AF in Fig. 1.4). In summer this front is not well defined in the region of Svalbard, as the Arctic air mass acquires a more maritime character (mA). On the other hand, a front can still be distinguished along the tundra–taiga boundary in west Eurasia (Krebs and Barry, 1970).

† In this dissertation the term Greenland-Norwegian-Barents Sea is used to refer to the whole oceanic area from the east coast of Greenland to Novaya Zemlya, north of 70°N and south of the Fram Strait, Svalbard, and Franz Josef Land.

Barents Sea† which may affect the Svalbard environment. The section describes the general atmospheric and oceanic circulation by which heat, moisture, and pollutants are transported to the North Atlantic sector of the Arctic, and ends with the description of present climatic conditions in Svalbard.

1.3.2- Atmospheric circulation and the Arctic Front

The upper atmosphere of the polar regions is dominated by the presence of a cold-core low which is observed at a height between 3 and 10 km (particularly between the 300 and 500 mbar pressure levels). These centres of low pressure result from the strongly negative energy balance of the polar regions. As a consequence, an intense pressure gradient exits between the Equator and the polar regions. The Coriolis force deflects the air from the direct path between high and low pressure and the air moves approximately in lines of equal pressure, resulting in a circumpolar vortex of upper westerly winds. The Northern Hemisphere vortex (in contrast to the Southern Hemisphere vortex) is not centred over the Pole and can have 2–3 centres and 2–5 waves. These waves appear to reflect the influence of the topography of the Northern Hemisphere and the inequalities of heating between continents and oceans (Lamb, 1972).

The north–south temperature gradient is far from regular, and is steeper in some areas than in others. It is represented at high altitudes (i.e. at about 10 km a.s.l.) by a maximum of the westerly winds. These atmospheric jet streams are associated with zones of intense baroclinicity (i.e. atmospheric fronts) at lower altitudes which represent the confluence of air masses with greatly differing characteristics. In the Atlantic region two frontal zones have been distinguished – one is known as the Atlantic Polar Front, marking the confluence of polar and tropical air in mid-latitudes, and oscillates from about latitudes 44° to 71°N over the year (Lamb and Mörth, 1978). The Atlantic Arctic Front, which is associated with the snow and ice margins of the high latitudes (Lamb and Mörth, 1978), is more relevant for this dissertation. It marks the confluence of the cold air mass of the Arctic Basin with the more maritime polar air which flows from the North Atlantic. During the winter the Arctic air mass expands, occupying a large fraction of the snow-covered continental land mass of North America and Eurasia (Barrie, 1986). The air masses acquire a more continental character and can be classified as cA (i.e. cold and dry Arctic air) according to the Køppen system. The thermal gradient between the air masses is increased and the frontal zone can be recognized in the latitudes between Svalbard and Iceland (AF in Fig. 1.4). In summer this front is not well defined in the region of Svalbard, as the Arctic air mass acquires a more maritime character (mA). On the other hand, a front can still be distinguished along the tundra–taiga boundary in west Eurasia (Krebs and Barry, 1970).

† In this dissertation the term Greenland-Norwegian-Barents Sea is used to refer to the whole oceanic area from the east coast of Greenland to Novaya Zemlya, north of 70°N and south of the Fram Strait, Svalbard, and Franz Josef Land.

Although the temperature distribution of a front is basically stable, instability can develop rapidly. These disturbances develop into major cyclones and anticyclones in a few days in the lower and middle troposphere, bringing together large volumes of air masses with opposite characteristics, and producing mixing and modification of these air masses. Thus the position and development of these superficial atmospheric disturbances are also related to the upper jet streams and so to the polar vortex, and the variations in the polar vortex affect superficial circulation. On the other hand, these lows and the high centres of pressure at the surface react on the vortex and distort the thermal pattern and the shape of the upper westerlies' flow (Lamb, 1982b). In summary, the circumpolar jet stream and the polar front are the key features in the formation and steering of the cyclones, which in their turn are the main mode of heat transport to the polar zones.

One of the characteristics of the polar vortex is that it is subject to variations in strength, wave length (thus in the number of main waves), amplitude (thus in the latitude reached by the main troughs and ridges), and eccentricity (the main centre can sometimes move as far as to 60–70°N of latitude; Lamb, 1972) at different time-scales, so affecting the strength and tracks of cyclones. During winter and spring or colder periods the vortex tends to have three centres (i.e. over the Canadian islands, Kamchatka, and Novaya Zemlya) and a 'meridional' pattern with large-amplitude waves which results in strong northerly and southerly winds (e.g. vortex pattern C in Fig. 1.3). A stronger meridional flow may result in the transport over the Northern Atlantic of moist warm air to near the Pole. At the same time, dry cold Arctic air affects a great part of the continent of Europe and North America as troughs expand (e.g. over Greenland, Scandinavia, and the Rocky Mountains), sometimes as far south as 40° of latitude (cf. Fig. 1.3). Some of the coldest periods (e.g. the 1560s, 1690s, 1750s, and 1950s) recorded in historical times in Europe were attributed to the expansion of a cold trough over Europe at the same time as a well-developed ridge advanced over the North Atlantic Arctic (Lamb, 1982) and increased the transport of the warm water of the North Atlantic Drift to the Norwegian coast. Thus one of the characteristics of colder periods is that different sectors of the Arctic may show climatic trends due to the increase in amplitude of the circumpolar vortex waves, in addition to great variability due to rapid changes in the wave position. In the extreme case of long waves with very large amplitudes, blocking may occur, and the flow becomes mainly 'meridional'. In the opinion of Lamb (1977, 1979) the period known as the 'Little Ice Age' (LIA) (cf. Section 1.4.3) was associated with big-amplitude waves and blocking. It is no surprise, therefore, that the LIA period is characterized by greater climatic variability when compared to this century (which shows a more 'zonal' flow) rather than by a constantly colder climate. For example, one of the coldest periods of the LIA in Europe, the late 17th century, also included some of the warmest years on record (Lamb, 1979). During warmer times, and summers in general, the vortex contracts (due to the reduction of the north–south temperature gradient), lying farther north, the amplitude of waves is reduced substantially, and the flow becomes more 'zonal'

(i.e. west–east), with a single mean centre near the Pole (pattern W in Fig. 1.3). Associated with this retraction, the mean position of the cyclone tracks also migrates farther north. Climatic conditions at the same latitude in the Northern Hemisphere become much more uniform, with the westerly winds occurring in a more restricted range of latitudes. The flux of water vapour to the central Arctic also increases.

The circumpolar vortex has also a tendency to show sudden changes in the number of waves (e.g. from 2 to 3). A two-wave pattern for the vortex is typical of warm climate and strong circulation, and the Norwegian and Barents seas are influenced by a ridge spreading from the south. This means that greater warmth and precipitation are brought by cyclonic activity from the Atlantic Ocean, which appears to have been the prevailing situation during the warmer period of this century (i.e. 1920s–1960s; cf. Section 1.4.2). In cooler times a third wave may develop in the Svalbard–Franz Josef Land region (associated with the expansion of cold Arctic air; Lamb and Mörth, 1978; Lamb, 1982b). The change in the number of waves frequently occurs abruptly, which implies rapid changes in the transport of heat to the Norwegian–Barents Sea region. It is no surprise, therefore, that the region shows some of the most abrupt changes in mean annual temperature (MAAT) ever recorded. In Section 1.4.2 it is seen that the MAAT can change by almost 8°C over a period of a few years, and Lamb (1982b) reports changes of more than 10°C in the mean temperature of some months in Franz Josef Land. In fact, Svalbard and Franz Josef Land have shown the greatest warming (between 1910 and 1920) and cooling (1960s) in the Arctic. Another characteristic of the vortex in this area is a quasi-biennial oscillation in its extent, and this appears to be reflected in some of the climatic time series for Svalbard (e.g. precipitation and total number of melting degree days; cf. Fig. A1.3-A1.8).

The major tracks of cyclones bringing moisture and heat to the Arctic are shown in Fig. 1.5. They reflect the major frontal zones and it can be seen that the Arctic coast is one of the commonest tracks in the winter (Fig. 1.5A). At this time of the year, as a result of the expansion of the Arctic air mass, the Arctic Front is pushed southward to the latitudes between Svalbard and Iceland in the North Atlantic. The point of convergence of the two principal tracks of cyclones coming from North America defines the Icelandic low (in the vicinity of Iceland), which is seen in the average atmospheric surface-pressure charts. The cyclones move from there along a track which follows the waters of the Norwegian Sea and progresses to the Barents Sea along the Eurasian coast. Fig. 1.4 shows the average values of surface pressure, winds, and the advance position of the frontal zones in the Arctic. It can be seen that the mean wind direction in the Greenland-Norwegian-Barents Sea and in northwestern Eurasia also reflects these tracks. Over Svalbard these winds acquire a strong E-NE component. It is clear from this wind pattern that in winter the main air-mass flows follow a route over the main centres of anthropogenic pollution in Europe (i.e. central and eastern Europe) before being deflected by the Siberian high towards the Arctic Basin, passing over Svalbard on the way. In this way the travelling depressions are loaded with continental

impurities (natural or anthropogenic) over Eurasia before moving to the Arctic, which naturally has important implications for the ionic composition of the snow and ice in Svalbard (cf. Chapter 5). In summer the Arctic air mass retracts and the Arctic Front is not so well defined. The mean track of the cyclones moves northward, sometimes reaching Svalbard. Atlantic warm and moist air is brought to the Archipelago much more frequently and winds acquire a mainly south-southeast direction.

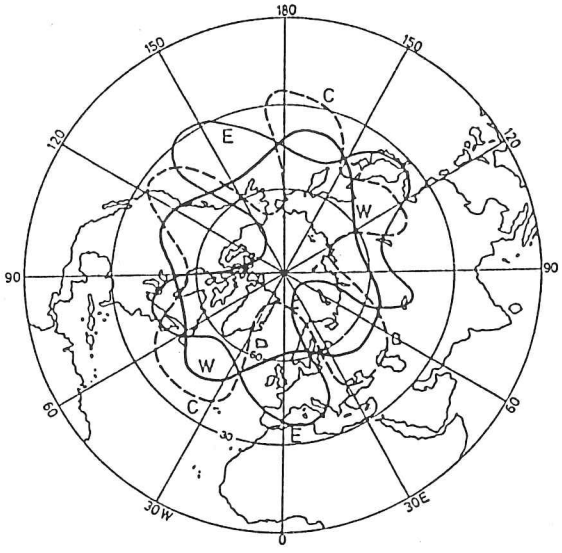

Figure 1.3- Types of variation in the circumpolar vortex. Slow-moving or stationary ('meridional') situations are shown by flow patterns with big meanders (C and E). Source: Lamb, 1972.

From the above observations it can be seen that climatological time series derived from Arctic ice cores should show greater similarity during warm periods (i.e. times of zonal flow). During colder periods greater variability may be observed from region to region, depending on whether the region under examination is under a vortex trough or ridge and how 'meridional' the atmospheric flow is. Furthermore, periods of general expansion of the Arctic air mass over continents will result in a greater concentration of exotic material (e.g. continental dust, pollens, and pollutants).

1.3.3- Present ocean circulation and the sea-ice limit

The climatic sensitivity of the Atlantic sector of the Arctic is further enhanced by three characteristics of the oceanic surface water there: 1) major mass and heat exchanges take place between cold and warm currents in the area; 2) the Fram Strait between Greenland and Spitsbergen is the main route of water entering and leaving the Arctic Ocean; 3) the area is subject to great variation in sea-ice cover, on both seasonal and longer time-scales, and it is coupled with variations in atmospheric and oceanic circulation.

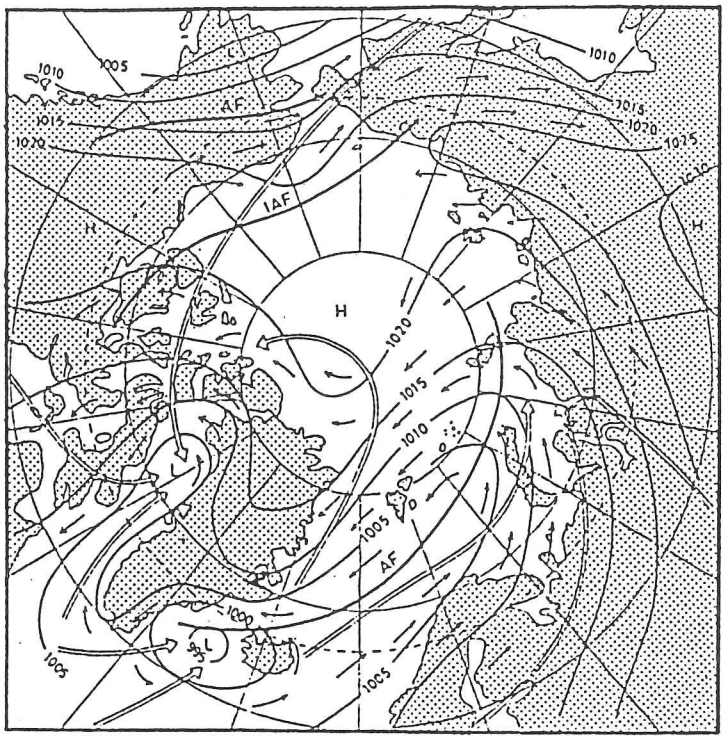

Figure 1.4- Average values of surface pressure, wind direction, and frontal zones in the Arctic during January. Note the advance position of the atmospheric Arctic Front in the North Atlantic between Iceland and Svalbard.

Source: Map from Heidam (1986).

Fig. 1.6 is a schematic diagram of the surface-water currents in the Greenland-Norwegian-Barents Sea. The West Spitsbergen Current (a branch of the Norwegian Atlantic Current, henceforward WSC) brings warmer water to the west coast of Svalbard and enters the Arctic Ocean through the Fram Strait. This current is responsible for an ice-free bay (Svalbardbukta or Whaler's bay) on the west-northwest coast of Svalbard every summer and in many winters. It is the northernmost area of open water in the Arctic. Although some warm water enters the Arctic through the passage between Spitsbergen and Norway, the Fram Strait is by far the most important route for warm water (in the form of a saline undercurrent; Parkinson et al., 1987). In fact, Aagaard and Greisman (1975) estimated that 75% of the mass exchange between the Arctic Basin and the rest of the world ocean takes place through this passage. The Fram Strait is also the main route for cold water leaving the Arctic. The Transpolar Drift Stream transports ice-laden water and, in the form of the East Greenland Current (henceforward EGC), extends sea-ice cover to the vicinity of Iceland. It is known that large interannual fluctuations occur in both currents, and the extent of sea-ice cover and of Svalbardbukta is strongly correlated with the strength of the WSC (Blindheim and Ljøen, 1972). It is known, for example, that the water volume transported by the EGC can vary by a factor of 10 (Lamb, 1979). Two secondary currents, the East Spitsbergen and Bear Island (Bjørnøya) currents, transport cold water and sea ice to the northeast of the Barents Sea. The East Spitsbergen Current is a net southwestward drift which transports ice around Sørkapp in winter, sometimes up to the latitude of Isfjorden, depending on the strength of the WSC. In general it ensures that the eastern coast of Svalbard remains ice-covered for a great part of the winter.

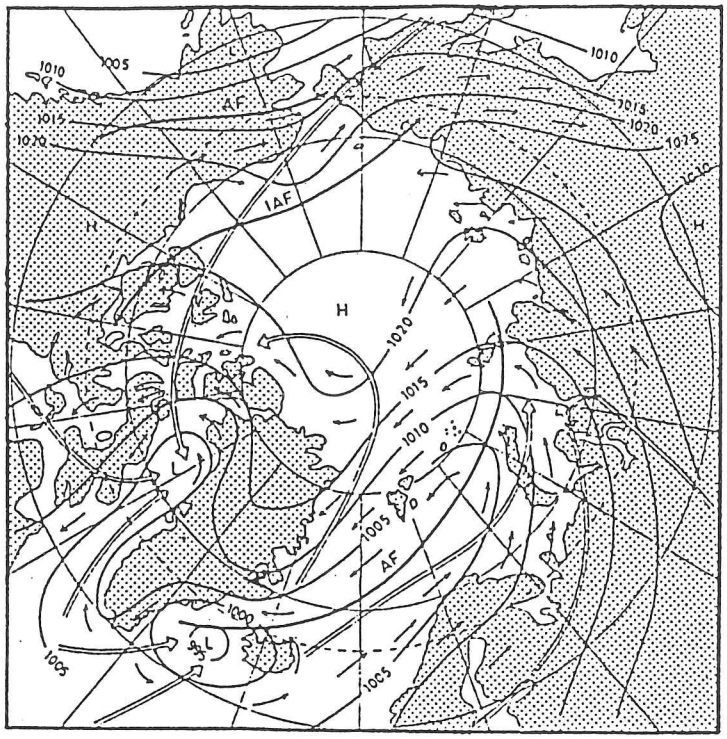

Figure 1.4- Average values of surface pressure, wind direction, and frontal zones in the Arctic during January. Note the advance position of the atmospheric Arctic Front in the North Atlantic between Iceland and Svalbard.

Source: Map from Heidam (1986).

Fig. 1.6 is a schematic diagram of the surface-water currents in the Greenland-Norwegian-Barents Sea. The West Spitsbergen Current (a branch of the Norwegian Atlantic Current, henceforward WSC) brings warmer water to the west coast of Svalbard and enters the Arctic Ocean through the Fram Strait. This current is responsible for an ice-free bay (Svalbardbukta or Whaler's bay) on the west-northwest coast of Svalbard every summer and in many winters. It is the northernmost area of open water in the Arctic. Although some warm water enters the Arctic through the passage between Spitsbergen and Norway, the Fram Strait is by far the most important route for warm water (in the form of a saline undercurrent; Parkinson et al., 1987). In fact, Aagaard and Greisman (1975) estimated that 75% of the mass exchange between the Arctic Basin and the rest of the world ocean takes place through this passage. The Fram Strait is also the main route for cold water leaving the Arctic. The Transpolar Drift Stream transports ice-laden water and, in the form of the East Greenland Current (henceforward EGC), extends sea-ice cover to the vicinity of Iceland. It is known that large interannual fluctuations occur in both currents, and the extent of sea-ice cover and of Svalbardbukta is strongly correlated with the strength of the WSC (Blindheim and Ljøen, 1972). It is known, for example, that the water volume transported by the EGC can vary by a factor of 10 (Lamb, 1979). Two secondary currents, the East Spitsbergen and Bear Island (Bjørnøya) currents, transport cold water and sea ice to the northeast of the Barents Sea. The East Spitsbergen Current is a net southwestward drift which transports ice around Sørkapp in winter, sometimes up to the latitude of Isfjorden, depending on the strength of the WSC. In general it ensures that the eastern coast of Svalbard remains ice-covered for a great part of the winter.

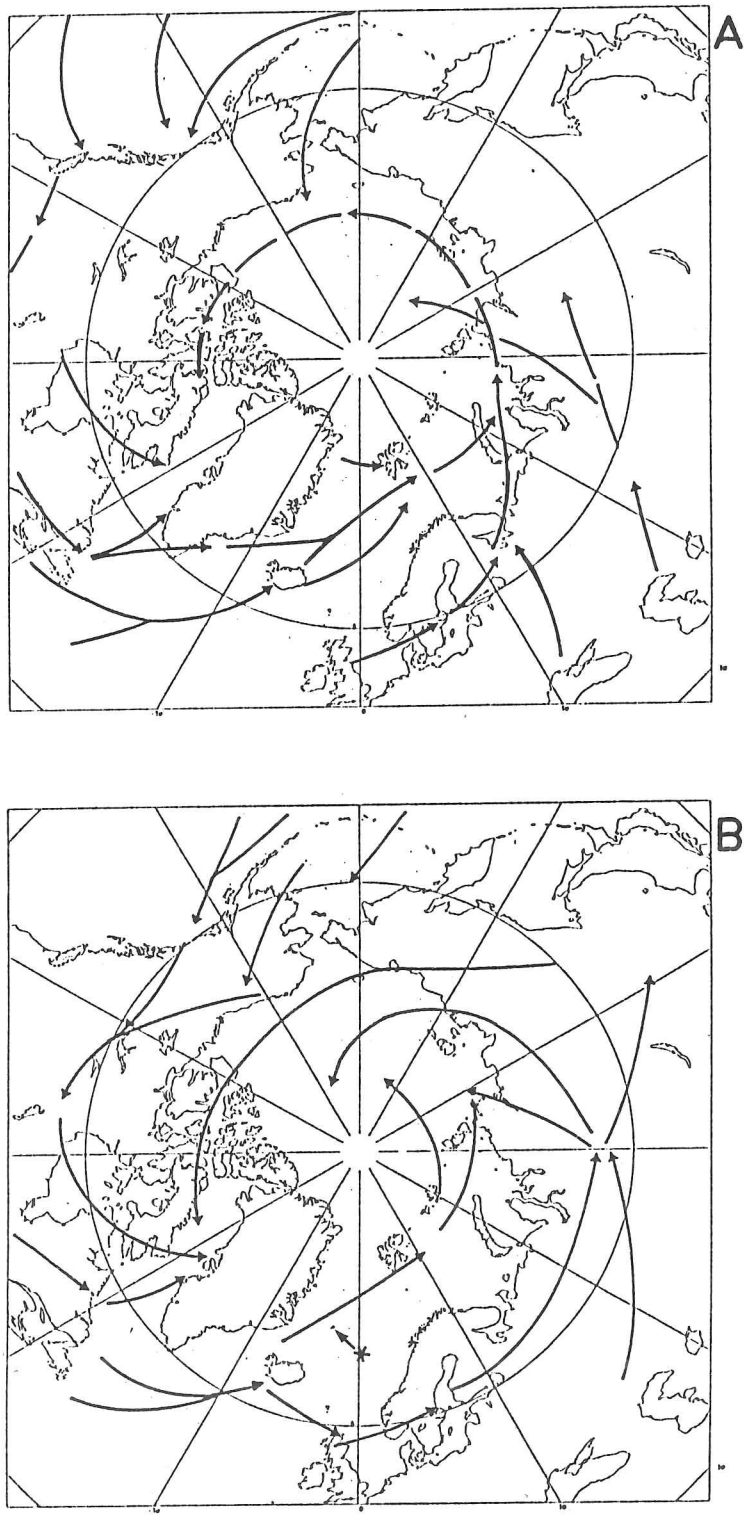

Figure 1.5- Principal Northern Hemisphere tracks of cyclones in January (A) and in July (B). Source: Klein (1957). Small arrow with a star in Fig. 1.5B marks the location of Jan Mayen.

Sea-ice conditions are dependent on both atmospheric and oceanographic factors. At the same time the sea ice affects atmospheric and oceanic circulation by complex interactions (Parkinson et al., 1987). For example, the presence of sea-ice cover restricts exchanges of heat, mass, momentum, and chemical constituents between ocean and atmosphere, it increases the albedo of the Earth's surface, and its growth and decay modify considerably the ocean-mixed layer (Barry, 1985). Furthermore, important feedback mechanisms operate among the other parts of the climatic system. For example, sea-ice growth increases the albedo of the Earth's surface and as a result decreases the atmospheric temperature, the lower temperature results in an increase of sea ice and further decrease in temperature, and so on. Hence sea ice is an integral part of the rest of the climatic system. The variability of the ice edge in the area of study is dominated by the seasonal cycle but it is also affected by synoptic-scale atmospheric forcing and longer-term changes in atmospheric and oceanographic conditions. It is therefore no surprise that the waters around Svalbard are characterized by some of the greatest variations in the sea-ice edge outside Antarctica.

Sea-ice cover to the east and to the west of Svalbard differs both in origin and in its seasonal variations. On the west side the sea-ice extent depends on the balance between the cold EGC and the warm WSC currents. The northernmost area of open water on the west coast, Svalbardbukta, shows the greatest seasonal variations and is frequently entirely covered with ice in late winter. However, this is not usual: there are great variations and open water has been observed at 83°N in the middle of December (Vinje, 1977). This area of open water has important consequences for the local climate, as the heat loss from an ice-free ocean at this latitude changes the heat balance markedly, besides promoting a source of local moisture for glaciers and ice caps in northern Spitsbergen and Nordaustlandet. Minimum sea-ice cover occurs during September and normally the whole of the south and west coast is ice-free then. In warmer years open water is observed all round the Archipelago. The ice begins to advance in October and by the end of the month open water is observed only on the west coast. The sea ice expands around the coast and in colder years the East Spitsbergen Current is able to transport some sea ice to the west coast as far as the latitude of Isfjorden. The disintegration of the ice cover begins in March and is rapid; by the end of the month the west coast is free of ice. However, interannual variations can be great, and the duration of the west-coast ice cover varies between 3 and 12 months (Wadhams, 1981). Further evidence for the variation in the sea-ice cover is the extension of the shipping season. The warming between the 1910s and the late 1930s resulted in an increase in the shipping season from 3 months to 7 at Isfjord (Lamb and Mörth, 1978) and it appears to have been associated with a more zonal flow of the upper westerlies. These variations in the sea-ice extent on the west coast are also clearly associated with fluctuations in the strength of the WSC. For example, from the 1910s to the 1930s the temperature of this current increased by 1.5°C (Goudie, 1983).

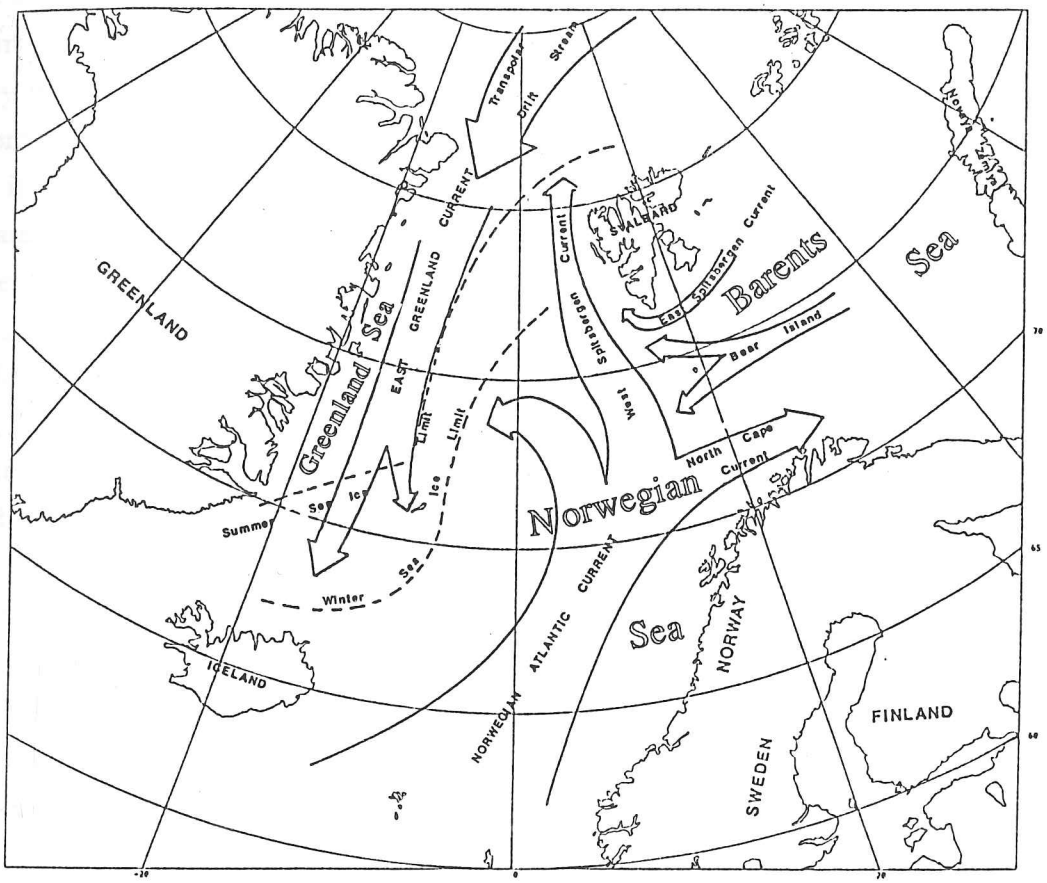

Figure 1.6- Ocean currents and mean sea-ice limit in the Arctic North Atlantic
Source: Map from Gathman (1986) and shown here in a modified form.

Farther west, the Greenland Sea has significant sea-ice cover throughout the summer months and the presence of ice is largely the result of advection of ice from the Arctic Ocean through the Fram strait (Wadhams, 1981). During March–April the ice goes beyond the southern tip of Greenland and reaches its minimum extent in August, when it may retreat to 72°N.

The ice cover to the east and south differs both in composition and in motion from the polar ice on the west coast. Sea ice is mainly transported southwestward by the East Spitsbergen Current around Sørkapp. In winter the ice extends as far as Bjørnøya, but the summer retreat is rapid and normally the sea-ice edge recedes to north of Kong Karls Land. The East Spitsbergen Current ensures that the east coast of Nordaustlandet remains ice-covered throughout many winters, but it is not unusual to find open water all around the Archipelago.

The comprehensive record of sea-ice extent in the areas near Svalbard is restricted to the period of satellite observations (e.g. microwave imagery from NOAA satellites). On the other hand, the longest historical record of sea-ice extent is the one for the Icelandic coast

which covers almost every year from A.D. 1600. These data have been extensively reviewed and tabulated (Koch, 1945; Thórarinsson, 1956; Bergthórsson, 1969; Sigtryggsson, 1972; Lamb, 1977). More recently Ogilvie (1984) has re-examined critically the estimates for the early period (i.e. 1600-1780), and presented a new decadal index. The Icelandic sea-ice record is used in this dissertation as an index of sea-ice conditions in the vicinity of Svalbard and it is frequently cited in Section 1.4.3. This methodology can be criticized. Iceland is situated more than 1500 km from Svalbard and may not be representative of local conditions there. The representativeness of the Icelandic sea-ice record has recently been assessed by statistical analysis (Kelly, Goodess and Cherry, 1987), however, and the results suggest that the Icelandic ice index is a fair representation of ice extent elsewhere in the Greenland Sea. In fact, the index correlates significantly with sea-ice extent on both the west and east Svalbard coasts. Sometimes, as in the period between May and August, the correlation reaches 0.7 (ibid.). Another important conclusion is that sea-ice extent is related directly to strong northerly and westerly winds over the Greenland Sea, and without doubt the index is a useful indicator of the character of the EGC (ibid.). These winds are associated with stronger development of the Greenland high and Icelandic low in late winter and spring, and the ice is transported southward because of the anticyclonic curl of the wind stress (Barry, 1985). This latter conclusion brings up the question of the relationship between sea-ice extent and atmospheric temperature. Although the sea-ice extent varies in relation to the gross changes in atmospheric temperature (Lamb and Mörth, 1978), the development of strong winds may make a significant contribution over short time-scales. In fact, a greater extent of sea ice in the Greenland Sea may be associated with the removal of ice from the Arctic Ocean by strong winds rather than by greater production (Lamb, 1982b). In some cases it can be associated with a warming of the Norwegian coast, as the intensification of the Icelandic low also implies strong south-southwesterly winds on the east side of the North Atlantic and, as a result of the intensification of the oceanic gyre in the North Atlantic, an increase in warmer air transported by the Norwegian Atlantic Current. Periods of expansion of sea ice in the Greenland Sea may also be related to changes in water temperature, and, for example, some of the periods of great ice extent (such as 1968–69 and 1979) were related to the migration southward of polar waters (Lamb and Mörth, 1978; Lamb, 1982b). The same appears to have happened between 1675 and 1705, when sea ice advanced between Iceland and the Faeroe Islands (Lamb, 1982b).

1.3.4- The present climate of Svalbard

The climate of the west coast of Svalbard may be classified as polar (tundra climate, ET in the Køppen classification), with a strong maritime influence. The mean temperature at Isfjord for the period 1912–75 was -4.8°C. Temperatures in the winter are relatively high when compared with other sites at the same latitude in the Arctic. The winter mean temperature for Isfjord (78°N, 13.6°E) during the period 1912–75 was -11.2°C. However, as referred to earlier and as explained in the following sections, the region is characterized by

great climatic variability and during warmer years the mean winter temperature may reach -4.7°C (as in 1932/33, for example). These relatively high temperatures result from the combined effect of the transport of warm air by cyclones travelling via Iceland and the heat provided by the WSC. Continentality increases towards the centre of Spitsbergen and, as expected, stations in the inner fjords show slightly warmer summers and cooler winters, and the mean annual atmospheric temperature (MAAT) is lower. For example, in the period 1957–75 the MAAT at Isfjord was -4.9°C and at Longyearbyen, which is situated about 50 km from the west coast, the MAAT was -5.9°C. Atmospheric temperature decreases towards the NE and the few measurements taken by expeditions indicate a lapse rate between 0.6 and 1.0°C/100 km (cf. Table 4.1 in Section 4.2). From 1989, data from an automatic weather station on Phippsøya will provide information on conditions on the northeastern coast of Svalbard (Hisdal, oral communication). The meteorological station nearest to the area of the field studies of 1985 and 1986 is in the mining town of Sveagruva (77°54'N, 16°43'E). It was opened in 1978 (May) and the MAAT for the period 1980–87 was -6.7°C. The station, which is situated at the head of Van Mijenfjorden, is the one with the most continental characteristics, which can readily be appreciated by the great difference between the winter and summer mean temperatures (-15.7°C in winter and 4.7°C in summer for the period 1980-87).

The coldest period, February–March, shows mean temperatures which vary between -8 and -16°C in Isfjord (Hisdal, 1985). However, the region is characterized by great temperature fluctuations at all time-scales. In Section 1.4 the temperature variations on annual and longer time-scales are reviewed. There are also great daily fluctuations in temperature: it is not unusual to have an increase in mean temperature of 20–25°C over a couple of days during the winter. In one case, in March 1985, temperatures near -30°C were immediately followed by days with temperatures close to 0°C and rain (N. Riley, personal communication). The main cause of abrupt fluctuations in the daily temperature is the alternation between cold Arctic air and moist warm air brought by cyclones. The latter arrive in the islands mainly from a S-SW direction and their incidence over Svalbard is directly related to the oscillations in the position of the Arctic Front over the Arctic North Atlantic. In winter the contrasts between the Arctic air mass and warmer cyclonic air are greater, and consequently surface-temperature variations will be greater (Hisdal, 1985; cf. Section 1.3.2).

Summer temperatures below 0°C are not unusual (Hisdal, 1985), although the mean temperature for July is 4.7°C in Isfjord (1912–75) and 6°C in Sveagruva (1980–1987). Mean daily maxima in this month can reach 8.4°C in Sveagruva. If a lapse rate of about 0.9°C is allowed for, it will be clear that even the glaciers on high mountains (i.e. above 1200 m a.s.l.) may suffer superficial melting in the summer. The maximum temperature officially recorded in Svalbard is 21.3°C at the Svalbard Lufthavn station in July 1979, and the lowest, at the former Green Harbour station (which was situated near the Barentsburg

mining town) in March 1917, was -49.2°C (Hisdal, 1985). As will be seen in the next section, this was the coldest year of the century. In such climatic conditions stratigraphic studies of snow and ice become meaningless, as ice layers can be formed at any time of the year, and destruction of some or all of the annual accumulation can occur (cf. Chapters 2 and 3).

Annual precipitation is low and is rarely above 400 mm (Hisdal, 1985). In Isfjord the long-term mean (1946–75) is only 403 mm, based on a range from 244 to 740 mm a^{-1}. The greater continentality of Sveagruva is apparent from the small mean annual accumulation for the period 1980–87, which is only 287 mm. Some years are relatively arid, and annual accumulation can be as low as 174 mm (e.g. in 1983). Rain and snow can occur at any time of the year (Hisdal, 1985). Few measurements have been made away from the weather stations, and the spatial distribution of the annual precipitation is still unknown. As a result, some authors have tried to interpret a snow-line altitude map by Liestøl and Roland (in Steffensen, 1982; Hisdal, 1985) as representative of the distribution of the annual net accumulation rate in Svalbard. They reasoned that the main factor controlling the snow line in Svalbard is the amount of snow (Hisdal, 1985). On the basis of this map, which is depicted in Fig. 2.3, the driest areas should be in central and northern Spitsbergen (around the central part of Wijdefjorden), which have the highest snow-line altitude, between 600 and 800 m a.s.l.. This approach can be questioned, as the snow line certainly depends on other factors (e.g. heat budget), in addition to showing great annual variability. The example in Svalbard that most clearly contradicts this generalization is the accumulation rate on Storøya. Although this small ice cap has a low snow line (less than 200 m a.s.l.), the accumulation rate is low (less than 400 mm a^{-1}; Heintzenberg et al., 1988). In fact, the ice cap owes its existence to special microclimatic conditions on the summit plateau. The summit is constantly covered by clouds in the summer and solid precipitation occurs all year round (Jonsson, 1982). A better approach to assessing variations in precipitation was that of Semb, Brækkan, and Joranger (1984), who measured the total accumulation at the end of the accumulation season (i.e. April–May) in snow cores from Svalbard glaciers in 1983. The distribution coincides more or less with the snow-line altitudes. The driest areas are without doubt the central part of Spitsbergen and Wijdefjorden, and precipitation is frequently less than 200 mm. There are three areas of high precipitation: in NW and SW Spitsbergen, and in Olav V Land in NE Spitsbergen. All these areas of high precipitation are associated with mountains. It seems, therefore, that precipitation in Svalbard is controlled strongly by orography. Another feature revealed by this survey is a corridor of low precipitation in the Isfjorden area. However, this may be only an artifact of the low elevation of some of the glaciers in the region, and so the sampled snow core represents a shorter period, as rain and melting occur more frequently later in the season than at high altitudes.

Precipitation is associated with the passage of cyclones over the Archipelago and as a consequence it shows strong seasonality and irregularity. Summer precipitation reaches Svalbard from the SW-S and winter precipitation comes mainly from the S-SE but also from the NE. The area is subject to great temporal variability in the precipitation (cf. Section 1.4), also because of the type of precipitation. The advance of the cyclone tracks during warm periods results in a greater precipitation rate. Warm periods will therefore be associated with greater precipitation, not only because the source areas will be nearer the Archipelago, but also due to greater penetration northward of the cyclones (Lamb, 1972). The annual maximum is reached in summer (mainly August–September) and can be as much as 40 mm per month in Isfjord.

The wind direction fluctuates from season to season and reflects the changes in cyclone tracks. In autumn-winter-spring, when the Arctic Front is at an advance position, E–NE winds prevail (cf. Fig. 1.4, and Steffensen, 1982). These winds have an important role in the transport of impurities from Eurasia (cf. Chapter 5). In summer, reflecting the migration northward of the main track of cyclones, the S-SW wind direction prevails, bringing relatively warm and moist air to the west coast of Svalbard.

1.4- The record of recent environmental change in Svalbard

1.4.1- Introduction

A detailed examination of the climatic changes during the instrumental period is made in order to provide a background for the ice-core studies and it includes the variations in mean annual atmospheric temperature, precipitation, and the summer 'warmth' index. The latter parameter is examined with a view to providing an index of the melting conditions but it is restricted to the last 40 years because the record was interrupted by the Second World War. The second part of this section examines the scanty data for environmental changes over the last 700 years, which encompass the period known as the 'Little Ice Age'. This review aims to provide a background for the discussions in Chapter 4.

1.4.2- Climatic variations in Svalbard during the instrumental period

In this section the record of environmental variations throughout the instrumental period are discussed in detail. The main objectives are to derive a time series of climatic parameters that can be correlated with measured ice-core parameters; to demonstrate the climatic sensitivity of Svalbard during the period; and to investigate whether the region is representative of climatic fluctuations elsewhere in the Arctic and in the Northern Hemisphere as a whole. The period under examination begins with the first instrumental records from the North Atlantic, dating from the 1880s, and goes up to 1986. The discussions in this section are based mainly on the summaries of the meteorological record by Steffensen (1969 and

1982) and Kelly et al. (1982) for the period from the 1880s to 1945. These are supplemented by observations on the meteorological tables published by the Norsk Meteorologisk Institutt (NMI) between 1946 and 1978, and by unpublished data for the Sveagruva meteorological station from 1979 to 1984. Elsewhere in this dissertation, there is, when relevant, a more detailed discussion of other climatic parameters important for glaciological studies (e.g. the number of melting degree days and the weighted temperature of days with precipitation).

The nearest meteorological station to the Skobreen ice-core site is at the mining settlement of Sveagruva, about 26 km north. Unfortunately this station was only opened in 1979. Further, no meteorological station in Svalbard has been operated continuously since records began in 1911. On the other hand, the mean daily and annual temperatures of the different stations in the Archipelago are highly correlated (i.e. $r > 0.96$ for all stations, at a high level of significance, $\alpha < 0.02$). On this basis, the mean annual conditions for Sveagruva were estimated from 1912 to 1978 from a series of linear regressions for the entire period (i.e. 1912–78) and supplemented with data from the station (1979–86). Other parameters (e.g. precipitation) do not show significant correlations and they were used only to give general insight into changes in the past. The procedures that were used to estimate the mean annual temperatures and other climatic parameters of glaciological importance are detailed in Appendix 1 - Climatic parameters relevant for glaciological studies in Svalbard.

1.4.2a - Mean annual temperature fluctuations

General trends

Records in Svalbard began at the Green Harbour meteorological station in 1911. Little is known about meteorological conditions in the Archipelago before this period. However, some information about the temperature trends can be obtained from expedition records (Steffensen, 1969) and from the general trends from 1880 for the Greenland Sea and NE Atlantic calculated by Kelly et al. (1982). This was extended to 1851 for the Arctic as a whole by Jones et al. (1986). The results can be considered reliable because there is good correlation between the general trends in the Greenland Sea and NE Atlantic as a whole and the Svalbard area (Fig. 1.7b and g). The period between the 1880s and 1906 was one of the coolest on record during the last 140 years. On the other hand, it was a period without marked trends in the region. This contrasts strongly with the trends in the Arctic and the Northern Hemisphere over the same time-scale. By the 1900s the Arctic had warmed by ~0.65°C and the Northern Hemisphere by ~0.25°C (Kelly et al., 1982). Further, the 1880s were the coolest decade in both regions. By 1906 temperatures were beginning to fall. When the record in Svalbard began temperatures were still falling towards the coolest year on record there, -11.0°C in Isfjord in 1917. A new trend towards higher temperatures characterized the inter-war period, and by 1938 the mean annual temperature had increased by ~1.8°C since 1880. From then onwards it dropped to a new minimum in the middle 1960s (i.e. it fell ~0.85°C from the mean

in 1938). This contrasts with the Svalbard area, which shows a relative minimum in the mid-1940s. In general, discussions in the rest of this section are based on temperature values for Isfjord. Sveagruva temperatures are used for the post-1978 period and frequently the estimated values are cited for earlier periods.

Mean annual atmospheric temperatures (henceforward MAAT) since 1912 have had four main trends: 1) a period of rapid warming (1912–23); 2) a 32-year period of relatively high temperatures (1924-56), slowly increasing to a maximum in 1954; 3) a sharp fall in temperature to 1968; 4) another increase in temperature to 1972. Between then and 1986 temperatures have been approximately constant, at -6.7°C (estimated for Sveagruva), with the exception of 1984, which was the warmest year on record (-3.5°C in Sveagruva). All these trends were interrupted from time to time by fluctuations in the opposite direction.

Figure 1.7g compares these trends in central Spitsbergen (calculated by the author) with temperature changes in different sectors of the Arctic and in the Northern Hemisphere as a whole (after Kelly et al., 1982). Temperatures are plotted as departures from the 1946–60 mean. Some of the Arctic sectors strongly reflect general Arctic trends and fluctuations. What is remarkable is the strength and swiftness of these fluctuations in mean annual temperature in some of the sectors. The Barents and Kara seas (Fig. 1.7c and d), and the Greenland Sea and NE Atlantic (Fig. 1.7b) sectors show the greatest and most rapid variations. Svalbard is on the boundary between the Greenland Sea/NE Atlantic and Barents Sea sectors, and the fluctuations there are similar to the fluctuations in these two sectors (Fig. 1.7g). Sometimes fluctuations in the Greenland Sea/NE Atlantic sector are stronger by a factor of 3 in relation to other sectors of the Arctic (e.g. the drop in temperature in the 1910s; compare Fig. 1.7b with the other Arctic sectors), which emphasizes the climatic sensitivity of the area. In making the above comparisons, it should be borne in mind that each one of the time series a – i has been compiled on the basis of data from different numbers of stations. Areas with a greater number of stations will have a higher signal-to-noise ratio, because the local anomalies are smoothed out by the averaging procedure. Therefore it is not possible, for example, to draw general conclusions from the changes observed in Central Spitsbergen and apply them to the Greenland Sea/NE Atlantic sector.

Soon after the 1917 minimum, temperature increased abruptly. In 7 years (1917–23) the mean annual temperature rose 7.9°C (i.e. to -3.1°C in Isfjord). This is one of the greatest increases recorded anywhere in the world and known to the author. There is evidence for it in different sectors of the Arctic (cf. Fig. 1.7) and it is certainly a good reference horizon for ice-core studies. This sharp shift in temperature is explained, at least partly, by the withdrawal northwards of the boundary of sea ice (Lamb, 1982a). The warming trend continued up to 1954, albeit interrupted intermittently by negative anomalies. In 1954 the temperature reached -2.0°C in Isfjord; the estimated value for Sveagruva is -3.9°C. This

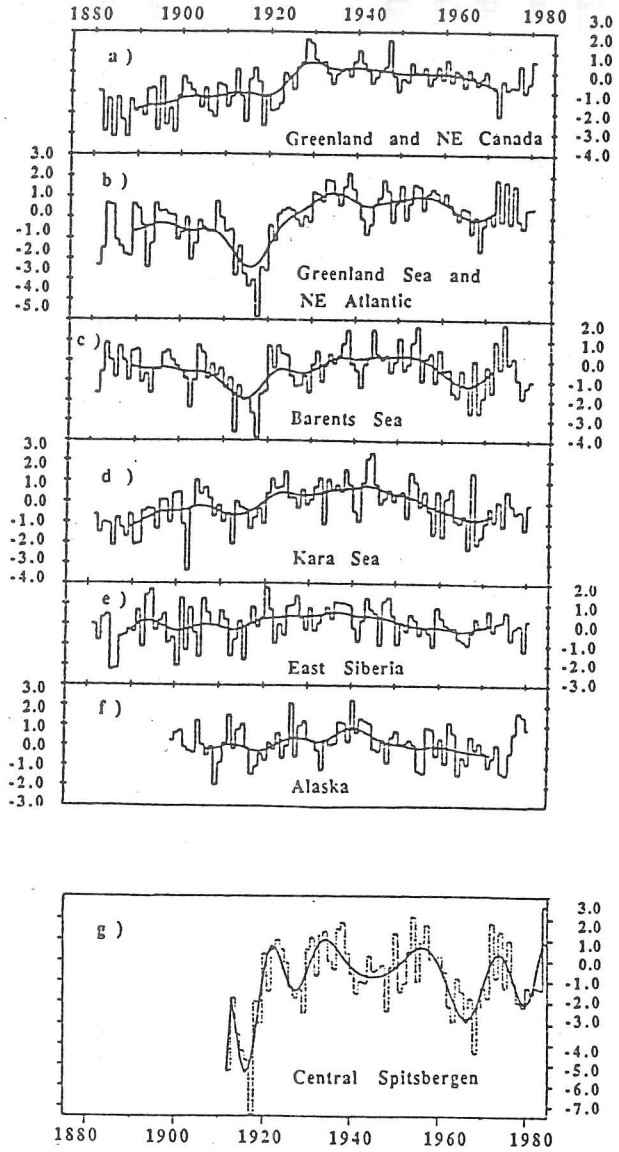

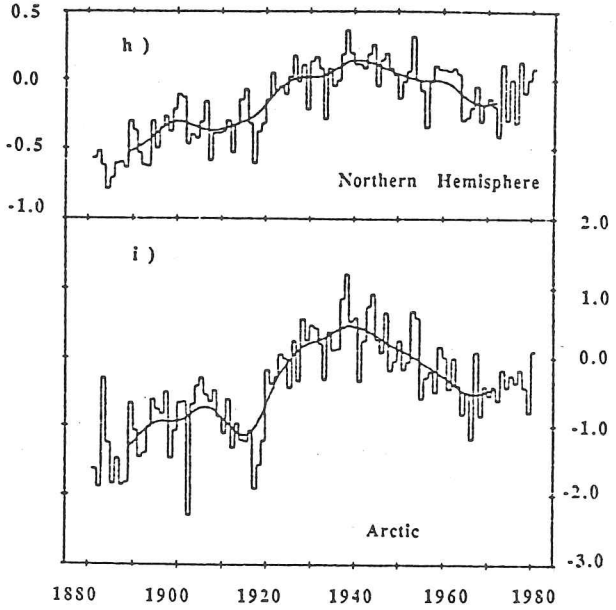

Figure 1.7- Annual temperatures (°C) time series for the different sectors of the Arctic (a - f), the Arctic (i), and the Northern Hemisphere (h) as departures from the period 1946-60. Source: Kelly et al. (1982), except graph g, which is by the author of this dissertation.

contrasts with what is frequently claimed for various ice-core studies in Svalbard (e.g. Gordiyenko et al., 1981), which consider that the maximum temperature was reached in the middle 1940s, apparently as a result of the incorrect use of 5–10-year running means (Steffensen, 1982; and Fig. 1.8), where the 1940s appeared as a warm phase, but the period is in fact relatively cool when compared with the 1930s and 1950s (Fig. 1.7g). The pseudo-high temperatures were created by the mean procedure. Further, as will be described in other sections, the mean temperature of days with precipitation (Fig. A1.3) shows even more strongly that the 1950s were the warmest period on Svalbard. Thus the isotope-ratio maximum should be correlated with the 1950s and not the 1940s.

After 1957 temperatures fell rapidly, from -2.4°C to a minimum of -8.1°C in Isfjord in 1968. A new rapid warming trend was observed until 1972, when temperatures reached -2.3°C. Since then, temperatures have fallen and have been more or less constant at about -6.7°C. If the 4 years with extremely high temperatures since 1972 are removed from the record, the temperature remains constant at about -5.1°C in Isfjord (or -7.3°C at Sveagruva), which should be borne in mind when correlating the mean isotope ratios. These anomalous years may not be reflected in the ice core, particularly if they were totally removed by flush-out during the summer. The maximum MAAT ever recorded was in 1984, when the mean annual temperature was -3.5°C in Sveagruva (i.e. equivalent to -1.7°C in Isfjord). This represents a range of about 9.3°C in the MAAT during this century in Isfjord.

The examination of temperature trends can be extended to 5-year running means (Fig. 1.8). These means may be more significant for comparisons with the ice-core data. As discussed elsewhere in this dissertation (Chapters 3 and 4), the percolation and refreezing of summer meltwater homogenizes the various measured parameters (e.g. $\delta^{18}O$) for a period of some years. The smoothed MAAT still shows the minima of the 1910s and 1960s. Three periods of high temperature can be distinguished – the first half of the 1920s, the 1930s, and the mid-1950s. The warmer years of the 1970s are shown as being slightly cooler than the later 1950s.

Fluctuations in the mean annual temperature provide some of the strongest evidence for the climatic sensitivity of the Svalbard region. The Greenland Sea and the NE Atlantic and the Barents sectors (which include Svalbard) show the greatest variations in temperature, which may be greater than similar variations in other areas of the Arctic by a factor of 3. Other areas underwent similar changes (i.e. the Kara Sea, and the Greenland and NE Canada sectors) but they were not so well defined. It is clear from the above observations that the strongest and most rapid variations in the MAAT (such as the warming by the end of the 1910s) occurred in areas where the production and decay of sea ice was greatest (e.g. the Greenland Sea and the NE Atlantic, and the Barents Sea) and these areas appear to represent well the short-term anomalies (i.e. less than five years). On the other hand, these areas are not

representative of temperature trends in the Arctic as a whole. Temperature fluctuation in the Kara Sea is a better illustration of the long-term temperature trends in the Arctic (cf. Fig. 1.7d and i; and Kelly et al., 1982).

Anomalous years

Years or periods of anomalous temperatures may be revealing for ice-core research in sub-polar areas, particularly when differences of the order of 5°C occur over a short time period (e.g. one–two years). They may represent the difference between the total preservation or destruction of one or several annual layers. They may also offer a reference horizon for the dating and correlation of ice cores.

In this century two periods of extremely low temperatures should be readily identifiable in any ice core from Svalbard. They are 1912–19 and 1962–68. For the record at Skobreen only the second period is relevant. The mean temperature at the site in 1968 is estimated to have been about -9.4°C. During this period some annual layers may have been preserved almost unaltered.

In this century there have been three periods of extremely high temperatures: 1937–38, 1954–57, and 1972–76 (cf. Fig. A1.2), when mean temperatures were -2.4°C, -3.1°C, and -3.6°C respectively. Ice masses in Spitsbergen were certainly affected by intense superficial melting during these periods (Baranowski, 1977b). However, other climatic parameters, such as the number of melting degree days and the duration of the melting season, are more useful as an index of melting. This is because a high mean annual temperature may be reflecting an increase in temperature only in winter months. These other parameters are therefore discussed below and elsewhere in the dissertation in the context of the interpretation of the ice-core record and the understanding of what controls the ablation of glaciers in Svalbard.

1.4.2b- Indexes of summer 'warmth'

Variations in MAAT are not useful as an index of summer warming because the mean temperature represents all the seasonal changes. In fact, the great majority of the years with an anomalously high MAAT in Svalbard were characterized by mild winters (Steffensen, 1982). It is therefore necessary to estimate a time series of parameters that gives some idea of the character of the ablation season, particularly of the days when the temperature was above 0°C. This is important for mass-balance studies (cf. Chapter 2) and to determine which periods were subject to intense superficial melting and altered the original ice-core record. In this section, variations in four parameters thought to be representative of the summer conditions are described: 1) mean summer temperature; 2) number of melting degree days; 3) length of the melt season; 4) and the mean daily maximum temperature in July. They were calculated

following the methodology described by Orheim (1972), Bradley and England (1978), and Hanson (1987). Details of the procedure and the significance of the variations for glaciological studies are given in Appendix 1 and Table A1.1. The variations in these four parameters, for the post-war period (1946–87) are depicted in the Appendix (Figs. A1.4-A1.7).

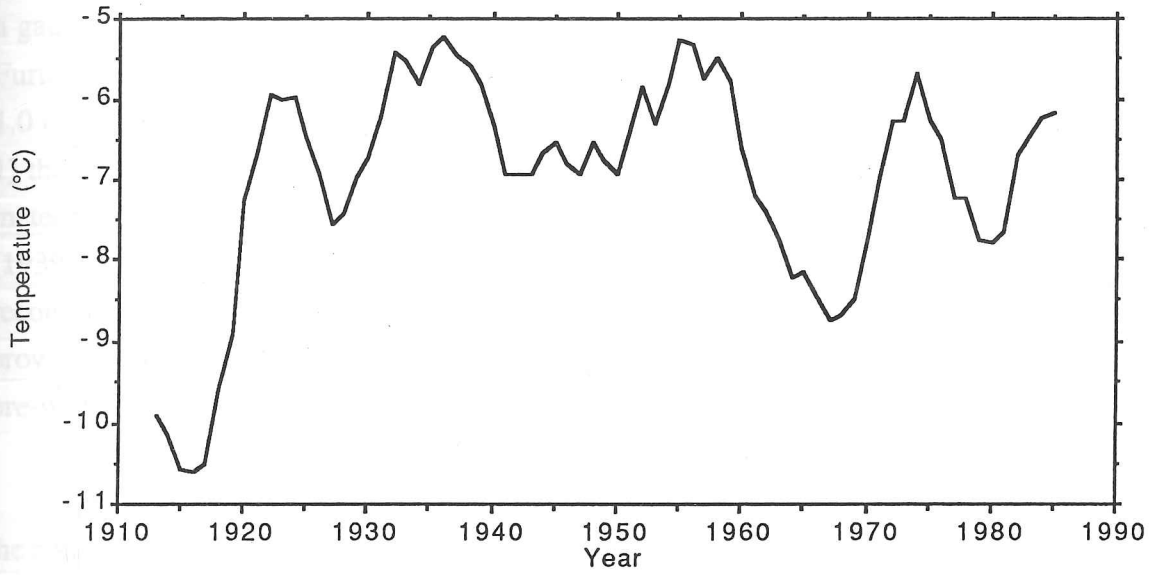

Figure 1.8- Mean annual air temperature for Svalbard (Sveagruva) smoothed by a 5-year running mean.

The only parameter to show any trend is the mean daily maximum temperature in July (July T_{max}) in the period 1955–79 (cf. Fig. A1.7). July T_{max} increased from 5.7°C in 1955 to a maximum of 11.7°C in 1979. Since then it has decreased slightly, reaching 7.3°C in 1987. Years with an anomalously high July T_{max} include 1960, 1966, 1969, 1974, 1979, and 1984 (all with July T_{max} greater than 9.5°C). The variations in the other parameters are irregular. The length of the melting season has ranged from 102 days (in 1960) to 224 days (in 1959) over the period 1946–87, and on average it lasts 146 days a year. The mean summer temperature during the same period was 4.4°C and a maximum was reached in 1953 (5.8°C). Other anomalously warm summers (mean temperature > 5.5°C) include 1971, 1972, 1974, and 1976. In recent years (1984–87) every summer has had a mean temperature above 5°C. The number of melting degree days (i.e. the sum of mean daily temperatures when these are > 0°C) is thought to be a better representation of summer conditions as it takes into account the length of the melting season and the accumulated warmth of the season (Bradley and England, 1978). This index had a mean of 487 during the period 1946–87,ranging from 299 (in 1962) to 663 (in 1954). Other years where the number of melting degree days (NMDD) was greater than 600 include 1951, 1954, 1971, 1972, 1974, 1976, and 1984. The summers of 1962 (299 NMDD) and 1982 (326 NMDD) were relatively cool. These sets of parameters indicate that the late 1950s, the early 1970s, and 1984 had extremely

warm summers, so the ice-core record for these periods may be greatly distorted or obliterated, as superficial melting may have been intense. The summers during the mid-1960s, on the other hand, were cool and the original record may have been preserved.

1.4.2c- Precipitation variations

When discussing precipitation variations one should bear in mind the difficulties of measuring the total daily precipitation in an environment like Svalbard. The problems of using a gauge to measure snowfall are well known when there are strong winds or drifting snow. Furthermore, there is a great number of days with precipitation amounting to less than 1.0 mm. There are other important drawbacks that should be taken into consideration: 1) there are no continuous observations for any of the stations for the whole period of meteorological observations in Svalbard; 2) the time series is incomplete for the war years (1939–45); 3) the great variability between stations does not allow the time series to be reconstructed by statistical methods. Therefore precipitation is discussed only with the aim of providing an indication of the variations in Svalbard. Only general comments are made on the pre-war record; the post-war record is plotted in Fig. A1.8.

Interannual precipitation variations in Svalbard have proved to be as highly variable as the annual temperature; during this century it has varied between 100 and 750 mm a^{-1} (Brázdil and Purkyne, 1988). The longest time series of records for the pre-war period is from the Green Harbour station and covers 1911 to 1930. Although great annual variability was observed (from 200 to 500 mm a^{-1}; Brázdil and Purkyne, 1988), there was an increase towards the 1930s (from 300 to 400 mm a^{-1}), and accumulation was still increasing during the 1930s. At the Isfjord station precipitation increased from 200 to 600 mm in the period 1930–36.

Fig. A1.8 plots the variation in total annual precipitation (in mm) for the post-war period. Discontinuities (i.e. changes in meteorological station) are marked by arrows. Isfjord station shows a substantial increase in precipitation from 1946 to 1962, when it reached 550 mm (i.e. an increase of almost 100%). This trend is statistically significant ($r = 0.57$, at $\alpha < 0.002$) and shows an annual increase of 7.3 mm. The maximum precipitation rates were reached by the end of the 1950s and in the warm years of 1972 and 1974. In Isfjord in 1972 (one of the warmest years of the century) precipitation was 740 mm. In the 1960s there was a slight fall in the precipitation but it did not reach the levels of the early 1950s. It seems from this observation that the general trend towards great precipitation followed, more or less, the trends in temperature for the first part of the century. In other words, the period of minimum precipitation was the 1910s, the coolest in the century, and then precipitation increased until the end of 1950s. The relative cooling of the late 1940s is represented by the low precipitation values at Isfjord (about 250 mm).

The precipitation time series had to be supplemented by data from Longyearbyen (1975–76), Svalbard Lufthavn (1977–79), and Sveagruva (1979–87), as Isfjord was closed in 1976. These stations are situated in the inner parts of fjords and so the precipitation is less. The last 10 years have shown greater variability in precipitation and in the case of Sveagruva precipitation has fluctuated between 174 mm and 462 mm since its opening in 1979.

1.4.3- The last 700 years: onset and termination of the Little Ice Age

This section reviews the development of environmental changes in Svalbard and the surrounding area over the last 700 years. This time span was chosen for two main reasons: first, it comprises the period covered by the great majority of the ice cores recovered from Svalbard so far (cf. Chapters 2 and 4), providing a reference background for the environmental changes in the Archipelago which are the subject of discussion in this dissertation. It is also important for the examination of short-term fluctuations which may be embedded in variations of lower frequency. The other reason is that this period comprises the so-called **Little Ice Age.**

The environment of Svalbard, and of a great part of the globe (cf. Grove, 1988), after the Hypsithermal in the early to mid-Holocene (Punning, Troitsky and Rajamae, 1976; Baranowski, 1977a and b; Lindner, Marks and Ostaficzvk, 1982; Lindner, Marks and Pekala, 1984) has been characterized by oscillations between cold and warm periods with a duration of hundreds of years (Werner, 1988). The last of the cold spells and the one characterized best in different paleoclimatological records is the **Little Ice Age** (LIA). This was a period of relatively low temperatures when compared with the present climate and was interrupted from time to time by intervals of more clement conditions. A pattern of complex climatic variability with cold and dry pulses, rather than a linear trend to colder times, prevailed (Wigley, 1979). Further, some of the warmest years in the record (e.g. 1665) were registered near the climax of the LIA in Europe (Lamb and Mörth, 1978). It has been recognized in a great part of the world, although the dearth of information from the Southern Hemisphere does not allow precise determination of the extent and duration there. The LIA is particularly well marked in several ice cores from the Arctic, including the northern Canadian islands, Greenland, and Svalbard (Johnsen et al., 1970; Dansgaard et al, 1975; Paterson et al., 1977; Hammer et al., 1978; Fisher and Koerner, 1981; Gordiyenko et al., 1981; Punning, Vaykmyae, and Tóugu, 1987). The LIA is said to have begun between the thirteenth and fourteenth centuries (Grove, 1988), sometimes in an abrupt way (e.g. Thompson and Mosley-Thompson, 1987). However, other authors place the onset at different times between 1300 and 1550 (e.g. Lamb, 1977; Wigley, 1979). The cooling of the period was coupled with changes in atmospheric and oceanic circulation (cf. Section 1.3), and in the Arctic North Atlantic it was frequently associated with the expansion of a trough of upper westerlies over the Norwegian-Barents seas (Lamb, 1979). Worldwide, the

environmental changes of the period include, for example, expansion of sea ice, glacier advances, changes in plant and faunal distribution, in patterns of agriculture in marginal areas (Grove, 1988), and (according to some authors) an unequivocal impact on human affairs (cf. Lamb, 1977; Grove, 1988).

In the rest of the section, the environmental conditions in Svalbard during this period are reviewed on the basis of various paleoclimatological studies by other authors. Glacio-sedimentological, glaciological, and historical evidence is examined. The ice-core record, which shows the best resolution for the period, is discussed thoroughly in Chapter 4. Despite its proximity to Europe, few paleoclimatological studies in the Archipelago have examined the development of the LIA. Thus it is necessary to refer frequently to environmental variations elsewhere in the western part of the North Atlantic (i.e. East Greenland and Iceland) which are thought to be concomitant with changes in Svalbard (cf. comments on the sea-ice extent in Section 1.3). Finally, as already mentioned, the sea-ice record in Svalbard is limited to the most recent decades and no time-series studies have been carried out, so the variations in sea-ice extent around Iceland are used as 'proxy' for conditions in the vicinity of Svalbard. The references to variations in sea ice off the Icelandic coast are based on the time series initially published by Koch (1945) and since updated by various authors (Thórarinsson, 1956; Bergthórsson, 1969; Sigtryggsson, 1972; Lamb, 1977). The time series from 1700 is plotted in Fig 4.10. For the early period, 1600–1700, the discussions are based on the review by Ogilvie (1984), who pointed out a great number of methodological errors in the pioneering work by Thoroddsen (1916/1917), on which all subsequent papers had relied heavily.

In spite of the climatic significance of Svalbard, there have been relatively few studies on the development of the LIA there. It is not surprising, therefore, that only a few paragraphs were devoted to the region in the recent and comprehensive review of the LIA by Grove (1988). Recently, Werner (1988) examined the sequence of glacial events during the Holocene on the basis of moraine and proglacial lacustrine sediment studies. It is clear from this and other studies on Svalbard (e.g. Baranowski, 1977a; Troitsky et al., 1981, 1985) that the late Holocene was characterized by multiple glacier advances, of which the LIA is the most recent. It is well marked in the upper 10% of a sediment core from Linnévatnet (Werner, 1988). Following the Medieval warm period (between the 8th and the 13th centuries), climatic conditions began to deteriorate.

There is still doubt about the timing of the onset of the LIA in Svalbard. The maximum age was established by ^{14}C dating of the uppermost fossil tundra below an advanced moraine in Werenskioldbreen in southern Spitsbergen (Baranowski and Karlén, 1976; Baranowski, 1977a and b) and the results give an age of 760 ± 145 years. Lichenometrical studies carried out by Werner (1988) in Svalbard indicate a stabilization of the ice by 650 B.P., which probably represents an upper limit for the onset. Lindner, Marks,

and Pekala (1987) reported a maximum extent for the glaciers at about 600 years B.P., based on ice-cored moraine studies. However, it is unwise to attribute these advances entirely to climatic deterioration, as Svalbard glaciers are prone to intermittent surging (cf. Section 2.2.2). It is reasonable to say, therefore, that the LIA began in Svalbard sometime between the 13th and the end of the 14th centuries, and soon reached a relative maximum, most probably about 650 years B.P. (Werner, 1988). These data would agree with evidence from other areas around the North Atlantic (i.e. East Greenland, Iceland, and Norway; cf. Grove, 1988). For the next two centuries there is no information from the moraine record on the development of the LIA , probably because moraines formed in the period have been overrun by later advances. Not much is known about this period in the North Atlantic. The little information available on sea-ice extent near the Icelandic coast confirms a cold period at about the end of the 13th century (particularly in the 1280s and 1290s) and another in the second half of the 14th century (1350–80). By this time regular contact with the Norse colonies in Iceland had been lost (Lamb, 1977, 1982b). A core from Crête (on the crest of the ice sheet in central Greenland, 71°07'N, 37°19'W) records the minimum $\delta^{18}O$ at the end of the 13th century which is the lowest value for the last 1000 years ($\delta^{18}O \approx -35.3‰$; Dansgaard et al., 1975). The history of environmental conditions up to the end of the 16th century in Svalbard has yet to be obtained. The Crête and Dye 3[†] stable-isotope records do indicate a relatively mild climate in the early 1400s, deteriorating towards the 1460s–1470s. The early part of this century was also characterized by a moister climate with warm summers, as demonstrated by an accumulation rate which was higher than the long-term mean and by the higher proportion of melt features in the Dye 3 core (Herron, Herron and Langway, 1981). At this time sea-ice conditions off Iceland appear to have worsened (Koch, 1945) and 1470 was apparently an extremely bad year, although this information is not totally reliable (Ogilvie, 1984). Information from Iceland indicates deteriorating climatic conditions, and the Denmark Strait (between Iceland and Greenland) was frequently blocked by sea ice in the summer at the end of the 16th century (Lamb, 1982b). On the other hand, the climatic conditions could not have been too much worse in the Norwegian-Barents seas, as Willem Barents was able to navigate to and discover Bjørnøya and Spitsbergen in 1596. Furthermore, the Crête core does not indicate any marked change (Dansgaard et al., 1975; cf. Fig. 4.10).

[†] This site is situated at 65°11'N, 43°49'W, 30 km to the east of the main ice divide of the Greenland ice sheet. It is known that accumulation comes mainly from the east and south (Robin, 1983) and so is representative of the conditions in the southwest part of the North Atlantic. On the other hand, the Crête station receives precipitation from both west and east because the site is at the north–south ice divide.

Data from two Dye 3 cores are used in this section: the discussions on the stable-isotope record refer to the 372 m core recovered in 1971 (Reeh et al., 1978), and the discussions based on the stratigraphy of melt features refer to the 2037 m ice core which was drilled (to bedrock) in 1980/81 (Herron, Herron and Langway, 1981; Langway, Oeschger and Dansgaard, 1985). The upper 80 m of the latter core were not sampled, and so there are no data for this century. Although both cores are near the Dye 3 station they are about 1 km apart (Herron, Herron and Langway, 1981). The Crête (405 m) core is the one recovered in 1974.

The picture that then emerges from the paleoclimatological record from Svalbard and other areas around the North Atlantic sector of the Arctic is one of continuous climatic deterioration for the next three centuries. On the other hand, this trend was interrupted by pulses of milder climate. In fact, one of the most marked but short warm intervals occurred in the first half of the 17th century. From 1620 to 1660 this short-term climatic amelioration allowed the development of the Dutch whaling town of Smeerenburg, on Amsterdamøya, in the northwestern corner of Spitsbergen (Hacquebord, 1981, 1984). Pollen variations in a core of sediments recovered near the station confirm that the trend of general climatic deterioration was interrupted by an amelioration between 1615 and 1650 (Van der Knaap, 1985). The historical records indicate that the whaling station was abandoned by the 1660s due to an increased incidence of sea ice (Hacquebord, 1984). This information agrees well with data from Iceland. The beginning of the 17th century was characterized by relatively heavy ice but by about 1630 conditions improved markedly, and in the 1650s almost no ice was reported off the Icelandic coast (Ogilvie, 1984). Until 1680 sea-ice concentration was relatively low but conditions deteriorated rapidly in the next two decades, reaching a maximum in 1695 (Lamb, 1977). In that year Iceland was surrounded by sea ice which came as far south as the Faeroe Islands. Lamb (1982a) thinks that this anomalous year was probably associated with the expansion of polar water across the entire surface of the Norwegian Sea and near Scotland, a phenomenon that was observed several times during the LIA. In fact this process is known to have affected the North Atlantic sector of the Arctic to different degrees during at least the last 225,000 years (cf. McIntyre, Ruddiman and Jantzen, 1972; Kellogg, 1976). In 1695 the sea temperature between the Faeroes and Iceland fell by about 5°C (Lamb, 1979). The warm period in the middle of the 17th century is reflected in the Crête stable-isotope record (cf. Fig. 4.10) and it was also followed by a rapid fall towards the end of the century. Finally, the proportion of melting layers in one of the Dye 3 cores indicates a period of warm summers in the middle of the 17th century, followed by a period of cool summers (Herron, Herron and Langway, 1981). This cold period is associated with the lowest accumulation rate found in the Dye 3 cores for the last 1000 years. The accumulation rate deviated from the long-term mean values (497 kg m^{-2} a^{-1} from the 11th to the 20th century; Reeh et al., 1978) by about 16%. Crête also recorded the lowest accumulation rate, in this case by 1640, when it deviated about 10% from the long-term mean for the 6th to the 20th century (266 kg m^{-2} a^{-1}, Reeh et al., 1978).

It is often stated that the LIA had reached its climax by this time, i.e. the end of the 17th and beginning of the 18th centuries (Lamb, 1977, 1982b; Wigley, 1979; Williams and Wigley, 1983). This is a generalization based mainly on the climatic conditions in Europe and on the impact on human life on the continent of the harsh years in the 1690s. However, this is not necessarily true for other areas. In fact, as the following paragraphs demonstrate, in the Arctic North Atlantic this period was only one of the short cold pulses which occurred in the next two centuries. This cold peak, albeit one of the strongest, was immersed in a general

trend to colder conditions towards the end of the 19th century – a conclusion strongly supported by the ice-core record from Svalbard and Greenland (Crête), as will be seen in Chapter 4.

It is not until the 19th century that is possible to obtain more information on environmental conditions in Svalbard. For the 18th century it is necessary yet again to rely on information from Iceland and Greenland. After the severe years at the beginning of the century, sea ice was restricted to the Iceland coast until the 1740s, when conditions deteriorated again (Ogilvie, 1984). By 1765 conditions had improved, but not for long. From the 1780s until the end of the 19th century the sea ice was extensive around Iceland, with the exception of a mild period from 1840 to 1854 (Sigtryggsson, 1972; Grove, 1988). The warming of the first half of the century is also reflected in the Crête core, which had $\delta^{18}O$ values similar to those for the present century (cf. Fig. 4.10), and in the Dye 3 cores (Dansgaard et al., 1975; Herron, Herron and Langway, 1981). On the other hand, from about the 1740s onwards conditions are shown as deteriorating continuously towards the 1780s-1790s. The Dye 3 core records a period of high melting at the end of the century (Herron, Herron and Langway, 1981).

Although several early expeditions in the 19th century reported the advanced position of the glacier fronts, and some took photographs, this kind of information cannot be used with confidence as a climatic index. Svalbard glaciers and ice caps are known to be subject to large surges at intervals that may vary between 20 and 100 years or more (Liestøl, in press, a; cf. Section 2.2). Other factors such as size, sub-glacial morphology, ice dynamics, and thermal conditions may play a role more important than climatic variation in determining the timing of their advance (Meier, 1965; Paterson, 1981). The interpretation becomes even more complex, as glaciers are known to respond with different time lags to fluctuations in the climatic conditions (Nye, 1961, 1963b), and it is not unusual to find glaciers advancing and retreating in the same area at the same time. On the other hand, studies by Werner (1988) indicate that several small cirque glaciers were able to exist only at the climax of the LIA in Svalbard during the 18th and 19th centuries and soon vanished as a result of warming in the 20th century. These glaciers have left moraines marking a maximum extent in about the 1880s. The Linné Valley, central-western Spitsbergen, is an example of an area with some of these cirques (Werner, 1988). In addition, André (1986) was able to date by lichenometry a major frontal moraine which had built up by the end of the last century in NW Spitsbergen.

Sea ice off the coast of Iceland during the 19th century was continuously severe, with the exception of the period between 1840 and 1854. Some of the years when sea-ice extent was greatest include: 1817, 1821, 1835, 1840, and 1866 (Lamb, 1977). The last two decades of the century saw some of the worst conditions ever recorded. In 1887 the sea ice grounded along the north coast of Iceland and in 1888 the island was again surrounded by sea ice

(Koch, 1945; Sigtryggsson, 1972; Lamb and Mörth, 1978; Grove, 1988). Polar water penetrated as far as Iceland and the Faeroes, and in 1888 an ice barrier was observed east and west of the Faeroes (Lamb, 1982a). Other paleoclimatological studies also show severe conditions in the 19th century. At Crête the $\delta^{18}O$ record is below the long-term mean throughout the century, except for a short period in about the 1850s, and it reaches a minimum at the end of the 1880s (cf. Dansgaard et al., 1975; and Fig. 4.10 in this dissertation). The accumulation rate reached a minimum at Dye 3 about this time, but at Crête this was observed in the first decade of the 20th century. An interesting observation is that the cold end of the century was associated with a high proportion of melting at Dye 3 (Herron, Herron and Langway, 1981), which appears to indicate high summer temperatures in that period. From the 1890s to the 1960s there was a continuous reduction of the sea ice around Iceland (particularly after 1915), and from 1880 to 1920 the number of weeks per year when there was sea ice off the coast of Iceland decreased from 12–13 to only 1.5. The increase in the ice-free period appears to have been associated with more 'zonal' atmospheric circulation (i.e. a long wave length), which results in greater penetration of cyclones in the Arctic (Lamb and Mörth, 1978). The 1960s experienced a new advance of polar water and in the years 1965, 1968, and 1969 there was heavy ice off the Icelandic coast. In 1968 Iceland was almost surrounded by sea ice, something that had not happened since 1880. In that year ice extended as far as Bjørnøya until April, and the area of Svalbardbukta was greatly reduced (Vinje, 1977), attesting changes in the strength of the WSC. But the 1970s witnessed great interannual variability in the sea-ice extent around Svalbard, and (as mentioned above) open water was observed in 1972 off the whole of the north coast of Svalbard as far as 83°N. Finally, the Crête and Dye 3 cores show a sharp increase in heavy stable-isotope content and accumulation rate (more than 10 and 20% respectively of the long-term mean) from the end of the 19th century to the 1950s, in agreement not only with the Greenland and Iceland records but also with the record from Svalbard. At Dye 3 these changes occurred in a relatively abrupt way at the end of the 19th century and beginning of the 20th century.

During the Swedish-Norwegian expedition of 1931 Ahlmann (1933c) noticed the general retreat of glaciers and ice caps on Nordaustlandet and NE Spitsbergen, although there were difficulties of interpretation due to surging glaciers (at least 69 glaciers have been observed to surge in the last 100 years; Liestøl, in press, b; cf. Section 2.2). Since then comparison with more recent terrestrial photographs has confirmed the continuous reduction of the ice cover in the Archipelago, after a maximum at the end of the 19th century, and since then the volume of some cirque glaciers have been reduced by half (Liestøl, in press, b). Other strong indications come from the general retreat of glaciers that are not known to surge. For example, Werenskioldbreen, in southern Spitsbergen, has retreated 1.5 km in the past 50 years (Baranowski, 1977b). Over the last 25 years mass-balance studies have been carried out by Norwegian and Soviet scientists (Liestøl, 1974, 1974, 1981, 1982, 1983; Guskov and Troitsky, 1987) and show considerable loss of mass. Results of the estimation

of the mass balance back to 1952 in Section 2.2 of this dissertation indicate considerable loss of mass from at least that year onwards. Koryakin (1985) has calculated that between 1900 and 1976 there was a reduction in the area covered by glaciers from between 4.2% in NE Spitsbergen to 11.7% in the southern part of the same island.

The above review indicates that the LIA began in about the 13th century in Svalbard. Climatic conditions deteriorated relatively rapidly and a secondary low in temperature was reached by the middle of the 14th century when glaciers deposited distinctive frontal moraines. From then until the end of the 19th century the climate in the region was characterized by the intercalation of cold and warm pulses of several decades' duration. There is no information on the 15th–16th centuries. On the other hand, the Iceland and Greenland records indicate a relatively mild climate, broken by two spells of cold in the 1460s–1470s and at the end of the 16th century. Historical and palynological studies show that the development of a whaling station in the extreme NW of Spitsbergen was possible because there was a short warm pulse between 1620 and 1660. After that, the climate deteriorated rapidly, reaching another secondary period of low temperature by the end of the century and shown by an increase in sea-ice extent in Svalbardbukta during the second half of the 17th century, which agrees with the Icelandic record. There is no information on the environmental changes in the 18th century other than the ice-core data (cf. Chapter 4), but the Iceland record indicates that the climate was relatively mild, with the exception of a period from 1740 to 1760. The Crête and Dye 3 cores indicate a relatively warm 18th century, but without great changes in the accumulation rate. The 19th century saw a continuous deterioration towards the 1880s, which seems to have been the coldest period in the LIA, when several glaciers reached their most advanced positions since the beginning of the Holocene. The last 100 years have been characterized by a general increase in temperature and as a result a great number of glaciers in Svalbard have been retreating. The increase in temperature was sometimes abrupt (e.g. 7.9°C in the MAAT from 1917 to 1923) and temperatures had reached a maximum by the mid-1950s. Sea ice increased again in the 1960s as a result of the decrease in temperature and changes in oceanic currents. MAATs have been increasing again since 1970, although in a irregular way (cf. Fig.1.7). The maximum MAAT ever recorded in Svalbard was in 1984 (i.e. about -1.7°C in Isfjord).

The paleoclimatological record for Svalbard appears to confirm the idea put forward by André (1986) and Werner (1988) of a LIA divided into two main cold stages: from 500 to 300 B.P., and the 19th century, when the main glacier advances occurred, interrupted by a relatively warm 18th century.

CHAPTER 2

THE GLACIOLOGY OF SVALBARD

2.1- Introduction

This chapter is divided into four sections which aim: (1) to introduce some aspects of the glaciology of Svalbard which are relevant to ice-core studies (e.g. ice thickness and accumulation rate) and which may provide guidelines for the selection of a site for future drilling; (2) to review glacio-environmental studies (e.g. ice-core and mass-balance studies) carried out in the Archipelago previous to this dissertation; (3) to summarize the fieldwork carried out by a team from SPRI in 1985 and 1986. In both these years glaciers and ice fields in central-eastern Spitsbergen were comprehensively surveyed by radio echo-sounding and also by pit and shallow ice-core studies (see Section 2.4). This summary does not include an account of the ice-drilling operations in 1986 which are detailed in Appendix 3 – Ice-core drilling operations on Skobreen; (4) to discuss in detail the glaciology of Skobreen, where the 23.1 m core, which provides the data for several of the discussions in this dissertation, was recovered. These discussions are based on data derived from RES and seismic measurements of the ice thickness, surface pits, a 9 m ice core, and theoretical considerations. This glaciological examination aims to check the suitability of the glacier as a site for ice-core studies, and also the sensitivity of the glacier to environmental changes (e.g. changes in the mean atmospheric temperature and net accumulation rate).

2.2- General glaciology of Svalbard

2.2.1- Ice thickness and internal reflecting horizons

The bulk of ice-thickness measurements in Svalbard were obtained by radio echo-sounding surveys carried out by the Scott Polar Research Institute (sometimes in association with the Norsk Polarinstitutt) and the Institute of Geography of the USSR Academy of Sciences – IG (USSR). Some expeditions carried out gravimetry (e.g. Hollin, 1956; Husebye, Sørnes and Wilhelmsen, 1965) and seismic (e.g. Ekman, 1971) surveys in the Svalbard ice masses and the results when compared with the RES results are within the expected range of error for the different techniques (Dowdeswell, 1984; Dowdeswell et al., 1984a). The RES by the IG (USSR) in the initial stages used an aircraft altimeter at 440 MHz (Macheret, 1976) and after 1978 a purpose-built sounder with a carrier frequency of

CHAPTER 2

THE GLACIOLOGY OF SVALBARD

2.1- Introduction

This chapter is divided into four sections which aim: (1) to introduce some aspects of the glaciology of Svalbard which are relevant to ice-core studies (e.g. ice thickness and accumulation rate) and which may provide guidelines for the selection of a site for future drilling; (2) to review glacio-environmental studies (e.g. ice-core and mass-balance studies) carried out in the Archipelago previous to this dissertation; (3) to summarize the fieldwork carried out by a team from SPRI in 1985 and 1986. In both these years glaciers and ice fields in central-eastern Spitsbergen were comprehensively surveyed by radio echo-sounding and also by pit and shallow ice-core studies (see Section 2.4). This summary does not include an account of the ice-drilling operations in 1986 which are detailed in Appendix 3 – Ice-core drilling operations on Skobreen; (4) to discuss in detail the glaciology of Skobreen, where the 23.1 m core, which provides the data for several of the discussions in this dissertation, was recovered. These discussions are based on data derived from RES and seismic measurements of the ice thickness, surface pits, a 9 m ice core, and theoretical considerations. This glaciological examination aims to check the suitability of the glacier as a site for ice-core studies, and also the sensitivity of the glacier to environmental changes (e.g. changes in the mean atmospheric temperature and net accumulation rate).

2.2- General glaciology of Svalbard

2.2.1- Ice thickness and internal reflecting horizons

The bulk of ice-thickness measurements in Svalbard were obtained by radio echo-sounding surveys carried out by the Scott Polar Research Institute (sometimes in association with the Norsk Polarinstitutt) and the Institute of Geography of the USSR Academy of Sciences – IG (USSR). Some expeditions carried out gravimetry (e.g. Hollin, 1956; Husebye, Sørnes and Wilhelmsen, 1965) and seismic (e.g. Ekman, 1971) surveys in the Svalbard ice masses and the results when compared with the RES results are within the expected range of error for the different techniques (Dowdeswell, 1984; Dowdeswell et al., 1984a). The RES by the IG (USSR) in the initial stages used an aircraft altimeter at 440 MHz (Macheret, 1976) and after 1978 a purpose-built sounder with a carrier frequency of

620 MHz (Macheret, 1981; Macheret and Zhuravlev, 1982; Kotlyakov, Macheret and Gromyko, 1982; Macheret, Zhuravlev and Bobrova, 1985). The great majority of the Soviet data were acquired in 1978/79 and other surveys included a detailed 50 km ground-base survey in the area of Austre Grönfjord-Fridtjovbreen and logging by RES of the Grönfjord-Fridtjovbreen borehole (Macheret et al., 1984). However, the bulk of the ice-thickness data was obtained by SPRI during four field seasons (1980, 1983, 1985, and 1986), using the SPRI MkIV 60 MHz unit, which is a development of the system described by Evans and Smith (1969). Since 1983 the system has included a digital recording system which allows quantitative estimates of echo power to be made and thus of bedrock reflection coefficients (Bamber, 1987a). These four surveys have covered a great part of the Spitsbergen and Nordaustlandet ice masses, and the most recent survey (1986) has also included the islands of Barentsøya and Edgeøya. Different kinds of platforms have been used, including a helicopter (Bell 206 Jetranger, 1980), a fixed-wing aircraft (de Havilland Twin Otter, 1983 and 1986), and a caboose pulled by a snow-mobile (1985). The operations, equipment, data reduction, and the results of the first two surveys are discussed comprehensively in the dissertation by Dowdeswell (1984) and other works (Dowdeswell et al., 1984a and b; Drewry and Liestøl, 1985). More recently, Bamber (1987a) examined the 1983 and 1985 data for Spitsbergen, and carried out a more detailed examination of the physical properties of the Svalbard ice which are important for RES. The work included modelling the dielectric properties of the ice and investigation of the causes of internal reflecting horizons (which were observed on 60% of the glaciers sounded in 1983; Bamber, 1987a). In 1985 a comprehensive overland RES survey was carried out on Paulabreen (a 15 km long glacier in central-eastern Spitsbergen) and two of its tributaries (Bakaninbreen and Skobreen), in association with seismic and topographical surveys. In 1986 the RES surveys in central-eastern Spitsbergen were extended to other glaciers. The operations and some of the results of the 1985 and 1986 surveys are summarized in Section 2.4 of this dissertation and described in detail in unpublished reports by Drewry (1985 and 1987b). The data of these two surveys are used in Section 2.5 to examine the dynamic conditions of Skobreen, the site of the 23.1 ice core recovered in 1986.

The above surveys detected a maximum ice thickness of 656 m in Spitsbergen (in Veteranen, a valley glacier in east Ny-Friesland, #2 in Fig. 1.2; Bamber, 1987a) and of 583 m in Nordaustlandet near the summit of Austfonna (Dowdeswell, 1984). Variety in ice thickness and sub-glacial morphology has been established, ranging from thin (tens of metres) with a steep and rough subglacial topography, to Austfonna which reveals ice thickness in the range of 300 m and a relatively flat superficial and sub-glacial topography in its eastern part. Austfonna appeared to be the ideal site in Svalbard for ice-core studies, as the relative flatness of the ice surface and bedrock would not require any complex model of the ice flow; furthermore, it is associated with an accumulation rate that guarantees about 4000 years of record (cf. Chapters 4 and 5). Unfortunately, as discussed in Chapters 2 and 4,

summer conditions at its summit (791 m a.s.l.; Dowdeswell, 1984) are relatively warm and substantial superficial melting occurs, thus altering the original record of the precipitation. Conditions for ice coring on Veteranen would be even less favourable, as the maximum ice thickness is to be found in the ablation area of the glacier at about 700 m a.s.l. On the other hand, the relatively low accumulation in the region (about 300 kg m^{-2} a^{-1}; cf. Fig. 2.4A) would give about 9000 years of record, and the bottom 10 m may represent accumulation from the end of the Last Glacial.

Two findings of the RES surveys in Svalbard can be used as a means of selecting an adequate site for ice-core studies with the objective of deriving environmental time series. From the first surveys it became clear that unambiguous bed echoes were rarely obtained for all the tracks sounded (the proportion of echoes varies from none to almost 100% of the track). Some of the most frequent areas without bottom returns are the accumulation areas and the areas near ice divides on thick glaciers (Macheret, 1981; Dowdeswell, 1984; Dowdeswell et al., 1984b). Dowdeswell et al. (1984b) attribute this phenomenon to the masking of bottom-echo returns by a large number of scatterers associated with melting and refreezing, and with water inclusions and other discrete inhomogeneities in relatively warm ice in the accumulation area (cf. Section 2.5.4). This is not unexpected, as most of the glaciers of Svalbard are of sub-polar thermal regime (Section 2.3.3) and so have ice near or at the pressure melting point in the accumulation area. Thus the proportion of returns in the accumulation area can give an indication of the bulk temperature of the ice (if other factors such as the total ice thickness remain the same). Examination of the glacier ice-thickness profiles plotted by Dowdeswell (1984) and Bamber (1987a) indicates that Svalbard glaciers and ice caps rarely show bed returns in the accumulation area, even at high altitudes (i.e. above 1000 m a.s.l.). Lomonosovfonna, one of the sites for ice-core studies, at 1120 m a.s.l. (cf. Section 2.3.1), was sounded unsuccessfully by both Soviet and British scientists. No return at all was recorded, whereas one would have been expected from the superficial conditions at the site (where a soaked firn layer up to 2 m thick has been observed; Kotlyakov et al., 1980) and from the stratigraphy of the Lomonosovfonna core, which shows numerous ice layers (Gordiyenko et al., 1981).

The other important observation is the presence of single continuous horizons (i.e. internal reflecting horizons – IRHs), ranging in depth from 70 to 200 m below the surface in Spitsbergen glaciers (Macheret and Zhuravlev, 1982; Dowdeswell, 1984; Bamber, 1987a and b). These IRHs can extend up to 20 km, showing a close relationship to the surface morphology, and they were detected in 60% of the glaciers sounded in 1983 (Bamber, 1987a). Furthermore, the IRHs show a greater concentration on the western side of Spitsbergen, as can be seen in Fig. 2.1B. Bamber (1987a and b) attributes these internal reflecting horizons to the presence of water-saturated zones, based on the examination of reflection coefficients from the 1983 SPRI surveys, Soviet borehole data and a radio-echo

logging experiment (Macheret et al., 1984). Therefore the glaciers with IRHs would not qualify as sites for ice-core drilling for the derivation of environmental data. On the other hand, it may provide further evidence for the character of the IRHs. Veteranen (in Ny-Friesland) may be an interesting site for drilling, as it appears to show internals caused by the presence of water and moraine material (Bamber, 1987a).

2.2.2- Surging activity and changes in the frontal position of glaciers

One of the main drawbacks of ice-core drilling in Svalbard from the point of view of a paleoclimatologist is that many of the glaciers surge from time to time. A surge is defined as a sudden and rapid advance of the glacier, associated with an increase in the ice velocity by a factor of 10 to 100 and lasting from a few months to several years, frequently occurring at regular intervals and separated by a longer quiescent period (Paterson, 1981). The phenomenon is accompanied by, for example, propagation of waves with increased thickness and velocity, intense crevassing of the surface, rapid vertical uplift and lowering of parts of the glaciers, contortion of moraines and, in the latter stages, rapid advance of the glacier front occurs. Interpretation of an ice core from a site subject to such rapid changes is therefore complex and it may be impossible to reconstruct the trajectory of an individual ice segment. Modelling of the ice flow becomes complex, because the abrupt changes in velocity certainly involve changes in the mechanical regime (i.e. from creep to basal sliding). Paleoclimatological studies based on moraine positions also become complex, as the moraines may represent a past surge rather than relate to an advance which is due to changes in environmental conditions such as mass balance. The retreat of some of the glaciers during this century may be a return to the normal front position rather than a retreat due to a general warming of the region. Many theories have been proposed to explain the surge phenomenon, and the mechanisms considered include, for example, thermal instabilities (Robin, 1955, Clarke, 1976), mechanical damming of water (Robin and Weertman, 1973), and deformation of an unlithified bed (Jones, 1979; Clarke, Collins and Thompson, 1984). Dowdeswell (1984) reviewed the mechanism applicable to Svalbard. Liestøl (in press, a; and Fig. 2.1A) reports that at least 57 glaciers have been observed to surge in Svalbard, including small valley glaciers (Liestøl, 1969, 1976), large tidewater glaciers (Liestøl, 1969), outlet glaciers of small ice caps (Dowdeswell, 1984), and major drainage basins of large ice caps (Schytt, 1969). The latter category includes the largest surge ever recorded, in which the ice front of the Bråsvellbreen basin of Austfonna moved about 20 km between 1936 and 1938 (Schytt, 1969). The most recently observed surge occurred on Bakaninbreen (#1 in Fig. 2.1A), a small valley glacier in central-eastern Spitsbergen, in the area of fieldwork covered by this dissertation (Drewry, 1987b; and Section 2.4.3). This glacier is still in an active phase four years after the first signs of surging were reported by Drewry (1985). Many other glaciers may have surged in Svalbard, as there is frequent evidence of (for example) looped moraines.

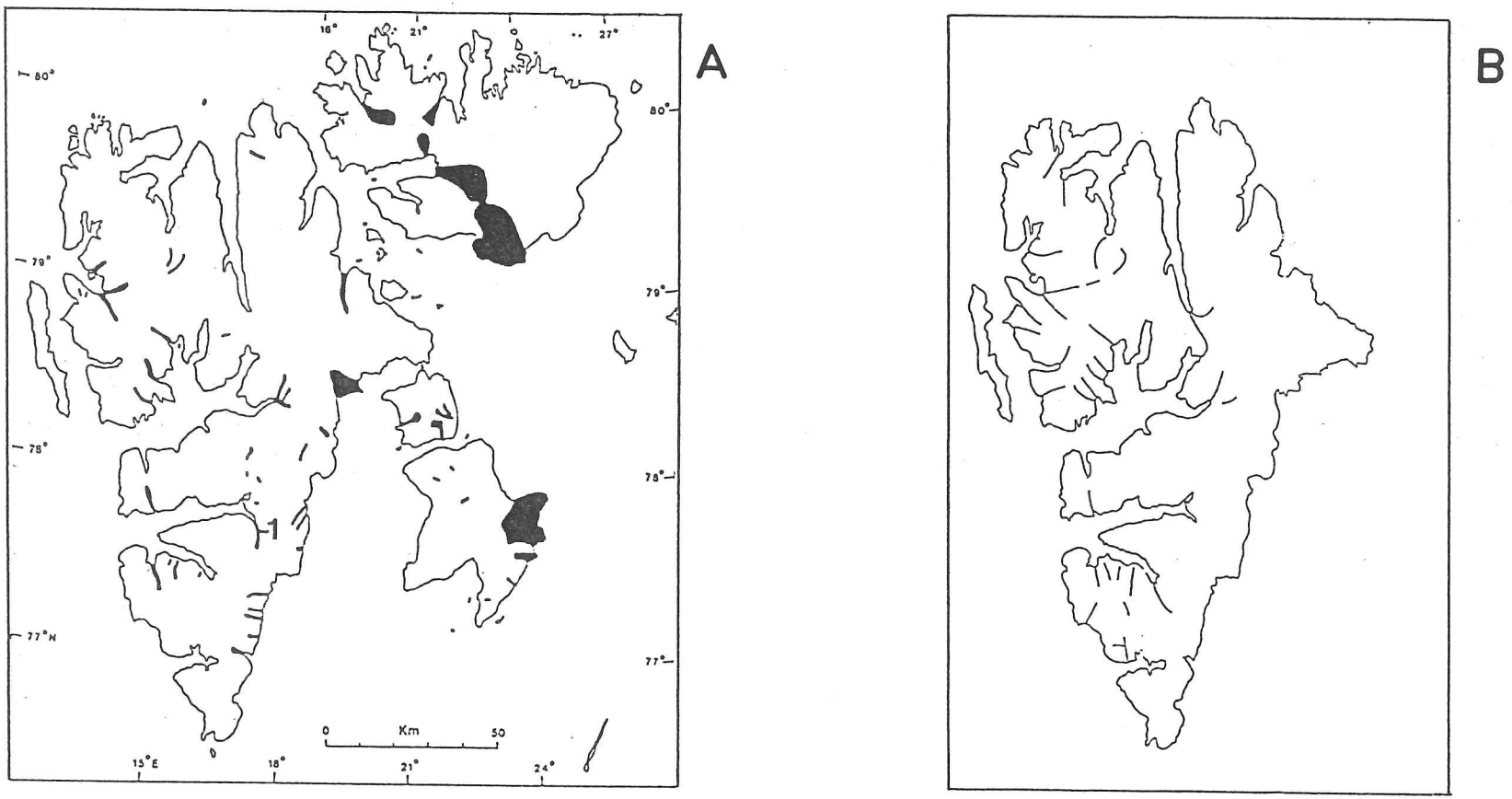

Figure 2.1- A) The location of glaciers in Svalbard which have been observed to surge. Source: Liestøl, in press; updated with the position of Bakaninbreen (1); B) Glaciers in Spitsbergen possessing internal reflecting horizons. Source: Bamber, 1987.

The general picture that emerges from reports on changes in frontal positions is one of general retreat during this century, despite the problems of interpretation caused by surging activity. Troitsky et al. (1975) reported that about 77% of the 490 observations of changes in frontal position (in 232 glaciers) during the period 1838–1967 refer to glacier retreats. Liestøl (in press, b) also reports a general retreat of the glaciers, based on a comparison of terrestrial photographs from the beginning of the century with more recent terrestrial and aerial photographs. More relevantly, he reports that some smaller cirque glaciers have lost more than half their volume this century, which naturally implies a strongly negative mass balance for the period. Dowdeswell (1986) examined the fluctuation of the outlet glaciers in Nordaustlandet from 1969 to 1981 based on Landsat multispectral scanner images, and 15 of the 22 glaciers examined retreated during this period. Bearing in mind that some of these retreats may have been caused by stagnation and thinning in the quiescent period between surges or by short-term iceberg calving (Dowdeswell, 1986), these changes may be reflecting the 20th-century warming. The direct cause of glacier retreats in Svalbard is most probably an increase in the proportion of the summer temperature degree days above 0°C rather than an increase in the mean temperature (cf. Section 2.3.2 and Appendix 3). Liestøl (in press, b) is of the opinion that the retreat is being caused by a reduction in precipitation rather than by an increase in ablation. However, this conclusion is not compatible with knowledge of the atmospheric circulation in the area. An increase in temperature in the Svalbard region would be coupled with a retreat of the Arctic Front (cf. Chapter 1), so it would become easier for moisture-laden cyclones to reach Svalbard. An increase in accumulation, rather than a decrease, is to be expected in warmer periods, as demonstrated in Fig. A1.8, which shows a increase in precipitation towards the warm 1970s.

2.2.3- Accumulation and equilibrium line

The spatial distribution of accumulation in Svalbard was obtained mainly from two surveys: (1) Schytt (1964) measured the total accumulation in Nordaustlandet by means of snow-stratigraphy studies (Fig. 2.3A); (2) more recently, Semb, Brækkan and Joranger (1984) measured the total accumulation through cores that sampled the snow since the formation of the last autumn ice layers (Fig. 2.4A). The values of the first survey are considered unrealistic; the result of ice-core studies on Austfonna indicate net annual accumulation rates of about 500 kg m^{-2} a^{-1} (cf. Chapters 2 and 5) at its summit (instead of 1000 kg m^{-2} a^{-1} as reported by Schytt, 1964). On the other hand, the trend to greater values at the summits of the two largest ice caps on Nordaustlandet has been confirmed by the measurements obtained by Semb, Brækkan and Joranger (1984). According to this survey, accumulation rates at the top of Austfonna and Vestfonna should fluctuate between 300 and 400 kg m^{-2}. As mentioned in Section 1.3.4, the spatial pattern of accumulation in Spitsbergen is strongly orographically controlled. Maximum accumulation rates are reached in the mountains on both coasts of Spitsbergen and can be as much as 700–800 kg m^{-2}. In

central parts of Spitsbergen and in a corridor in Isfjorden (the 'arid' areas of the Archipelago) accumulation is as little as 150 kg m^{-2}.

A map of equilibrium-line altitude, based on Landsat imagery, aerial photographs, and some ground data sets, has been produced by Liestøl and Roland (in Steffensen, 1982). It has frequently been interpreted, erroneously in the opinion of the author of this dissertation (cf. Section 1.3.4), as equivalent to the precipitation distribution (e.g. Steffensen, 1982). As a matter of fact the map, shown in Fig 2.3B, would be more representative of the snow-line altitude than the equilibrium-line altitude. In sub-polar glaciers the two lines do not coincide and there is considerable formation of superimposed ice between the two lines. Furthermore, superimposed ice is difficult to distinguish from glacial ice in Landsat imagery and even in air photographs. The altitude of this 'snow line' tends to increase towards the centre of Spitsbergen, where it can be as high as 800 m a.s.l. It may be reflecting the sum factors, such as a greater summer temperature (due to a greater continentality) and lower accumulation.

2.3- Introduction to glacio-environmental studies in Svalbard

2.3.1- Ice-core and pit studies

This section is an introduction to the pit, borehole, and ice-core studies carried out in Svalbard before this dissertation. The cores are discussed only briefly here; more detailed discussions are to be found at the appropriate sections as indicated. Fig. 2.2 shows the location of these studies.

The first pit observations carried out in Svalbard had as their main objective the acquisition of information on the state of the mass balance of the Nordaustlandet ice caps. Ahlmann (1933a) carried out the first systematic snow and ice stratigraphy studies on these ice caps during the Swedish – Norwegian Arctic Expedition (1931) and obtained a mean net accumulation rate (a_n) between 60 and 70 kg m^{-2} a^{-1} from 19 pits. This work was followed by the observations of the Oxford expedition of 1935–36, when a total net accumulation rate of 370 kg m^{-2} a^{-1} and an a_n of 75 kg m^{-2} a^{-1} were estimated for a site on the top of Vestfonna (Moss, 1938; Glen, 1941). Different results were obtained by Schytt during the Swedish International Geophysical Year (IGY) Expedition. The net accumulation between 1956 (when he placed a layer of dye in a shallow pit) and 1958 was 590 kg m^{-2} a^{-1}. The different net accumulation rates obtained by these expeditions bear witness to the complexity of the snow stratigraphy of glaciers and ice caps subject to intermittent melting in the superficial layers. Variations in the degree of summer melting, followed by percolation and refreezing, make it difficult, if not impossible, to identify the annual layers by visual examination alone with confidence. This point is discussed elsewhere in the dissertation, and

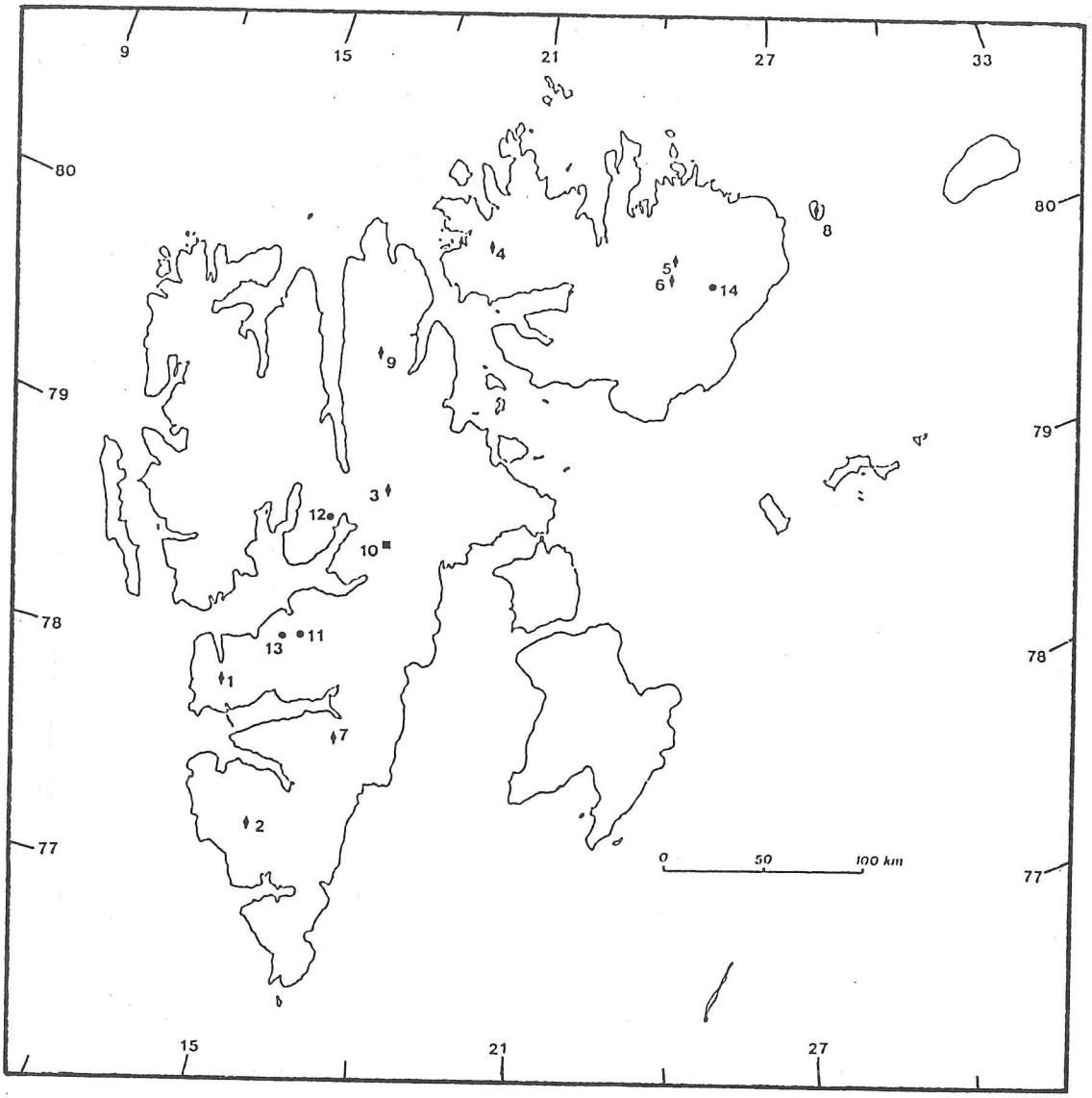

Figure 2.2- Location of main pit, borehole and ice-core studies in Svalbard. Ice cores include: **Amundsenisen** (2), **Åsgårdfonna** (9), **Austfonna** 1981 (5) and 1986 (6), **Grönfjordbreen-Fridtjovbreen** (1), **Lomonosovfonna** (3), **Skobreen** (7), **Storøya** (8), **Vestfonna** (4). Boreholes: **Austfonna** (14), **Bertilbreen** (12), **Bogerbreen** (13), and **Foxfonna** (11). Only the detailed **Malte Brunfjellet** pit study (10) by Mulvaney (1987) is included in this map.

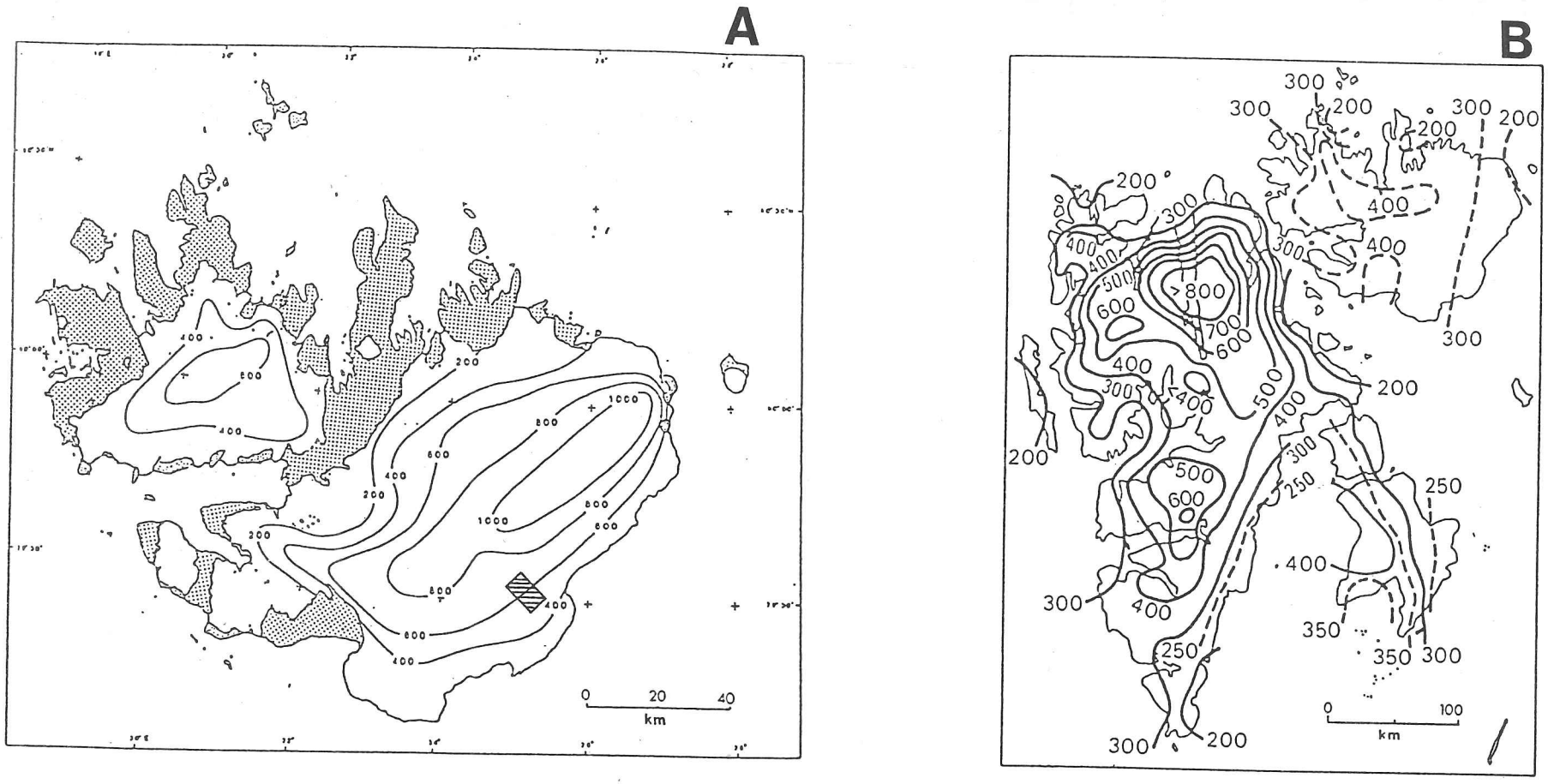

Figure 2.3- A) The total accumulation distribution on Nordaustlandet in 1957-58 (by Schytt, 1964) the shaded rectangle marks the area with net mass-balance measurements by a SPRI team in 1983 (Dowdeswell, 1984). B) Glacier equilibrium-line altitudes derived from aerial photographs, Landsat imagery and direct observations (by Liestøl and Roland in Steffensen, 1982).

Accumulation rates are given in kg m^{-2} a^{-1} and the equilibrium-line altitudes in metres.

with particular reference to Austfonna in Section 5.5.3. During the IGY expedition Schytt also carried out a transverse of the Nordaustlandet ice caps, when the total accumulation before the melt season was measured in several pits. The results are presented in Fig. 2.3A and there is a clear trend to high values towards Austfonna. This trend indicates that the air masses bringing moisture come mainly from the east during the winter. The spatial distribution of accumulation and the net accumulation rate in Austfonna determined by Schytt were confirmed by the Soviet expedition of 1984/85 (Arkhipov et al., 1987). Dowdeswell (1984) measured a total accumulation of between 740 and 950 kg m^{-2} a^{-1} from the end of the melting season to early May 1983 in the shaded area in Fig. 2.3A, extending eastwards the area of high accumulation in Austfonna.

More detailed pit studies began when Gorham (1958) examined several pits and exposed crevasse walls in Nordaustlandet for ionic analysis. Gjessing (1977) reported similar measurements for snow pits in Austfonna, mainly with a view to obtaining information on the main anthropogenic pollutants such as sulphates and nitrates. More recently Semb, Brækkan and Joranger (1984) carried out a detailed examination of the spatial distribution in Svalbard of major ionic species (i.e. Ca^{+2}, Cl^{-}, H^{+}, K^{+}, Mg^{+2}, Na^{+}, NH_4^{+}, NO_3^{-}, and SO_4^{2-}), as well of the total precipitation between the summer of 1982 and April 1983, by examining snow cores. A strong orographic control of accumulation in the Archipelago, with maximum accumulation on the west coast and a relatively dry area in the centre of Spitsbergen, was one of the main findings. There is also a strong seasonality in some of the ions. Some of the ions examined show a trend to greater values towards the east. This trend was attributed to the transportation of anthropogenic pollution from Eurasia in the winter (cf. Chapter 5). Fig. 2.4 shows the spatial distribution of some of the measurements carried out by Semb, Brækkan and Joranger (1984). Finally, Mulvaney (1987) dug a 5 m pit in Malte Brunfjellet, Sabine Land, Spitsbergen, to examine the variation in chlorides, nitrates, and sulphates. There is a more detailed discussion of the results of these studies in Chapter 5, which deals with the record of anthropogenic pollution in the Archipelago. Table 2.1 summarizes the ionic concentration measurements† made in superficial snow at several sites in Svalbard.

Ice-drilling activities in Svalbard began in 1966 when Soviet scientists drilled some shallow boreholes (Kotlyakov, 1985). Since then a successful programme of ice-core studies has been undertaken in Svalbard by the Institute of Geography, USSR Academy of Sciences – IG (USSR) – based mainly on the use of an electro-thermal drill. The main objective of these studies was to derive a history of environmental changes for the last 600–800 years by the examination of variations in the stable-isotope content and chemical species (Punning, Vaykmyae and Tóugu, 1987), thereby establishing the development of the Little Ice Age in

† Unless otherwise stated, all concentrations cited in this dissertation have been converted to μEq l^{-1} to facilitate comparisons.

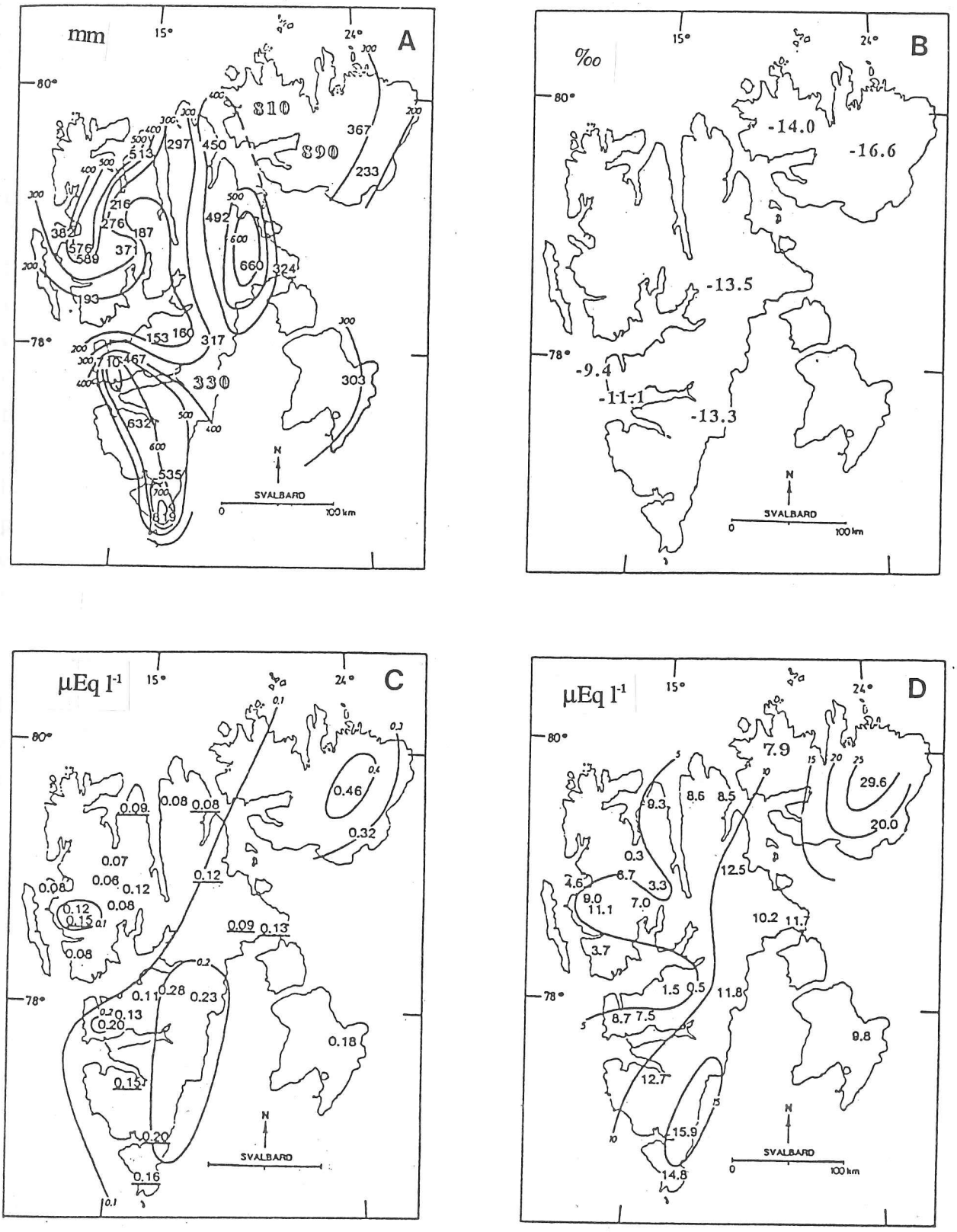

Figure 2.4- Spatial distribution of snow cores in water equivalent in mm (A), $\delta^{18}O$ (B), acidity (D) and excess sulphate (C). A, C, and D are by Semb, Brækkan and Joranger (1984); B and the outlined values in A (which are data based on ice-core data; see text for details) are by the author of this dissertation. The stable-isotope values refer to the decade of 1960, for which there is data for all ice cores from Svalbard.

The following units are used in plots A-D: mm of water equivalent (A); ‰ (B), µEq l^{-1} (C and D).

the Archipelago. The studies also included the examination of the structure and hydrothermal regime of the Svalbard glaciers and ice caps, and the recent changes in their chemistry (to obtain an idea of the extent of anthropogenic pollution in the area). Other studies included density variation, light transmissivity, type of ice formation, and concentration of dust and radioactive isotopes (Kotlyakov, 1985). The main studies and other details for each Svalbard core are summarized in Table 2.2. In general the interpretation of the ice-core record in the Archipelago is complicated by a complex fractionation process of the air masses reaching Svalbard (cf. Chapter 4), and by the high summer temperatures, which caused significant melting. The quality of the cores is far from ideal and no detailed studies like the ones on the Greenland ice cores (e.g. Langway, Oeschger and Dansgaard, 1985) have been possible. The difficulty of interpreting these cores is the result of the percolation and frequent flush-out of the lighter stable-isotope and radioactive products used to estimate net mass balance (e.g. ^{90}Sr, ^{137}Cs, and ^{3}H; cf. Section 3.2.5). Nonetheless, some of the cores recovered may be considered a closed system (i.e. the melting is not sufficiently intense to saturate the snow pack, and the meltwater refreezes *in situ*) over longer time-scales (e.g. 10 years). On the other hand, there is still no core from this Archipelago which allows high-frequency fluctuations (e.g. occurring every 5 years or less) to be examined.

The first ice core was recovered from the ice divide of Grönfjordbreen and Fridtjovbreen (450 m a.s.l.) in 1975 (Vaykmyae et al., 1977; Punning et al., 1980). The 213 m core was analysed mainly for $\delta^{18}O$ and ion content, and a detailed stratigraphic examination was carried out. From this examination of the Grönfjord-Fridtjovbreen core it was clear that the intense melting, percolation, and precipitation in the form of rain in the summer had altered the stable-isotope seasonal variations beyond recognition, ice formation occurring mainly as a result of percolation and refreezing of meltwater and frequently forming ice layers without bubbles (Zagorodnov and Zotikov, 1981a). Furthermore, the long-term $\delta^{18}O$ fluctuations do not accord with the record from other Svalbard cores (Fig. 4.10), even after considerable smoothing. It can be seen that the increase in stable isotopes in about A.D. 1300 and at the end of the 16th century, although observed in all the cores, is proportionally greater in Grönfjord-Fridtjovbreen, most probably due to greater melting and flush-out of the lighter isotopes. This core is not, therefore, considered a reliable guide to the relationship between climate and isotope concentration, and it is no surprise that Punning et al. (1980) did not find any relationship between the temperature and stable-isotope ratios. In 1980 a 368 m ice core was recovered from Amundsenisen, in south Spitsbergen. Borehole measurements indicate that Amundsenisen is close to the melting point throughout (Zagorodnov and Zotikov, 1981a). As was to be expected from a temperate ice mass, the stable-isotope record from this core had been totally obliterated (Zagorodnov, personal communication). The stratigraphy consists mainly of an intercalation of bubble and clear ice layers, with micro 'water-filled canals' and cavities ranging from 10 to 200 mm^2 in cross-

section (Zagorodnov and Zotikov, 1981b). The borehole was extended to a depth of 586 m with a hot-point thermal drill.

Table 2.1- Ionic concentrations in Svalbard. All concentrations are in $\mu Eq\ l^{-1}$.

Site	Altitude	Period	Cl^-	SO_4^{2-}	$[SO_4^{2-}]^*$	NO_3^-	References
Amundsenisen	700 m	-1980	14.1				*Punning, Vaykmyae and Tóugu* (1987)
Austfonna	700 m	1580-1985	28.2				*Punning, Vaykmyae and Tóugu* (1987)
		1977		2.6	1.5	0.5	*Gjessing* (1977)
		1983	21.5[d]	11.7	9.5	1.0	*Semb, Brækkan and Joranger* (1984)
Central-eastern Spitsbergen		1983	41.0[b]	9.0[c]	4.8		*Semb, Brækkan and Joranger* (1984)
Central-western Spitsbergen		1983	73.0[b]	11.8[c]	4.2		*Semb, Brækkan and Joranger* (1984)
Grönfjord-Fridtjovbreen	450 m	1150-1975	987.3				*Punning, Vaykmyae and Tóugu* (1987)
Lomonosov-fonna	1120 m	1130-1976	155.2				*Punning, Vaykmyae and Tóugu* (1987)
		1930-1976	104.6	27.1	16.3		*Punning and Vaykmyae* (1985) [a]
Malte Brunfjellet		1985-1987	12.3	3.9	2.5	0.9	*Mulvaney* (1987)
Skobreen	600 m	1929-1984	19.9	7.3	5.3	1.3	This dissertation
Vestfonna	580 m	1100-1981	42.3				*Punning, Vaykmyae and Tóugu* (1987)
		1100-1981		16.7	14.6		*Yevseyev and Korzun* (1985)

Notes:
(a) Data appeared in graphic form only
(b) estimated from the $[SO_4^{2-}]^*$ concentration
(c) estimated from $[SO_4^{2-}]^*$ and Na^+ relationship
(d) estimated from Na^+ concentration, assuming that crustal sources in the winter are negligible

Hitherto Lomonosovfonna has been the core site that has produced the best record in terms of preservation of the original precipitation. The high altitude of the site (1120 m a.s.l.) guarantees restricted summer melting, percolation of meltwater is restricted to about the upper 3–4 m, and the snow density after the ablation season changes only from 410 to 490 kg m^{-3} (Zagorodnov et al., 1984). The first core collected at this site, in 1976, has been thoroughly analysed (Gordiyenko et al., 1981) and in Sections 4.3 and 4.4 its stable-isotope record is compared with the Skobreen core record, climatic time series, and other environmental data from the North Atlantic Arctic. Anomalously high isotope and ion values cast doubt on the environmental interpretation of this core. The upper 40 m, which had been analysed in detail for $\delta^{18}O$ by Gordiyenko et al. (1981), was redated by the author of this dissertation and a statistically significant relationship with temperature was obtained. These

	Ice Cores										Boreholes			
Site name	*Grönfjord-Fridtjovbreen (1)*	*Amundsenisen (2)*	*Lomonosov-fonna (3)*	*Vestfonna (4)*	*Austfonna (5)*	*Austfonna (6)*	*Skobreen (7)*	*Åsgårdfonna (8)*	*Storøya (9)*	*Malte Brunfjellet (10)*	*Foxfonna (11)*	*Bertilbreen (12)*	*Bogerbreen (13)*	*Austfonna (14)*
Elevation (a.s.l.)	450 m	700 m	1120 m	580 m	700 m	750 m	600 m	1200 m	238 m			475 m		
Ice thickness	220 m	586 m	≈ 220 m	208 m	560 m	566.7	135 m	85.6 m				108 m		
Length of the ice core	213 m	368 m (ice core) 586 m (borehole)	201 m (1976) 135 m (1982)	208 m	204 m	566.7 m	23.1 m	85.6 m	6 m	5 m (snow pit)	75 m	367 m		136 m
Deposition yr. deepest layer	≈ 1150		≈ 1130	≈ 1100	≈ 1600		1929							
Mean accum. rate (w.eq.)	57 cm/yr		83 cm/yr	81 cm/yr	89 cm/yr		33 cm/yr		40 cm/yr					
10 m temperature	-0.16°C	0.0°C	-2.6°C	-0.6°C	-0.9°C		-2.8°C			----------				-6.2°C (15 m)
Drilling year	1975	1980	1976 and 1982	1981	1985	1987	1986	1987	1980	1987	1972	1980	1980	1986
Drilling method	Electro-thermal	Electro-thermal (HP)	Electro-thermal	Electro-thermal	Electro-thermal	Electro-thermal	Electro-mechanical	Electro-mechanical						
Drilling agency	IG (USSR)	IG (USSR)	IG (USSR)	IG (USSR)	IG (USSR)	IG (USSR)	SPRI	NIPR	Ymer	PEG	NPI	IG(URSS)	IG(USRR)	LGGE / SPRI
Main studies	St, $\delta^{18}O$, β, CO_2 Ions (13), pH, RES borehole logging	T Ions	$\delta^{18}O$, β, Cl^-	Ions (13), pH, β	St, ρ, $\delta^{18}O$, T, ^3H, β, Cl^-, EC, Fab	EC, Mi, SO_4^{-2}, NO_3^-, Cl^-, pH, EC,	St,ρ, $\delta^{18}O$,δD, ^3H,pH,EC,Mi, Ions (3)	St,ρ, $\delta^{18}O$,δD,T	Mi	St,β,SO_4^{-2}, NO_3^-,Cl^-		T	T	T

Table 2.2- Summary of the main pit and ice core studies on Svalbard. For symbols see the relevant list on page xiv.

Sources: general (Kotlyakov, 1985; Punning, Vaykmyae and Tóugu, 1987); **Amundsenisen** (Zagorodnov, 1981 and 1988); **Åsgårdfonna** (Watanabe and Fujii, 1988); **Austfonna** (Arkhipov et al., 1987; Zagorodnov, in preparation; Zagorodnov and Arkhipov, in preparation); **Austfonna borehole** (M. Vallon, written communication); **Bertilbreen and Bogerbreen** (Zagorodnov, 1981); **Foxfonna** (Liestøl, 1974); **Grönfjordbreen-Fridtjovbreen** (Vaykmyae et al., 1977; Punning et al., 1980; Kotlyakov et al., 1980; Zagorodnov and Zotikov, 1981; Macheret et al., 1984); **Lomonosovfonna** (Gordiyenko et al., 1981; Zagorodnov et al., 1984); **Malte Brunfjellet** (Mulvaney, 1987); **Skobreen** (this dissertation); **Storøya** (Heintzenberg et al., 1988); **Vestfonna** (Zagorodnov and Zinger, 1982; Vaykmyae et al., 1985; Yevseyev and Korzun, 1985; Punning et al., 1986).

Abbreviations: EC - Electroconductivity; **LGGE** - Laboratoire de Glaciologie et Géophysique de l'Environnement, Grenoble, France; **IG (USSR)** - Institute of Geography, USSR Academy of Sciences; **PEG** - Polar Exploration Group, Chesterfield, UK; **NIPR** - National Institute of Polar Research, Tokyo, Japan; **NPI** - Norsk Polarinstitutt; **SPRI** - Scott Polar Research Institute; **St** - stratigraphy; **Ymer** - University of Stockholm, Sweden; β-β-activity.

points are discussed in Chapters 4 and 5. A second core of 135 m was drilled in 1982 (Zagorodnov et al., 1984) and, apart from the analysis of the ice structure, no other study is known to have been published.

In recent years ice-coring activities by the Soviet expeditions have been concentrated on the Nordaustlandet ice caps. A 208 m core was recovered from Vestfonna in 1981 (at 580 m a.s.l.) and two from Austfonna, in 1985 (204 m), and 1987 (566.7 m). The latter core reached bedrock, confirming the ice thickness measured by radio echo-sounding carried out by the SPRI in 1983 (Dowdeswell, 1984). It also confirmed that the ice cap is at the pressure melting point (-0.42°C; Zagorodnov and Arkhipov, in preparation) at the bottom in the centre. A colder environment, because this island is situated farther north and east, was thought to guarantee better preservation of the original record, but even there the results were not so promising. Melting and percolation can be intense in some years. For example, it is normal to find in Austfonna an intercalation of snow and water-saturated firn, with superimposed ice in the upper layers. The water saturation is intense enough to form an aquifer horizon in the boundary between the firn and ice layers at different levels (Zagorodnov, in preparation). The presence of water is a major drawback for drilling activity, because it frequently percolates into the borehole and refreezes, thus closing it. On the other hand, the proportion of firn layers tends to increase below a depth of 45 m, confirming reduced melting before this century. Despite the problems caused by high melting, the stable-isotope record from the Nordaustlandet ice caps and from Lomonosovfonna shows the same long-term fluctuations and trends (cf. Chapter 4). In general, the seasonality of the stable-isotope ratios has not been preserved. However, Punning et al. (1986) reported that seasonal variations in chloride concentrations made it possible to identify annual layers in Vestfonna.

The variations in the chemistry of all the Nordaustlandet cores have been examined but no detailed profile is known to have been published. Yevseyev and Korzun (1985) summarized the ionic concentrations in Vestfonna and concluded that the upper layers are contaminated by pollutants. The chemistry of the Svalbard pits and cores is discussed in Sections 5.4 and 5.5 with a view to interpreting the record of anthropogenic pollution in Svalbard. The net accumulation rate in these cores was estimated for the period after the first thermonuclear explosion (1951) by the examination of β-activity. Estimates for different sites varied from 570 kg m^{-2} a^{-1} (for Grönfjord-Fridtjovbreen) to 890 kg m^{-2} a^{-1} (for Austfonna). However, these values have frequently been revised and various authors have cited different net accumulation rates for the same site (cf. Section 5.5.3). This fact emphasizes once again the difficulty of interpreting the stratigraphy of the Svalbard ice cores.

Most recently the Japanese National Institute of Polar Research (NIPR) drilled an 85.6 m core in the Høghetta ice dome on Åsgårdfonna, northeastern Spitsbergen (Fujii, 1989). The altitude of this site (1200 m a.s.l.) and the geographical position were

thought to be good indicators of a well-preserved record. The first results show an extremely low accumulation rate, and transformation from snow to glacial ice at about 1 m below the surface (Kameda et al., 1989). Finally, a shallow ice core (6 m) was recovered by the Swedish Ymer expedition to Storøya in 1980. Microparticles were analysed for chemical composition and a regular seasonal pattern was encountered, which indicates a mean annual net accumulation rate of about 400 kg m^{-2} a^{-1} at the top of Storøyajøkulen, Storøya (Heintzenberg et al., 1988). This contrasts with the results obtained by Jonsson (1982), which indicate a net mass balance of about 230 kg m^{-2} a^{-1} in this ice cap.

Finally, boreholes have been drilled in Bertilbreen and Bogerbreen (Zagorodnov, 1981) and Foxfonna (Liestøl, 1974), and temperature distribution has been measured in the first two cores.

2.3.2- Mass-balance studies

Mass-balance studies have been carried out in Svalbard since 1966 by the Norsk Polarinstitutt and the Institute of Geography - Academy of Sciences (USSR). Overall, 12 glaciers have had their mass balance measured but not all continuously (Troitsky, 1988). Fig. 2.5A shows the location of these glaciers and it can been seen that the studies have been concentrated in the Isfjorden and Kongsfjorden areas. The most detailed and extensive studies were done on Austre Brøggerbreen (# 1 in Fig. 2.5A) and Midre Lovénbreen (2) on Brøggerhalvøya (78°N, 12°E), where measurements exist from 1967 onwards. Other glaciers for which there are mass-balance measurements include: Bertilbreen (5), Bogerbreen (9), Daudbreen (7), Finsterwalderbreen (12), 14th July (3), Grönfjordbreen (11), Longyearbreen (8), Nordenskiöldbreen (6), Sveabreen (4), and Vöringbreen (10) (Liestøl, 1974, 1976, 1982, 1983, 1984, 1986; Gokhman, Troitsky and Tyuflin, 1988).

The net mass balance of all the glaciers has been negative in most years, except 1982, when a cool summer resulted in low ablation (cf. Fig. 2.5B). In some years summer melting was enough to form superimposed ice in the upper reaches of several glaciers. In the balance year of 1983/84 the mass balance was negative (between -25 and -50 kg m^{-2}) even at the top of Vöringbreen, Bogerbreen, and Bertilbreen (i.e. 500 m a.s.l.; Guskov and Troitsky, 1987). For the period 1967–86 Brøggerbreen and Lovénbreen had a net deficit of 858 and 714 kg m^{-2} respectively. More recently (1986) an 136 m borehole was drilled in Austfonna (Table 2.2 and Section 2.3.3).

Fig. 2.5B plots the mass-balance data for three of these glaciers, which are thought to be representative of mass-balance conditions encountered in Spitsbergen. Lovénbreen is representative of the mass balance of glaciers situated on the west coast, and Bogerbreen and Bertilbreen reflect the mass balance of glaciers subject to increased continentality. It is apparent that summer ablation controls the annual variations in net mass balance; winter accumulation has been relatively constant at all the sites over the years. On the other hand,

there is a spatial trend to more negative values of net mass balance towards the interior, due to less winter accumulation (from a mean annual value of 76.0 ± 3.8 kg m^{-2} on Lovénbreen to 41.1 ± 2.0 kg m^{-2} on Bertilbreen). This distribution of accumulation is in agreement with the known spatial distribution of accumulation in Spitsbergen (cf. Fig. 2.4A).

The graphs in Fig. 2.5B demonstrate that the annual variations in net mass balance in Spitsbergen are determined mainly by variations in the summer balance (b_s). If the environmental processes that determine the ablation rate can determined, it will be possible to reconstruct the historical record of net mass balance throughout the instrumental period. This record would be important, for example, for checking the trends in net accumulation rates determined from an ice core and also for examining the relationship between glaciers and climate (e.g. chapter 14 in Paterson, 1981). This is a complex study which requires, among other things, a detailed examination of the heat-budget terms and their relationship to variations in climatic elements, as the distribution of the mass balance of a glacier results from interaction between atmospheric (e.g. radiation, precipitation) and glacier (e.g. albedo) conditions (Hanson, 1987), and is beyond the scope of this dissertation. On the other hand, several authors have correlated the summer mass balance with standard measurements taken at weather stations and with indexes derived from these measurements (e.g. Orheim, 1972; Bradley and England, 1978). A similar methodology has been adopted in this dissertation: the summer ablation of all the glaciers was correlated with parameters thought to represent the character of the ablation season, such as the number of melting degree days, the length of the melt season, and the mean summer temperature (cf. the discussion on the variations in these parameters in Section 1.4 and Appendix 1). Unfortunately no linear relationship exists between any of the indexes of summer 'warmth' and the summer mass balance of the glaciers mentioned above, in contrast to glaciers situated in other parts of the Arctic (e.g. the Canadian High Arctic - north of 74°N; Bradley and England, 1978). However, a multiple correlation between the b_s and the number of melting degree days (NMDD), combined with the mean daily maximum temperature in July (July T_{max}), gives a coefficient of $r = 0.89$ for Lovénbreen. This coefficient explains about 79% of the variance. The record from this glacier was used because it is one of the longest in Svalbard. The number of melting degrees gives an index of the number of days where the temperature was greater than 0°C (cf. Section 1.4), therefore of the days with melting, and the July T_{max} gives an index of the month when the greater part of ablation occurs. Fig. 2.6 shows the measured and estimated summer mass balance for Lovénbreen, based on the resulting relationship: $b_s = -0.20$ NMDD - 15.44 July T_{max} + 128.55, with $\alpha < 0.001$. The record could not be extended back farther than 1952, as this is the first year for which there are published data on the maximum daily temperature for any station in Svalbard. Furthermore, this regression could certainly be improved by using data from the nearby Ny-Ålesund weather station, rather than the values estimated from central Spitsbergen. Unfortunately, it has not been possible to obtain data for these stations for the years since 1980. If the winter mass balance since 1952 has been similar

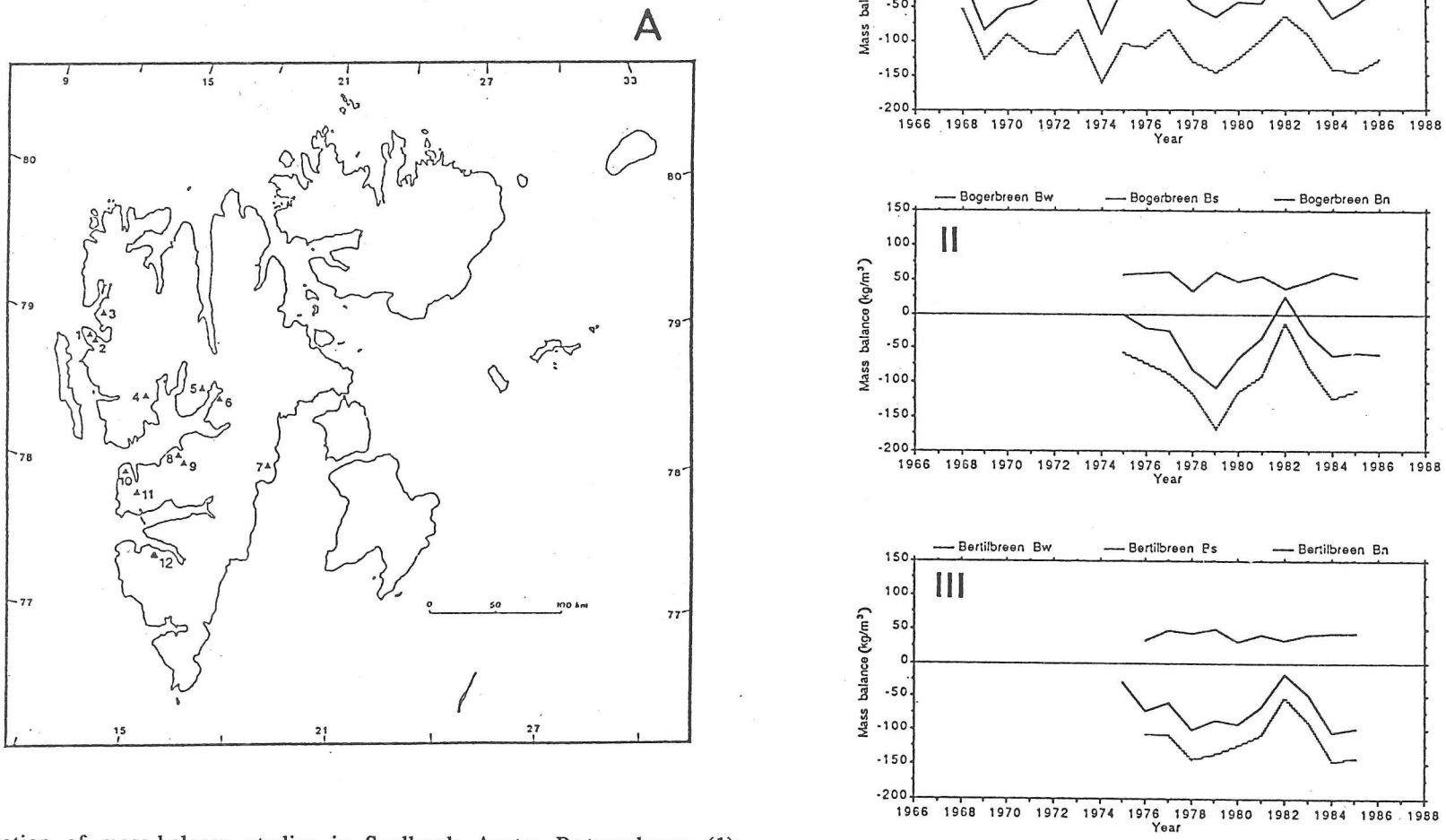

Figure 2.5- A) Location of mass-balance studies in Svalbard: Austre Brøggerbreen (1); Bertilbreen (5); Bogerbreen (9); Daudbreen (7); Finsterwalderbreen (12); 14th July (3); Grönfjordbreen (11); Longyearbreen (8); Midre Lovénbreen (2); Nordenskiöldbreen (6); Sveabreen (4); Vøringbreen (10). B) Mass-balance time series for glaciers representative of different regions of Svalbard (see text for details): (I) Lovénbreen; (II) Bogerbreen; (III) Bertilbreen.

to that in the 1970s and 1980s (i.e. about 76.0 ± 3.8 kg m^{-2}), the graph in Fig. 2.5 represents a cumulative loss of 853 kg m^{-2} between 1952 and 1985. On the other hand, this is not realistic, as the level of precipitation before 1963 was significantly greater (about 50%) than the present level (cf. Section 1.4). In any case, the great majority of years would still show a negative net mass balance over that period. This has probably also been true for all the years since the cool 1910s.

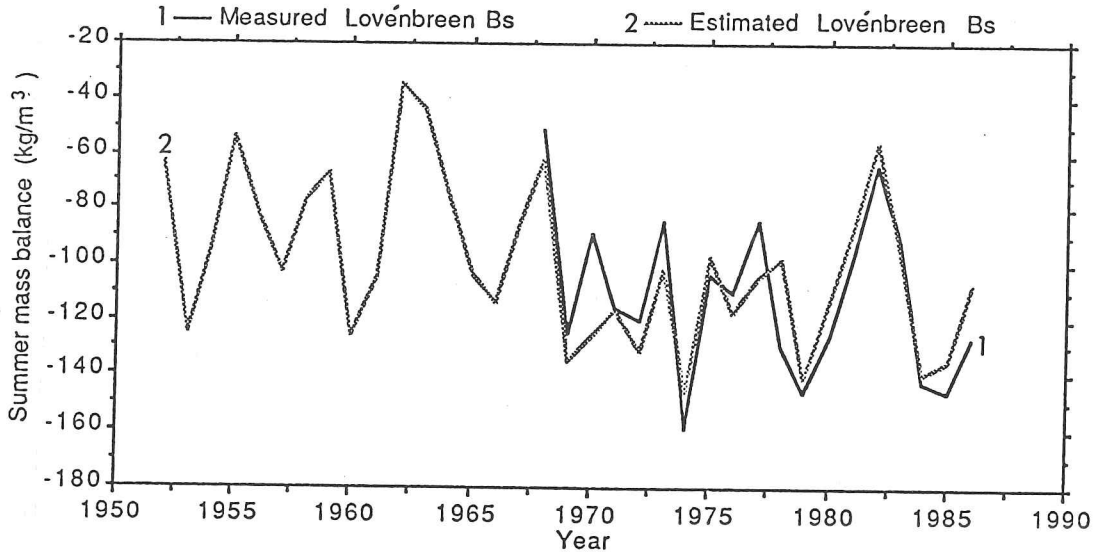

Figure 2.6- Measured (continuous line) and estimated (shaded line) summer mass balance for Lovénbreen. The measured data represent the period from 1968 to 1987 and they are derived from the mass-balance surveys by the Norsk Polarinstitutt. The estimated values and extension of the record back to 1952 is based on a multiple linear regression between the summer mass balance and the number of total melting degree days combined with the mean daily maximum temperature in July (see text for details).

2.3.3- Temperature profiles and the thermal regime of Svalbard ice masses

In this dissertation the geophysical classification by Lagally (1932) and Ahlmann (1933a) is used to describe the bulk (gross) thermal conditions of the whole of the glacier or ice cap. This classification divides glaciers into three categories: – temperate, sub-polar, and polar, according to the ice temperature below the superficial layer affected by the seasonal changes in atmospheric temperature (i.e. the upper 10–15 m). Temperate glaciers are at the pressure melting point† throughout and polar glaciers are below that temperature. The great majority of the glaciers and ice caps of Svalbard have a complex thermal structure. Part of the ice may be at the pressure melting point and part below it. Frequently the accumulation-area ice is at or near the pressure melting point and the ablation-area ice is colder (e.g. Sverdrup,

† The term 'pressure melting point' is used in this dissertation on the understanding that it takes into account both the pressure and the chemical composition of the ice (Harrison, 1972), reflecting its conventional use in glaciological literature.

1935; Schytt, 1964; Baranowski, 1975). Ahlmann (1933a) used the term 'sub-polar' for these ice masses. For example, it is common to find in Svalbard glaciers and ice caps with the accumulation area at the pressure melting point and the ablation area frozen to bedrock. Only some of the small valley and cirque glaciers at high altitudes are entirely below the melting point in the winter and could be classified as polar (Liestøl, in press, b). Unfortunately not much more is known about the internal distribution of the temperature of Svalbard ice. There have been few deep borehole measurements and they have rarely reached bedrock.

To describe the conditions of the superficial layers it is more useful to use the terminology of Benson (1962) and Müller (1962). This classification divides the surface of an ice mass into categories according to its temperature and degree of wetness. The great majority of the accumulation areas of the Svalbard ice masses are at or near the pressure melting point by the end of the summer, and suffer intense melting to the extent that the formation of superimposed ice layers is frequent. According to Benson (1962) and Müller (1962), these areas are in the percolation and wet-snow zones of the accumulation area. One of the conventional glaciological techniques, the use of 10–15 m temperatures to obtain information on the mean annual atmospheric temperature – MAAT (Paterson, 1981) – is not useful in these thermal conditions. In the dry-snow zone, 10–15 m is the depth at which the glacier-temperature response to seasonal changes in the atmospheric temperature becomes insignificant. In Svalbard, however, the great majority of glaciers and ice caps suffer intense melting of the superficial layers of snow/firn to different degrees. Several expeditions have reported the presence of water-saturated layers and the subsequent formation of superimposed ice layers (e.g. Zagorodnov and Arkhipov, in preparation). At Austfonna an intercalation of superimposed ice layers and water-saturated firn is encountered up to a depth of 30 m (Zagorodnov, personal communication). The refreezing of this meltwater increases substantially the temperature of the snow pack by the release of latent heat. The intensity of this process in Svalbard can be appreciated when the 10 m temperature is compared with the estimated atmospheric surface temperature for some of the sites (cf. Table 4.1). At Lomonosovfonna, for example, the refreezing process is strong enough to increase the 10 m temperature to -2.25°C (Zagorodnov and Zotikov, 1981a) at 1120 m a.s.l.. This temperature may represent a difference of about 10°C from the MAAT. Furthermore, there is great annual variability in the 10 m temperature, and on the crest of Vestfonna measured temperatures range from -6.5°C to 0°C (Dowdeswell, 1984; Palosuo, 1987). These differences are most probably caused by variations in the intensity of the refreezing process.

There have been few deep borehole measurements that reached a depth greater than 50 m. Soviet scientists have measured temperature at two of the sites of Spitsbergen glaciers (Grönfjord-Fridtjovbreen and Lomonosovfonna; Zagorodnov and Zotikov, 1981) and, more recently, a team of scientists from the Laboratoire de Glaciologie et Géophysique de l'Environnement (Grenoble) and SPRI measured the temperature distribution in a 136 m

borehole in Austfonna (79°45N, 25°36E). The Grönfjord-Fridtjovbreen profile was measured at the ice divide: it is relatively featureless below the layer affected by the winter 'cold wave' and, as expected, tends to greater temperatures. The glacier is most probably at the melting point at the ice divide. The Lomonosovfonna profile reaches only the upper 100 m and the temperature increases from about -2°C to about 0°C at a depth of 30 m. This reverse temperature gradient was probably caused by the warm period from 1920 to 1960, when melting at the site would have been more intense. Temperatures decrease below 30 m, reaching -2.4°C at a depth of 100 m. This decrease in temperature was most probably caused by cooling during the Little Ice Age (cf. Sections 1.4 and 4.4). Unfortunately it is not possible to confirm this observation, as the site is 1 km from the ice divide and no dynamic parameters are given. The Austfonna profile is 478.5 m a.s.l. in the ablation area (cf. Fig. 2.7) and, after an increase in temperature (from -6.2 to -3.7°C) between the surface and 60 m depth, the temperature stabilizes around -4.1°C, so the ablation area of Austfonna may be frozen to bedrock. On the other hand, results from a new borehole drilled to bedrock (566.7 m) in 1985 indicate that Austfonna is at the pressure melting point (-0.42°C; Zagorodnov and Arkhipov, in preparation) at the ice divide, providing support for the hypothesis put forward by Schytt (1969) that Austfonna has a warm centre surrounded by an annulus of colder ice.

Fig. 2.7 shows the shallow snow/ice temperature measurements that have been made in accumulation areas in Svalbard. The location of deep (>50 m) temperature measurements is also indicated. The general trend to lower temperatures towards the north and east is confirmed by the spatial distribution of the 10 m temperature. These trends in the shallow-ice temperature reflect the trend of decreasing superficial melting towards the east rather than the gross thermal structure of the ice masses. On the other hand, the few deep-ice temperatures supported the idea of cooler ice masses towards the east. This appears to be confirmed also by RES results, such as higher reflection coefficients and a greater concentration of internal reflecting horizons towards the west (Dowdeswell, 1984; Bamber, 1987). However, as Bamber (1987) emphasized, it is not possible to generalize about the thermal distribution of glaciers in Svalbard. Other factors, such as the ice thickness, are also important for determining the temperature of the glacier. The classical examples for Svalbard are the glaciers in northwestern Spitsbergen (e.g. Haakon VII Land), of which the ice thickness is 100–200 m near the pressure melting point. Thinner glaciers in central Spitsbergen are colder and may be frozen to bedrock (e.g. Foxfonna; Liestøl, 1984). In the ablation areas of the Svalbard ice masses the 10 m temperatures are in general lower than in the accumulation areas (by 2–8°C). This is a result of the impermeability of the ice. Although melting is more intense in the ablation area, the meltwater runs off the system instead of refreezing.

Figure 2.7- Shallow-ice temperatures (10 - 15 m) in the glaciers and ice caps of Svalbard. Only temperatures at the highest altitude in the accumulation area are given (see text for details).

A study in which the stable-isotope composition of an ice core is compared with the temperature variations in a borehole has yet to be carried out on Svalbard. The temperature distribution of a deep borehole can be used to derive past temperature changes by way of heat-conduction models and can be cross-checked with the temperature changes indicated by the variations in the stable-isotope ratio (e.g. Robin, 1976, 1983). Unfortunately, none of the ice cores for which there are stable-isotope studies have been measured for temperature throughout the depth of the borehole. Although these measurements (i.e. $\delta^{18}O$ and temperature) have been carried out for the recently recovered ice core from Austfonna (1987), the results have not been published (Zagorodnov and Arkhipov, in preparation).

2.4- The area of glaciological fieldwork in 1985 and 1986

2.4.1- Introduction

In 1985 and 1986 a team from SPRI carried out a comprehensive glaciological survey of central-eastern Spitsbergen (Fig. 2.8). The fieldwork aimed mainly to collect information on the ice thickness and sub-glacial morphology by means of radio echo-sounding. The RES surveys were complemented by glaciological studies at the surface on three glaciers in the area. These studies, which include snow pits and shallow-ice cores, provided new information on the environmental conditions, both in space and time, for this area.

The fieldwork was divided into two phases: (1) in 1985 a detailed overland RES survey of three valley glaciers of the Paulabreen system (i.e. Bakaninbreen, Paulabreen, and Skobreen; # 3, 2, 1 respectively in Fig. 2.11) was carried out, together with pit studies and the drilling of a 9 m core; (2) in 1986 an airborne operation successfully sounded 40 glacier systems of central Spitsbergen (Fig. 2.8). That year the fieldwork was complemented by the drilling of a 23.1 m ice core in Skobreen. This section is an introduction to the glaciology of central-eastern Spitsbergen and summarizes the fieldwork undertaken in the two seasons. This summary includes information on the operations, equipment used, and estimated errors in determination of the ice thickness and surface elevation. The main objective is to set the glaciological scene for a detailed examination of Skobreen, the site of the 1986 ice-core drilling, in Section 2.5. A more detailed account of the operations and of the radio-echo results can be found in the reports by Drewry (1985 and 1987b) and in the dissertation by Bamber (1987a).

Figure 2.8 shows a map of the area of study in 1986. The stippled square identifies the area of fieldwork in 1985. The main morphological features of the area are plateaus of Tertiary sedimentary rock, reaching maximum altitudes between 800 and 1000 m and dissected by cirque and valley glaciers (Fig. 2.10). Some of the plateaus are covered by small ice fields. The total area depicted in Fig. 2.8 comprises about 3340 km^2, of which

about 69% are ice-covered. Many of the main Spitsbergen valley glaciers are in this area (e.g Doktorbreen and Paulabreen) and they may be more than 15 km in length. The great majority of these glaciers originate from ice fields up in the plateaus and descend to Van Mijenfjorden, Van Keulenfjorden, and Storfjorden. According to the map by Liestøl and Roland reproduced in Fig. 2.3 and from examination of aerial photographs (Fig. 2.9), the snow-line elevation would appear to fluctuate between 300 and 400 m a.s.l.. Total accumulation in the area from the formation of the last autumn ice layer to May was about 400 kg m^{-2} in 1982/1983 (Semb, Brækkan and Joranger, 1984; cf. Section 2.2.3).

Glaciological information about the area was relatively scarce before 1985 and was based mainly on glacio-sedimentological studies. Punning, Troitsky and Rajamae (1976), basing their work on dated driftwood in the moraines of Svea Lowland (in the northeastern margin of Van Mijenfjorden, SW of Sveagruva), concluded that Paulabreen extended down Rindersbukta and across Van Mijenfjorden during the first stages of the LIA (i.e. 500 – 600 years B.P.). Rowan et al. (1982) examined the same sequence of moraines and also concluded that Paulabreen reached a maximum extent between 250 and 600 B.P., placing the maximum Late Holocene glacial extent of the glacier at Conwentzodden on Van Mijenfjorden (i.e. about 19 km distant from the present front; Fig. 2.8). However, they attributed the advanced position of the glacier during the LIA to a surge rather than to climatic deterioration. This conclusion was based on the presence of fjord clay that had been pushed and incorporated into the Lowland sediments by the surging glacier. Further evidence of intermittent surging activity in the area was provided by a seismic and sedimentological survey of Van Mijenfjorden by Elverhøi, Lønne and Seland (1983). A coarser-grained and acoustically opaque (at 3.5 kHz) sediment unit deposited near a sill off Conwentzodden was identified as a surge sequence (ibid.). These observations on the frontal position of Paulabreen emphasized once again the difficulties of interpreting variations in the extent of glaciers subject to surges. Finally, some information on the retreat of Paulabreen since the end of the last century is provided by maps and terrestrial photographs taken by earlier expeditions. On the basis of this sort of information, Koryakin (1974) estimated that Paulabreen retreated 7 km between 1898 and 1967, and Horvath and Fahn (1975) cited a retreat velocity of 95 m a^{-1} between 1898 and 1913, and 70 m a^{-1} between 1913 and 1924. This retreat is well marked by the substantial thickness of glacial sediments left on the sides of Rindersbukta (Figs. 2.8 and 2.9).

2.4.2- The 1985 and 1986 RES field seasons

2.4.2a- Methods

Twenty kilometres of three valley glaciers of the Paulabreen system (i.e. Bakaninbreen, Paulabreen, and Skobreen) were surveyed by RES in May 1985 on an overland operation. The SPRI survey followed a line of stakes previously established and

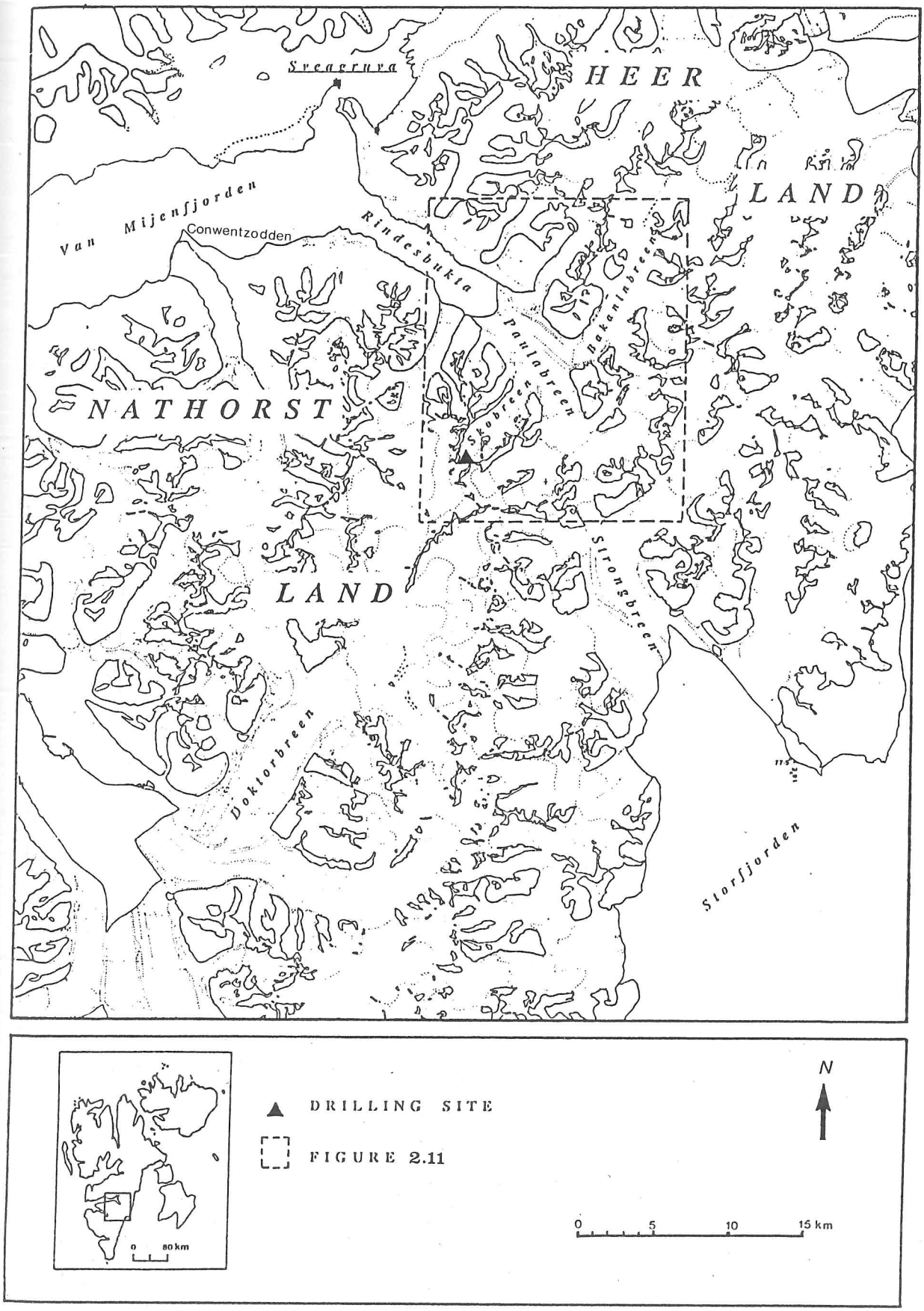

Figure 2.8- Location of area of studies in 1986 in central-eastern Spitsbergen and of ice-drilling site (triangle). The stippled square identifies the area of the Paulabreen system, the main area of glaciological studies in 1985 and 1986.

sounded by seismic reflection by Horizon Exploration, who also surveyed the topography of the ice surface along this track. All these activities were part of a British Petroleum – Norway programme carried out to evaluate techniques of geophysical exploration in valley glaciers of mountainous Arctic terrain. In May 1986 an airborne operation allowed the sounding of 40 glacier systems in central-eastern Spitsbergen (in the area depicted in Fig. 2.8). This section summarizes the operations and methodology used to obtain the ice thickness and surface elevation. The reader is directed to the reports by Drewry (1985 and 1987b) and the dissertation by J.L. Bamber (1987a) for more details.

The echo-sounding data were collected by A.P.R. Cooper and M.R. Gorman in both field seasons; J.L. Bamber participated in the 1985 operations. Extraction and processing of the ice-thickness data was carried out at SPRI by A.P.R. Cooper and J.L. Bamber, using the University of Cambridge mainframe computer.

Radio echo-sounding equipment

The SPRI Mk. IV 60 MHz system was used in both field seasons to sound the ice, but with different platforms. The equipment is a development of the Mk. II system described by Evans and Smith (1972) and has undergone several modifications since then. It was tested successfully in 1980 in Svalbard (Drewry et al., 1980) and in 1983 it was used to sound more than 4900 kilometres of flight track there (Dowdeswell, 1984).

In 1985 the SPRI Mk. IV 60 MHz and recording systems were mounted in a caboose on a sledge and towed by one or two snow-mobiles, depending on the surface conditions. The antenna was a single folded dipole drawn 3 m behind the sledge. A calibrated wheel-odometer triggered the radar transmitter at 1 m intervals. Part of the recording was carried out with a fast digitizing system which transferred each return wave form to a magnetic tape (Drewry and Liestøl, 1985). The system was able to record a minimum ice thickness of 80 m (Bamber, 1987a) and had a minimum system performance of 130 dB. Part of the survey had to be recorded on Super-8 ciné film, due to a fault in the recording and control unit of the RES equipment (Bamber, 1987a). The film was later digitized, using an automatic scanning system. A Z-modulated display (i.e. range and intensity of return signal versus time) was available from a fast thermal printer during the operations. The digital ice thickness was then extracted by a tracking algorithm developed by A.P.R. Cooper.

In 1986 the radar and recording systems were mounted in a de Havilland Twin Otter which operated from the airport at Longyearbyen. The system followed the configuration described by Dowdeswell (1984) but significant improvements had been made to the recording system. The antenna consisted of two half-wave dipoles mounted under the wings of the aircraft. In this configuration the wings act as reflectors, giving 8 dB of forward gain. System performance was 160 dB. Two improvements in the recording procedure are major

advances when compared with the previous system used by SPRI in Svalbard, and result in easy and rapid data reduction: (1) radar and navigation data were gathered and written to tape in a 2-second cycle and in the same stream of data; (2) the data were recorded directly onto IBM-compatible magnetic tapes. This recording procedure was controlled by a S-100 bus Z-80 based micro-computer. Finally, Z-scopes are also available on heat-developed paper.

In both surveys the ice thickness was determined using an electromagnetic propagation velocity of 168 m μs^{-1}. No corrections were made for the upper snow/firn layer because it is restricted to a few metres even in the accumulation area (as shown by the Skobreen core stratigraphy) and therefore the error incurred should be insignificant.

The seismic sounding results reported for Skobreen in Section 2.5 were processed by Horizon Exploration, using a mean 'P' wave velocity in the ice of 3650 m s^{-1}. Each sounding was about 125 m apart (with a 230 m spread; the geophones were 10 m apart).

Errors in navigation, in the determination of the ice thickness, and surface elevation

Errors in determination in surface elevation and navigation were eliminated in 1985, as the RES survey followed a line of stakes which had been surveyed topographically with a vertical accuracy of ±5 cm and horizontal accuracy of ±1 cm. Parts of the track were sounded more than once to assess the system accuracy, and 85% of the differences lay in the ±10 m range. These differences closely fitted a normal distribution and so Drewry (1987b) considered that the standard deviation of the differences (±4.6 m) gave the uncertainty of any ice-depth measurement. The maximum error in determination of the ice thickness by the seismic-reflection method is estimated to be ±5 m at the most, taking into account all the sources of uncertainty (e.g. identification of the shot instant, identification and timing of the bed return; Drewry, 1987b).

In 1986 navigation data were obtained from an Omega VLF navigation system. The data were tied to major navigational check points, logged by the navigator and the RES observer, and to fixes taken from vertical aerial photographs. Drewry (1987b) estimated that this methodology results in a circular error in position of ±100 m at any fix point, and not more than 250 m between fixes. The accuracy of the ice-thickness measurements is estimated to be at worst ±5 m and this should be added to the system accuracy of ±10 m cited above. Finally, an unknown error may be present in the 1986 survey, due to difficulties in the determination of the aircraft elevation. The procedure adopted in previous RES surveys was to take the raw aircraft elevation from the pressure altimeter and correct that to allow for changes in atmospheric pressure at the surface. This is done by establishing the terrain clearance when over the sea and so fixing the aircraft elevation relative to the sea-level. The error between this fixed elevation and the pressure altimeter reading is then distributed

linearly between fixes (Drewry, 1987b). Unfortunately, in 1986 it was impossible to avoid rapid changes in aircraft elevation (due to a low cloud ceiling), so an uncertainty remains because the pressure altimeter responds slowly to these rapid changes in aircraft elevation. Drewry (1987b) estimated that the error for surface elevations from the radio-echo altimetry is of the order of 10–12 m.

Finally, an indication of the absolute error of the RES technique in Spitsbergen ice is provided by comparing the sounding at Austre Grönfjord-Fridtjovbreen in 1980 and drilling by Soviet scientists (Macheret et al., 1984). The SPRI Mk. IV 60 MHz system recorded an ice thickness of 205 m and drilling reached the bed at a depth of 211 m (i.e. a difference of less than 3%).

2.4.2b- Summary of the results

About two thirds of the 40 glacier systems sounded showed returns along more than 60% of the track. In general, as in other RES surveys in Svalbard, no returns were recorded for the accumulation areas of the glaciers. In fact, it was rare that any glacier showed a bed return when the ice surface was at an altitude over 500 m. This is probably due to ice at high bulk temperature (i.e. at or near the pressure melting point) and to a greater concentration of impurities and inhomogenities (associated with melting and refreezing) that make the ice more 'lossy' to electro-magnetic energy (Dowdeswell et al., 1984a). Discontinuity or absence of bed returns were also observed in two other situations (Drewry, 1987b): (1) where the ice surface was heavily crevassed; (2) on small steep-sided glaciers. In these two cases scattering of the electro-magnetic waves from the facets of the broken surface or adjacent mountain walls masked the identification of the bottom returns (Smith and Evans, 1972).

Maximum ice thickness sounded by the SPRI Mk. IV system was 418 m and maximum surface elevation was 782 m a.s.l.; both were obtained near the divide between Scheelbreen and Barlaupfonna (just west of Skobreen; cf. Fig. 2.8). Minimum bedrock elevation was found in Arnesenbreen (-117 m), on the east coast of Spitsbergen. The complete data set for central-eastern Spitsbergen has been plotted by Drewry (1987b).

2.4.3- The Paulabreen system

As already mentioned, the fieldwork in 1985 was restricted to the Paulabreen system. This system is formed by the trunk glacier, Paulabreen, and six main tributaries which drain from Heer and Nathorst lands into Rindersbukta, at the head of Van Mijenfjorden (Figs. 2.8 and 2.11). Paulabreen, a typical tidewater glacier, is one of the largest in Spitsbergen, extending over about 15 km. Characteristics such as very low gradient, absence of extensive crevassing, a semi-permanent surface meltwater drainage network, and lack of changes in the moraine features appear to indicate that it is moving slowly. However, glacio-

sedimentological studies in the area indicate that this glacier has surged at least twice during the Holocene (Rowan et al., 1982; cf. discussion above). Two tributaries of Paulabreen, Bakaninbreen and Skobreen (# 1 and 3 in Fig. 2.11), were also surveyed in 1985.

Bakaninbreen enters the Paula valley from the northeast side, turning sharply through 90 degrees (Fig. 2.8 and 2.9), and then flows parallel to Paulabreen for about 6.5 km. A major medial moraine separating Bakaninbreen from Paulabreen indicates that these two glaciers flow independently of each other. The lower part of Bakaninbreen is deeply covered with moraine and it has been retreating together with the front of Paulabreen. In 1985 Bakaninbreen showed the first signs of surge activity (e.g. the formation of a steep ice ramp not correlated with any subglacial feature, a small side lobe heavily crevassed and overriding the lateral moraine, Fig. 2.12A). Since then the glacier has been going through a major surge, with substantial morphological and dynamic changes. By spring 1986 the ramp (which marks the surge front) had moved forward 1700 ± 150 m and risen by 25 m. The upper basin suffered considerable down-draw of the ice surface and the surface was highly crevassed (Fig. 2.12B). For the last three years the surge front has been propagating down-glacier and by mid-July 1989 it was recognizeable as a 30 m wave in the Paula valley, at about 4 km from the terminus (Ian Frearson, Arctic Group, Derby; personal communication). The surge front has thus moved about 1600 m in this period, i.e. there has been a total dislocation of 3200 m since 1985. The ice surface is heavily crevassed behind the surge front, and in the upper basin the surface has lowered by as much as 50–100 m (ibid.). In moving into the Paula valley, the front surge distorted and crevassed the medial moraine separating Bakaninbreen from Paulabreen.

Skobreen is a small tributary of Paulabreen and flows into it from the southwest. This glacier was the site of the drilling of the 23.1 m ice core discussed in other chapters of this dissertation and so its glaciology is examined in detail in Section 2.5.

Figure 2.11 shows the tracks of the ice-thickness measurements carried out in the Paulabreen system. All three glaciers were depth-sounded at least three times along the longitudinal profile (twice by RES in 1985–86, and once by seismic reflection in 1985). Paulabreen was also sounded in 1980 by RES. A secondary longitudinal profile of lower Bakaninbreen and a cross-profile of Skobreen, both done in 1985, completed the sounding in the area. The maximum thickness sounded in the system was 254 m in the upper part of Paulabreen and the ice thickness in the other two glaciers ranged from 114 to 223 m.

A comparison carried out by Drewry (1987b) of ice-thickness measurements obtained by RES and seismic reflection revealed that the seismic results are higher by at least 15 m in 50% of the cases examined on Paulabreen and parts of Bakaninbreen (where differences of up to 64 m were observed). The average error of ±17.2 m is well outside the accuracy of the

Figure 2.9- Vertical aerial photo mosaic of the Paulabreen system. The black dot identifies the site of the shallow ice core recovered in 1986 in Skobreen. Aerial photographs taken in August 23rd 1970.

two techniques. Drewry (1987b) therefore suggested that these two glaciers may be underlain by a layer of moraine or basal till. This hypothesis is supported by the extensive quantity of glacial sediments both in and on the sides of Rindersbukta. This moraine/till layer is difficult to penetrate with electromagnetic energy but not with seismic waves, so the seismic reflection would represent the till–bedrock interface and the RES returns the ice–till boundary. On Skobreen, however, the opposite case is observed: seismic measurements in general reveal thinner ice. Possible explanations for this observation are discussed in Section 2.5.

Figure 2.10- Aerial view of the Paulabreen system in summer (courtesy of J.A. Dowdeswell). The photograph was taken in the middle of August (1987) from over Rindersbukta looking southeast. Note the moraine to the left of centre separating Paulabreen from Bakaninbreen. The arcuate moraine in the centre-right of the photograph marks the snout of Skobreen.

2.5- The glaciology of Skobreen: the ice-core site in 1986

Skobreen is a 7900 m long valley-glacier tributary of Paulabreen (Figs. 2.9 and 2.11), ranging in altitude from 230 to 750 m a.s.l.. It is separated from Paulabreen by a moraine. Two cirque glaciers and a small valley glacier join Skobreen from the southwest (# 1, 2 and 3 in Fig. 2.13). The main valley glacier has a mean width of about 1400 m. Near the equilibrium line it has a roughly parabolic cross-section with a total area of 118,225 m^2. The four glaciers comprise a total area of 9.4 km^2, resting on Tertiary sandstones, siltstones and shales (Flood, 1971). The snout lies exactly over the contact between the Tertiary sequence and the Cretaceous.

A reconnaissance glaciological survey was conducted on Skobreen during 1985. In addition to RES, the survey included snow-pit studies, the drilling of a 9 m ice core, and the examination of the variations in the ice surface over the last 50 years. They had as an

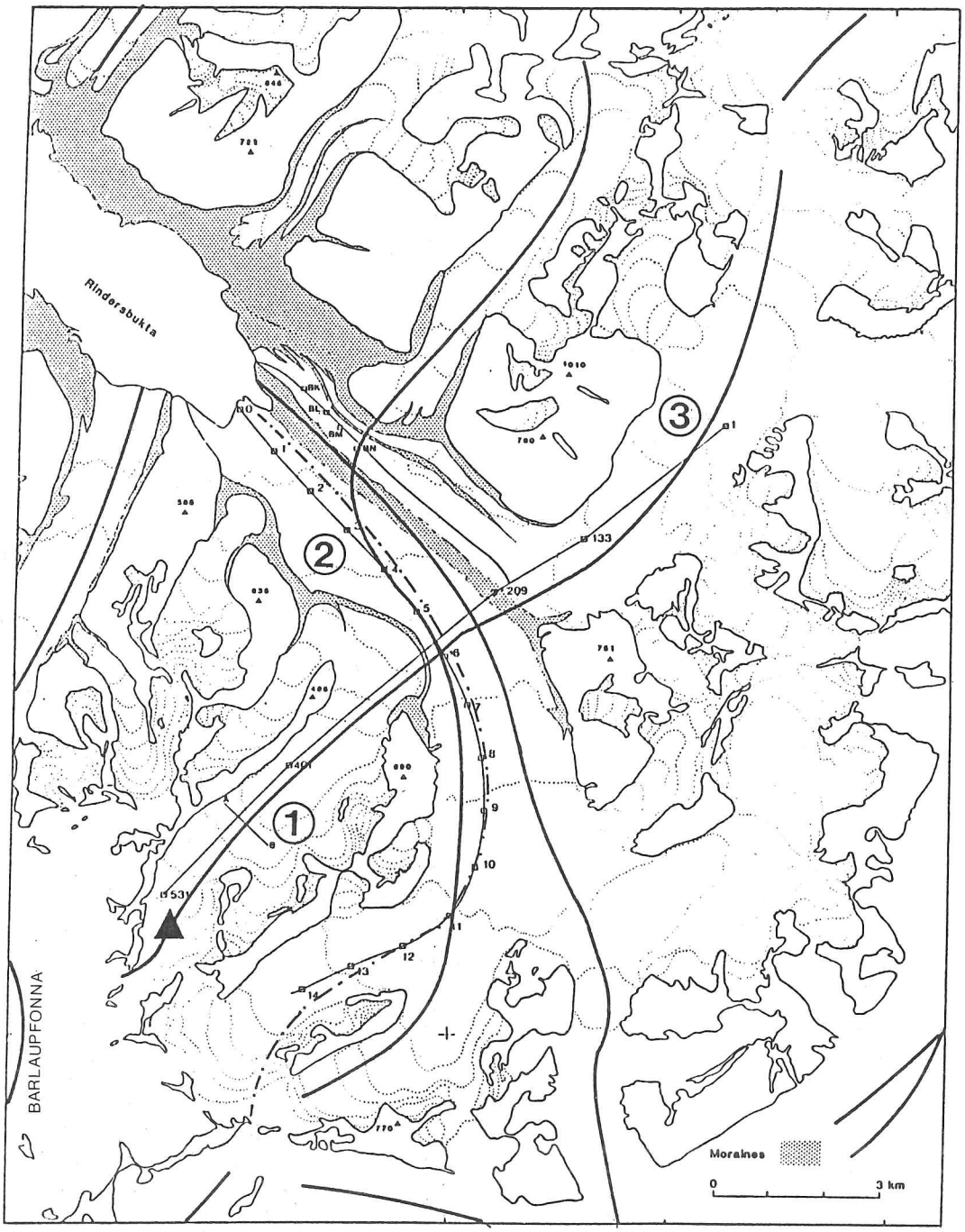

Figure 2.11- The Paulabreen system: the area of studies in 1985 and 1986. The triangle marks the site of the 23.1 m ice core recovered in 1986. The lines mark the location of the radio echo-sounding tracks in 1980 (stipple and dotted line), 1985 (continuous thin lines), and 1986 (continuous thick lines). The seismic survey in 1985 followed the same track of the RES that year. See Fig. 2.13 for details of the Skobreen surveys.

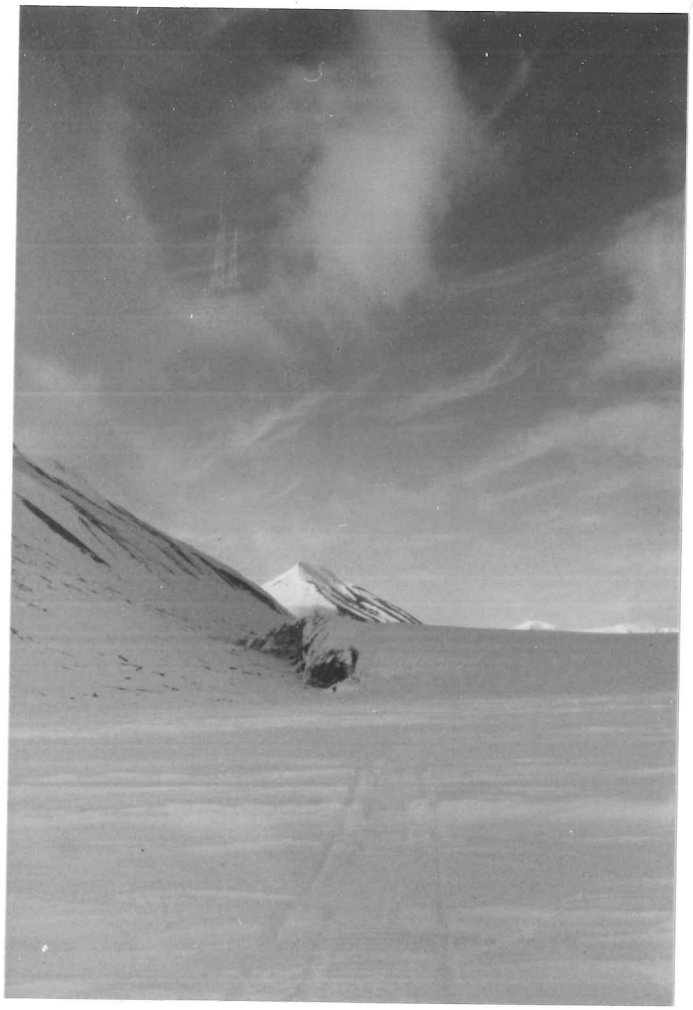

A

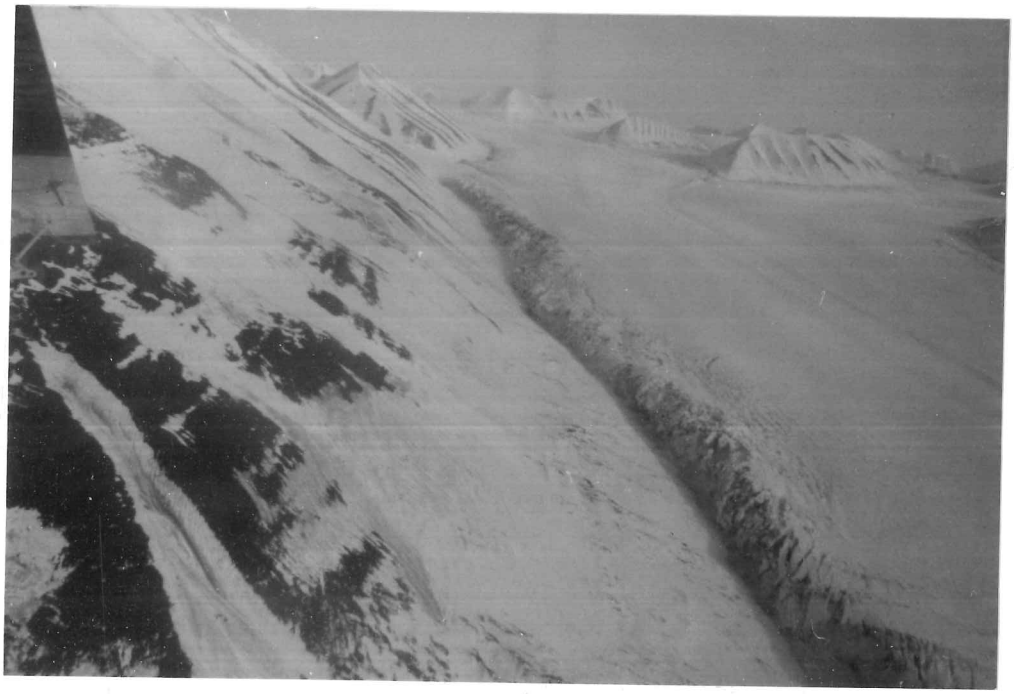

B

Figure 2.12- Surging activity on Bakaninbreen. Fig. 2.12A shows a side lobe observed in 1985 and identified as one of the first signs of surging. Fig. 2.12B shows the same lateral wall in 1986. The highly crevassed margin confirmed the surge.

objective the examination of aspects of the thermal and dynamic structure of the glacier, its stability, and the present distribution of some of the parameters used to derive environmental information (i.e. accumulation and stable-isotope ratios).

Before the glaciological surveys of 1985 and 1986 little was known about this glacier. The only source of information was three aerial photographic surveys, done in 1937/38 (oblique), 1970, and 1977 (vertical). The Norsk Polarinstitutt has published a topographic map (NPI, Braganzavågen sheet), scale 1:100,000, based on the survey of 1937/38. On the basis of this map and the 1970 aerial photographs the morphological and glaciological aspects of the surface of Skobreen are described.

2.5.1- Snow and ice zones

Three snow/ice zones are observed in the aerial photographs taken in August 1970: (1) a relatively dry-snow zone, (2) a firn/superimposed ice zone and (3) a blue-ice zone (Fig. 2.13).

In the first instance the uppermost part of the glacier appeared to be dry enough for ice-core research. The pit studies described below show that ice layers and lenses in this zone do not exceed more than a few millimetres of winter accumulation. It was thought that during the summer the melting and refreezing would be restricted to the surface (i.e. not more than a few centimetres in depth), which would not have been a great problem for a straight environmental interpretation of an ice core that it was planned to recover in 1986. Melt phenomena can in fact be useful for determining annual boundaries and for providing information about summer climate, and would affect only slightly the initial distribution of chemical species. Several studies were carried out successfully in similar areas (e.g. at Dye 3; Hibler and Langway, 1977). For 1970 at least, this part of the glacier could be classified as a percolation zone according to the terminology proposed by Benson (1962) and Müller (1962). However, close examination of the stratigraphy of the 23.1 m ice core revealed that this is not true for some years (Section 3.2) – the area can be affected strongly by melting and percolation in a warm year. Total loss of some years' winter accumulation is possible even at 600 m. Accordingly, it is more appropriate to call this upper area and **site of the ice-core a wet-snow zone.**

An extensive area of firn is observed from 450 to 370 m. This firn disappears gradually, showing glacial ice in the ablation area. The **firn line** was at about **370 m** a.s.l. in 1970. In non-temperate glaciers it is often the case that the snow line does not coincide with the equilibrium line. This is because a zone of superimposed ice is formed between the snow and the equilibrium line, and is a consequence of the intense melting and refreezing in summer. In aerial photographs it is very difficult to distinguish the superimposed from the glacial ice. Only an estimate of the mean annual snow line for 1970 can be given (somewhere

between 350 and 370 m). This would be in good agreement with mass-balance studies carried out elsewhere in Spitsbergen in the same year. These showed an equilibrium line at about 370 m on Werenskioldbreen (Baranowski, 1975) and Lovénbreen (Liestøl, 1974, 1976, 1982; and Fig. 2.3).

It is clear from these observations that the equilibrium line in Spitsbergen ice masses may be subject to considerable inter-annual variation. For example, on Lovénbreen the equilibrium line oscillated between 280 and 650 m from 1967 to 1982 (Liestøl, 1968). This demonstrates that even the heads of glaciers like Skobreen are not free from periods of intense melting. The distribution of the different zones varies greatly from year to year. This is to be expected for the region, as a result of the great variation in the mean annual temperature and the mean number of degree days (cf. Section 1.4). It is important to note that the summer of 1970 was relatively cool. In warmer years the firn line may go to 600 or even to 650 m a.s.l., and superimposed ice will form in the upper reaches of the glaciers.

At about 400 m the firn and snow are saturated sufficiently to allow the development of a dense network of supraglacial streams. The existence of thick ice layers in the accumulation area indicates that there is considerable meltwater runoff but it should be restricted to the surface snow strata by thick layers of superimposed ice. It can be observed that some of the streams survive over several years, which is thought to be characteristic of slow-moving glaciers, particularly glaciers with a low activity index (i.e. low accumulation and ablation; Hambrey, 1977).

The two zones described above constitute the 'accumulation' area and they cover a total area of 5.8 km^2 (which includes the three tributaries). The ablation area covers an area of about 3.6 km^2 and terminates against a **moraine** band (Fig. 2.13). This moraine was first thought to be a terminal moraine. Close examination reveals that it is a lateral moraine of Paulabreen that has been pushed by Skobreen some time in the past. At present the moraine seems to be stationary. At about 800 m from the snout a band of discontinuous supraglacial moraine is observed. This debris is carried to the surface by flowlines and is concentrated by the intense summer meltwater flow.

The glacier snout has been in the same position for at least the last 50 years, as may be seen from the aerial photographs and topographic map. Although information is lacking about exactly when it was formed, it may have been during the second half of the 19th century. This was the last period of general glacier advance in Svalbard (cf. Section 1.4.3). Furthermore, no crevasses have been observed in the ablation area and this emphasizes the extremely slow movement of the glacier. In addition, moraine material can be observed in the ablation area. This too has been in the same position for the last 50 years. It seems from these observations that the glacier is stagnant.

† Naturally, this estimate is only valid for the time when the aerial photographs on page 63 were taken (i.e. August 23rd 1970) because the snow-line altitude oscillates over the year and from year to year depending on the environmental conditions.

2.5.2- Pit studies

Six pits (S_1–S_6 in Fig. 2.13) were dug along Skobreen in 1985 to determine the present winter accumulation and the present value of stable-isotope ratios and their variations with altitude. The pits were excavated down to the glacier ice or to the first thick ice layer thought to identify the late summer horizon. The snow was sampled every 20 cm along the pit wall, and samples were collected in sealed glass bottles (22 cm^3 capacity). No major melting alteration was observed, except thin ice layers of less than 0.5 cm. The melted samples were mixed in the laboratory and the bulk sample for each pit was analysed for stable-isotope content (i.e. $\delta^{18}O$ and δD). All the samples were measured with respect to Standard Mean Ocean Water (SMOW; Craig, 1961b, and Section 3.2.4 of this dissertation). These analyses were carried out at the Stable Isotope Laboratory of the BGS Hydrology Group, by courtesy of Dr. W. Darling.

Table 2.3 and Fig. 2.14 give the results of these studies. The three variables increase in an approximately linear way, reaching a limit at about 500 m a.s.l. $\delta^{18}O$, δD, and accumulation have a slope of 0.85‰/100 m, 8.90‰/100 m, and 17.30 cm/100 m respectively with elevation. Bearing in mind that the precipitation originates from the same altitude (and at the same temperature), no trend should have been observed. This is plausible for the short extension of Skobreen. For larger ice masses, with greater differences of altitude between the head (or ice divide) and the terminus, we would expect a linear decrease with altitude. This results from the temperature dependence of isotope fractionation during condensation at different temperatures (i.e. as the air mass becomes colder with altitude, the precipitation is depleted of heavier isotopes; Dansgaard, 1964). The most probable cause of the inverted trend on Skobreen is that the sampled data refer to different time intervals. In other words, all the winter accumulation in the upper parts of the glaciers had been sampled. This covers about seven months (October–April). In the lower parts the interval is shorter and covers a shorter period later in the season and therefore colder isotopically. The late-autumn accumulation in the lower parts had melted and flushed out. This last observation is supported by the total accumulation at the nearby Sveagruva meteorological station of 155 mm of water for these seven months. Finally, the hypothesis is supported by the value of *d* (deuterium excess). During ablation (melting and evaporation) the snow pack not only becomes richer in heavier stable isotopes, but also shows a general decrease in *d* (Stichler et al., 1982). The mean value of *d* for the pits, 14.5 ± 2.6 (σ), is near the mean value for the Archipelago, 12.29 ± 4.08 (σ) (International Atomic Energy Agency, 1969–79). It can be concluded that the snow samples have not been affected substantially by melting.

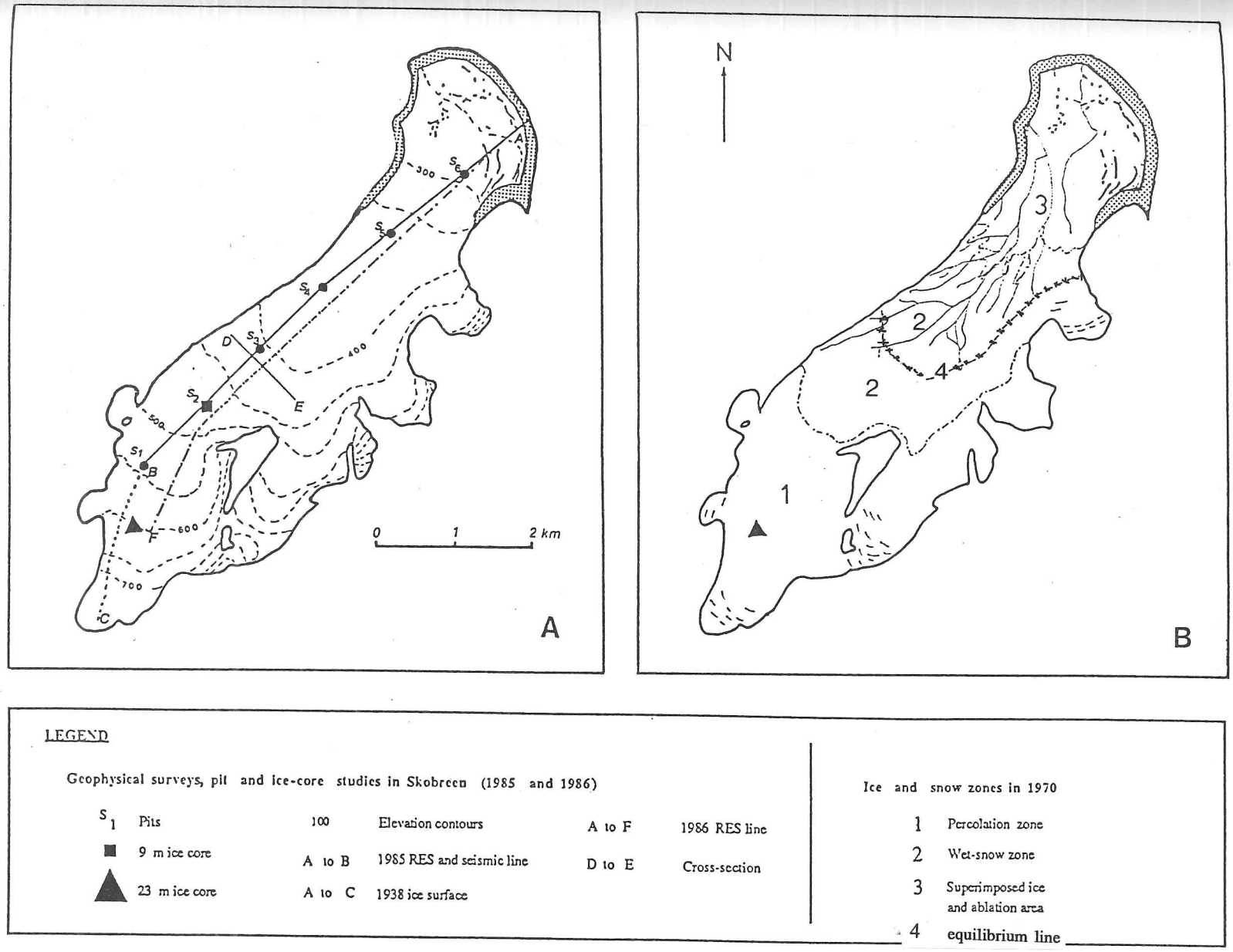

Figure 2.13- Location of geophysical surveys, pit and ice-core studies (A), and ice and snow zones (B) on Skobreen.

Table 2.3- Skobreen pit and ice-core data

Pit or ice core	Elevation (m a.s.l.)	Snow depth (m)[a]	$\delta^{18}O$ (‰)	δD (‰)	Temperature (°C)
23.1 m IC	600.0	2.10	-12.6 [b]	-82 [b]	
S_1	558.2	2.01	-11.9	-77	
S_2	488.8	2.10	-12.2	-84	
9.0 m IC	488.8		-11.7 [b]	-82 [b]	-2.8
S_3	427.3	2.00	-11.6	-82	
S_4	397.2	1.85	-13.2	-92	
S_5	347.4	1.64	-13.2	-90	
S_6	297.5	1.58	-14.3	-98	

IC = Ice-core depth
[a] Winter accumulation, not corrected for density
[b] Mean values

2.5.3- 9 m ice core

A drilling team from SPRI (D.J. Drewry, J.A. Dowdeswell, and J.C. Simões) recovered a 9 m ice core from the site of pit S_2. The equipment used was a standard 10 m SIPRE ice-coring drill (Fig. 2.15). The main object was to establish the mean net accumulation for Skobreen during the last two decades.

Ice drilling was difficult, due to considerable ice-layer formation. Several times the drill was trapped in the ice. The ice core was of very poor quality and was recovered in pieces. Every 20 cm was sampled for tritium and stable-isotope analysis ($\delta^{18}O$ and δD), and samples were analysed at the Stable Isotope Laboratory of the BGS Hydrology Group. The sampling rate turned out to be inadequate. There was no previous information on the accumulation in this area, and it had been wrongly estimated to be about 50–70 cm water equivalent (w.eq.) per year. Cross-comparison of the 1985 and 1986 ice cores (described below) shows that it is, at most, 25 cm w.eq.

The peaks in tritium due to the atomic tests of the 1960s were not found (J.A. Dowdeswell, personal communication). The flush-out is intense enough at the site to have obliterated the 1963/64 tritium peaks, so no absolute dating was possible. On the other hand, the snow which had accumulated in 1968 was used as a reference horizon. This was the coldest year in Svalbard since the 1910s and it is easily recognized in the various Svalbard ice cores (see Sections 3.3.5 and 4.3.3), including the two ice cores recovered from Skobreen, which are more than 2 km apart (Fig. 3.5). This cross-comparison gives a mean net mass balance for the period 1968–85 of 0.20–0.25 m a^{-1} w.eq. at pit S_2.

Table 2.3- Skobreen pit and ice-core data

Pit or ice core	Elevation (m a.s.l.)	Snow depth (m)[a]	$\delta^{18}O$ (‰)	δD (‰)	Temperature (°C)
23.1 m IC	600.0	2.10	-12.6 [b]	-82 [b]	
S_1	558.2	2.01	-11.9	-77	
S_2	488.8	2.10	-12.2	-84	
9.0 m IC	488.8		-11.7 [b]	-82 [b]	-2.8
S_3	427.3	2.00	-11.6	-82	
S_4	397.2	1.85	-13.2	-92	
S_5	347.4	1.64	-13.2	-90	
S_6	297.5	1.58	-14.3	-98	

IC = Ice-core depth
[a] Winter accumulation, not corrected for density
[b] Mean values

2.5.3- 9 m ice core

A drilling team from SPRI (D.J. Drewry, J.A. Dowdeswell, and J.C. Simões) recovered a 9 m ice core from the site of pit S_2. The equipment used was a standard 10 m SIPRE ice-coring drill (Fig. 2.15). The main object was to establish the mean net accumulation for Skobreen during the last two decades.

Ice drilling was difficult, due to considerable ice-layer formation. Several times the drill was trapped in the ice. The ice core was of very poor quality and was recovered in pieces. Every 20 cm was sampled for tritium and stable-isotope analysis ($\delta^{18}O$ and δD), and samples were analysed at the Stable Isotope Laboratory of the BGS Hydrology Group. The sampling rate turned out to be inadequate. There was no previous information on the accumulation in this area, and it had been wrongly estimated to be about 50–70 cm water equivalent (w.eq.) per year. Cross-comparison of the 1985 and 1986 ice cores (described below) shows that it is, at most, 25 cm w.eq.

The peaks in tritium due to the atomic tests of the 1960s were not found (J.A. Dowdeswell, personal communication). The flush-out is intense enough at the site to have obliterated the 1963/64 tritium peaks, so no absolute dating was possible. On the other hand, the snow which had accumulated in 1968 was used as a reference horizon. This was the coldest year in Svalbard since the 1910s and it is easily recognized in the various Svalbard ice cores (see Sections 3.3.5 and 4.3.3), including the two ice cores recovered from Skobreen, which are more than 2 km apart (Fig. 3.5). This cross-comparison gives a mean net mass balance for the period 1968–85 of 0.20–0.25 m a^{-1} w.eq. at pit S_2.

Skobreen winter accumulation

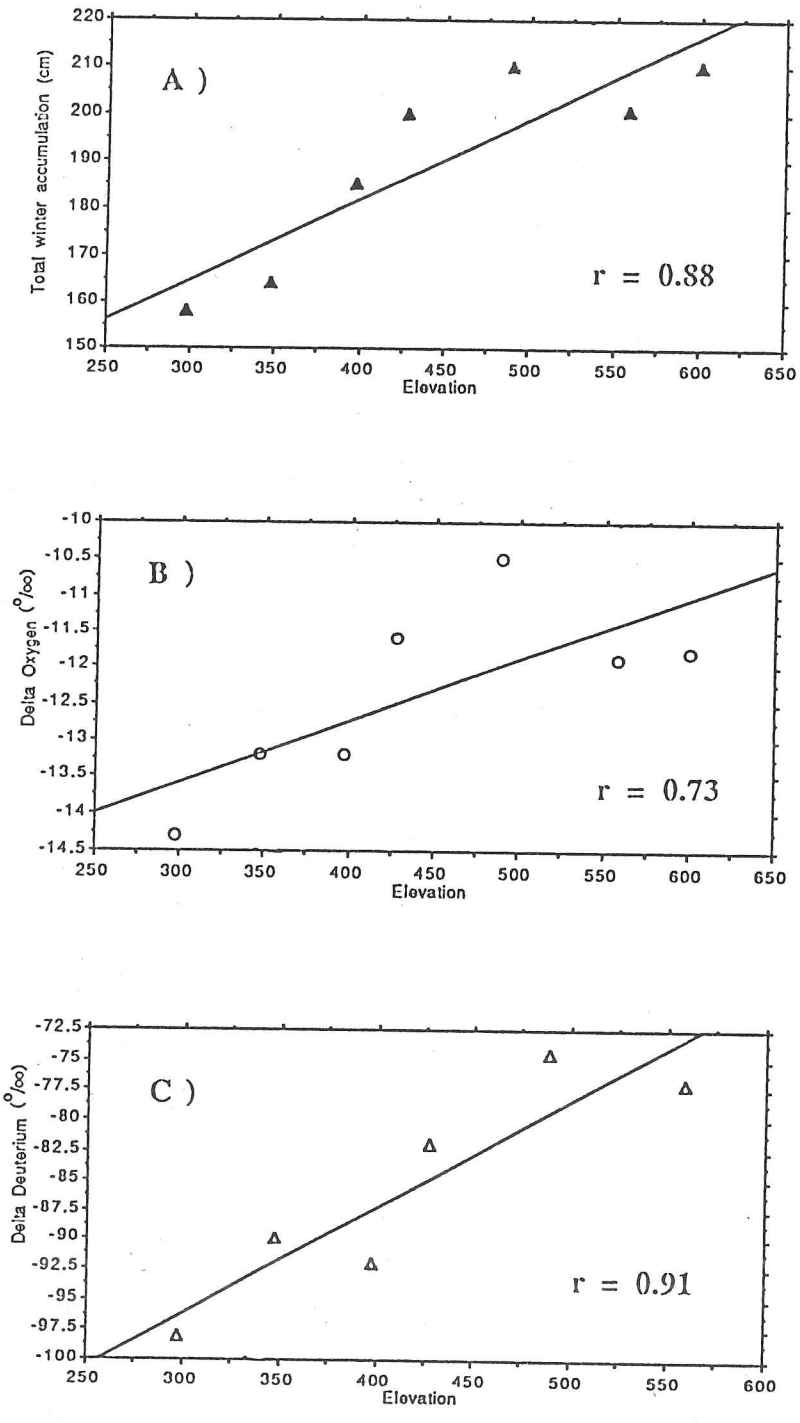

Figure 2.14- Total winter accumulation (in cm and not corrected for density) and its isotopic composition (in ‰) plotted against the elevation (m) of the sites of collection on Skobreen. 'r' is the coefficient of linear correlation between the x and y values. Source: Drewry, 1985.

Figure 2.15- Shallow-ice coring on Skobreen using a SIPRE 10 m drill.

The δD and $\delta^{18}O$ vertical profiles (Fig. 2.16A and B) show that no seasonal variation can be recognized. This is a consequence of the wrong sampling frequency and the homogenization of the isotopic ratios due to melting and refreezing. The mean $\delta^{18}O$ for the whole ice core is -11.71‰ ± 0.94 (σ) and for the deuterium content is -82.0‰ ± 7.2 (σ). Although the degree of melting and flush-out is high, cross-comparison with the 1986 ice core (Fig. 3.5) shows that the general features remain identifiable. Furthermore, Fig. 3.6 shows that the deuterium excess - *d* in the 1986 core is approximately constant along the ice core, with the exception of the top 5 m. The decrease in *d* reflects the great extent of melting over the last 10 years, particularly in 1984. This is to be expected, as 1984 was the warmest year since records began and had anomalous days with a maximum temperature of 6.5°C in the middle of December.

2.5.4- Ice-surface and thickness measurements

Skobreen was surveyed by RES in 1985 and 1986 by a team from SPRI. Equipment, methods, and errors have been summarized in Section 2.4 and in Drewry (1985, 1987b). Ice thicknesses ranging from 114 m near the head of the glacier to 199 m near the equilibrium line (about 400 m a.s.l.) were observed.

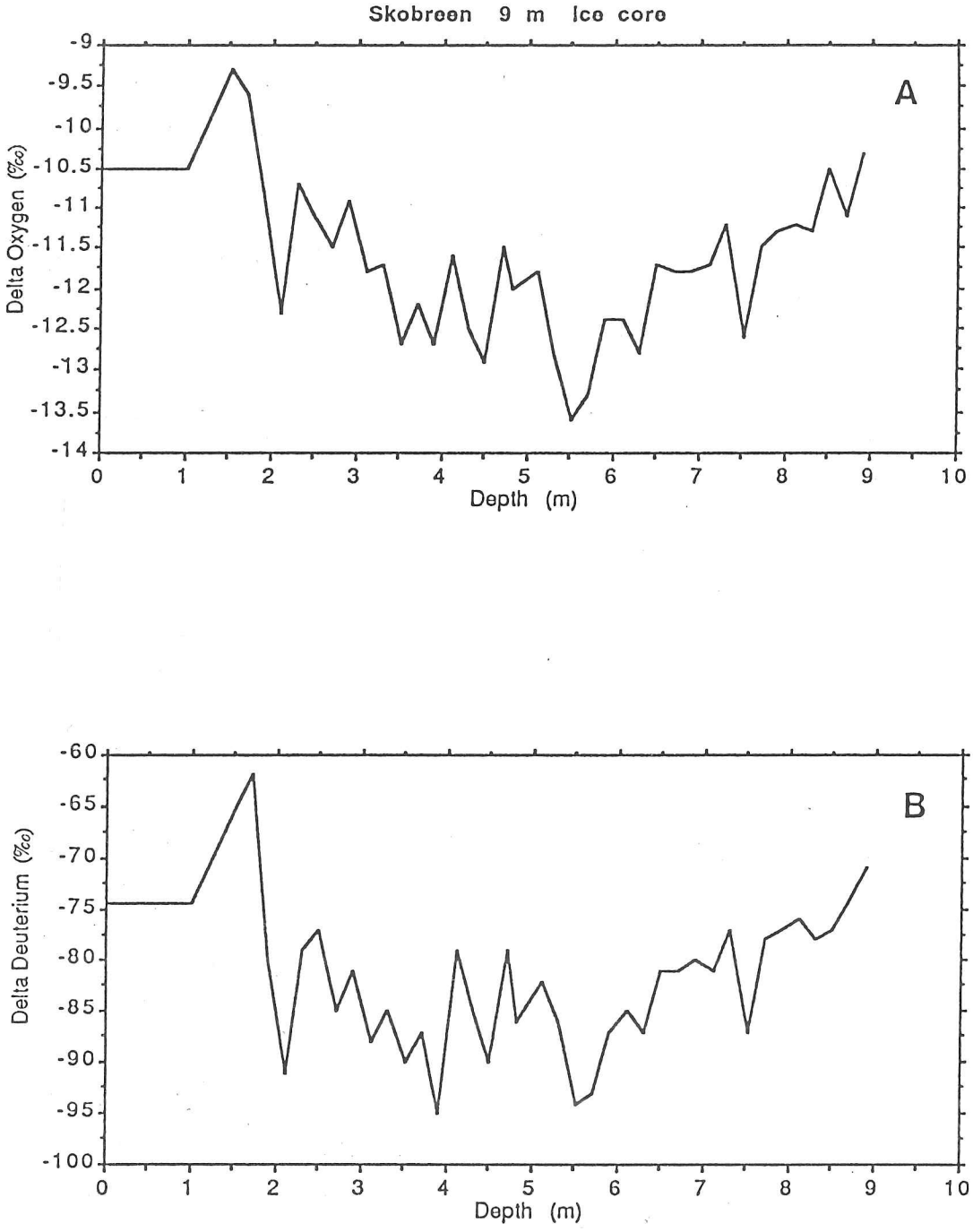

Figure 2.16- $\delta^{18}O$ (A) and δD (B) of a 9 m core from Skobreen. The profiles have not been corrected for density.

Radio echo-sounding results from Skobreen show an unambiguous bed echo for almost the whole of the 6.6 km surveyed in 1985. In contrast, it can be seen in Fig. 2.17*I* that the airborne survey of 1986 did not show bed returns for two sections of the glacier: in the upper part of the glacier (above 500 m) and in the ablation area (between 250 and 350 m). The lack of returns represents 35% of the total track of 7.6 km. The proportion is typical for glaciers in south-central Spitsbergen (Dowdeswell et al., 1984a). The 1986 results show a mean ice thickness of 175 m.

In ice masses at relatively high temperatures (i.e. near or at the melting point) the bedrock may remain undetected due to high scattering and absorption of radio waves (Robin, Evans and Bailey, 1969; Smith and Evans, 1972; Goodman, 1975). In this 'warm' ice the bed echo may be attenuated by scattering due to a great number of inhomogeneities (Smith and Evans, 1972) associated with melting and refreezing (e.g. soaked firn, ice layers, and lenses). Furthermore, the bottom return may be concealed by the return of many discrete scatterers (Smith and Evans, 1972). The frequent lack of bed returns in the accumulation areas of Svalbard sub-polar glaciers may be the result of these phenomena (Dowdeswell et al., 1984a and b; Drewry, 1985). This would seem to be an explanation for the lack of returns at Skobreen. The temperature in the accumulation area is close to -2.8°C, and it is known from ice-core stratigraphy that there is great variability in the density of the firn (ice layers up to 2 m thick are intercalated) and a great quantity of impurities (cf. Chapter 3). On the other hand, since most of the accumulation area shows a well-defined bottom return this explanation is not adequate. Moreover, it would not account for the lack of returns in the ablation area, and another explanation for the lack of bed returns must be sought. Airborne RES with the system configuration used in 1986 was not able to detect ice less than 100 m thick (M. Gorman, personal communication), as a consequence of the high scattering angle of the ice surface, due to sastrugis and other irregularities. The problem can be avoided by carrying out over-snow surveys similar to that undertaken in 1985. There is also the problem of internal scattering due to several thick ice layers and discrete inhomogeneities (e.g. water layers) in the firn and ice of the accumulation area (see Section 3.2.1). The same explanation is given for the lack of bottom returns in the ablation area: the area where there are no returns is located over a sill and the ice is very thin.

In Fig. 2.17*I* the two RES surveys are compared. This plot was fixed through the 1985 ice surface and bedrock. The first survey produced better results because it was an over-snow survey, so less scatter occurred. Furthermore, the topography of the ice surface was surveyed with a vertical accuracy of ±5 cm and a horizontal accuracy of ±1 cm. In general the differences between the two RES surveys in the lower part of the glacier are within the system accuracy, which is ±10 m (Drewry, 1985; and Section 2.4.2 of this dissertation). At about 2400 m from the snout of the glacier the longitudinal RES profiles begin to differ markedly. A difference in bedrock elevation is explained by the different tracks

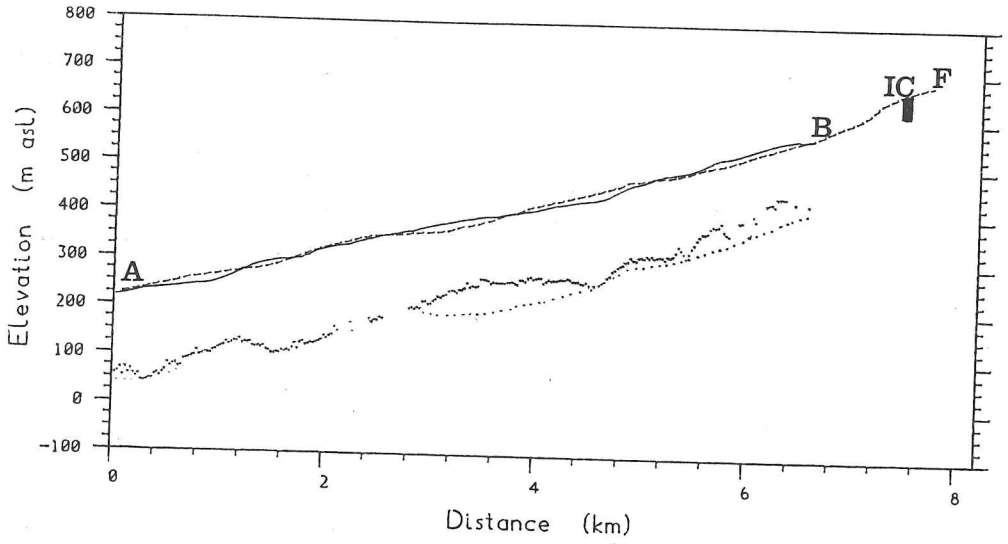

I) Ice-surface and bedrock elevations from the 1985 and 1986 radio echo-soundings. A-F (stippled line) is the ice surface determined by the airborne survey of 1986 (see text for details). IC is the location where the 23.1 m core was recovered. The dots mark the bedrock returns obtained during the 1986 airborne RES. Sources: Drewry, 1985 and 1987b.

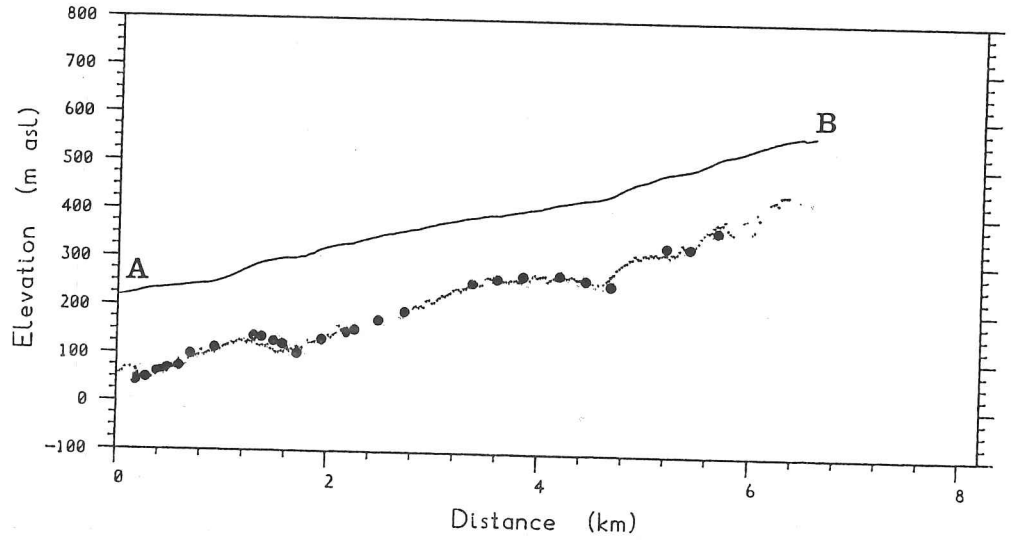

II) Ice surface in 1985 and bedrock determined by the the RES in 1985 and a seismic survey (black dots). Sources: Drewry, 1985 and 1987b.

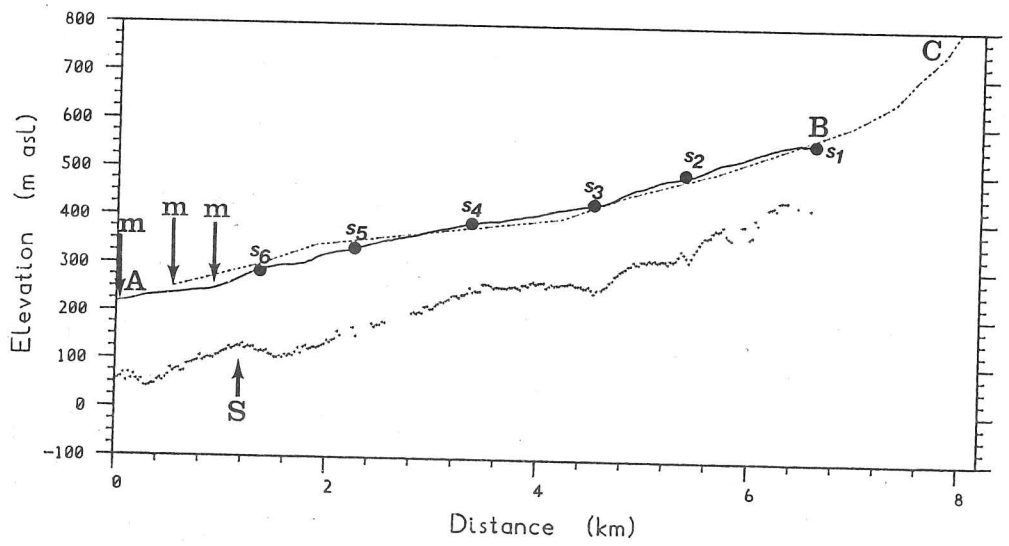

III) Location of pit studies (s_1-s_6), and moraines (m) on the Skobreen ice surface as determined in 1985. A-C (stippled-dotted line) marks the ice surface in 1937-38. S is the subglacial sill near the snout of Skobreen. The 1937-38 ice surface is derived from a topographic map published by the Norsk Polarinstitutt in 1983 (Braganzavågen sheet, 1:100,000).

Figure 2.17- Longitudinal RES and seismic profiles of ice thickness on Skobreen. In all the profiles (I-III), A-B (continuous line) marks the ice-surface elevation as determined by a topographical survey on Skobreen in 1985, and the tiny triangles mark the bedrock returns obtained by an overland survey in the same year (see text for details). The spatial location of the survey and the features on Skobreen are also marked in the map of Fig. 2.13. Source: Drewry, 1985.

followed in 1985 and 1986. As the cross-section (Fig. 2.18) shows, the 1985 survey did not follow the deepest part of the glacier valley (i.e. the thalweg). In 1986 the flight line attempted to follow the central line of the valley, which is in approximately the same position as the thalweg. The differences in these profiles agree well with the differences observed in the cross-profile (i.e. 40–50 m).

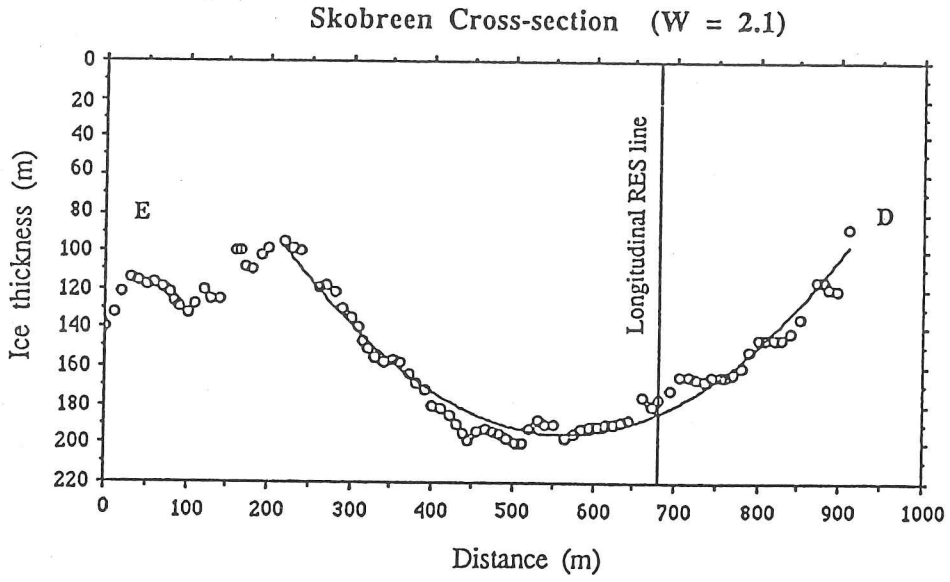

Figure 2.18- Cross-section profile of ice thickness on Skobreen, as determined by an overland survey in 1985. The location of this cross-section is marked in Fig. 2.13 (E–D). The vertical line in the profile marks the location of the RES longitudinal profile depicted in Fig. 2.17*I*. Source: Drewry, 1985.

A bedrock sill associated with a significant surface slope marks the end of the Skobreen valley. This is followed by a relatively flat area towards the moraine band (surface slope <0.6°). We concluded that this lower part of the glacier is stagnant; this is supported by the slight slope, permanent supraglacial drainage, and the stationary state of the moraine band separating Skobreen from Paulabreen and of the supraglacial moraines in Skobreen.

The shallow seismic-reflection survey referred to in Section 2.4 produced results that differed in some respects from those of the coincident 1985 RES survey. On average the RES results were 9.3 m deeper than the seismic ones. The maximum difference was 28 m (Fig. 2.17*II*). These values far exceed the level of uncertainty of the RES and seismic surveys (i.e. 4.6 and 5 m respectively; Drewry, 1987b). Drewry (1985, 1987a) first suggested that this was caused by a line of sounding close to one of the valley walls (NW; Fig. 2.13), which would result in seismic reflections from the wall that are nearer than the bottom. This would not happen in the RES survey because a narrow beam is used. However, the areas with the greatest differences and nearest to the wall did not bear this out and he abandoned the hypothesis. The areas with the greatest differences were over the sill and it is not possible to provide another explanation without more field data. Drewry (1987b) also

suggested that the steep gradients of the sill on both sides could cause the nearest returns to be migrated, thus affecting the results.

Table 2.4- Details of the measurements of ice thickness at Skobreen

Year	Total track (km)	Track with bed (%)	Max depth (m)	Min depth (m)
1985	6.6	≈100	193	114
1986	7.6	65	199	132
Seismic	6.6	———	190	127

Fig. 2.17*III* illustrates the changes in ice elevation since 1937/38. The ice elevation in 1937/38, and the ice surface and bedrock profiles obtained from the RES surveys of 1985, are plotted against the distance from the snout. The 1937/38 map has a contour interval of 50 m, a maximum error in height of ±2.5 m, and a horizontal error of 20 m (Trond Eiken, written communication). The contour intervals are derived from the 1937/38 aerial photographs. Thus, the area affected by ablation was as much as 30 m lower than in 1937/38, taking into account the accuracies of the map based on the 1937/38 aerial photographs and the topographic survey of 1985 (i.e ±5 cm vertical error and 0.1 cm horizontal error). This represents about 0.60 m per year and follows the general trend of the Spitsbergen glaciers that have been the subject of mass-balance studies (i.e. Austre Brøggerbreen and Midre Lovénbreen, Liestøl, 1984; and Werenskioldbreen, Baranowski, 1975). It is relevant that the snout of Skobreen is almost 200 m higher than the snout of these other glaciers. Below the sill the ice surface becomes flat (α <0.6°). Fig. 2.17*I* compares the RES profiles of 1985 and 1986. It can be observed that there has been hardly any change in the ablation area. The differences observed are within the instrumental error.

There were no measurements of ice velocity in the 1985 and 1986 surveys. On the other hand, the velocity at the centre line can be estimated from glaciological theory. Valley glaciers do not deform in plane strain (Paterson, 1981), as the stresses and velocities are modified by the support action of the valley walls. Therefore, in order to estimate the velocity at the centre line of Skobreen, it is necessary to take account of the effects of the valley walls on the ice flow. On the other hand, it is known that at the centre line the shape of the velocity profile versus depth is close to that for laminar flow, and shear stress deviates only slightly from being linear with depth for a half-width greater than one, i.e. $W > 1$ (Raymond, 1980). Furthermore, Nye (1965) introduced a shape factor F into the calculation of the τ_{xy} (for laminar flow τ_{xy} is supposed to be the only basal shear-stress component different from zero). F quantifies the effect of the valley sides on the flow of a cross-section. It can be

expressed by: $\tau_{xy} = -F\rho gh \sin\alpha$. F will depend on the the form of the glacier channel (i.e. parabola, half of an ellipse, rectangle) and of W, the ratio of half-width to depth. The cross-section of **Skobreen** (Fig. 2.18) is roughly parabolic and W is about 2 (W = 2.1). For this value, $F = 0.646$ (Paterson, 1981). The basal shear stress combined with the ice-flow law and integrated down from the surface gives:

$$(u_s - u_b) = [\, 2A / (n + 1)] \; (\rho \, g \, F \, h \sin\alpha)^n \, h \qquad \text{(Raymond, 1980)}$$

Examination of the thermal conditions at the accumulation area indicates that the glacier is marginally at the pressure melting point at the bottom (cf. Section 2.5.6). The ablation area shows a less steep slope and thinner ice. It is reasonable, therefore, to assume that the ablation area is frozen to bedrock. Thus the basal sliding component (u_b) is believed to be zero. 'A' is affected by the temperature gradient and variations in different properties of the ice (e.g. impurity content). Different parts of a sub-polar glacier may have different temperatures, so the ice velocity was calculated at 0° and -5°C to provide a range of probable velocities. We obtained velocities between 0.75 and 2.35 m a^{-1} in the centre of the cross-section (h = 200 m, sin α = 0.045). If the cross-section shape and W hold for the ice-core site, the annual velocity ranges between 0.52 and 1.64 m a^{-1} (h = 125 m, sin α = 0.075). For these calculations A = 16.71 x 10^{-2} a^{-1} bar^{-3} and 5.36 x 10^{-2} a^{-1} bar^{-3}, for ice at 0° and -5°C respectively. These estimates give an idea of the scale of the ice velocity. Even if there were some sliding contribution (say ten times the ice deformation), it would still be very small ($u_s < 25$ m a^{-1}), which confirms the glaciomorphological observations that the glacier is moving very slowly. It is thus not necessary to correct the ice-core profile for horizontal velocity.

2.5.5- Stability of the glacier

One of the principal concerns when choosing a drilling site is the possibility of glacier surging. Many Svalbard ice masses surge from time to time (Liestøl, 1969, and Liestøl, in press, a; Schytt, 1969; Horvath and Fahn, 1975; Drewry and Liestøl, 1985; and Section 2.2.2 of this dissertation). Furthermore, some of the glaciers in the Paulabreen system are known to have surged (e.g. Paulabreen and Bakaninbreen; Drewry, 1987b), and several others show looped moraines (Fig. 2.9), which have been interpreted as evidence of past surging (Paterson, 1981). This would make the environmental interpretation of an ice core extremely difficult, if not impossible. For example, rapid changes in elevation could result in rapid changes in the stable-isotope ratios and give a false idea of rapid climatic change. Skobreen does not have any of the characteristics of a surging glacier, and no major changes have been observed over the last 50 years.

2.5.6- Thermal conditions

A string of thermistors was lowered into the borehole and left for 24 hours to stabilize thermally. The 9 m temperature was -2.8°C. This is markedly different from the estimated present mean temperature for the area at this altitude, -11.5°C. This observation is based on a mean temperature in Sveagruva (near sea-level) of -7.0°C and a mean lapse rate for the Van Mijenfjorden area of 0.9°C/100 m (in fact the lapse rate varies between 0.6 and 1.6°C/100 m; Ottar, Pacyna and Berg, 1986). The difference in temperature can be attributed to heating of the snow/firn pack by latent heat release during refreezing. It was not possible to estimate the extent of heating of the snow pack by expulsion of latent heat (Holdsworth, 1984), because the variations in density along the ice core were not measured. On the other hand, the high percentage of ice at this shallow depth and the homogenization of the isotope content confirm that the site is subject to a high degree of melting, percolation, and refreezing. The latter process releases enough latent heat that the firn temperature is greater than the mean annual temperature (Paterson, 1981), and it is not possible to equate the 10 m temperature with the mean annual air temperature (see Section 2.3.3 on 10 m temperatures in Svalbard). The other factor that can explain the differences in temperature, i.e. the difference between mean annual screen and ground temperatures, can contribute only a few degrees to the difference in the Arctic (Paterson, 1981). The mean temperature and, perhaps more important for melting, the maximum temperature and the number of degree days, have varied substantially in Svalbard, so it is not possible to generalize about the thermal structure of the glacier without measuring the vertical temperature profile. Nevertheless a simple moving-column model was run in order to estimate the internal distribution of temperature at the site of the S_2 pit and to test the sensibility of the glacier to small changes in surface temperature and net accumulation.

A simple column model (Budd and Radok, 1971; Paterson, 1981) was used because there was insufficient input data (e.g. past surface temperatures and accumulation rates, strain-rates along a deeper ice core) to apply more sophisticated and non-steady-state models (e.g. Paterson and Clarke, 1978). The main drawback is that the model considers that the advection term of the heat transfer function does not vary with depth. On the other hand, this is not important for our case because of the low velocity.

The model calculates the temperature every 15 m through the numerical solution of the following equation (Paterson, 1981):

$$\partial T/\partial y = (\partial T/\partial y)_b \, e^{(-y_b^2/l^2)} + (Wl/k)\, I\, (y_b/l) \qquad (1)$$

where $(\partial T/\partial y)_b$ is the basal temperature gradient, $l^2 = 2kh/b_n$, b_n is the net mass balance, h is the total ice thickness, y_b is the vertical distance from the bedrock, W is the warming of the column, k is the thermal diffusivity constant (1.15×10^{-6} m^2 s^{-1}; Paterson, 1981), and I is Dawson's Integral (which is tabulated). It was run initially with the measured data.

The horizontal velocity was not measured. However, the contribution of the ice deformation is only of the order of a few metres per year at the equilibrium line, as described above, and the snout appears to be frozen to bedrock. Therefore a mean value of 10 m a^{-1} can be used safely, bearing in mind that the sliding contribution is expected to be small, if any. A net accumulation of 25 cm a^{-1} was used, obtained from the shallow ice-core studies (see discussion above). For this estimate, it was assumed that the ice column had a mean density of about 800 kg m^{-3}. Surface slope at the site was determined from the topographic survey of 1985 ($\alpha = 0.069$). An ice thickness of 165 m for the site was determined by the 1985 RES survey. Drewry (1985) cited a measured geothermal gradient at Sveagruva of 0.02°C m^{-1}.

The resulting vertical temperature profile is shown in Fig. 2.19A (**I**). The bed is at the pressure melting point (approx. -0.11°C) with a melt rate of 0.8 mm a^{-1}. Curve **II** in the same figure shows the results when the surface temperature is reduced from -2.8 to -3.5°C. The ice becomes frozen to bedrock (T = -0.29°C). It is important to note that the last decade is not representative of the surface temperature in Svalbard in recent centuries. In fact, this temperature reflects the warm 1970s, so the internal distribution should resemble curve **II** rather than curve **I**. Curve **III** shows the results given by the model when run with data for the site provided by Drewry (1985), who assumed that the site was much nearer to the equilibrium line and that the net mass balance was near 0. In this case the melt rate is slightly higher, 1.2 mm a^{-1}. In addition, the model was run for a net mass balance of 0.35 m a^{-1} (run **VI**), resulting in a profile similar to curve **I** (melt rate = 0.6 mm a^{-1}) and a new net balance and temperature at the same time (curve **IV** in Fig. 2.19B). The latter resulted in further decrease in the basal temperature (-0.46°C). Reduction in the surface velocity to 2 m a^{-1} had insignificant impact (curve **V** in Fig. 2.19C). In general, these results demonstrate clearly the climatic sensitivity of sub-polar glaciers at the theoretical level. Small changes in temperature and net accumulation can have a major influence on the temperature distribution and in consequence on basal conditions and ice dynamics.

It may be concluded on theoretical grounds that Skobreen has a complex thermal structure, as reported for many Svalbard glaciers. It has a warm thermal regime in the accumulation area and a cold regime in the ablation area. During the high summer, melting occurs over the whole surface, with substantial percolation and refreezing in the accumulation area. Some of the ice is at or near the melting point, as shown by the surface temperature and model above. On the other hand, there is some evidence that the ablation area is frozen to bedrock (e.g. permanent supraglacial drainage). Skobreen appears to be extremely sensitive to small variations in temperature and net balance. It could be said that it is a maritime sub-polar glacier at high latitude (Baranowski, 1977b).

Table 2.5- Input parameters and results of a moving-column temperature model for Skobreen.

Run	Surface temp. (°C)	Mass balance (m a^{-1})	Surface velocity (m a^{-1})	Surface slope	Geothermal gradient (°C/m)	Ice thickness (m)	Basal temp. (°C)	Melting rate (mm a^{-1})
I	- 2.8	0.25	10	0.069			- 0.11	0.8
II	- 3.5	0.25	10	0.069			- 0.29	-----
III	- 2.8	0.01	10	0.026	0.02	165	- 0.11	1.2
IV	- 3.5	0.35	10	0.069			- 0.46	-----
V	- 2.8	0.25	2	0.069			- 0.11	0.4
VI	- 2.8	0.35	10	0.069			- 0.11	0.6

2.5.7- Conclusions

Skobreen is a stable glacier, at least it has been for the last 50–100 years. It is moving slowly (< 25 m a^{-1} at the equilibrium line) and should be almost stagnant at its head. This makes the interpretation of any core easier, because the horizontal strain does not need to be taken into consideration. Characteristics of surging glaciers common elsewhere in Svalbard (e.g. contortion of moraines, rapid advance of the glacier snout, intense crevassing of the surface) have not been observed for the last 50 years. On the other hand, theoretical modelling of the thermal regime indicates that the glacier may be at the pressure point in the accumulation area, and that it may also be extremely sensitive to small variations in atmospheric temperature and net accumulation (cf. Section 2.5.6). The accumulation area is building up slowly. Further information which might reveal whether Skobreen has surged is not available. These observations question the possibility of non-stable behaviour in the past. Furthermore, it appears from the examination of data from RES in the snout that the glacier spilled over the sill, pushing towards the Paulabreen valley. Therefore, the possibility of surge behaviour with a long quiescent period cannot be ignored. Other disadvantages of Skobreen as a site for ice-core drilling include intense superficial melting in summer (even at 600 m a.s.l.) with the formation of thick ice layers, and the presence of impurities derived from the valley walls which certainly alter the chemistry of the deposited snow.

It is not advisable, therefore, to drill deeper in valley glaciers in this region for ice-core studies, because the environmental record in the ice will be blurred. One of the ice fields at higher elevation in the area (e.g. Barlaupfonna) would be the most suitable place to drill in central Spitsbergen. As an ice core only 23.1 m in length was recovered, these observations will not affect our interpretation. On the other hand, drilling in different areas of Skobreen and other valley glaciers in the area would give an insight into the thermal regime, helping, perhaps, to explain the response of sub-polar glaciers to changes in environmental conditions.

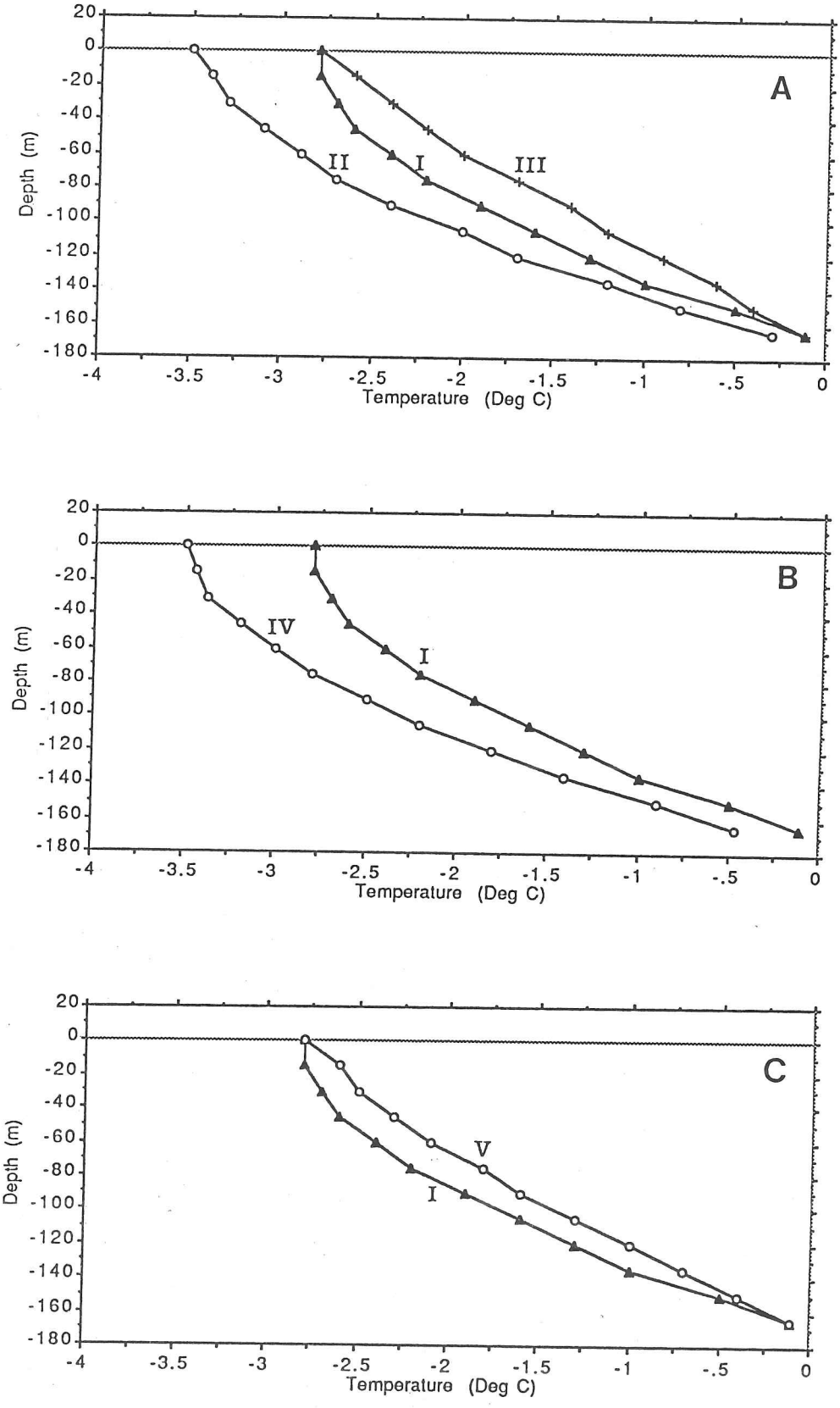

Figure 2.19- Estimated vertical temperature profiles for Skobreen based on a simple column model (see text for details). Graphs A-C depict the results of different runs (I-V), using the input data detailed in Table 2.5. The model calculates the temperature every 15 m; the temperatures are represented by a small triangle, dot or cross.

CHAPTER 3

THE SKOBREEN ICE CORE

"It is a common feature of causal investigations that today's noise is tomorrow's explained variance!"

Chorley and Kennedy, 1971

3.1- Introduction: the ice-core site

In the spring of 1986 a 23.10 m ice core was retrieved from Skobreen in central Spitsbergen. This was one of the first times that an electro-mechanical drill had been used in Svalbard and it was the first dry borehole there of more than 10 m depth. The initial plan was to drill a 125 m ice core. The main objective was to obtain a time series of environmental data for the past 600 years. Until 1986 there were only three ice cores from the whole Archipelago (i.e. Grönfjordbreen, Lomonosovfonna, and Vestfonna) for which there were substantial published environmental analyses. The core would have allowed a detailed study of environmental changes throughout the Little Ice Age in this very sensitive area (see Chapters 1 and 4) . Unfortunately, a major fault in the drilling equipment frustrated this plan. Details of the field operations are given in Appendix 3.

The ice-core site is located 600 m a.s.l. (measured by pressure altimeter with a precision of ±10 m). It was important to select a site as free as possible from undulations and sastrugi, which can affect significantly the annual layer thickness, even over a short distance (Mosley-Thompson et al., 1985). The upper reaches of Skobreen are relatively flat and the small wind drifts (shown in the Frontispiece) do not affect the results. These drifts have amplitudes of only a few centimetres and therefore are one order of magnitude smaller than the mean annual accumulation.

The main characteristics determining the selection of this site, which is fully described in Section 2.5, were: 1) high elevation, in order to minimize surface melting (unfortunately the elevation was inadequate, as discussed); 2) location as near as practicable to the ice divide (towards the head, as it is a valley glacier), where there is less horizontal flow; 3) a dynamically stable glacier (several of the glaciers in Svalbard surge from time to time); 4) ice thick enough to provide about 600 years' precipitation, as demonstrated by the 1985

RES survey; 5) representative of the central-eastern part of Spitsbergen; 6) no ice core had previously been taken from Heer Land and Nathorst Land; 7) the possibility of obtaining data from a nearby weather station (Sveagruva, 26 km north); 8) logistic limitations: the ice-coring activities were part of a major RES survey in central Spitsbergen by the Scott Polar Research Institute. Naturally the ideal site would be on an ice-cap divide, but unfortunately no information about ice thickness in the region had been available before the SPRI survey of 1985/86 (except for that of Paulabreen, which, however, is known to have surged; Rowan et al., 1982). Results of the 1986 RES survey (Drewry et al., 1987b) suggest that Barlaupfonna could provide a better environmental record.This ice cap is 700 m a.s.l. and is probably thicker than Skobreen (the estimated **h** is about 300 m). Unfortunately the RES record did not show a good bedrock return at the ice divide.

3.2- Laboratory work and analytic techniques

In this section the methodology and results of the chemical and physical analyses carried out in samples of the Skobreen core are described. Melting, percolation, and refreezing are the great drawback of the Skobreen core. Frequently it was necessary to use a methodology that could provide information about the alteration of the initial record by the meltwater (e.g. the use of the deuterium excess - *d* to help the interpretation of the stable-isotope variations). Analyses carried out included the stratigraphic examination of the core through transmitted light, density determination, tritium concentration, acidity (through the measurement of pH), electrolytic conductivity, ionic concentration (Cl^-, NO_3^-, and SO_4^{2-}), examination of the dust layers through a Scanning Electron Microscope (SEM), and crystal-size determination of two thin sections of the core. Table 3.1 summarizes the studies carried out on the Skobreen core.

3.2.1- Stratigraphic analysis

The examination of the ice core by transmitted light was useful for determining the main variations in density. Firn is less translucent than ice because it has a greater number of pore spaces. As a result, firn/ice transition is easily discernible (Fig. 3.1A). These variations turned out to provide a good representation of the general density profile (Fig. 3.2). No cycles were evident from this first examination and the profile clearly denotes a rapid change to glacier ice. This observation shows that refreezing of meltwater in firn makes a great contribution to the formation of ice at this site. It was evident that the site is subject to significant melting and refreezing on an irregular basis in the summer, sometimes forming ice layers of different thickness, at other times forming superimposed ice. Therefore it was impossible to use any stratigraphic criteria (e.g. melt phenomena and wind crusts) to identify annual accumulation cycles. This is a useful procedure for analysing cores from polar ice (e.g. Schytt, 1958; Benson, 1962; Langway, 1970) but not for analysing ice affected strongly by melting and percolation.

Table 3.1- Summary of the studies carried out on the Skobreen core

	$\delta^{18}O$ (‰)	δD (‰)	Tritium (TU)	Acidity (μ Eq l^{-1})	EC ($\mu S\ cm^{-1}$)	SO_4^{-2} (μ Eq l^{-1})	Cl^- (μ Eq l^{-1})	NO_3^- (μ Eq l^{-1})
Mean value	-12.60	-82.3	92.3	3.09	4.9	7.33	19.94	1.29
Standard deviation	0.82	6.6	81.7	1.49	5.1	6.00	16.05	1.34
Variation range	-14.48 -9.82	-97.0 -67.5	16.0 327.3	0.19 7.94	1.7 54.1	2.12 28.62	4.15 75.12	0.03 7.08
Precision of measurements	±0.15	±0.3	±6.4 [a]	± 0.002 [b]	±0.1	10%	10%	10%
Number of samples	211	61	71	211	211	34	38	29

Notes: (a) mean value.

(b) pH measurements were converted to H^+ concentration. The given precision is valid, therefore, only for pH = 7 or 0.1 μEq l^{-1}. This is because of the logarithmic scale of the pH.

The top 2.1 m was examined in the pit and was compacted snow; no structures were observed. In the next 2 m granular snow was intercalated with firn. A great number of ice layers were present below 2.1 m. Initially they were about 2–3 cm thick but at 4 m deep the first thick layer (60 cm) was observed. This suggests that in some years there was complete saturation of the snow cover during the summer (Koerner, Paterson and Krouse, 1973), perhaps even with some flush-out. In other years the melting was not so intense and the melted water may have been retained. From this point there is an irregular intercalation of firn and ice layers of different thickness. It results in the preservation of some of the snow/firn layers, which could be evidence of colder summers. Only by studying other parameters that may indicate a seasonal variation (e.g. stable-isotope ratios and ionic concentrations) can annual layers be defined. The ice sections were characterized by the intercalation of bubbly and clear ice (Fig. 3.1B). The latter identifies the previous summer surface where the melting was intense. Clear ice is in general associated with dust layers. Thirteen dust layers were pinpointed and the debris was examined under an electron microscope (see Section 3.3.9). Several times these layers were associated with clear ice with high density (i.e. $\rho > 880$ kg/m^3). In these cases the dust layers clearly marked summer melt horizons: they occurred at depths of 2.11, 13.95, 15.65, 16.28, and 17.71 m in water equivalent

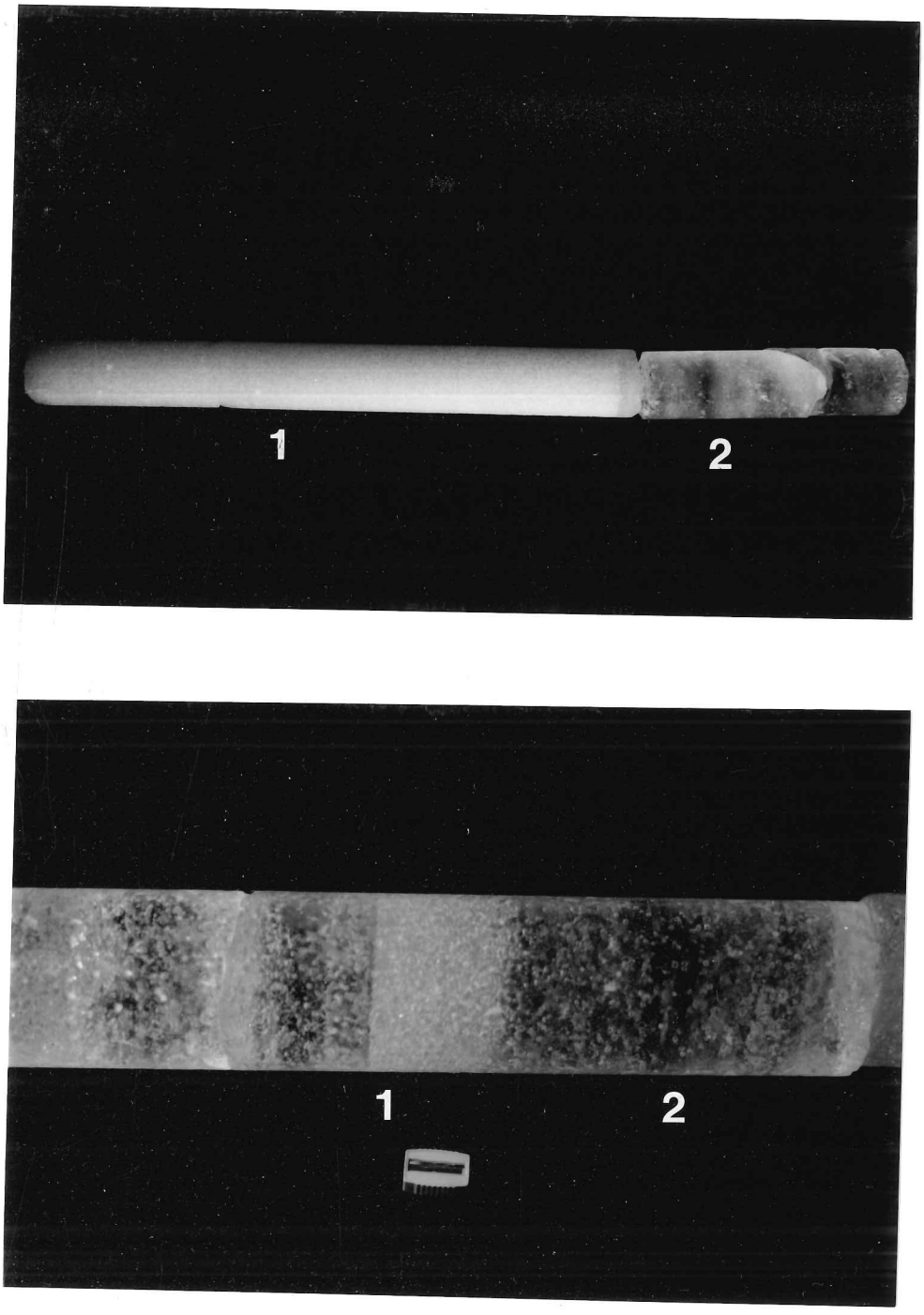

Figure 3.1- **A)** An 1 m section of the Skobreen ice core examined through transmitted light and showing the intercalation of firn (1) and ice layers (2). **B)** Detail of intercalation of firn and ice layers with different bubble concentrations. Note that the ice layer which suffered intense summer melt (2) contains fewer bubbles and is darker in the photograph. The remaining firn layer (1) of this section is very porous and is white. The difference in colours is due to light reflection and absorption processes. The sharpener used as a scale is about 2 cm in length.

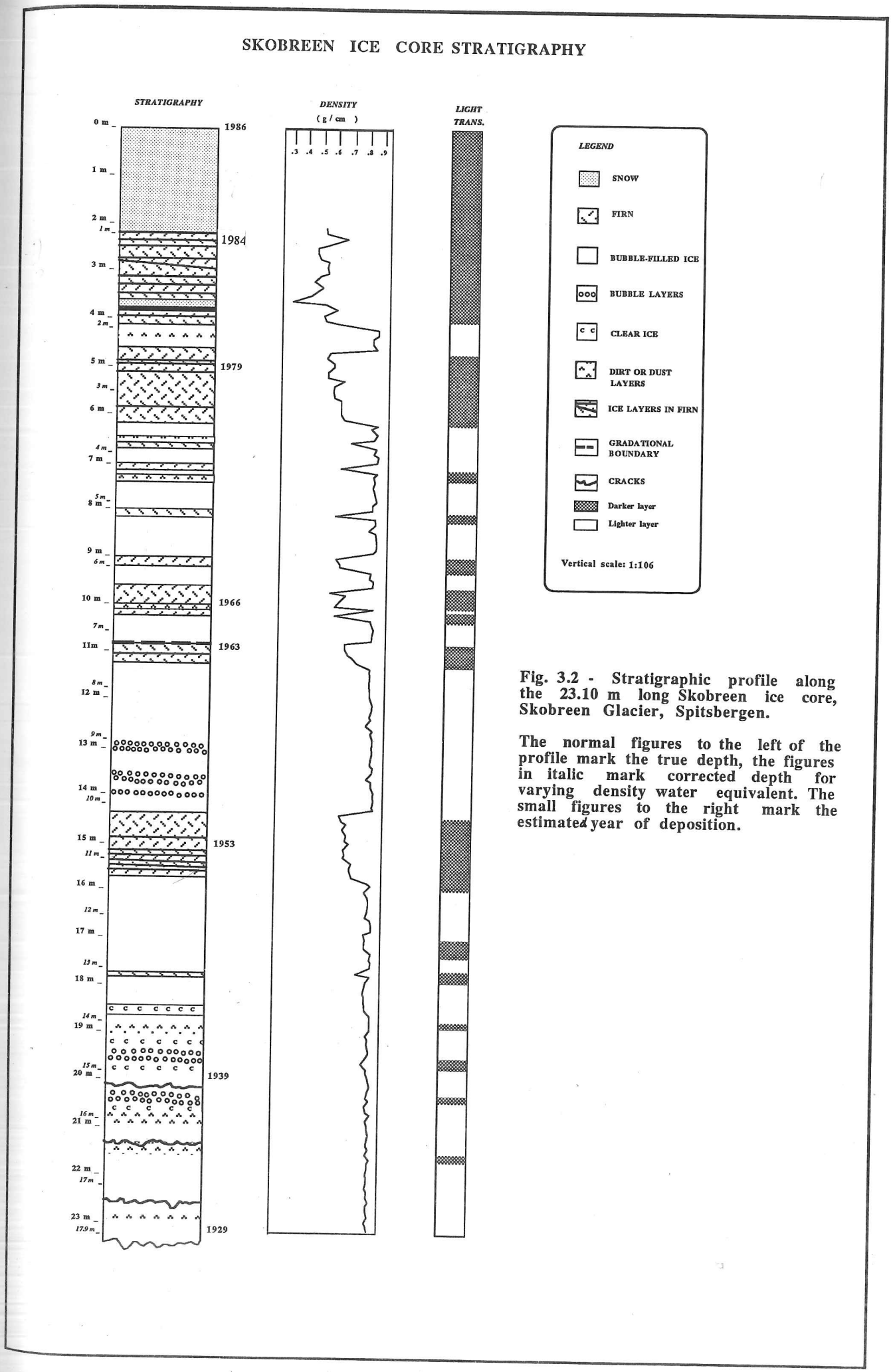

Fig. 3.2 - Stratigraphic profile along the 23.10 m long Skobreen ice core, Skobreen Glacier, Spitsbergen.

The normal figures to the left of the profile mark the true depth, the figures in italic mark corrected depth for varying density water equivalent. The small figures to the right mark the estimated year of deposition.

(Fig. 3.4K). No systematic cyclic sequence or periodicity that may have suggested annual layers was observed in the ice-core structure.

3.2.2- Sampling

A sample frequency of 10 samples per metre was chosen, bearing in mind an estimated mean annual net accumulation of 50 cm. This would be safe for examining seasonal changes (i.e. there was no danger of aliasing). Thus, after the stratigraphic examination the core was cut into 211 sections each 10 cm in length. Each segment would be measured and weighed if it was firn. The segments were then split parallel to the longitudinal axis by band saw in the clean cold-room in BP's Cold Regions Section. Half the section was sampled in different studies and the other half was stored.

About 25 cm^3 of each section was to be taken for density measurement, if it was ice. To reduce contamination, about 1.5 cm of the outside of the core was removed before placing the remainder in plastic bags for melting. Throughout the sampling process, tenon saws covered with PTFE and plastic gloves were used. The meltwater was then resampled in sealed plastic bottles of 22 cm^3 capacity and sent to the relevant laboratories for different studies.

Two 10 cm sections (from depths of 16.40 and 22.80 m) were kept intact for thin-section studies. The methodology of preparation is described in Section 3.3.10. Part of these sections was used by J. Bamber (1987) for the study of dielectric properties.

Figure 3.3 illustrates the ice-core sampling procedure. Section A was stored for further studies.

3.2.3- Density determination

Density was determined for all 211 samples. Firn sections were measured by the volume and weighing technique. Each 10 cm cylindrical section was weighed in an electronic balance with an accuracy of ±0.1 g. Volume was measured by ruler and caliper with a vernier (accuracy 0.01 cm). The density of the ice sections was measured by the hydrostatic method, following the procedure developed by Langway (1970). This allows information on the smaller variations to be obtained. Twenty-five cubic centimetres of ice was immersed in trimethylpentane 2,2,4, which is immiscible with water. It has a known coefficient of cubic expansion (c.c.e.) that is linear for the range of temperatures used (ρ = 711.76 kg m^{-3} at -4.5°C and c.c.e. = 1.07 x 10^{-3}/°C). The density was calculated from the following equation:

$$\rho_s = \frac{w_a \cdot \rho_{lt}}{w_a - w_l}$$

where ρ_s = density of the sample, w_a = weight in air, w_l = weight in liquid, and ρ_{lt} = density of the liquid corrected for temperature t_x. The density of trimethylpentane at t_x is given by: $\rho_{lt} = \rho_{l\text{-}4.5°C} \times [1 + 0.00107 (-4.5 - t_x)]$. The ice pieces were weighed in a beam balance accurate to 0.05 g. The temperature of the liquid was measured with a thermometer graduated to 0.2°C. The maximum error by the weight–volume method is of the order of 2%, and for the hydrostatic method it is of the order of 0.5% (Langway, 1970).

The density profile is plotted in Fig. 3.2, and Appendix 2 presents all the results. The mean ice-core density is relatively high, 806 kg m^{-3}, and ranges from 335 to 914 kg m^{-3}. It confirms the stratigraphic observation that there is a rapid change to glacier ice. The firn/ice transition is the result of the freezing of meltwater rather than of the recrystallization of snow and firn. Superimposed ice layers are intercalated with firn layers. No cyclicity of the annual density variations remained. The density profile confirms the visual stratigraphic observations and there is a good correlation between density and light transmissivity. After correction for density the Skobreen core is reduced to 17.90 m water equivalent.

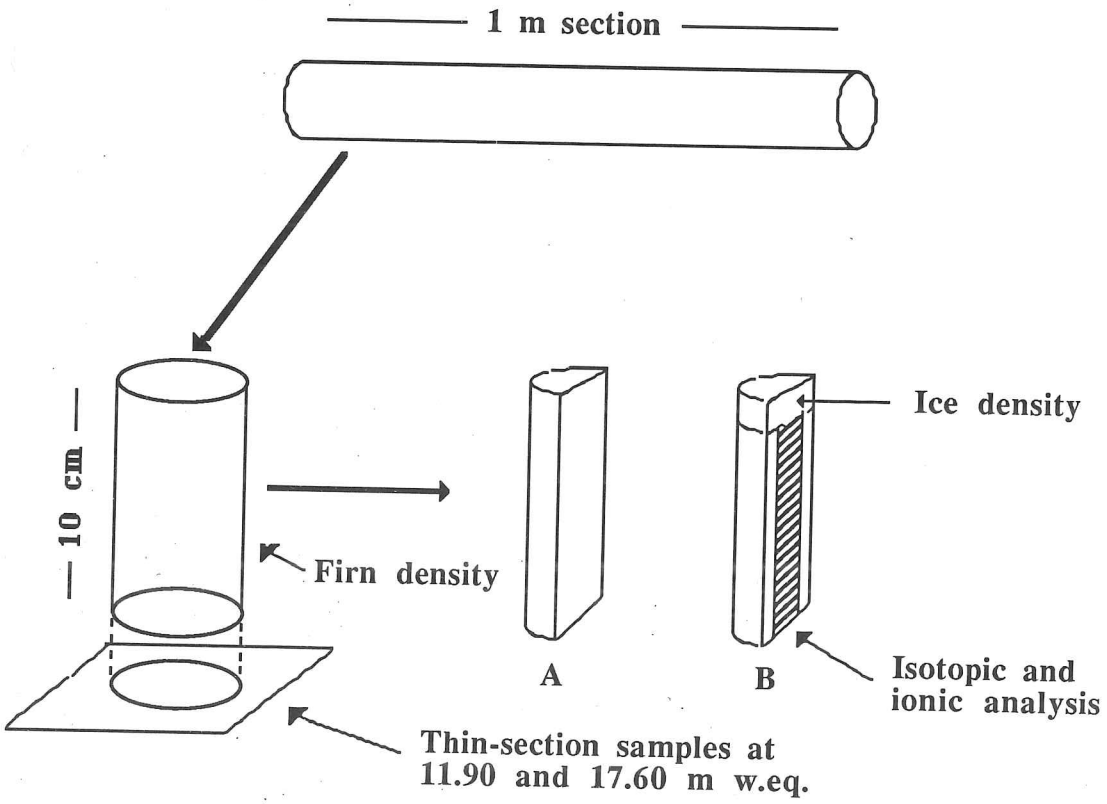

Figure 3.3- Ice-core sampling procedure

3.2.4- Stable isotopic content

3.2.4a- Introduction

The study of variations in the stable-isotope composition of snow, firn, and ice is one of the main tools of glaciology. It has played an increasing part in ice-core research since Dansgaard (1954) and Epstein (1956) drew attention to its potential for glaciology, and Epstein and Benson (1959) demonstrated that summer snow is generally heavier isotopically than winter snow. These studies are based on the fact that the contents of stable isotopes of oxygen and hydrogen are controlled by fractionation phenomena (cf. Section 4.2). In snow and ice, fractionation occurs at the liquid–vapour, solid–liquid and solid–vapour phase boundaries (Moser and Stichler, 1980).

In snow and ice which are not affected substantially by secondary processes (e.g. summer melting), the original isotope ratios are preserved. This condition is fulfilled in polar snow and ice, where it is possible to determine variations in the isotope content with depth and, if the core has been dated, the variations over time. In contrast, stable-isotope investigations in sub-polar and temperate glaciers are not very successful. Post-depositional processes such as melting, percolation, and refreezing frequently obliterate the initial isotope record. In general they render impossible the determination of the net annual accumulation, dating, and comparisons with the temperature curves. In addition, the accumulation in these areas is not usually distributed regularly throughout the year; it is concentrated in two or three periods. The net accumulation also varies substantially from year to year. For these reasons stable-isotope studies in non-polar snow and ice masses were practically abandoned after an initial wave of exploratory work in the late 1960s and early 1970s (e.g. Deutsch, Ambach and Eisner, 1966; Ambach et al., 1972; Schotterer et al., 1977). These studies have been revived in the 1980s by the use of new techniques (for example, the measurement of the relation between $\delta^{18}O$ and δD ratios) which may give better resolution of the seasonal values.

The precipitation in Svalbard shows a seasonal difference of only 2.7‰ (cf. Section 4.2). Besides, it was clear from the ice-density profile that the ice-core site at Skobreen is subject to extensive melting in the summer, so a significant homogenization of the isotope variations was to be expected. Nevertheless the stable-isotope ratios were measured in the ice samples to determine if some cyclicity or quasi-cyclicity had been preserved; to see whether they reflected the general trends and longer-term variations in the mean temperatures at the nearby Sveagruva station (Section 4.3 of this dissertation); and whether it was possible to date the ice core by cross-comparison with the mean-temperature curves.

3.2.4b- Methodology

All 211 samples were analysed for $\delta^{18}O$ by mass spectrometry. Ideally, all the samples should be analysed simultaneously for deuterium content. This would make possible a detailed analysis of the variations in *d* - deuterium excess. The oscillations of *d* may resolve the yearly annual firn and ice layers better than the oscillation of δD and $\delta^{18}O$ (Stichler et al., 1982 and below). Unfortunately this was not possible because resources were limited. Another advantage in measuring δD is that the kinetic effect is relatively small (Jouzel et al., 1987). Sixty-one samples were selected for these studies. Four 1 m sections were continuously sampled for more detailed examination. The oxygen ratios were measured by Prof. W. Dansgaard's team at the Department of Glaciology of the University of Copenhagen. The deuterium content was measured at the Centre d'Études Nucléaires de Saclay, France, courtesy of Dr. J. Jouzel. For these analyses the oxygen isotope ratios were determined with an analytical error of 0.15‰ and the hydrogen ratios were determined with an error of 0.3‰.

In this dissertation, following normal practice, the stable-isotope content of both hydrogen and oxygen in a sample are expressed with reference to **SMOW** - 'Standard Mean Ocean Water'[†] content (Craig, 1961b) . This is given by δ values from the following formula:

$$\delta x = \frac{R_{Sample} - R_{SMOW}}{R_{SMOW}} \times 1000\ (‰)$$

where x is ^{18}O or D (deuterium), and R is the ratio $\delta^{18}O/^{16}O$ or $\delta D/H$.

3.2.4c- Results

The $\delta^{18}O$ profile (Figs. 3.4C and 3.6A) displays highly damped oscillations and in general it is impossible to identify annual layers with confidence. At best, it may be possible to determine the yearly variations for some periods (e.g. between 5 and 7 m), but even these appear to have been distorted. The mean $\delta^{18}O$ for the profile is -12.66‰, but (more importantly) the standard deviation is only 0.82‰, showing the extent of damping. Further, the $\delta^{18}O$ ranges from -14.48‰ to -9.82‰ and the extreme variation in a year is only about 3.5‰. These observations reveal that the isotope values were subject to considerable homogenization. The most damped part of the core is generally associated with high density. Hence the homogenization can be attributed to percolation and the refreezing of meltwater.

---

† As a matter of fact, SMOW is not a real water body (Dansgaard et al., 1973). It is the zero point in the δ-scale which is defined on the basis of a water sample in the National Bureau of Standards, USA. Secondary standards exist in Vienna at the Section of Isotope Hydrology of the International Atomic Energy Agency.

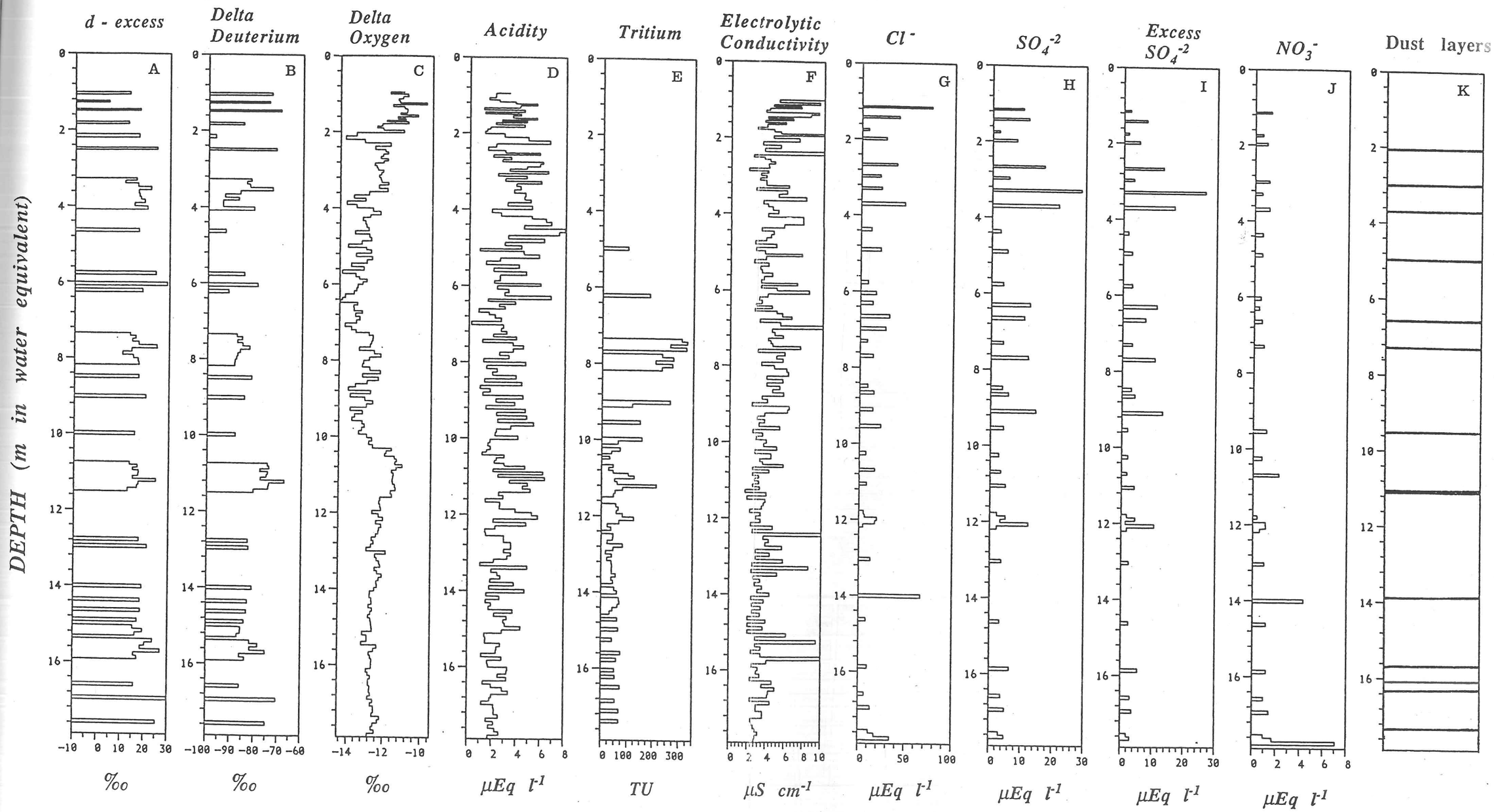

Figure 3.4- Depth variations of the different analyses carried out for the 23.1 m Skobreen ice core. Depth has been corrected for density.

Normally (i.e. in polar snow and ice) a less negative isotope ratio can be associated with warmer conditions. This is not true of the conditions encountered in Svalbard glaciers. Melting, percolation, refreezing, and flush-out may affect the superficial layers, altering the original isotope sequence. Many processes can alter the initial sequence of non-polar glaciers (see Koerner, Paterson and Krouse, 1973) and frequently occur in Skobreen and other Svalbard cores: 1) layers with low $\delta^{18}O$ and high density which are identified as summer layers (e.g. at 2.1 and 3.9 m in Fig. 3.4C). The explanation for the formation of these layers is simple. During periods of extreme warmth the upper layers will be subject to intense melting and be removed from the system (i.e. flushed out). The winter layers are left, with their low $\delta^{18}O$. Sometimes more than one annual layer can be ablated; 2) layers with high $\delta^{18}O$ and low density. The melting is not so intense, or the upper layers are at or near the pressure melting point. Meltwater percolates through the snow/firn pack. Fractionation will occur between the meltwater and snow (enriching the snow in ^{18}O at the expense of the meltwater, and the lighter isotopes will be flushed out (e.g. between 10.2 and 11.6 m in Fig. 3.4C); 3) in other years melting is restricted as a result of a cooler summer. The summer precipitation is retained, giving the impression of an isotopically warmer period.

Five major sections can be distinguished in the profile of Fig 3.4C, showing different mean isotope values and different variations in $\delta^{18}O$ from peak to trough.† These are described from top to bottom:

1) 0.87–2 m deep - an upper part with low density and showing four summer $\delta^{18}O$ peaks. This section has the highest mean values for the core, -11.04‰. The mean isotope difference between peaks and troughs is about 1.5‰. The high variability of the isotope content (associated with very low densities) indicates that melting, refreezing, and homogenization were restricted. This is confirmed by the small $\delta^{18}O$ difference between the upper part of this section and pit S_1 (588 m a.s.l.) of the 1985 survey. The δ values are -11.2 ± 0.3 and -11.9 ± 0.2 respectively.

The sequence is terminated by a relatively abrupt fall in the isotope ratio. This lower layer has the lowest ^{18}O content in the core and high density (ρ = 900 kg m^{-3}). It therefore marks a period of intense melting, with the flush-out of the summer layer (see observation above) and formation of superimposed ice. This interpretation is reinforced by the high concentration of large particles (i.e.> 20 μm), which indicated that they were supplied by the adjacent valley walls (see section on the particles analysis).

† All discussions here and in the following sections refer to the density-corrected profiles (i.e. in water equivalents) unless otherwise stated.

The upper 87 cm were not sampled, but are assumed to represent one year, or at most two years, of accumulation, so the abrupt reduction in $\delta^{18}O$, at 2.1 m depth, should represent the summer of 1980 or 1981.

2) 2.1–4.0 m deep - the seasonal variations in $\delta^{18}O$ are highly damped. Fractionation between the snow/firn and percolating water may have been the cause. The density is low and this suggests that at the time of the percolation the snow pack was at or near the pressure melting point so no refreezing occurred and the lighter isotope was removed. The sequence is terminated by another layer of superimposed ice with low $\delta^{18}O$ that may have had the same genesis as the layers at 2.1 m.

3) 4.0–10.2 m - the lowest isotope ratios are encountered in this section. The greater variability of density and $\delta^{18}O$ indicates that summer temperatures were sufficient to melt only part of the superficial layers. Meltwater percolated the underlaying layer and refroze. The seasonal variability is not clear. Differences between troughs and peaks are at most 2‰. It would be risky to interpret them as seasonal variations in view of the complexity of the process affecting the snow/firn pack.

In the lower part of the section (i.e. from about 7.5 m w.eq.) the increase in density points to more intense melting, so the isotope record may also have been altered by fractionation with meltwater.

4) 10.2–11.6 m - at 10.2 m there is a relatively abrupt increase in $\delta^{18}O$ (i.e. 2.8‰). The $\delta^{18}O$ is associated with low-density layers. Although melting in the core as a whole is high, some of the original firn layers were preserved at this depth. It seems, therefore, that the layers just above this section were subject to intense and rapid melting, forming superimposed ice which isolated the firn from further alteration. The period is relatively warm isotopically, although it may represent post-deposition fractionation rather than the original conditions of the precipitation.

5) From 11.6 - the record is totally damped, with a mean value of -12.57‰. It is certain that it been subjected to intense melting, followed by percolation. The homogenization was so intense that the standard deviation of the mean $\delta^{18}O$ is only 0.26‰. Some layers may have been obliterated. The high homogenization may have been caused by intense melting during a warm period, possibly at the time of deposition of the layers in section four. Meltwater would have percolated through 10.2–11.2 m and refrozen in the lower layers.

From the density observations it is clear that melting is intense enough to form superimposed ice layers even at this altitude (i.e. 600 m a.s.l.). The original isotope ratios will rarely be retained in these conditions. However, if the flush-out is not very intense, the

The upper 87 cm were not sampled, but are assumed to represent one year, or at most two years, of accumulation, so the abrupt reduction in $\delta^{18}O$, at 2.1 m depth, should represent the summer of 1980 or 1981.

2) 2.1–4.0 m deep - the seasonal variations in $\delta^{18}O$ are highly damped. Fractionation between the snow/firn and percolating water may have been the cause. The density is low and this suggests that at the time of the percolation the snow pack was at or near the pressure melting point so no refreezing occurred and the lighter isotope was removed. The sequence is terminated by another layer of superimposed ice with low $\delta^{18}O$ that may have had the same genesis as the layers at 2.1 m.

3) 4.0–10.2 m - the lowest isotope ratios are encountered in this section. The greater variability of density and $\delta^{18}O$ indicates that summer temperatures were sufficient to melt only part of the superficial layers. Meltwater percolated the underlaying layer and refroze. The seasonal variability is not clear. Differences between troughs and peaks are at most 2‰. It would be risky to interpret them as seasonal variations in view of the complexity of the process affecting the snow/firn pack.

In the lower part of the section (i.e. from about 7.5 m w.eq.) the increase in density points to more intense melting, so the isotope record may also have been altered by fractionation with meltwater.

4) 10.2–11.6 m - at 10.2 m there is a relatively abrupt increase in $\delta^{18}O$ (i.e. 2.8‰). The $\delta^{18}O$ is associated with low-density layers. Although melting in the core as a whole is high, some of the original firn layers were preserved at this depth. It seems, therefore, that the layers just above this section were subject to intense and rapid melting, forming superimposed ice which isolated the firn from further alteration. The period is relatively warm isotopically, although it may represent post-deposition fractionation rather than the original conditions of the precipitation.

5) From 11.6 - the record is totally damped, with a mean value of -12.57‰. It is certain that it been subjected to intense melting, followed by percolation. The homogenization was so intense that the standard deviation of the mean $\delta^{18}O$ is only 0.26‰. Some layers may have been obliterated. The high homogenization may have been caused by intense melting during a warm period, possibly at the time of deposition of the layers in section four. Meltwater would have percolated through 10.2–11.2 m and refrozen in the lower layers.

From the density observations it is clear that melting is intense enough to form superimposed ice layers even at this altitude (i.e. 600 m a.s.l.). The original isotope ratios will rarely be retained in these conditions. However, if the flush-out is not very intense, the

long-term variations and trends may be recognizable. Fig. 3.5 compares the $\delta^{18}O$ profile of the 23.1 m ice core with the 9 m ice core recovered in 1985. The main variations and trends are similar, although the resolution of the 9 m core is restricted by the sampling (only 1 sample from each 20 cm). The correspondence of $\delta^{18}O$ confirms that the variations are representative of the mean conditions of the initial precipitation. Such correspondence would not be expected if a glacier was strongly affected by flush-out. The net accumulation and changes in the isotope ratios would be irregular over the whole glacier surface. It is known that ice cores from temperate glaciers recovered less than 100 m apart show substantially different $\delta^{18}O$ profiles (e.g. Schotterer et al., 1977). On Skobreen the two ice cores were drilled about 2 km apart and the difference in altitude is 112 m. Therefore it can be concluded that the ice-core site on Skobreen is not subject to great flush-out of meltwater, although it can be affected by substantial melting. In other words, the melting water in general refreezes at the site and the system can be considered closed. The mean $\delta^{18}O$ of the 9 m core is -11.7‰ and the corresponding section in the 23.1 m core has a mean of -12.7‰. The difference is explained by more intense melting at a lower elevation and therefore a stronger flush-out of the lighter isotope. As discussed below, the latter conclusion is corroborated by a lower *d* - excess deuterium in the 9 m core.

Fig. 3.6 compares the $\delta^{18}O$, δD, and excess deuterium profiles. A polynomial is fitted to the three profiles to represent the main variations. The δD ranges from -97.0 to -67.5‰. Although the number of samples is restricted (only 61), there are obvious similarities between the δD and $\delta^{18}O$ profiles. In the four 1 m sections (I–IV) the difference between the isotope troughs and peaks is slightly more marked. Nevertheless they do not allow the determination of the net annual accumulation. The two low $\delta^{18}O$ values associated with ice layers at 2.1 and 3.8 m depth are well represented in the ^{2}H content profile. The lowest values are found at 2.2 m. Finally, the abrupt reduction in the δ values at 10.2 m is represented by a change of 15‰ of the deuterium content.

The relationship between δD and $\delta^{18}O$ in the 61 samples from the Skobreen ice core is plotted in Fig. 3.7. The relationship does not follow Craig's meteoric water line (cf. Section 4.2). This is to be expected: first, because the original isotope record has been altered by intense melting, percolation, and refreezing; second, because condensation in the Archipelago does not occur in thermodynamic equilibrium and is altered by different processes when precipitation is falling, as described in Section 4.2. The regression obtained for the Skobreen core samples ($\delta D = (6.0 \pm 0.6)\ \delta^{18}O - (7.8 \pm 7.9)$‰) is not significantly different from the relationship for the precipitation samples from Isfjord (Fig. 4.5). The high uncertainty reflects the clustering of isotope values. Further, as a consequence of the *d* versus $\delta^{18}O$ antiphase correlation the δD versus $\delta^{18}O$ diagram shows a slope less than 8 (Johnsen, Dansgaard and White, in press) even though the great majority of the samples have values close to Craig's equation.

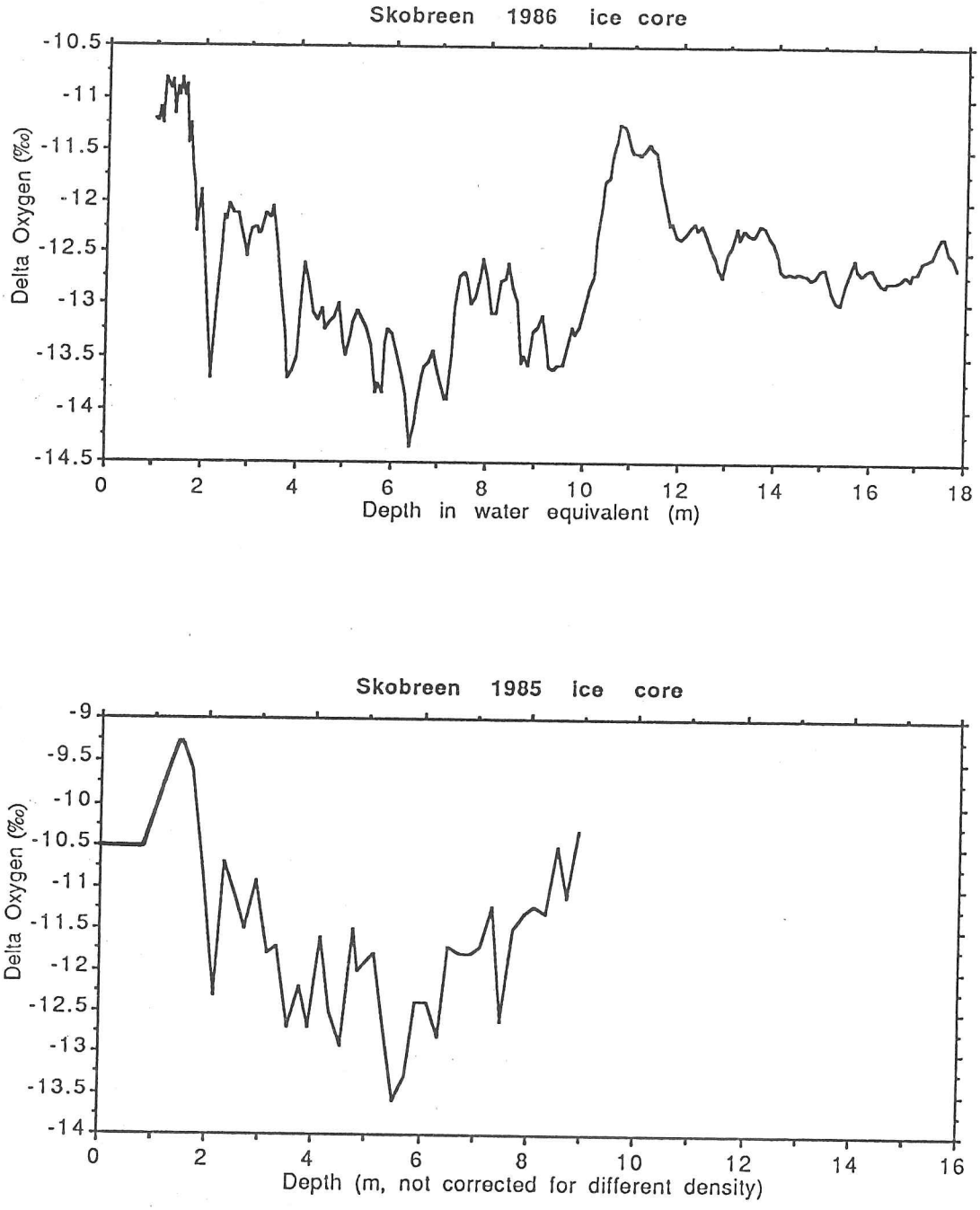

Figure 3.5- Comparison of the $\delta^{18}O$ (‰) profile of the ice core recovered in 1985 (9 m) with the core recovered in 1986 (23.1 m). Note that the profile of the core recovered in 1985 has not been corrected for variations in density.

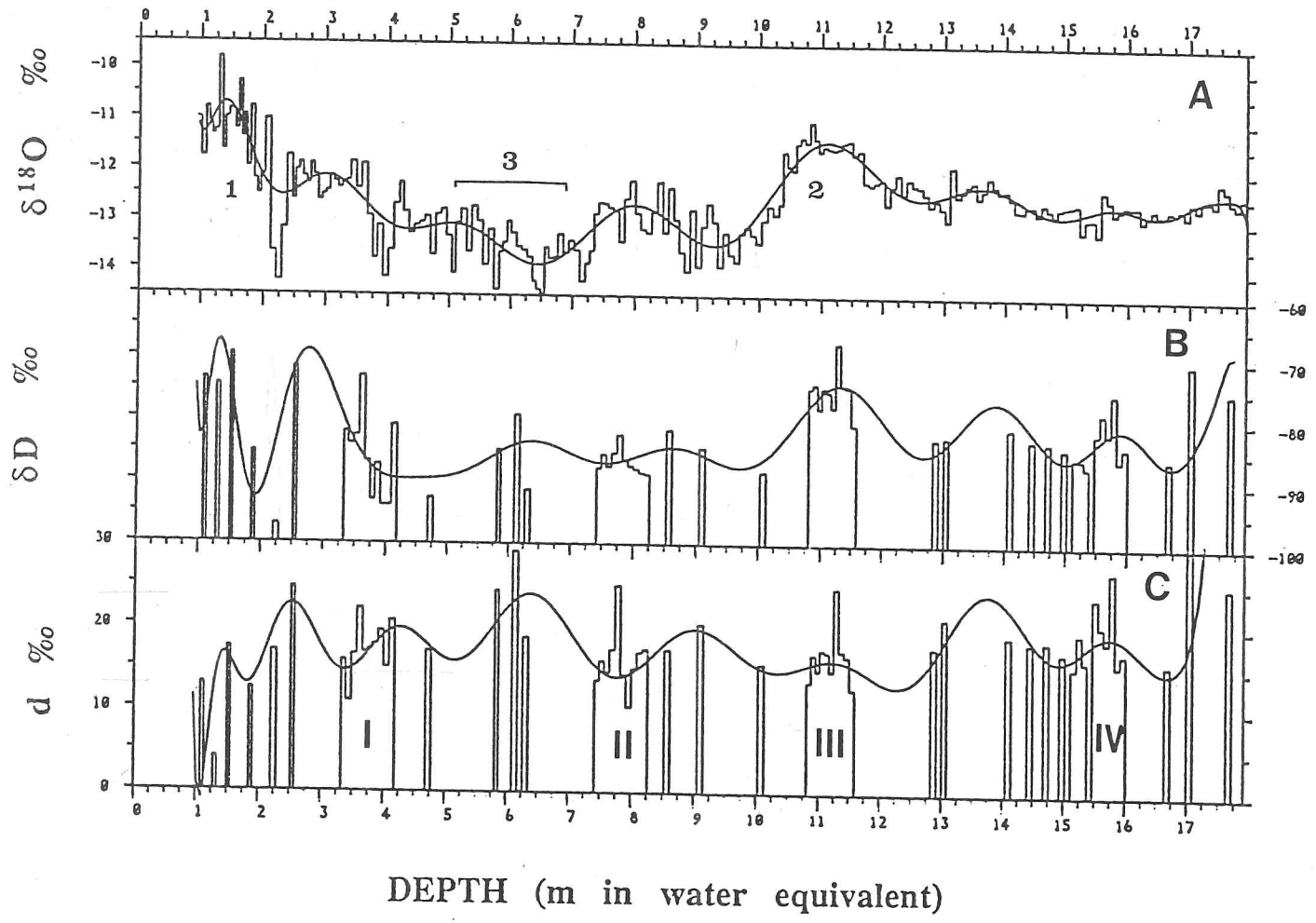

Figure 3.6- Variations of the stable-isotope ratios and excess deuterium - *d* in the 23.1 m Skobreen ice core. A polynomial is fitted to the three profiles to represent the main variations. Areas identified by the numbers 1-3 in the $\delta^{18}O$ profile refer to discussions in Section 3.2.4.

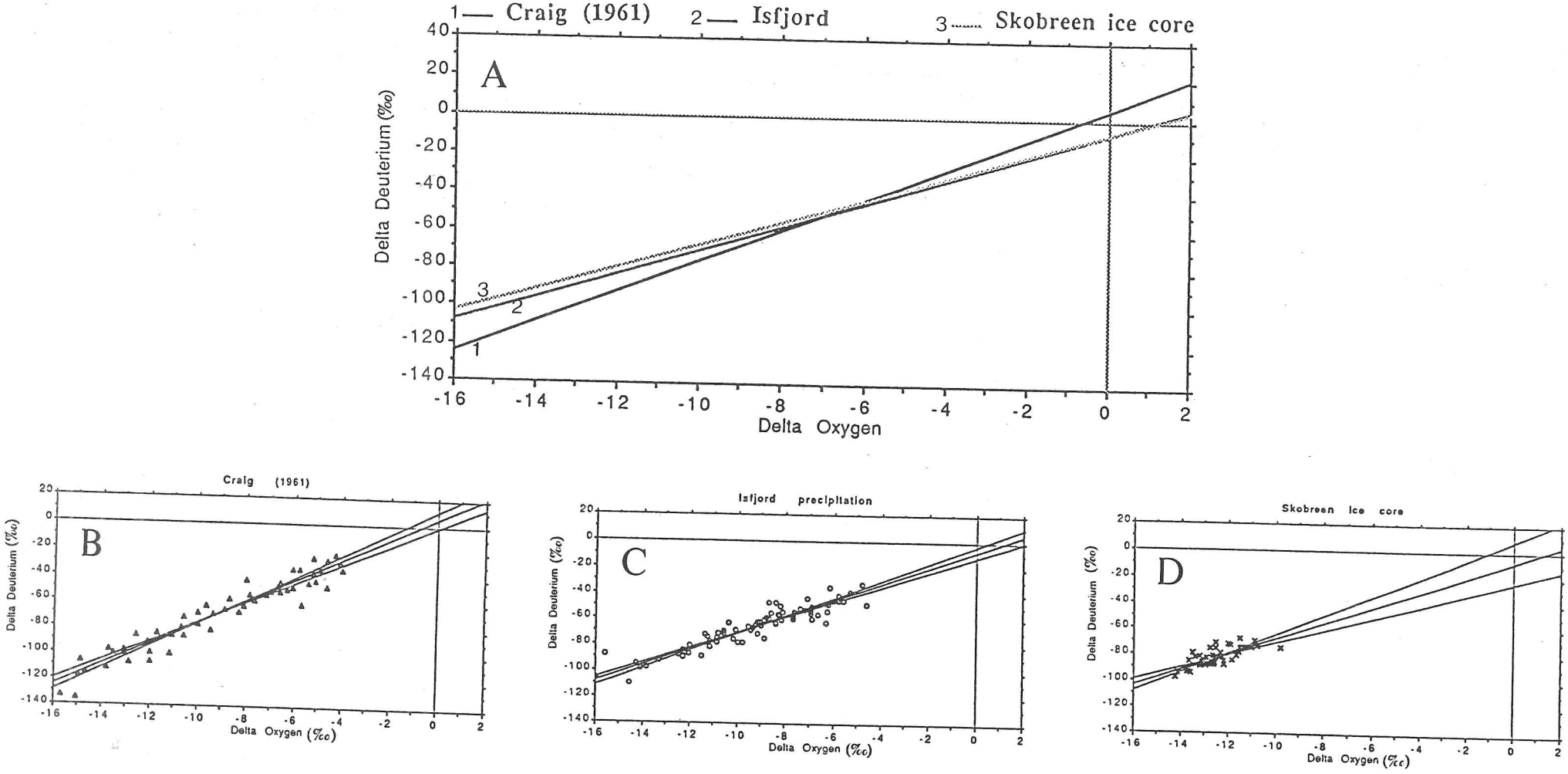

Figure 3.7- Comparison of the δD-$\delta^{18}O$ relationship of samples collected at the IAEA network station at Isfjord and from the meteoric water line (Craig, 1961). Figs. 3.7.B-D represent the δD versus $\delta^{18}O$ relationship for each set of samples. The two lines equidistant from the correlation line represent the 95% confidence limits for the slope of the correlation. Compare with Fig. 4.5, which also plots the δD-$\delta^{18}O$ relationship for Isfjord samples collected in the winter.

The Skobreen isotope record shows why studies in firn and ice samples from temperate and sub-polar glaciers have been restricted. The interpretation of the isotope values is complex, if not impossible. More recent studies (Stichler et al., 1982; Baker et al., 1985; Oerter et al., 1985) show, however, that it is feasible to determine the annual layers by the examination of variations in the so-called excess deuterium - *d*. The deuterium excess is expressed as the relationship between δD and $\delta^{18}O$ and is given by: $d = \delta D - 8\delta^{18}O$. Furthermore, *d* can give some insight into the processes that alter the isotope ratios. Stichler et al. (1982) demonstrated that during melting and evaporation the deuterium excess will decrease while the stable-isotope ratios increase (cf. Fig. 3.8). The opposite is true during condensation. At night, for example, the formation of hoar frost increases *d* in the top 1–2 cm of the the snow surface (Stichler, 1982). As shown in Section 4.2, there is a also a marked seasonality in *d* in precipitation from Isfjord. The summer *d*, already lower, will be reduced further. Hence layers with low *d* can be identified as summer layers.

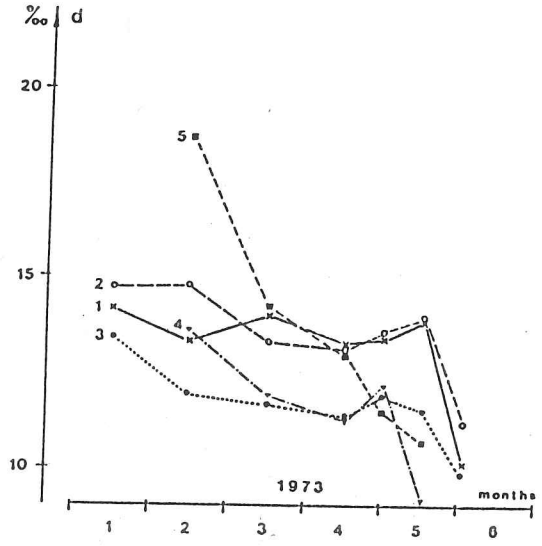

Figure 3.8- Depletion of deuterium excess - *d* in different layers (nos. 1–5) during the melting process of the natural snow cover at Weißfluhjoch/Davos, Switzerland, between January and June, 1973. Source: Martinec et al., 1977.

A year-by-year resolution is not possible for the Skobreen ice core, as the deuterium content profile is not continuous. On the other hand, some general conclusions can be drawn. The deuterium excesses of Skobreen are high when compared with values at Isfjord; they have a mean value of 17.8 ± 0.6‰ and range from 4.1 to 29.9‰. The difference can be explained by an altitude effect. For instance, the lower temperature will reduce the proportion of rain and re-evaporation. The variations in *d* are much greater than the isotope-ratio variations. The main oscillations of *d* are in antiphase with the $\delta^{18}O$ values. The sections identified as warm periods, from 0.87–2.1 m and from 10.2–11.2 m (# 1 and 2 in Fig. 3.6), have a lower *d* value. This low *d* value confirms that these sections were subject to

melting.The cooler part of the record (i.e. from 5 to 7 m) has the highest *d* (area # 3 in Fig. 3.6).

The four continuous 1 m sections provide information on the net accumulation for several years. Layers with peaks in the δD and $\delta^{18}O$ profile and a trough in *d* were interpreted as being summer layers. Net accumulation varies from 18 to 43 cm a^{-1} in w.eq. These great variations are to be expected. Ablation and accumulation conditions are known to vary greatly from year to year in Svalbard (cf. Section 2.3.3). In the upper 1 m section (from 3.4 to 4.2 m depth) three annual layers have been identified and they show accumulation ranging from 20 to 33 cm a^{-1}. In the cooler isotope period the accumulation increases to 40 cm a^{-1} from 7.5 to 8.1 m and it is reduced to 27 cm in the lower section at 15.1 m. The association of high *d* with low δD and $\delta^{18}O$ values also identifies a winter layer in the rest of the profile.

3.2.5- Tritium content

3.2.5a- Introduction

Tritium and other by-products of thermonuclear explosions have been used intensively in glaciology for the last 25 years. Picciotto and Wilgain (1963) demonstrated that reference horizons were formed by stratospheric fall-out of radioactive debris from thermonuclear explosions, thus making possible the dating of ice cores and determination of the mean net accumulation rate from the time of fall-out and the collection of the sample (Crozaz, Langway and Picciotto, 1966; Hammer et al., 1978).

In nature tritium is formed by the interaction of cosmic rays with the upper atmosphere, and the estimated natural level ranges from 4 to 25 TU (Gat, 1980). Since 1952 (the Ivy experiment) the atmosphere has been swamped with artificial tritium produced by thermonuclear explosions. The dates of these weapons tests are well known and therefore serve as reference horizons. The greatest injections of tritium from weapons testing occurred in 1954, 1955, 1958, and again in 1961–62. The all-time maximum occurred at the end of 1962 as a result of a series of tests by U.S.A. and U.S.S.R. The most powerful explosions were in Novaya Zemlya and should, therefore, be well represented in firn and ice in Svalbard, particularly the explosion of 58 Mt (Holdsworth et al., 1984). Subsequently, the People's Republic of China and France carried out a series of smaller weapons tests. The Chinese explosions of 1967–70, and later in 1973/74, 1976, and 1978, may have left an imprint in Svalbard snow and ice. The French explosions (from 1973 to 1980) occurred in the Southern Hemisphere and were on a smaller scale, so they are not expected to be recognizable in Svalbard.

Residence time in the atmosphere should be taken into account when identifying a layer. On average the first tritium fall-out would be traced a year after tests carried out in the

same hemisphere as the deposition site and two years later if in the other hemisphere. Another important feature of tritium content in the atmosphere is a yearly cycle of maximum concentration in spring and summer in the Northern Hemisphere. Thus it provides an additional method of counting annual layers.

A new reference level in the Northern Hemisphere was created by the nuclear accident at Chernobyl (USSR). The gross β–activity measured in snow and samples from Alpine glaciers are of the same order of magnitude as the contamination of the firn in 1963 (Ambach et al., 1987). On Austfonna β-radioactivity of 8.84 Bq kg^{-1} was measured in May 1986 (Pourchet et al., 1988), so this horizon may be used as a new reference horizon in Svalbard.

3.2.5b- Sampling

The mean net accumulation rate was estimated to be between 50 and 70 cm a^{-1} w.eq. before the drilling of the ice core, and so the 1963 peak in tritium concentration was expected to occur between 11.5 and 16.1 m. The lower 8 m of the core were sampled, taking this estimate into account. For each 10 cm section a 20 ml sample was collected and sent in sealed bottles to the Physikalisches Institut at the University of Bern, where the samples were analysed by Professor H. Oeschger and his team. The first results showed that the net accumulation had been overestimated, and additional measurements were carried out for samples from between 4 and 10 m depth. Unfortunately, these later analyses had to be restricted as the ice core had been used by then for other analyses.

Until these studies, no results had been published on the tritium content of snow and ice on Svalbard.* Soviet scientists have been using the measurement of the gross β-activity to identify the bomb-produced radio-isotope layers. This process is less expensive than the measurement of tritium concentration (Julian Paren, personal communication). However, the process is not appropriate for glaciers with dust layers. It is known that dust horizons act as filters for ^{210}Pb, ^{137}Cs, and ^{90}Sr. In addition, some clays absorb ^{137}Cs, creating false β-activity peaks (Schotterer et al., 1977).

3.2.5c- Results

Fig. 3.4E shows the tritium profile of the core. The values range from 16 to 327 TU (tritium units†). All samples were decay-corrected for the time of collection (i.e. May 1986). The maximum tritium value was encountered at 7.4 m depth (Fig. 3.4E). No seasonality in tritium content is observed throughout the core.

† 1 TU (tritium unit) is equivalent to $T/H = 10^{-18}$. 1 TU – 3.2 pCi or 0.12 Bq per litre of water.

* Drewry and Liestøl (1985) reported the use of tritium to estimate the net accumulation rate in Austfonna, but no figures for the tritium content are given.

The ^{3}H profile can be divided into three sections with different patterns. From a depth of 4–10.4 m the distribution of tritium forms a bell shape. The tritium content increases from 96 TU to an absolute maximum of 327 TU at 7.4 m, decreasing then to 30 TU at 10.4 m. All the values in the section are above natural levels. The layers at about 7.4 m are, therefore, interpreted as having been deposited within the years 1961–64. If the peak at 7.4 m is taken as 1963, this will result in a mean net accumulation ratio of 32 cm a^{-1} w.eq.

If the peak at 7.4 m is decay-corrected for 1963 it represents about 1100 TU. According to the precipitation data from Svalbard the value to be expected is about 5000 TU (IAEA, 1969). The additional decrease in the tritium content suggests an intense wash-out or percolation to lower layers (Oerter and Rauert, 1982). The latter process is more probable, as tritium levels at the bottom of the core are greater than the natural level (i.e. > 25 TU). Exchange between the meltwater and snow/firn layers would have increased the original tritium levels (Theodórsson, 1977). The relatively high values in the two shallowest samples may represent the explosions carried out by the People's Republic of China in the 1970s. On the other hand, these two samples with high tritium content may have been a result of percolation of meltwater coming from higher up the glacier. It is not possible to comment further without a more detailed profile.

In the second section a maximum of 212 TU is reached at 11.2 m depth and it decreases to 22 TU at 12.2 m. One could interpret this second increase in tritium as the result of thermonuclear explosions between the years 1952 and 1954. If the peak value is considered to have been deposited in 1953 (i.e. the Castle explosion of 1952), it will result in a mean net accumulation of 34 cm a^{-1} for the period 1953–86, and 39 cm a^{-1} for the period 1953–63. On the other hand, bearing in mind the high melt rate at the site, this interpretation is uncertain. The relatively high values may represent contamination from the layers above. It is necessary, therefore, to use other methods to confirm the mean net accumulation rate. This is done in Section 3.3, where the dating of the core is discussed (cf. Table 3.3)

No strong variations are observed along the lower section (i.e. from 12.2 m to the bottom). However, a mean value of 52 ± 3 TU in this section indicates that these layers were intensively contaminated by percolation before the transformation to ice. Assuming that the firn/ice transition was 15 m from the surface, as it is now, these layers may have been enriched with tritium from all the explosions which occurred between 1951 and 1964.

3.2.6- Acidity

3.2.6a- Introduction

The study of acidity profiles from ice cores is valuable for revealing past vulcanism and for providing a record of anthropogenic acid emissions. The acidity of the Skobreen core

was investigated to evaluate recent observations of high acidity in superficial snow on Svalbard (Semb, Brækkan, and Joranger, 1984), and to obtain an acidity time series. It aimed to provide a historical record of atmospheric pollutants arriving in Svalbard from northeast Scandinavia and the USSR (the record of anthropogenic pollutants in snow and ice in Svalbard is discussed in detail in Chapter 5). It aimed also to examine whether the volcanic impurities from a volcanic eruption had left an imprint in the ice-core chemistry, and if so to use the resulting peaks as reference horizons.

Acidity measurements are useful for investigating trends in anthropogenic emissions of pollutants in the Northern Hemisphere. The increase in tropospheric pollution in the 20th century has been successfully revealed by ice-core acidity measurements in the Canadian High Arctic (Koerner and Fisher, 1982; Barrie, Fisher and Koerner, 1985) and Greenland (Finkel, Langway and Clausen, 1986). These studies have also confirmed that it is possible to recognize seasonal variations in acidity. From Arctic haze studies it is well known that there is a strong seasonality in acidity and other pollutants in the Arctic atmosphere (Barrie, Fisher and Koerner, 1985; Barrie, 1986; Ottar and Pacyna, 1986). This is because the Arctic lower troposphere is loaded with man-made pollutant emissions mainly from December to April (Barrie, 1986). The pollutant material originates from the industrial areas of Eurasia; in particular, central Europe, Scandinavia and the USSR produce a high concentration of strong acids (i.e. H_2SO_4, HNO_3, and HCl), due to smelting, other industrial processes, and fossil-fuel combustion, associated with other impurities (e.g. Pb, Zn, and Ni; Ottar and Pacyna, 1986). In the Arctic, the archipelagos of Svalbard and Franz Josef Land are the first land masses in the pathway of air masses coming from Eurasia (cf. the discussion of pollution meteorology in Chapter 5, and see Fig. 5.1A). Therefore, they are the first sink for the pollutants and the precipitating snow contains a high concentration of impurities. Semb, Brækkan, and Joranger (1984) confirmed that the winter precipitation in Svalbard is highly acidic (pHs range from 4.53 to 5.01, or from 29.6 to 9.8 $\mu Eq\ l^{-1}$). If some seasonality in H^+ concentration could be identified in the ice core, this would provide an additional method by which to recognize annual layers and to help date the core.

There are some local sources of air pollution, particularly the emission of sulphur by a coal-burning electric power plant in Longyearbyen. Ottar, Pacyna and Berg (1986) report the effect of local sources, natural and anthropogenic, on a layer of polluted air at low altitude (i.e. below 1500 m) in summer. This may increase the background acidity in summer. On the other hand, the predominant wind directions in Longyearbyen (S-SE) will take any pollutant in the opposite direction to Skobreen. The coal mined in winter in Sveagruva accumulates in heaps in the open air and may have contributed to impurities to the Skobreen core. It is not possible to separate the local and long-range sources without further studies.

Several studies on variations in acidity have been carried out on Arctic (Hammer, 1977; Hammer et al., 1981a) and Antarctic (Delmas et al., 1985) ice cores. They have demonstrated that it is possible to derive a sequence of major volcanic eruptions, for different time-scales. The peaks in H^+ result from large quantities of sulphates which originate from the emissions of H_2S and SO_2 by volcanic activity in the atmosphere. The peaks can be detected by static electrical conductivity analysis, electroconductivity of the meltwater, and measurements of sulphate content in ice cores, in addition to the acidity (Hammer, 1977; Delmas et al., 1985). The date of some of these eruptions is well known and therefore can be used as reference horizons to help date ice cores. For the time-scale thought to be covered by the Skobreen ice core, no major eruption is known, with the exception of Gonung Agung in 1963. However, this volcano is located in the Southern Hemisphere (Bali) and its acid peak would have been reduced. Ice cores retrieved from the Canadian Arctic islands and Greenland (Barrie, Fisher and Koerner, 1985) do not record this explosion.

The volcanic eruption in Beerenberg on Jan Mayen (71° 00'N 08° 20'W) in 1970 is the only one that might have left some imprint in Svalbard ice masses over the time-scale covered by the Skobreen ice core. This eruption was small compared with eruptions that injected dust and gases into the stratosphere on a global scale. On the other hand, the location, timing, and characteristics of the eruption may have influenced the transport of acidic components to Svalbard. Jan Mayen is not only relatively near to Svalbard (i.e. about 1000 km to the SE; see Fig. 1.5) but it is situated in the track of the main cyclones that move from Iceland to Svalbard in the summer season (the eruption was in September). Therefore some of the ejected material could have been transported by tropospheric circulation, although the lifetime of dust in this layer of the atmosphere is short. Furthermore, the volcanic cloud was observed to reach an altitude of 10 km, so it reached the stratosphere and may have injected gases into the Junge layer. In this layer the emitted SO_2 is converted into fine sulphuric acid aerosols and transported to higher latitudes (Delmas et al., 1985). It should be added that a strong smell of sulphur was observed in the area (Siggerud, 1972). Therefore one of the objectives was to find a peak in acidity associated with liquid conductivity and the sulphate content of the Skobreen ice core, for use as a reference horizon and to help date the core.

3.2.6b- Methods

Acidity was measured in all the ice-core samples with a pH meter. The equipment used was a pH stick, Gallenkamp PHK-120-B, with a precision of 0.01 at pH 7; it was calibrated with buffers of pH 4 and 7. The pH results were converted to a concentration of H^+ in $\mu Eq\ l^{-1}$ and are plotted in Fig. 3.4D.

The main problem when measuring pH is the uptake of atmospheric CO_2, which appears as H_2CO_3 in melted snow and ice samples and reduces the pH. The literature cites

several ways of reducing the influence of CO_2: for example, the purging of CO_2 by bubbling nitrogen gas in the melted samples and measuring the pH in a nitrogen atmosphere (Paren, 1970). Nitrogen is inert and does not form ions in solution. Hammer and Clausen (1986) melted the samples in a microwave oven to reduce the CO_2 uptake. It is advisable also to use other techniques, such as acid titration (Legrand, 1980; Aristarain, Legrand and Delmas, 1982), to control the results. Unfortunately, it was not possible to use either of these methods because resources were limited. The pH was measured after the sample bottle had been open for 10 minutes (to achieve equilibrium with the atmospheric CO_2) in a well-ventilated clean room at ambient temperature (i.e. 21°C). This procedure results in a constant H_2CO_3 background for all the samples, so the variations in acidity cannot result from varying CO_2 uptake. For one in four samples the pH was also measured after another 4 and 8 minutes. No substantial difference was observed between the extra measurements. This confirms that the uptake of CO_2 achieved an equilibrium. A sample of three-distilled deionized water (pH ≈ 5.7) was used as reference and was repeated measured over time.

3.2.6c- Results

The acidity profile in Fig. 3.4D shows rapid variations, contrasting with the stable-isotope profiles. Four to five acidic peaks may be observed in a 1 m section. The difference between the peaks and the adjacent troughs varies between 3.5 and 5 $\mu Eq\ l^{-1}$. This is a little less than the values observed for seasonal differences elsewhere in the Arctic (e.g. Koerner and Fisher, 1982). Forty-seven peaks were identified. If these peaks are interpreted as annual late winter–early spring maxima, the mean annual net accumulation rate (a_n) will be about 36 cm a^{-1}. On the other hand, some uncertainty exists about this estimate as the variations in acidity appear to have been damped in some sections (e.g. 12.5–13.5 m and 14.5–15 m in Fig. 3.4D). Percolation of H^+ to lower layers may have been the cause. Another 3–4 peaks may be added and would result in $a_n \approx 33$ cm a^{-1}. The number of cycles per metre of this time series are examined by spectral density analysis in Section 3.3 to confirm these observations (or not).

There is a general increase in acidity from bottom to top, with a rate of change of 0.088 $\mu Eq\ l^{-1}\ m^{-1}$ (st. error = 0.011). A maximum acidity of 7.9 $\mu Eq\ l^{-1}$ is measured at a depth of 4.5 m. However, this increase is interrupted by a fall in acidity where an overall minimum of 0.2 $\mu Eq\ l^{-1}$ is reached (at a depth of 6.9 m). The most probable reason for this reduction in acidity is neutralization due to reaction with alkaline dust layers coming from the valley walls (Delmas and Aristarain, 1978; Souchez and Lemmens, 1987; and Section 5.5.1 in this dissertation). In support of this hypothesis, some of the extremely low values are known to be associated with dust layers (e.g. at 2 m, 5 m, 6.3–6.5 m, and 15.7 m depth). In Fig. 5.5A a 3-cycle moving average of the maximum and minimum values is plotted in order to identify any trend there may be. The maximum values have a mean of $4.8 \pm 0.19\ \mu Eq\ l^{-1}\ a^{-1}$ and increase at a rate of 0.054 $\mu Eq\ l^{-1}\ a^{-1}$ from the bottom to the top of the core. The trend of

the minimum values is not so well defined. Only the last 15 peaks show a rapid increase. This difference in the behaviour of maxima and minima is to be expected if the ice core represents trends in atmospheric pollution in the Arctic. As discussed elsewhere in this dissertation, there is a strong seasonal component, and maximum values are reached in winter. The minimum values are supposed to occur in summer. At this time of the year cyclones arrive in Svalbard via Iceland and are greatly depleted of pollutants from North America (Fig. 5.1A). As a consequence, increase in the acidity of the precipitation is greater in winter. The high minimum values in the upper part of the core could be caused by more intense contamination in recent years, or merely reflect greater homogenization of the core due to more intense melting. The last hypothesis appears to be the likely one, as the decreases in the minimum values is accompanied by a decrease in the maximum values. The interpretation of the peak values as winter layers is supported by atmospheric observations in the winter, as well by snow-pit studies which demonstrated that the pH increases substantially in winter-time (Gjessing, 1977; Semb, Brækkan and Joranger, 1984) due to the increase in the load of pollutants. Another important observation is that the difference between peaks and troughs tends to increase in the top part of the core, illustrating the increase in acidity in one season more than the other. In Section 5.5 the trends of the increase in acidity are explored in more detail after the core has been dated.

Baseline data for acidity have been obtained from pre-industrial-revolution ice from a core recovered recently in Austfonna (Zagorodnov and Arkhipov, in preparation). Acidity at that period oscillated between 2.5 and 2.8 $\mu Eq\ l^{-1}$. This suggests that the Skobreen core is loaded with pollutants from a depth of 15 m upwards (cf. Fig.3.4D). In the upper 5 m the mean value for peaks is $5.8 \pm 0.3\ \mu Eq\ l^{-1}$, representing a net increase of 2.8–3.3 $\mu Eq\ l^{-1}$ (i.e. 75–107% of the levels at the bottom of the core). The H^+ concentration, however, is relatively low when compared with the present acidity of snow, as derived from a survey by Semb, Brækkan and Joranger (1984). The winter snow in central-eastern Spitsbergen shows an acidity of $\approx 12\ \mu Eq\ l^{-1}$ (Fig. 2.4). No layer of the ice core gives such a high value. The difference in acidity may be caused by various factors, such as scouring of the later winter – early spring layers, melting and wash-out of the upper layers, neutralization by carbonates, or perhaps by a combination of these activities. Therefore the observed increase should be a minimum limit and the acidity may have been increasing still more. A greater increase in acidity has been observed in an ice core from Nordaustlandet (cf. Chapter 5).

3.2.7- Electrolytic conductivity

3.2.7a- Introduction

Electrolytic conductivity (EC) is a measure of the ability of a solution to conduct an electrical current. It is an easy and quick way to obtain an index of the total dissolved chemical species, hence it has been used intensively in glaciological (Barrie, Fisher and

Koerner 1985; Delmas et al., 1985) and glacio-geological studies (Drewry, 1986; Fenn, 1987). However, the total EC does not result only from the sum of individual ionic conductivity as it does in simple solutions. In natural waters, which of course include melted snow and ice, the EC (i.e. the liquid conductivity of meltwater) will be affected by various factors, such as the proportion of different ions, water temperature, pH, atmospheric CO_2, sediment load, and dissolved organic material (Fenn, 1987). Further, ion association and ion pairing may occur (Fenn, 1987). This will neutralize or reduce the conductance of otherwise dissociated ions.

In clean polar snow and ice from the interior of the Antarctic and Greenland ice sheets, some of the problems cited above are reduced or non-existent. The total EC can in general be related to variations in ionic concentration. Further, the main contributor to total EC is the H^+. This is because of the much larger specific conductivity of the proton (Delmas et al., 1985). The concentration of H^+ depends mainly on the strong acid content of the sample (i.e. HCl, HNO_3, and H_2SO_4). A strong relationship is observed, therefore, between acidity and EC. Before the industrial revolution the main sources of strong acids were limited to material injected into the atmosphere by volcanic eruptions (e.g. SO_2, which reacts in the atmosphere to produce sulphuric acid). The EC technique has been a useful method for identifying layers laden with impurities of volcanic origin, when it is associated with measurements of acidity, solid electroconductivity, and sulphate content (Hammer, 1977; Hammer et al., 1978; Hammer et al., 1981a and b; Delmas et al., 1985). The major volcanic explosions reported in the historical record (e.g. Tambora, 1815; Krakatoa, 1883; Mt. Agung, 1963) have been identified and used as reference horizons.

Interpretation of EC profiles from outside the central parts of the two ice sheets is more complex. Near the coast the EC is controlled by the concentration of sea salts, and a good relationship with acidity is not to be expected. The peaks which indicate the presence of volcanic material will be concealed. On the other hand, the EC may show strong seasonality because the sea-salt concentration will be related to periods when there was open water and/or stormy weather (Palais et al., 1984). Layers with high EC could in this case be identified as having been precipitated in summer, therefore providing an extra method for dating a core. For the case of valley glaciers, the situation is even less promising. The surface of the glacier is constantly enriched by wind-blown particles from the valley walls. In warm summers, ice layers with a high concentration of solids will form. These dust layers alter the EC in a complex way (cf. Section 5.5.1).

A complex EC profile for the Skobreen ice core is to be expected. The glacier is not only a valley glacier but it is near open water in summer (i.e. only 10 km from Van Mijenfjorden). Consequently, the EC peaks should reflect the higher concentration of ions in summer.

Bearing in mind the complexity of interpreting an EC profile from a valley glacier near open water, the studies in this section have the following objectives: 1) to derive an index of all the dissolved material for the Skobreen core, establishing whether any seasonality may be observed which could help to date the core; 2) to examine the relationship between EC and the acidity profile and determine which are the main factors controlling EC (i.e. the pollutant concentration, sea salts or dust layers); 3) to examine trends and variations in both peaks and background values, establishing whether the increase in the input of anthropogenic material into the troposphere is recognizable in the ice core, despite the high contribution of local impurities. These points are discussed in Sections 3.2.7c, 3.3, and 5.5.1.

3.2.7b- Methods

The electrolytic conductivity was measured continuously along the Skobreen core, using a Philips PW 9505 conductivity meter with automatic correction for the ambient temperature (21°C) and a precision of ± 0.1 μS cm^{-1}.

EC measurements, like acidity, may be affected by the uptake of CO_2. The conductivity may be increased by bicarbonate and hydrogen ions resulting from the dissolution of carbon dioxide (Fenn, 1987). Hence, the same methodology used for measuring acidity was followed. In other words, the sample bottles were left open for 10 minutes before measurement to achieve equilibrium with atmospheric CO_2. The conductivity cell was then immersed in the meltwater for about 2 minutes before reading.

3.2.7c- Results

The EC ranges from 1.7 to 11.5 μS cm^{-1}, with a mean value of 4.2 ± 0.1 μS cm^{-1}. Three anomalous peaks of 16.6, 30.0, and 54.6 μS cm^{-1} were considered to be due to contamination, as they are not associated with any anomalously high values of the acidity, ionic content, or dust layers. The EC appears to vary semi-regularly, like the acidity values. Fifty-two peaks were recognized. If they are taken as annual maxima, it will result in a net accumulation rate of 33 cm a^{-1} w.eq. On the other hand, the difference between peaks and troughs is not so marked as in the acidity profile. At a depth of 10.4 m (Fig.3.4F), there is a relatively abrupt change in the values of EC. This is associated with similar changes in the acidity and $\delta^{18}O$ profile.

Table 3.2 shows the mean and the standard deviation (σ) for the top 10.4 m and for the rest of the core. The abrupt reduction in all three parameters, and their standard deviation, suggest that the bottom part of the core was intensely homogenized. The fact that the seasonality of these parameters can still be distinguished in the top part of the core confirms that the homogenization was not total. Towards the top there is a difference in the increase

between peaks and troughs. The difference can sometimes reach 8 μS cm^{-1}. This is greater than the seasonal EC variations described elsewhere in the Arctic (e.g. in the Agassiz ice cap, Barrie, Fisher and Koerner, 1985; and the Penny ice cap, Holdsworth, 1984). As expected, some of the highest EC values are associated with dust layers (e.g. at 2.2, 3.7, and 15.7 m depth). The process that increases EC in dust layers is explained in Section 5.5.1.

Table 3.2- Mean and one standard deviation of $\delta^{18}O$, acidity, and EC for the upper and lower (i.e. depth >10.4 m) parts of the Skobreen ice core.

	$\delta^{18}O$		Acidity		EC	
Depth interval	Mean	σ	Mean	σ	Mean	σ
0.85–10.4 m	-12.8	1.0	3.4	1.6	4.7	1.9
10.4–17.9 m	-12.4	0.5	2.8	1.2	3.5	1.3

Fig. 5.5B plots the peak and trough values separately, to establish any trend there may be. The values are smoothed by a three-sample moving average. The background value oscillates at about 2 μS cm^{-1} in the bottom part of the core. In the rest of the core both peaks and troughs increase towards the surface. There is an increase in the annual maximum of (0.032 ± 0.012) μS cm^{-1} a^{-1} where $r = 0.36$ and $\alpha < 0.01$. The interpretation of this trend is not straightforward, as it may have been caused, for example, by an increase in the concentration of strong acids or by sea salts. Finally, although there is a cyclicity in the EC peaks at about the frequency of the acidity peaks (i.e. 3.2–3.4 cycles m^{-1}, cf. Section 3.3.2), there is no significant correlation between EC and acidity. This is not unexpected for the environment of Skobreen. This observation no doubt reflects the great contribution of other cations which derived from crustal weathering to EC. In fact, some of the EC peaks are associated with dust layers, so it is not possible to derive an index of the dissolved H^+ from the EC as other ions appear to be affecting the total conductivity. In this case, each ion collaborates in different proportions to the EC in respect of its ionic conductivity and concentration. In Section 5.5.1 the relationship between EC and acidity is examined in more detail in order to elucidate which factors control the EC.

3.2.8- Ionic concentrations

3.2.8a- Introduction

The chemistry of polar snow and ice reflects the composition of the atmospheric aerosol. The analysis of variations in the concentration of chemical species can provide proxy information on environmental conditions and their evolution over time. Over the last thirty years several studies have produced, for example, information on past volcanic activity

(Delmas et al., 1985; Legrand and Delmas, 1987); climatic conditions at different time-scales up to 160,000 years B.P. (e.g. Legrand et al., 1988), including the examination of atmospheric conditions during the Last Glacial – Interglacial climatic cycle; anthropogenic pollution (Busenberg and Langway, 1979; Herron, 1982; Wolff and Peel, 1985; Finkel, Langway and Clausen, 1986); solar activity (Raisbeck et al., 1982); and atmospheric composition from the examination of gases in the bubble inclusions (Delmas, Ascensio and Legrand, 1980; Neftel et al., 1982).

The chemical species measured for these studies include all the major impurities found in snow and ice (i.e. H^+, SO_4^{2-}, NO_3^-, Cl^-, Na^+, Ca^{2+}, NH_4^+, Mg^{2+}, and K^+), trace elements (e.g. Pb, Cu, Cd, and Zn), and organic compounds and gases (e.g. CO_2). The high purity of polar snow and ice allows pre-industrial baselines to be determined, as there is no production of trace substances on an ice sheet.

Beyond the two ice sheets, however, chemical studies have been restricted. The reasons for this lack of studies include high local contamination due to nearby outcrops of rock which release chemicals during crustal weathering, and post-deposition alterations caused by the melting and percolation of some of the snow and ice. Hence the studies beyond the ice sheets have been limited in general to ice caps and to glaciers at high altitudes (e.g. Mt. Logan, Quelccaya Ice Cap), preferably in an accumulation area where there is little or no melting.

Glaciological conditions in Svalbard are not ideal (e.g. there is melting, and irregular distribution of precipitation over the year) for studies of chemical impurities. All the sites already examined are affected by various degrees of melting in summer. Elution of some or all of the main ionic components is frequent. In summer, the contribution of weathering impurities is high, particularly in Spitsbergen, so the Skobreen core was sampled in order to derive general trends and to discover how much the core had been affected by melting.

Svalbard and Franz Josef Land are the first land masses in the pathway of air masses coming from Eurasia (Fig.5.1A). They are, therefore, ideal places for monitoring the input of anthropogenically derived pollutants. Semb, Brækkan, and Joranger (1984) have shown that the winter precipitation is heavily loaded with pollutants, in particular H_2SO_4. One of the main objectives of the ionic analysis was to derive an excess-sulphate (i.e. the non-sea salt SO_4^{2-}) profile that would extend over time the observations of high concentration at the surface. The resulting time series could then be compared with records of pollutant emissions, e.g. European emissions of SO_2 (Möller, 1984). This last analysis is written up in Chapter 5.

3.2.8b- Methodology

Thirty-eight samples were selected for Cl^-, SO_4^{2-}, and NO_3^- analysis. The samples were analysed by Dr. R. Mulvaney at the British Antarctic Survey (BAS). Two blanks were analysed together to assess the degree of contamination during preparation and analysis. It was necessary to pass all the samples through a Millipore 0.45 μm filter, due to the high quantity of solids. All the anions were measured by ion chromatography, using a Dionex model 2010i. The ionic concentration was determined with an accuracy of 10%. The two blanks, which contained water that had been distilled three times, showed concentrations of less than 0.6 μEq l^{-1} of SO_4^{2-}, <0.5 μEq l^{-1} of Cl^-, and <0.2 μEq l^{-1} of NO_3^-. Similarly prepared water was used to clean the plastic storage bottles.

The core was sampled, bearing in mind an estimated mean annual net accumulation of 50 cm a^{-1}. The results of the acidity, $\delta^{18}O$, and EC profiles show that this is a gross overestimation, of at least 50%. The real mean net accumulation rate is between 30 and 33 cm a^{-1} (cf. Section 3.3). Therefore there is at most one sample for each period of two–three years. A 50 cm section was sampled continuously for more detailed examination (giving from 11.7 to 12.2 m w.eq.).

3.2.8c- Results

The variations in three anions and in excess sulphate are plotted in μEq l^{-1} in Fig. 3.4G – 3.4J. Excess sulphate, $[SO_4^{2-}]^*$, was calculated from the known sea-salt ratio of sulphates to chlorides, $[SO_4^{2-}]^* = [SO_4^{2-}] - 0.103\ [Cl^-]$ (Mulvaney and Peel, 1988). This calculation assumes that all chloride is derived from sea-salt spray. This may be questionable in the case of Svalbard, where the input of HCl coming from Eurasia may be important. Unfortunately, the Na^+ concentration was not measured and it is not possible to confirm the proportion of sea salt from the Cl^-/Na^+ ratio.

Chlorides

Cl^- values range from 4.15 to 75.12 μEq l^{-1}, with a mean value of 19.94 ± 2.60 μEq l^{-1} †. The profile appears to be depleted of Cl^- in the lower parts of the core. Semb, Brækkan and Joranger (1984) measured a Na^+ concentration for central-eastern Spitsbergen of about 0.81 mg l^{-1}. This results in a Cl^- concentration of 1.46 mg l^{-1}, or 41 μEq l^{-1} if all Na^+ is assumed to be marine and the sea-water ratio $[Cl^-]/[Na^+]$ is taken as 1.82 (Clausen and Langway, 1989). On Austfonna before the 20th century the mean Cl^- is about 33 μEq l^{-1} (Punning, Vaykmyae and Tóugu, 1987). It appears, therefore, that some Cl^- has been flushed out of the system in Skobreen, and there is an abrupt change in the mean

† The numbers after ± of the mean concentrations are the standard error of the mean, unless otherwise stated.

value at a depth of 4 m. The profile, nevertheless, has not been totally homogenized. There is still a significant correlation with total sulphates ($r = 0.50$ at $\alpha < 0.003$). In an elution sequence the SO_4^{2-} is the first anion to be flushed out and Cl^- the last (Brimblecombe et al., 1985). Further, the SO_4^{2-}/Cl^- ratio would decrease rapidly as the elution is also differential (i.e. sulphates are removed faster). It can be concluded that the profile is still representative of the original values, although impaired. Otherwise no correlation would be observed.

Peaks in Cl^- can also be created by hydrochloric acids resulting from volcanic explosion (Herron, 1982). These peaks are about 4.2 $\mu Eq\ l^{-1}$ in the two ice sheets (Herron, 1982), which is less than the background level at Skobreen. Therefore they are expected to be masked in the profile if there is a record at all. Finally, no clear increase in Cl^- concentration in the atmosphere has been observed during Arctic haze episodes (Pacyna and Ottar, 1985).

It may be concluded that the Cl^- concentration reflects mainly the contribution from sea-salt spray. Some Cl^- has been eluted, but the core is not totally homogenized. The mean concentration is considered to be consistent with the geographical position of the site.

Sulphates

The sulphate concentration varies from 2.12 to 28.62 $\mu Eq\ l^{-1}$, with a mean of $7.33 \pm 1.03\ \mu Eq\ l^{-1}$. Sulphate concentrations in Skobreen and elsewhere in Svalbard are greater than the concentrations in modern snow in Greenland by a factor of 2–10. For example, the SO_4^{2-} concentration at Camp Century is 2.5 $\mu Eq\ l^{-1}$ for the year 1976–77, and 2.7 $\mu Eq\ l^{-1}$ at North Central for 1973–77 (Herron, 1982). The reason for the higher concentration in Svalbard is the greater concentration of sea-salt sulphates (e.g. $NaSO_4$), as the open sea is much nearer. No long-term sulphate record has previously been published for Svalbard, so it is impossible to obtain a baseline. The only long-term data are the mean sulphate concentration for the whole Vestfonna core, which includes modern snow and ice (cf. Section 2.3). It has a mean of $16.7 \pm 7.7\ \mu Eq\ l^{-1}$ at one standard deviation (Punning et al., 1987).

On average 30% of the Skobreen SO_4^{2-} originates from sea salt. The maximum proportion is 78%. These percentages were calculated from the excess-sulphate relationship. No significant trends are obtained from the total sulphate record. As in the Cl^- profile, the record appears to have been homogenized below a depth of 4 m. The high concentrations between 2 and 4 m are similar to the sulphate concentration measured by Semb, Brækkan, and Joranger (1984) in winter snow layers from central-eastern Spitsbergen (cf. Table 2.1).

The excess-sulphate variations show a profile similar to that for the total sulphate. The mean concentration for the profile is $5.28 \pm 0.92\ \mu Eq\ l^{-1}$. This value is similar to the measurements obtained by Semb, Brækkan and Joranger (1984) for the region and of the

same order of magnitude as observations on Austfonna. The Svalbard concentrations are greater by a factor of 2–5 than the excess-sulphate concentrations found elsewhere in modern snow in the Arctic. For example, 1.7 μEq l^{-1} at Dye 3 for 1983 (Mayewski et al., 1986); and 2.3 μEq l^{-1} between 1976 and 1977 at Camp Century (Herron, 1982). The profile shows the same abrupt increase at about a depth of 4 m as the Cl^- and total SO_4^{2-} profiles. The concentrations in the top part of the core are very similar to concentrations measured in winter in central and southern Svalbard (about 30 μEq l^{-1}).

Excess sulphate can originate from H_2SO_4 ejected into the atmosphere by volcanic eruptions and from the photolytic oxidation of sulphurous gases. These gases in their turn can originate either from the biological activity of marine organisms or, increasingly importantly, from fossil combustion (primarily coal). For the period covered by the Skobreen record (cf. Section 3.3 on the dating of the core) no major volcanic eruption had occurred apart from that of Mt. Agung. As already discussed in the section on acidity, there is no record of this eruption in the Skobreen firn and ice, perhaps because it is masked by the high contribution of excess sulphate from marine and anthropogenic sources. The same is true for the eruption at Beerenberg, Jan Mayen, in 1970. This source is therefore disregarded in respect of excess-sulphate concentration in Svalbard snow and ice. It remains to find a way of distinguishing the excess-sulphate background due to marine organisms activity from that due to the anthropogenic contribution.

Normally it is assumed that the $[SO_4^{2-}]^*$ concentration from before the industrial revolution is entirely due to biogenic activity, discounting peaks of volcanic origin. It is also reasonable to assume that the production by marine organisms of sulphur gases has not varied substantially in recent centuries. A baseline for pre-industrial $[SO_4^{2-}]^*$, therefore, could be obtained from intermediate and deep ice cores, in this way making it possible to establish the modern anthropogenic contribution to excess sulphate. Unfortunately, no such record has been published for Svalbard and it is necessary to look elsewhere. The concentration in the ice cores recovered in Greenland is not representative of the conditions encountered in Svalbard. All the Greenland sites are far too distant from the coast and the marine contribution should be much less than in Svalbard. James Ross Island, Antarctic Peninsula, is one of the best analogues. The sea-ice margin is near the island in summer and thus its geographical position is similar to that of Svalbard. Further, no anthropogenic contribution has been detected in sulphates from Antarctica (Clausen and Langway, 1989). Finally, the concentrations encountered at this site are relatively high, due to a zone of high biogenic production in the Weddell Sea (D. Peel, personal communication). Therefore the measured modern $[SO_4^{2-}]^*$ concentration of 1.3 μEq l^{-1} (Aristarain, 1980) may be said to be representative of the natural background level for sites near the coast. This concentration approaches the summer concentration measured in Nordaustlandet, 2.4 μEq l^{-1} (Gjessing, 1977). The latter may be considered as the maximum value for biogenic $[SO_4^{2-}]^*$

in Svalbard, as the anthropogenic contribution is small at this time of the year. Bearing in mind the observations on the biogenic contribution to excess sulphate, 2 $\mu Eq\ l^{-1}$ was subtracted from the values to derive the anthropogenic contribution. In Section 5.5.5 the resulting profile is compared with the estimated European emissions of SO_2.

There is a marked increase in excess sulphate towards the top of the core, although no significant linear trend was obtained. The lack of a trend is attributed to the low values, which may represent summer accumulation when the anthropogenic contribution is restricted and the flush-out is intense. The mean anthropogenic contribution increases from 2.1 ± 0.7 in the lower 13 m to 7.4 ± 3 in the upper part of the core, again showing the same abrupt change. The concentrations in the upper part are also consistent with the values measured in modern Svalbard snow (cf. Table 2.1). Nevertheless, the core is enriched with sulphates of anthropogenic origin. If only the upper part of the core is taken into consideration, which is reasonable as it does not appear to have been greatly altered by melting, the mean concentration is comparable to the concentration measured in modern snow from glaciers in continental Europe (e.g. Colle Gnifetti, 4.4 $\mu Eq\ l^{-1}$; Wagenbach et al., 1988). If 2 $\mu Eq\ l^{-1}$ is taken as the pre-industrial level, concentration in Skobreen may have increased by up to 14 times. Some sites on Svalbard show snow concentrations of up to 34 $\mu Eq\ l^{-1}$ (Semb, Brækkan and Joranger, 1984; Section 2.3 of this dissertation), or 17 times the background level. There is enough evidence to conclude that the snow and ice of Skobreen is as heavily contaminated by anthropogenic pollutants (i.e. mainly H_2SO_4) as some glaciers in continental Europe, even after partial elution. A more comprehensive discussion of the anthropogenic effect on Svalbard ice masses is to be found in Chapter 5.

Both Cl^- and SO_4^{2-} profiles show an abrupt increase towards the surface, at a depth of 4 m. At first glance this could be interpreted as an increase in pollution or as climatic variability. More detailed examination reveals that this is not the case. Below 4 m both profiles have been homogenized, which is reflected in a decrease in the standard deviation of the mean concentrations. The Cl^- reduces from a mean value of 34.9 ± 7.3 to $15.0 \pm 2.2\ \mu Eq\ l^{-1}$, and the SO_4^{2-} reduces from 13.0 ± 3.1 to $5.4 \pm 0.7\ \mu Eq\ l^{-1}$. The mean concentrations in the upper 4 m are greater than in the rest of the core by a factor of 2.4. Finally, the change in concentrations is associated with an abrupt increase in the proportion of ice to firn.

Similar phenomena have been observed in an ice core from Folgefonni ice cap (60°04'N, 06°23'E), Norway. The differences in concentration between the upper 12 m and the rest of the 61 m core may be of one order of magnitude (Davies, Vincent and Brimblecombe, 1982). Further, the values in the upper part before spring melting are similar to the concentration measured in winter snow in Svalbard. In both cases, Skobreen and

Folgefonni, the abrupt increase in ionic concentration suggests that each year water percolates through snow and firn, removing some of the original impurities.

Nitrates

Nitrate has a mean concentration of 1.3 ± 0.3 μEq l^{-1}, which is in agreement which observations by Mulvaney (1987) on Malte Brunfjellet, Sabine Land, Spitsbergen, 0.9 μEq l^{-1}, and by Semb, Brækkan and Joranger (1984) on Austfonna, 1.0 μEq l^{-1}. These concentrations are similar to concentrations in Greenland (e.g. 0.9 μEq l^{-1} at Dye 3 for 1975–81; Herron, 1982). The profile shows little variation, with the exception of two peaks, at 13.9 m (4.31 μEq l^{-1}) and 17.7 m (7.08 μEq l^{-1}). No explanation has been found for these relatively high concentrations. The lack of any systematic trend is anomalous as an increase in concentration in the last forty years is to be expected due to the increasing combustion of fossil fuel and biomass burning (Neftel et al., 1985). Another explanation is that the NO_x is rapidly oxidized to HNO_3 and removed by rainfall over a short time-scale and near the source area (Brimblecombe, 1986). The featureless profile could indicate an intense flush-out of the original material, but this is not to be expected, as the other two anions do not show such strong damping.

3.2.9- Examination of dust layers

The original plan was to analyse comprehensively the insoluble material, such as microparticles (i.e. <20 μm) and pollens, expected to be found in ice and snow. The analysis of the physical and chemical properties of microparticles, for example, has provided information on past volcanic activity (Thompson, 1977; Thompson and Mosley-Thompson, 1981a and b). Further, microparticle concentration may vary strongly from season to season, with a maximum in spring (Koerner, 1977b). It was hoped to use this fact as a way of helping to date the core. Unfortunately the site of the core is not appropriate for such studies. The high concentration of particles up to 1 mm in diameter masked any other material. It would be extremely difficult and time-consuming to try to separate microparticles and pollens from the local contribution. It was decided, therefore, to examine only the dust layers which were identified with the naked eye. The objective of the analysis was to obtain an idea of the chemical composition of the dust layers that could help to explain the variations in other parameters.

Thirteen black dust layers were identified during the stratigraphic examination and are marked in Fig. 3.4K. The melted samples of the snow and ice contained in these layers were first passed through a Millipore 0.45 μm filter. In the process, the filters frequently became clogged, so high was the concentration of particles of varying size. The 13 filters were stored in sterile Petri dishes and taken to the Earth Sciences Department at the University of Cambridge for sample preparation.

Sample preparation

The filters were washed in distilled water and the particles were collected in plastic tubes of 50 ml capacity. A bach of four tubes at a time was taken to the centrifuge for about 10 minutes. The precipitate was then collected in a pipette and two or three drops were spread evenly on stubs with a net for Scanning Electron Microscope (SEM) examination. After being left to dry for three days, the stubs were finally double-coated with gold.

3.2.9a- Methodology

The 13 stubs were examined through a SEM. Concurrently, the chemical composition of some of the particles was determined in a semi-quantitative way by dispersive x-ray analysis (EDX). The equipment used was a Philips 501B SEM, with a dispersive x-ray analyser, Link-AN 10000, attached to it.

Examination through a SEM is a widely used and well-known technique in Earth Sciences, so it is considered unnecessary the describe the principles on which it is based. Any textbook on clay mineralogy contains information on the subject. Energy-dispersive x-ray analysis is a fast and low-cost technique for determining chemical elements in a sample. On the other hand, the results are only semi-quantitative. The technique is based on the fact that each element in the sample produces x-rays at a characteristic energy level when it is being scanned by the microscope's electron beam. These x-rays are analysed by an attached energy-sensitive Si(Li) detector (Welton, 1984). The equipment used had a resolution of 150 eV. The system is able to identify any element with atomic number greater than 11 (Na). The different x-rays are separated according to energy level and each element yields a peak on an EDX spectrum at its own specific level. The peaks in the EDX spectrum represent the chemical composition of the mineral. The gold (Au) peak represents the coating on the stubs and it is ignored. The peaks of Si, Al, K, and Ca are proportional to their concentration. However, peaks at both extremes of the spectrum are altered by absorption in the window of the detector and they are not proportional to the concentration. Nevertheless, an indication of the chemical composition is obtained. To identify a mineral, the resulting EDX spectrum and the crystal morphology are compared with typical EDX profiles and microphotographs in one of the SEM petrology atlases (e.g. Welton, 1984).

The EDX analysis was restricted to 10 samples of each stub, as the aim was only to identify the main components. Five particles on each of the two axes were chosen at random and isolated at 20.000 X for examination.

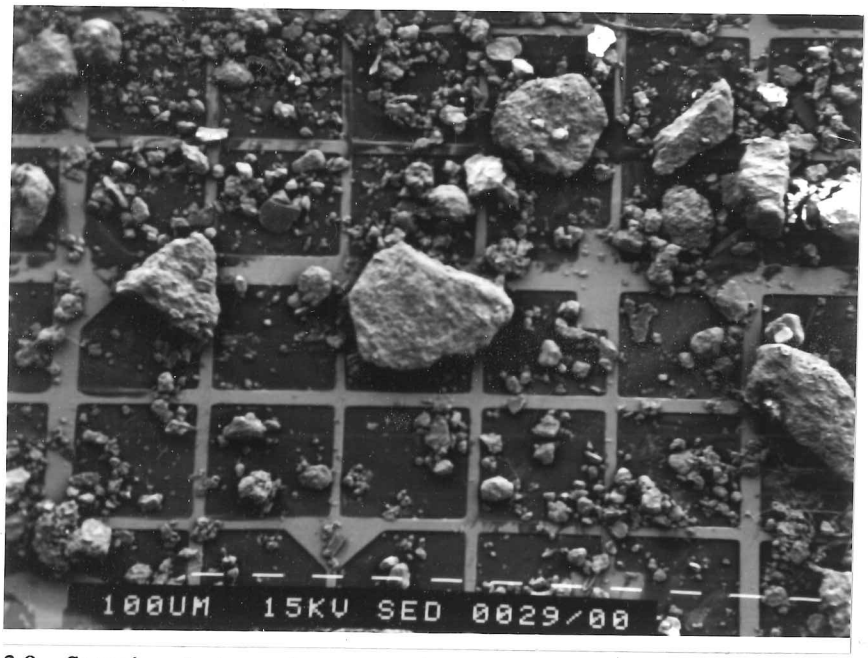

Figure 3.9- Scanning electron microscope micrograph of dust-layer particles found in the 23.1 m Skobreen ice core. Note the relatively large size of some particles (> 0.5 mm).

3.2.9b- Results

The minimum particle size is about 1 μm in diameter and the maximum is 1 mm. Finer material was rarely observed. The large sizes prove that the particles originate from the surrounding areas. The atmosphere can rarely transport particles with a radius greater than 20 μm over a long distance (Mosley-Thompson, 1980). Small pieces of shales and sandstones are identifiable, as well semi-euhedral feldspars and mica crystals (Fig. 3.9).

The mineralogical composition of the 13 layers is similar. The examination of a total of 100 particles by EDX revealed a mineralogical composition typical of immature sandstones: Quartz (SiO_2), Potassic feldspars ($KALSi_3O_8$) and Plagioclase ($NaAlSi_3O_8$ - $CaAl_2Si_2O_8$), Biotite ($K(Mg,Fe)_3AlSi_3O_{10}(OH)_2$), Muscovite ($KAl_3Si_3O_{10}(OH)_2$) and clays [e.g. Chlorite $(Mg,Fe,Al)_3$ $(Al,Si_4O_{10}$ $(OH)_2.(Mg,Al)_3(OH)_6$), and Illite ($KO_2Al_4(Al_2,Si)_8O_{20}(OH)_4$)].

The mineralogical composition associated with the presence of pieces of sandstones and shales leaves no doubt that they reflect the lithology of the valley walls and surrounding outcrops. No particles of exotic composition were identified. If they are present, the great quantity of local impurities will mask them. Finally, the 13 layers are interpreted as representing periods of intense melting. Therefore they are used as reference horizons to mark summer layers.

3.3.10- Crystal size

3.3.10a- Introduction and methodology

Two thin sections were cut from the Skobreen core for examination of the crystal size. The technique for preparation and analysis of thin sections of ice is the one described by Langway (1958).

The thin sections were prepared in the SPRI cold-rooms at about -10°C. Two 10 cm sections were taken from the core at 11.9 and 17.6 m w.eq. and were cut with a tenon saw to a thickness of about 1 cm. The flat surface of each of the sections was put into contact with a slightly warmed clean glass slide. The warmth is enough to melt a thin film of the ice, which immediately refreezes, bonding the ice to the glass. This process does not alter the crystal-size. Using a standard biological microtome, the two sections were reduced to a thickness of 0.4 mm.

The two sections were examined on a Rigsby-type universal stage and photographed under cross-polaroids with a 100 ASA black-and-white film (Fig. 3.10). The photographs were printed on a scale of 2:1 and the crystal boundaries were digitized in order to determine the 'average' area and diameter. A Fortran program for counting and measuring ice floes from aerial photographs, developed by the SPRI Sea Ice Group, was used to compute the dimensions of the crystals.

3.2.10b- Results

There is a marked increase in area and diameter and a decrease in the number of crystals with depth. At 11.9 m the mean crystal area is 9.29 ± 9.38 mm^2 and the mean diameter is 2.72 ± 1.42 mm. At 17.6 m the mean area increases to 13.39 ± 14.52 mm^2 and the mean diameter to 3.035 ± 1.76 mm. The number of crystals reduces from 857 at 11.9 m to 572 at 17.6 m.

The difference of 44% in the mean area of the crystals in less than 6 m w.eq. is not unexpected. Ice is formed by the refreezing of meltwater in some years, and the size of crystals can differ greatly even in neighbouring layers. This fact has been observed in several Svalbard ice cores (Zagorodnov and Arkhipov, in preparation). In some years superimposed ice is formed and the crystal size will depend on the degree of saturation of the snow pack and on the temperature of the snow (Koerner, 1968).

3.3- Dating of the Skobreen ice core and determination of the net mean annual accumulation rate

To obtain a reliable time series of environmental changes in an ice core, accurate dating of the ice layers is essential. This is a difficult task in the case of the Skobreen core. Dating of ice cores from sites which undergo intense superficial melting in summer is complex. The techniques normally used for dating polar snow and ice, such as visual examination of the stratigraphy, seasonality of chemical and physical parameters, concentration of microparticles, and reference horizons (Hammer et al., 1978), are rarely

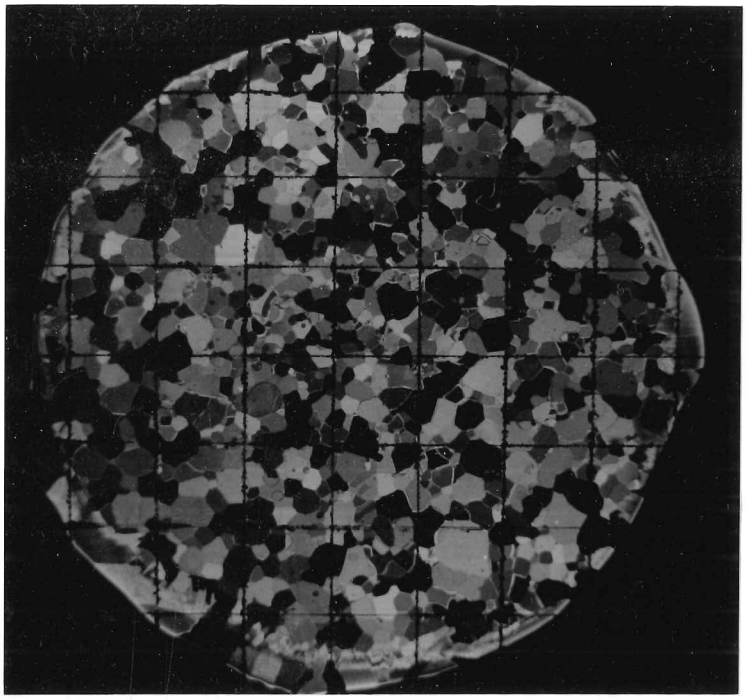

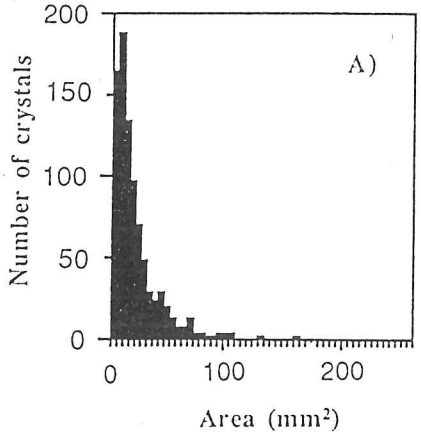

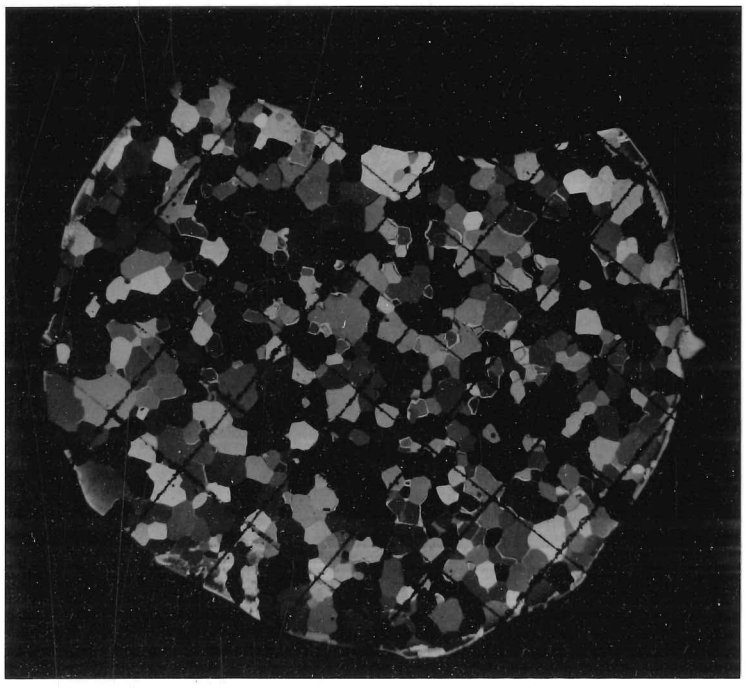

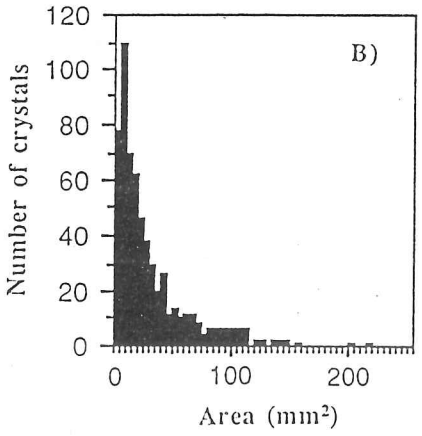

Figure 3.10- Photographs of two thin sections from the Skobreen core. The photographs were taken under cross-polaroids and are presented in actual-size. The thin section A comes from a depth of 11.9 m w.eq. and section B from a depth of 17.6 m w.eq. The diagrams show the change in crystal number and area. The narrow band of fine-grained ice at the perimeter of the sections should be disregarded. This band is the refrozen meltwater of the bonding process.

applicable. Melting followed by percolation of meltwater through the upper layers homogenizes any seasonal variation. In warmer summers some meltwater is taken from the system. As discussed in previous chapters, this removal is not uniform for isotopes and chemical species. Isotopic fractionation, and preferential and differential elution of the ionic species, can alter the original record beyond recognition. As a result there is a great uncertainty in the identification of seasonal maxima and minima, as shown by the description of the Skobreen core in Chapter 3. Furthermore, scouring due to glacier winds might have altered the initial record, and an entire season have been removed. Even the use of less accurate techniques, such as the estimation of the age of layers by flow models, is inadvisable. The mean net accumulation rate is highly irregular and some years may be missing due to net ablation.

The best approach for the interpretation of an ice core such as Skobreen is to examine independently all the physical and chemical properties that may show some seasonality or quasi-seasonality, or that may be used as reference horizons, then cross-compare all the results (i.e. the use of a multiple-dating technique methodology). In dating the Skobreen core, therefore, five sequential steps were adopted: 1) the determination of the net mean accumulation rate since 1963 by examining the tritium profile; 2) to check the resulting net mean accumulation rate by spectral analysis of the parameters with continuous time series (i.e. acidity, $\delta^{18}O$, and EC); 3) to identify the maximum number of annual layers from the stable-isotope and excess deuterium - *d*, acidity, and EC profiles, using the dust horizons as reference horizons for summer seasons; 4) to compare the results with a simple Nye flow model, calculated on the basis of the mean net accumulation rate determined from the upper layer; 5) and, finally, to cross-compare the results with the the mean annual temperature time series, to establish whether an 'anomalous' warm or cold year has left an imprint in the core that could be used as a reference horizon.

3.3.1- Determination of the mean net accumulation rate for the period 1963–86

The 1963 tritium peak was identified at a depth of 7.4 m, representing a net accumulation rate of 32.0 cm a^{-1}. There is some uncertainty about the position of the 1963 layer as few measurements have been made above this depth. That some tritium percolates in the summer is demonstrated by the profile in Fig. 3.4E, therefore the identification of the 1963 year layer at this depth gives a maximum estimate of accumulation rate.

3.3.2- Time-series analyses

In ideal conditions (i.e. dry polar snow), seasonal variations in stable isotopes and other parameters can be recognized. The almost regularly spaced variables can be interpreted as annual variations and dating the core is relatively easy. This is not the case for Skobreen. It

was necessary to find a technique that could separate any cyclic variation from the random noise caused by post-deposition processes: in other words, the application of a spectral-analysis model to the continuous time series.

The three continuous and irregularly spaced time series (i.e. acidity, $\delta^{18}O$, and EC) were first converted to equally spaced sequences by rectangular integration (Davis, 1986). This is necessary because the computation of spectral analysis requires observations that represent constant intervals of space or time.

The power spectrum of the three time series was calculated in a NAG routine (G13CBF) using spectral smoothing by the trapezium frequency (Daniel) window. Fig. 3.11 plots frequency (in cycles m^{-1}) against power (in $unit^2$ $cycles^{-1}$ m^{-1}) of the time series. The error bars represent the 95% confidence intervals for the peaks identified. As expected, no peaks are recognizable in the $\delta^{18}O$ profile. The record is flat, emphasizing the degree of homogenization. On the other hand, both the acidity and the electrolytic conductivity show significant peaks at, respectively, 3.2 and 3.4 cycles m^{-1} (or one peak each 31 and 30 cm). These results, therefore, confirm a cyclicity with a period of about 31 cm a^{-1}.

3.3.3- Identification of annual layers

A multi-parameter approach was adopted to determine the greatest number of annual layers. The different time series were examined concurrently to identify which sections were deposited in summer or winter. The interpretation would be accepted when three or more variables pointed to the same period of the year. For example, a decrease in the stable-isotope ratios associated with high excess deuterium, high acidity, and low conductivity would be interpreted with confidence as a winter layer. The presence of dust layers would mark a summer layer. However, some assumptions and uncertainties in these interpretations are discussed below.

1) Acidity and EC

Both properties have been shown to have a cyclicity of about 31 cm a^{-1} w.eq. and are interpreted as seasonal variations. It is known that the highest acidity levels occur in winter and the highest EC in summer (cf. Section 5.5.1).

2) Stable isotopes and deuterium excess - *d*

Only a few variations remain in the record, and these are interpreted as seasonal (cf. Section 3.2.4). The variations in peaks and troughs are small. To improve the reliability of the procedure, annual layers were accepted as such only when two troughs were separated by two samples and the intervening peak was greater

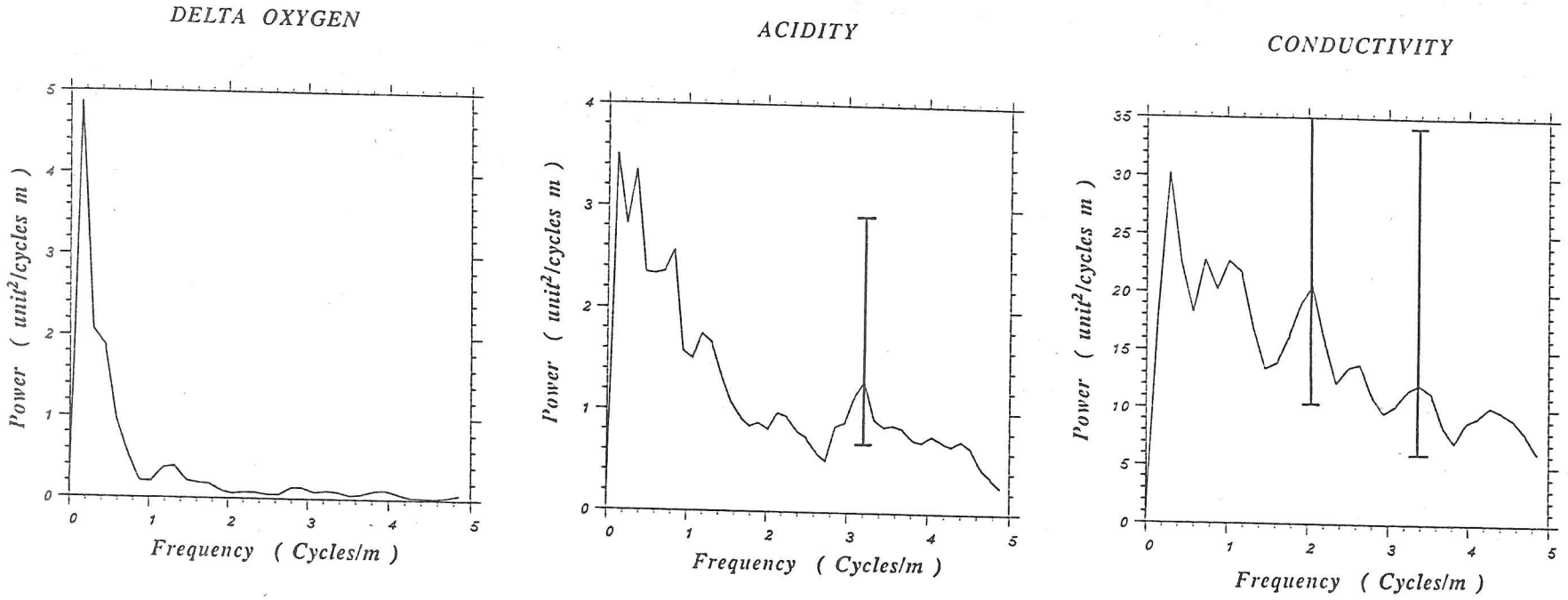

Figure 3.11- Power spectrum of the $\delta^{18}O$, acidity and electrolytic conductivity time series for the Skobreen ice core. The error bars represent the 95% confidence intervals for the identified peak. Note the total homogenization of the $\delta^{18}O$ variations. The peaks representing a frequency between 3.2 and 3.4 cycles m^{-1} (or one peak every 30-31 cm) are supposed to identify the seasonal cyclicity in acidity and electrolytic conductivity.

than one standard deviation of the mean of the $\delta^{18}O$ (i.e. 0.82‰). This reduced the number of misidentifications due to double annual peaks.

In total, 56 layers were identified and are shown in Fig 3.13. Dashed lines between layers indicate that there is some uncertainty in their identification. Layer thickness ranges from 18 to 62 cm w.eq., with a mean of 30.0 ± 0.95 cm w.eq. The core represents a period of 58 years, if 2 years are added to account for the upper 0.85 cm w.eq. which was not sampled. The bottom layer was thus deposited in 1929. The main uncertainty in the procedure would be caused by net ablation in one or more years.

3.3.4- Dating by dynamic model

The age of ice layers can be estimated with flow models. A Nye flow model (Nye, 1963a; Haefeli, 1963) was applied in order to estimate the age of the layers at Skobreen. In this model, the vertical strain-rate is assumed to be constant, the glacier is assumed to be in steady state, and the ice is assumed to be frozen to bedrock. The last two assumptions imply that the annual vertical velocity (v) at the surface is equal to the annual net accumulation in ice equivalent (a_{ice}) and is zero at bedrock. So, $v = a_{ice}(1- y/h)$ (Paterson, 1980). The time (t) that each layer was deposited in relation to the present is given by the integration of v from the surface to the depth of the layer at present (y), or:

$$t = \int_0^y v^{-1} dy$$

$$= \int_0^y \frac{dy}{a_{ice}\left(1 - \frac{y}{h}\right)}$$

$$\text{therefore} \quad t = -\left(\frac{h}{a_{ice}}\right) \ln\left(1 - \frac{y}{h}\right)$$

where h is the ice thickness at the site.

The core site is near the head of the glacier. It is reasonable to assume, therefore, that the horizontal velocity is close to zero, and the analysis carried out in Section 2.5 demonstrated that the horizontal velocity of the glacier is probably small even near the equilibrium line. Thus, it can be accepted that the vertical strain-rate is nearly constant at the core site, at least in the upper layers. The melting at the ice/bedrock interface is also negligible (i.e. less than 1.0 mm a^{-1}; cf. Section 2.5). The main cause of uncertainty in the model is the irregular net accumulation rate. In the computation of the age of the layers a mean net accumulation rate of 0.345 m a^{-1} ice equivalent was used. This value was obtained from the

examination of the $\delta^{18}O$ variations from the top four layers, which have not been damped. However, the glacier appears to have been ablating for the last 50 years (cf. Section 2.5), so the steady-state condition is not fulfilled. Nevertheless, the model was applied in order to compare the results with those obtained from other methods, summarized in Table 3.3. Differences are found in the bottom 9 m of the core. This is the section of the core where the variations are mostly damped, and perhaps some of the layers were not recognized as such. On the other hand, the differences may be caused by net accumulation higher than the mean. The late 1950s and early 1960s were years of heavy precipitation (cf. Appendix 1 – Fig. A1.8) and the net accumulation rate may have increased. This later hypothesis appears to be confirmed by the layer thickness attributed to the period (i.e. 61 cm a^{-1}).

3.3.5- Cross-comparison with the meteorological record

The dating of the $\delta^{18}O$ profile was based on the above results and compared to the mean annual temperature to establish whether an 'anomalous' warm or cold year has left an imprint in the isotope composition of the core. Fig. 3.12 plots the two profiles. Two major features are identifiable in the isotope profile, albeit displaced in time: the minimum temperature of 1968 which is registered in the core in 1967, and the high temperature of 1957 which appears in the core in the layer dated to 1954. The misidentification of the 1968 layer could have been caused by the identification of a non-existent extra layer. Melting of the layers with high $\delta^{18}O$ and percolation to the lower layers would explain the dislocation of the 1957 peak.

Table 3.3- Age of the ice at different depths of the Skobreen core; depths in water equivalent.

Depth	Tritium	Seasonal variations	Flow-model
1.0 m		1984	1984
5.0 m		1971	1971
7.4 m	1963	1963	1963
10.0 m		1956	1954
15.0 m		1939	1936
17.9 m		1929	1927

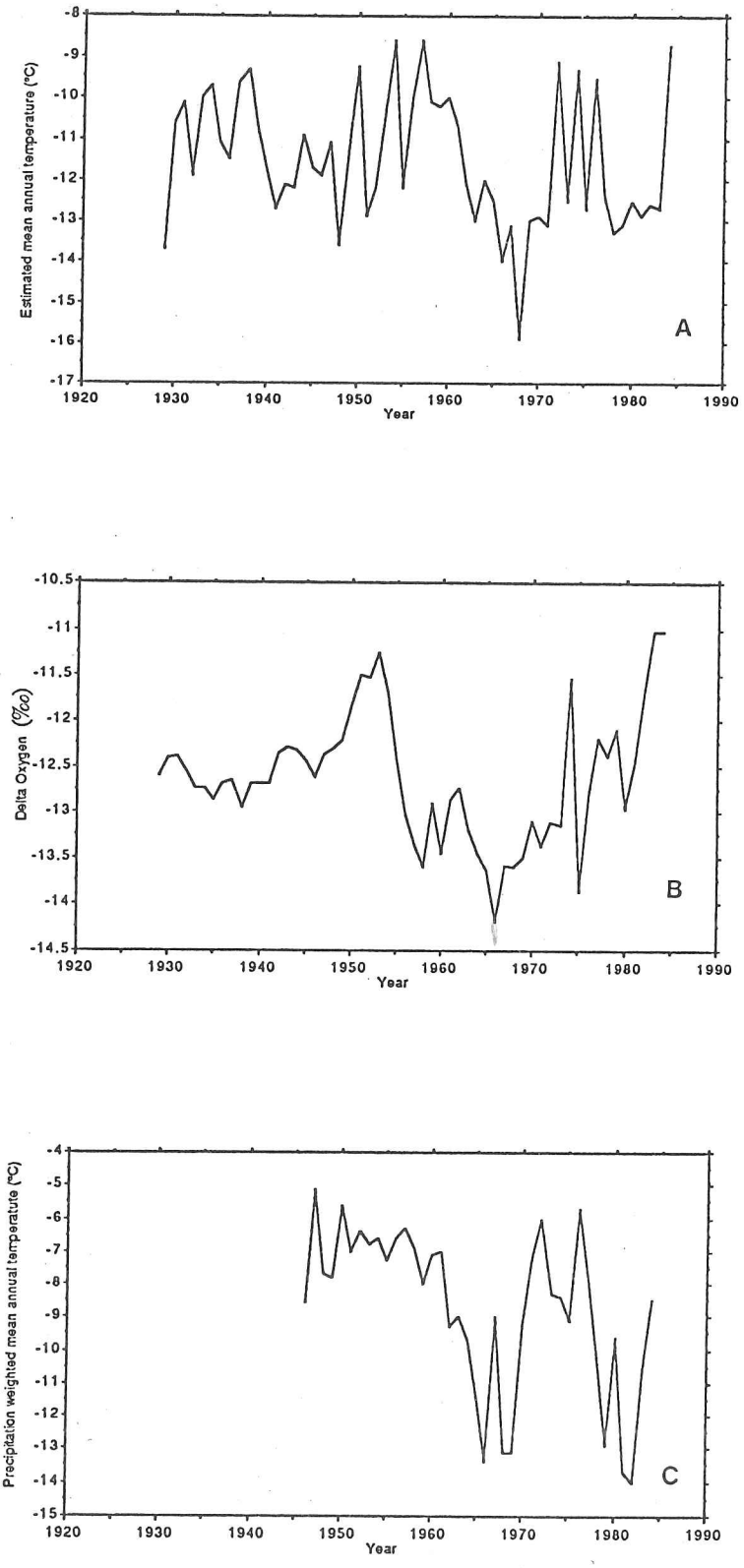

Figure 3.12- Comparison of the mean annual $\delta^{18}O$ (B) in the Skobreen core; the mean annual temperature (A) and the precipitation-weighted mean annual temperature time series have been estimated at 600 m a.s.l. for central-eastern Spitsbergen

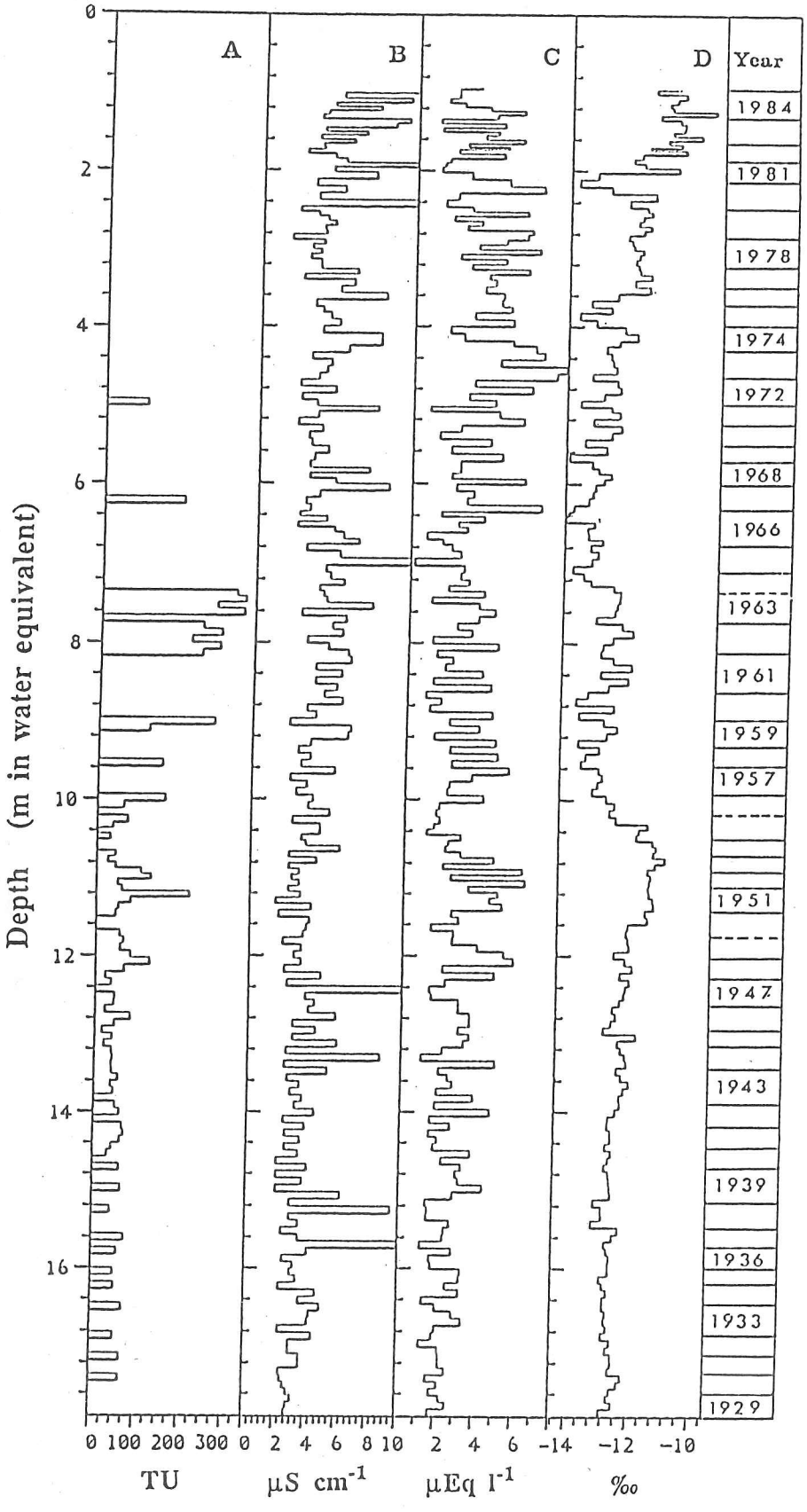

Figure 3.13- The dated 23.1 m Skobreen ice core: A) tritium; B) electrolytic conductivity; C) acidity; D) $\delta^{18}O$. Time-scale (years) shown to the right, depth scale (m) to the left in water equivalents.

3.3.6- Conclusions

The mean net accumulation rate is between 30 and 33 cm a^{-1} w.eq. It is not possible to date the core in annual detail with confidence. The different methods show results that differ by up to 3 years over about 56–59 years of deposition. Some seasonality is still recognizable, which helps the dating, but great uncertainties remain. Parts of the core still show some regular variations in $\delta^{18}O$, acidity, and EC, but these variations are not continuous and sometimes they are not clear. The bottom 9 m of the core show the greatest uncertainty, as the record is strongly homogenized. It is clear that the record cannot be used for more detailed studies: for example, to derive a $\delta^{18}O/\delta T$ gradient. In the following sections the environmental record of the Skobreen core is discussed on the basis of this dating. Despite the lack of resolution, the core is expected to provide information about major trends.

3.4- Summary and conclusions

An ice core has been drilled in central-eastern Spitsbergen, providing a record of the environmental conditions of glaciers in the area. The core indicates that even at an altitude of 600 m a.s.l. melting can be extensive. This is shown by an intercalation of firn and superimposed ice and by the rapid change of the snow pack to glacial ice. Percolation, refreezing, and flush-out of material have impaired the original record of variations in acidity, EC, ionic concentration, stable-isotope ratios, and tritium. The site is not suitable for studies of annual detail. Nevertheless, the variations have not been totally obliterated and a quasi-seasonality in the acidity and EC profiles is observed. There are still vestiges of seasonal variations in the stable-isotope ratios. Variations in deuterium excess - *d* have been better preserved and help to identify the annual layers. For detailed studies, however, it will be essential to have a continuous *d* profile.

The mean net accumulation, determined by the identification of the 1963 tritium layer, is 32 cm a^{-1} for the period 1963–86. However, there is some uncertainty about this figure, as downward percolation of tritium occurred. The rarely preserved seasonal variations in stable isotopes, and the variations in *d*, acidity, and EC suggest net accumulation rates between 18 and 43 cm a^{-1}. The electrolytic conductivity and acidity variations, if interpreted as seasonal, point to mean net accumulation rates between 33 and 36 cm a^{-1} for the whole period covered by the core. In other words, the core could represent between 50 and 55 years of deposition, but this is not precise enough, for example, to obtain a transfer function between mean annual temperature and variations in the $\delta^{18}O$. It was necessary, therefore, to find a way of improving the recognition of the annual layers, which would at least allow a comparison with the mean climatic conditions for longer periods (i.e. for more than 5 years). Spectral analysis of the variations in acidity and EC, a Nye flow model, and comparison of the results with the climatic record indicate a mean annual net accumulation between 30 and

32 cm a^{-1}, confirming the tritium dating. Therefore, the bottom layer of the Skobreen ice core was deposited between 1927 and 1930.

Variations in acidity and EC have been preserved and both show increasing values towards the surface, although they are not very significant statistically. On the other hand, examination of the trends of the annual maximum points to a marked increase in acidity. This is to be expected if a marked seasonality exists in the precipitation of strong acids in the Archipelago. The upper 5 m of the core have a mean H^+ concentration of 5.8 ± 0.3 μEq l^{-1}, which represents an increase between 75 and 107% from baseline values for the Archipelago. This high concentration is similar to concentrations in the Agassiz ice cap, Ellesmere Island (Barrie, Fisher and Koerner, 1985). The concentration of H^+, on the other hand, is lower than concentrations measured by Semb, Brækkan and Joranger (1984) in central Spitsbergen. This last observation is associated with the fact that all the ionic profiles show abrupt reduction in the mean concentration below 4 m, indicating that the core has suffered partial elution of H^+ and other ions. The electrolytic conductivity also increases towards the surface but the trend is not highly significant. Furthermore, there is no relationship between acidity and EC, indicating that other factors besides the concentration of H^+ control the conductivity of the meltwater.

All ionic profiles show evidence of partial elution below a depth of 4 m. Nevertheless, the mean concentrations are still above the baseline levels. The excess-sulphate profile indicates an increased anthropogenic contribution towards the surface. The $[SO_4^{2-}]^*$ can be greater than the baseline levels by more than an order of magnitude. This high excess sulphate, associated with high H^+ concentration, indicates that the snow precipitating at Skobreen is heavily polluted by anthropogenic sources.

Finally, as a suggestion for future work in the area, it would be advisable to drill in one of the small ice caps such as Barlaupfonna. Reduced melting and less dust would guarantee a better record and easier interpretation of the environment than was possible in the case of the Skobreen core. Nevertheless, it would still be advisable to obtain a detailed excess deuterium - *d* profile in order to have an annual resolution of the core, because melting will still affect the surface of these ice caps, although to a lesser degree. Our experience demonstrated that an electro-thermal or thermal drill should be used so that the equipment does not stick in the ice.

CHAPTER 4

THE STABLE-ISOTOPE RECORD IN SVALBARD

4.1- Introduction

This chapter investigates stable-isotope variations in space and time in Svalbard. The study has three main objectives: (1) to determine which factors control the stable-isotope composition of precipitation in Svalbard. The variations in the stable-isotope ratios at the IAEA station (Isfjord) in the course of the year are examined on the basis of the relationships between the two-stable isotope ratios δD and $\delta^{18}O$, and between the mean monthly $\delta^{18}O$ and atmospheric temperature. The study also investigates whether there is any regular relationship between the stable isotope-ratios and the environmental parameters (e.g. temperature) that may contribute to the interpretation of the Svalbard ice cores. The present stable-isotope values of the ice-core sites are compared with the results obtained from a simple model of the isotope fractionation mechanism; (2) to study the relationship between the stable-isotope variations in the upper part of the Lomonosovfonna core and atmospheric temperature. This study is carried out in the hope of providing an oxygen-isotope/air-temperature gradient which would permit the interpretation of shifts in the stable isotope in terms of temperature changes; (3) to re-interpret the long-term stable-isotope record in the Svalbard cores which have been recovered by Soviet scientists since 1975 (main references: Gordiyenko et al., 1981; Kotlyakov, 1985; Arkhipov et al., 1987; Punning, Vaykmyae and Tóugu, 1987). The stable-isotope profiles of the three best-preserved cores (i.e. Austfonna, Lomonosovfonna, and Vestfonna) are examined for the last 700 years, allowing the reconstruction of the main events of the Little Ice Age in the Archipelago. This re-interpretation is necessary because new mean annual net accumulation rates have been determined by the author of this dissertation for both the Austfonna and Lomonosovfonna cores. Furthermore, the environmental interpretation of these records is based on the knowledge obtained from these studies of the fractionation process in the region, and is supported by variations in other parameters (e.g. the proportion of percolation ice). Finally, the stable-isotope time series are compared with the Crête (Greenland) core stable-isotope record and to the sea-ice variations off the Icelandic coast in order to establish whether changes in Svalbard were contemporaneous with changes in other parts of the Greenland Sea/NE Atlantic region.

4.2- Stable isotopes in precipitation: seasonal and spatial variations in the Archipelago

In this section the variations in the isotope ratios in the precipitation at the International Atomic Energy Agency (IAEA) network station (i.e. Isfjord) are examined. It aims to check two basic assumptions in the interpretation of ice cores: (1) there is a strong seasonal variation in the stable-isotope values which allows the identification of annual layers; (2) there is a regular relationship between the isotope values and the atmospheric temperature of the precipitation. The relationship between $\delta^{18}O$ and temperature at the surface of the ice-core sites is examined to obtain a $\delta^{18}O/\delta T$ gradient. This will make possible (or not) the determination of a transfer function in order to relate changes in $\delta^{18}O$ along the depth of an ice core to past temperature fluctuations. Finally, the relationship between δD and $\delta^{18}O$, and the spatial distribution of the $\delta^{18}O$, is examined to elucidate the factors controlling the isotope composition (e.g. altitude, latitude, and distance from the water-vapour source) throughout the Archipelago.

4.2.1- Seasonal variations

Isotope studies in ice cores presume that there is a marked difference in the ratio of heavy isotopes in summer (δs) and winter (δw) precipitation at high latitudes (Epstein, 1956), which allows the identification of annual layers, the dating of an ice core, and the determination of accumulation rates (Dansgaard et al., 1973). This assumption is true for high polar glaciers, where the difference $|\delta s - \delta w|$ may be greater than 10‰, mainly due to the temperature effect. On the other hand, it is not common for sub-polar island stations (like Svalbard), which show a complex distribution of isotope values in the course of a year. The identification of the annual layers is additionally complicated by intense melting and percolation (Ambach et al., 1972), and rain-water infiltration (Moser and Stichler, 1980). Fractionation between the liquid and solid phases, followed by flush-out of the lighter isotopes, further alter the initial record (Arnason, 1969) and cause rapid isotope homogenization or the obliteration of the annual layer, particularly if the $|\delta s - \delta w|$ is small.

Fig. 4.1 shows the unweighted and precipitation-weighted monthly means of the isotope values for the period 1961–75. The isotope values were obtained from the IAEA survey (IAEA, 1969–79). The isotope composition varies little, which becomes clearer when it is compared with the variation in temperature during the year: there is a difference of 17.6°C between February and July. The unweighted mean difference of $\delta^{18}O$ between the summer (May–October) and winter (November–April) months is only ~2‰. It is important to note that this difference exists only over a longer period. Dansgaard (1964), for example, noted an anomalous seasonal effect for the years 1961–62. He found that $\delta^{18}O$ at Isfjord increased in winter (i.e. $\delta s - \delta w = -2.7‰$). The difference between the isotopically warmest (July) and coolest (March) months is also small, only 4.3‰, and would make the identification of

summer peaks difficult. Furthermore, this is not a regular feature of precipitation in Svalbard. It is not abnormal to find winter precipitation with high isotope values. In fact, the highest value ever measured in Svalbard was -4.6‰ during March. The weighted mean $\delta^{18}O$ values show a similar picture: the lowest $\delta^{18}O$ value occurs in February. Weighted monthly mean values are more representative, as the lighter precipitation events can be affected greatly by fractionation during the fall (i.e. amount effect at high temperatures). For ice-core studies the precipitation-weighted mean is more relevant as it will give more weight to the wettest periods.

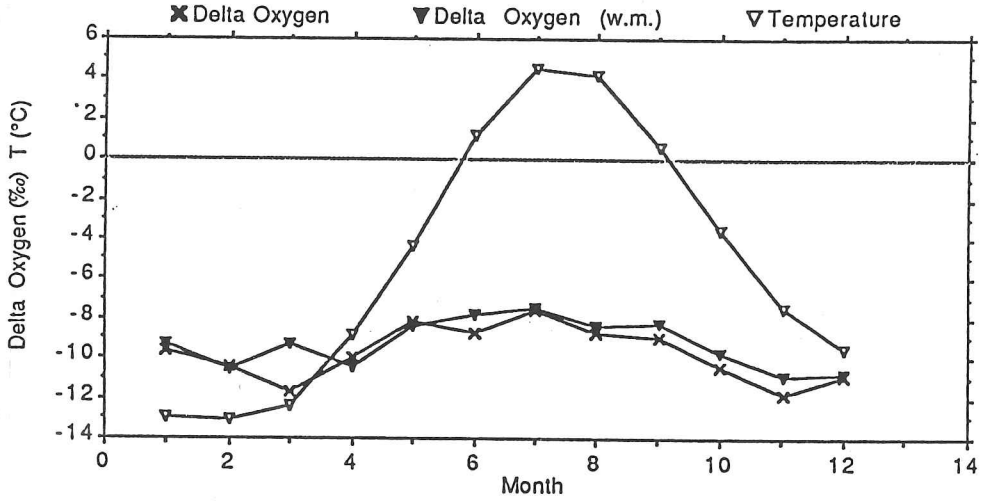

Figure 4.1- Mean monthly $\delta^{18}O$ and temperature of the Isfjord precipitation (see text for details). The multiplication sign represents the mean $\delta^{18}O$ and the closed triangle the mean $\delta^{18}O$ weighted for the amount of precipitation; the open triangles represent the mean temperature of the precipitation.

The great variability in the δ values in the course of any one year is due to the type of precipitation in Svalbard. Precipitation is associated with frontal activity and varies sharply with the passage of cyclones (Punning and Vaykmyae, 1985). These rapid changes are especially great in winter. From time to time the cold Arctic air is broken by a cyclone bringing moisture from mid-latitudes with high $\delta^{18}O$. This last observation has important implications for the isotope ratios during colder periods. The mean position of the Arctic front will move southward during colder periods or during periods of more meridional flow. The cold Arctic air mass will be more stable over the Archipelago. As a result, cyclones bringing precipitation will move over the Archipelago less often in the winter, and they will be more depleted of heavier isotopes when they reach Svalbard, which will result in a greater difference in isotope content between summer and winter precipitation. Annual layers may therefore be identified more easily during colder periods, because of a greater $|\delta s - \delta w|$ and better preservation due to reduced melting and percolation.

The small seasonal isotope differences, the rapid changes in $\delta^{18}O$ values, and homogenization due to post-deposition processes would make the identification of annual layers difficult. The variations due to change in circulation are greater than the seasonal isotope variations in Isfjord. However, snow samples collected at the surface of the ice-core sites in Svalbard show greater |δs - δwl: Grönfjord-Fridtjovbreen (4.1‰; Vaykmyae et al., 1977), Skobreen (3‰), Lomonosovfonna (5.7‰; Gordiyenko et al., 1981), and Austfonna (6–8‰; Arkhipov et al., 1987). Probably the main cause of these variations is the greater continentality of these sites, which would increase the seasonal differences in temperature, and consequently the stable-isotope differences. Nevertheless, even the differences in these δ values may be reduced rapidly in present summer conditions in Svalbard. It is thus not possible to use isotope variations for the identification of different seasons. A new approach is needed for annual-layer identification: for example, the analysis of other properties that are not strongly affected by post-deposition processes. This approach is examined in Chapter 3.

4.2.2- Relationship between $\delta^{18}O$ and mean air temperature

In this section the relationship between $\delta^{18}O$ and temperature in precipitation at Isfjord is examined. The aim is to check whether the variations in $\delta^{18}O$ are related to changes in temperature. This in turn may allow (or not) the determination of an equation relating temperatures on the surface to $\delta^{18}O$ fluctuations.

The isotopic fractionation of precipitation depends on several factors: the origin of the water vapour; the past history of the precipitation cloud system; the type of cooling of the air masses (i.e. isobaric, adiabatic), the mean evaporation and condensation temperatures and the processes of condensation and evaporation (Jouzel and Merlivat, 1984), and the distance from the source of water vapour (Fisher and Alt, 1985). Further, isotopic fractionation is related to different geographical parameters such as latitude, altitude, distance from the coast, and the amount of precipitation (Dansgaard, 1964). However, the isotope composition of precipitation depends mainly on the condensation temperature (Picciotto, DeMaire and Friedman, 1960; Dansgaard, 1964; Dansgaard et al., 1973). In general, studies have tried to establish a relationship between surface temperature and $\delta^{18}O$ values, as there have been few measurements of condensation temperatures. Dansgaard (1964) and Dansgaard et al. (1973) demonstrated that the mean annual $\delta^{18}O$ correlates with the mean annual surface temperature. For the North Atlantic coastal stations Dansgaard (1964) determined the following relationship: $\delta^{18}O = 0.695\ T(°C) - 13.6$. Yurtsever (1975), using a multiple linear regression analysis of the $\delta^{18}O$ of precipitation and latitude, altitude, amount of precipitation, and temperature, confirmed that the temperature variations can generally be established from isotope variations. He obtained the following relationship: $\delta^{18}O = (0.521 \pm 0.014)\ T(°C) - (14.96 \pm 0.21)$. These observations agree well with values calculated from a simple Rayleigh condensation model. The Rayleigh process holds that condensation occurs at equilibrium and that the condensate is removed immediately from the system after condensation (Dansgaard,

1964). Nevertheless, these observations are true only for regions where the mean condensation temperature is approximately the same as the mean surface temperature. This is rarely the case in Svalbard, which is affected by frontal activity, so a good linear relationship might not be expected between temperature and $\delta^{18}O$. Furthermore, in summer conditions precipitation may fall as water, and re-evaporation and exchange with the vapour alter the initial $\delta^{18}O$ (Aldaz and Deutsch, 1967; Peel and Clausen, 1982). In recent years increasing criticism has been levelled at this methodology, because there is no physical reason for the MAAT to correlate with the condensation temperature of a few days with precipitation (Bradley and Eischeid, 1985; cf. Section 4.3).

Unfortunately, it is not possible to verify the relationship between mean annual temperature and the $\delta^{18}O$ of precipitation in Svalbard. Monthly $\delta^{18}O$ measurements are only available for 4 years. In Fig.4.2, the monthly mean $\delta^{18}O$, averaged over a period of 15 years (1961–75), is compared with the monthly mean temperature at Isfjord (i.e. the sampling site). The resulting regression, $\delta^{18}O = (0.15 \pm 0.05)\ T(°C) - (8.96 \pm 0.37)$, is highly significant (i.e. $\alpha < 0.01$) where $r = 0.73$. On the other hand, the high scatter shows that temperature cannot explain all the isotope variability. A relatively low slope of the regression line, 0.15‰/°C, indicates that the condensation processes do not follow a Rayleigh model (i.e. condensation processes do not occur in equilibrium conditions). This is to be expected because the air masses are unstable as a result of frontal activity and the high summer temperatures. Soviet scientists observed rapid variations in $\delta^{18}O$ which were not related to temperature changes (Punning and Vaykmyae, 1985). Precipitation occurs in the form of rain in summer, sometimes at temperatures higher than 10°C, so the precipitation undergoes considerable alteration as it falls. The initial isotope values are altered by isotopic exchange between the falling drops and the environmental vapour and by re-evaporation. Moreover, the kinetic effect can be important when precipitation takes the form of rain, and the $\delta^{18}O$ of the precipitation may sometimes approach the **SMOW** value. This demonstrates that the local contribution may be important and it is discussed in the following sections.

Usually the mean $\delta^{18}O$ for a period of years is related to the mean surface temperature for the same period at a station or ice-core site. This will smooth out the high scatter (shown in Fig. 4.1) due to the processes outlined in the previous paragraph (i.e. re-evaporation, etc.). For example, data have been correlated elsewhere with the 10 m ice-core temperature (e.g. Peel and Clausen, 1982) to derive the $\delta^{18}O/\delta T$ gradient. This methodology cannot be applied to the Svalbard ice-core sites. The 10 m temperature is increased by the release of latent heat due to refreezing of meltwater. In the following paragraph the estimated surface temperature for the ice-core sites is used to determine the spatial trends in the Archipelago. However, only broad conclusions can be reached. Meteorological information from the interior of the Archipelago is lacking, so the estimated temperatures cannot be accurate (cf.

Table 4.1). In Section 4.3 the estimated temperature time series for Lomonosovfonna and Skobreen are compared with their respective $\delta^{18}O$ time series.

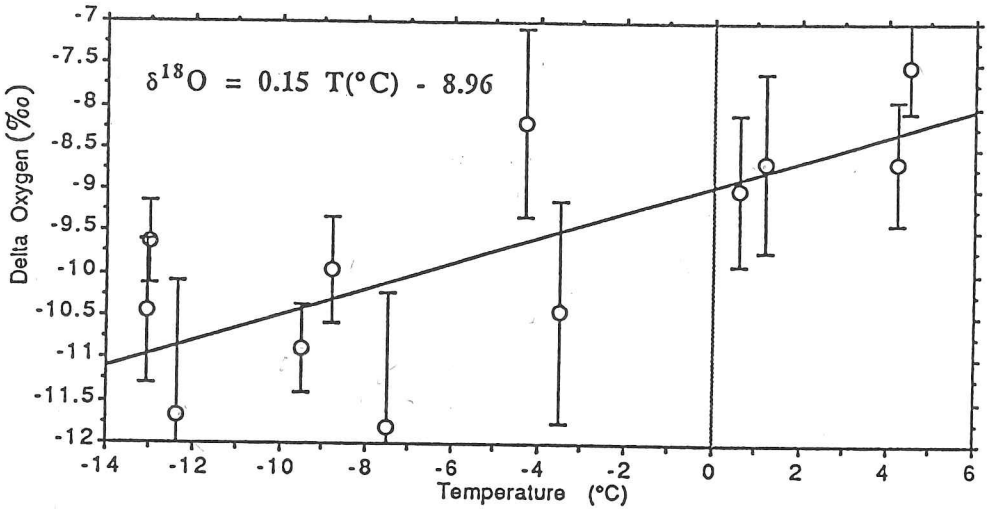

Figure 4.2- Relationship between the isotope composition and temperature of the Isfjord precipitation. The error bars represent one standard error of the monthly mean.

In Fig. 4.3 the stable-isotope ratios ($\delta^{18}O$ values) are plotted against the estimated mean annual air temperature at the Svalbard ice-core sites (triangles). The mean temperature for a period of 10 years (1960–69) for each ice-core site was estimated from the sparse meteorological information for the interior. The isotope values refer to the same period. The three curves (*a* – *c*) represent the values predicted by a simple model of fractionation under Rayleigh condensation conditions which tries to explain the precipitation process throughout the Archipelago. Each curve represents possible air-mass temperature/pressure histories for precipitation over Svalbard. The methodology used to calculate curves *a* – *c* was the one used by Peel and Clausen (1982). In this model the $\delta^{18}O$ (‰) value at a temperature *t* is given by:

$$\delta_t = \left[\frac{\alpha_t}{\alpha_{t+\Delta t}} F^{(\alpha_m - 1)} (1 + \delta_{t+\Delta t}) - 1 \right] \times 1000,$$

where α_t is the fractionation factor at temperature *t*, α_m is the fractionation factor at $(t + \Delta t/2)$, and F_v is the remaining fraction of the vapour phase at *t* compared with that at $t + \Delta t$. $H_2{}^{18}O$ fractionation factors for temperatures below 0°C have not been derived yet. On the other hand, Peel and Clausen (1982) demonstrated that fractionation factors between water and vapour determined by Majoube (1971) for the 0 – 100°C range can be extrapolated up to -20°C. The results obtained by using the extrapolated factors deviated less than 2% from the

results calculated by using HDO fractionation factors (Merlivat and Nief, 1967) and then converted to $\delta^{18}O$ by the relation $\delta^{18}O = \delta D/8$. The curves assumed that condensation occurs as water throughout. This is a reasonable assumption for the range of mean temperatures encountered in Svalbard (in general above -16°C). As in Peel and Clausen (1982), F_v was calculated as the mixing ratio at pressure p_t and temperature t divided by the mixing ratio at $p_t - \Delta t$ and $t - \Delta t$. The values for the mixing ratio were derived from tables 73 and 74 of List (1949). In the case of adiabatic cooling (curve ***c***), the pressure p at a given temperature was determined from tables of p versus t along saturation pseudo-adiabats (Letestu, 1966; table 4.15.1). The temperature was reduced by 1°C at each step.

The airmass is assumed to have cooled isobarically in the North Atlantic, arriving at Isfjord (7 m a.s.l.) with an ^{18}O content of -9.4‰. This is considered to be the dominant cooling process in air masses moving over oceans and sea ice towards higher latitudes (Peel and Clausen, 1982). On the other hand, if the mean annual $\delta^{18}O$ values for Isfjord (i.e. -9.4‰ where T = -5.8°C) are compared with values for Reykjavik (i.e. -7.5‰ at T = 4.8°C), it becomes clear that the air masses moving from Iceland take up some of their vapour over the Arctic North Atlantic. It would be necessary for air masses to be in equilibrium with SMOW at +3.5°C (curve ***a***) to explain the relatively high isotope values in Svalbard. Curve ***b*** represents the case where the air masses, after passing Isfjord ($\delta^{18}O$ = -9.4‰), continue to cool isobarically towards the northwest. This is not an unreasonable assumption, at least for the western part of Spitsbergen. Indeed, the condensation altitude may be the same for all the sites. Isotope differences between sites would have resulted from in-fall alteration. Nevertheless the calculated values lay outside the error of the estimated temperature and isotope values in Svalbard. Furthermore, the distribution of accumulation over the Archipelago (Fig. 2.4A) indicates a strong orographic control. It appears that air masses are subject to rapid uplift and cooling on the western side of Spitsbergen, precipitating as a result. In this case the precipitation on the eastern side of Svalbard would be controlled by the circulation type that is dominant in the winter, when cyclones come mainly from the east (cf. Section 1.3), so curve ***c*** assumes that after passing Isfjord the air masses cool adiabatically as they are uplifted by the topography. The influence of the topography would be particularly strong on the east and west coasts of Spitsbergen, where there are mountains more than 1000 m a.s.l. Mountains can also retard the movement of a depression, thereby increasing the cyclonic precipitation (Barry and Chorley, 1982). For both curves the initial conditions are t_o = -6.0°C and p_o = 1000 mbar.

The fractionation process appears to be explained better by curve ***c***. A linear regression for the set of points representing the five Svalbard stations (i.e. Isfjord, Grönfjordbreen-Fridtjovbreen, Skobreen, Vestfonna, and Austfonna) gives: $\delta^{18}O = (0.87 \pm 0.10)$ T(°C) - (3.86 ± 1.05). The slope 0.87‰/°C lies between the theoretical slopes for isobaric and adiabatic condensation determined by Dansgaard (1964) from the range of

temperatures for Svalbard. Lomonosovfonna (closed triangle) was not included, as the $\delta^{18}O$ value is anomalously 'warm' for the estimated temperature, even if large margins of error are allowed for (horizontal bars in Fig.4.3). Two hypotheses are put forward: (1) scouring of winter precipitation by katabatic winds may occur, since Lomonosovfonna has a steep surface slope (the topography falls from 1200 to 0 m in 20 km); (2) the high $\delta^{18}O$ could result from a relatively high proportion of local moisture (i.e. from Isfjord) in summer. A process which may explain this high local contribution is discussed in Section 4.2.4.

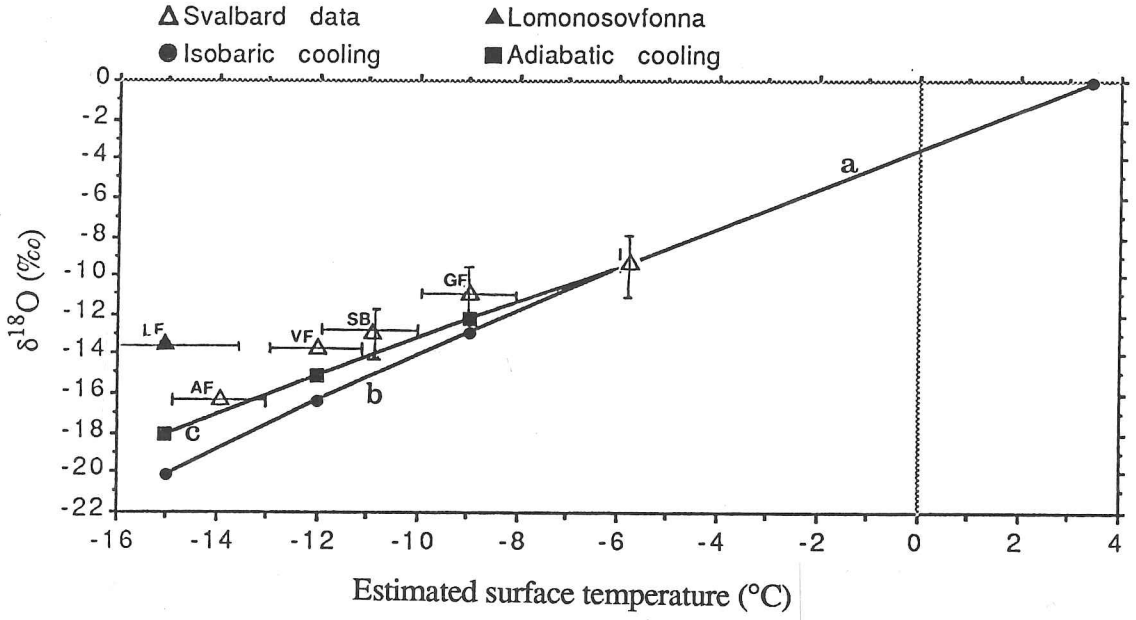

Figure 4.3- Comparison of the mean stable-isotope ratios ($\delta^{18}O$ values) of the Svalbard sites, with the results obtained from simple models of the isotope fractionation mechanism. All curves assume that condensation occurs as water throughout and were calculated with p_o = 1000 mbar. **a**: t_o = 3.5 °C. Air mass cooled isobarically to -5.8°C. **b**: t_o = -5.8°C. Air mass cooled isobarically throughout. **c**: t_o = -5.8°C. Air mass cooled adiabatically throughout. Svalbard data are marked by open triangles, except Lomonosovfonna (**LF**, closed triangle); **AF** (Austfonna), **GF** (Grönfjord-Fridtjovbreen), **I** (Isfjord), **SB** (Skobreen), and **VF** (Vestfonna). The horizontal bars are the errors in the estimated surface temperature (see Table 4.1 for details). Vertical bars represent one standard error in the mean isotopic composition.

The hypothesis of adiabatic cooling appears to be strengthened by the relationship between $\delta^{18}O$ and altitude of the site (Fig. 4.4A). If the Lomonosovfonna value is not taken into consideration, the resulting relationship is: $\delta^{18}O = (-0.0089 \pm 0.0027)$ altitude (in m) – 8.72 ± 1.39, which is significant at $\alpha < 0.05$, with $r = 0.89$. However, the rate of stable-isotope depletion in Svalbard is slower than might be expected from the fractionation model. This slower rate may be reflecting the local contribution of moisture, particularly in summer. This hypothesis is supported by the correlation between the $\delta^{18}O$ and distance from each site to the nearest open water, which gives $\delta^{18}O = (-0.11 \pm 0.06)$ distance (in km) - 9.83 ± 0.79.

The correlation coefficient (r) for this relationship is 0.93 and is significant at $\alpha < 0.008$ (Fig. 4.4B). More importantly, it applies to all the cores (i.e. also that from Lomonosovfonna). Open water means any area which is free of sea-ice cover for at least part of the year. For example, in the case of Lomonosovfonna the nearest water is the head of Isfjorden in summer. In the case of Austfonna the distance between the centre of the ice cap and the coast was taken into account. The sea ice varies substantially from year to year in this area, and sometimes does not melt in summer. On the other hand, satellite observations show that in some years open water can extend to 83°N north of Svalbard, in the middle of winter (Vinje, 1977; cf. Section 1.3). From these observations it appears that the extent of sea ice off the coast of Svalbard plays an important role in stable-isotope composition in the area. In the following sections this point is discussed in more detail by comparing the ice-core records with the record of the sea-ice extent off Iceland.

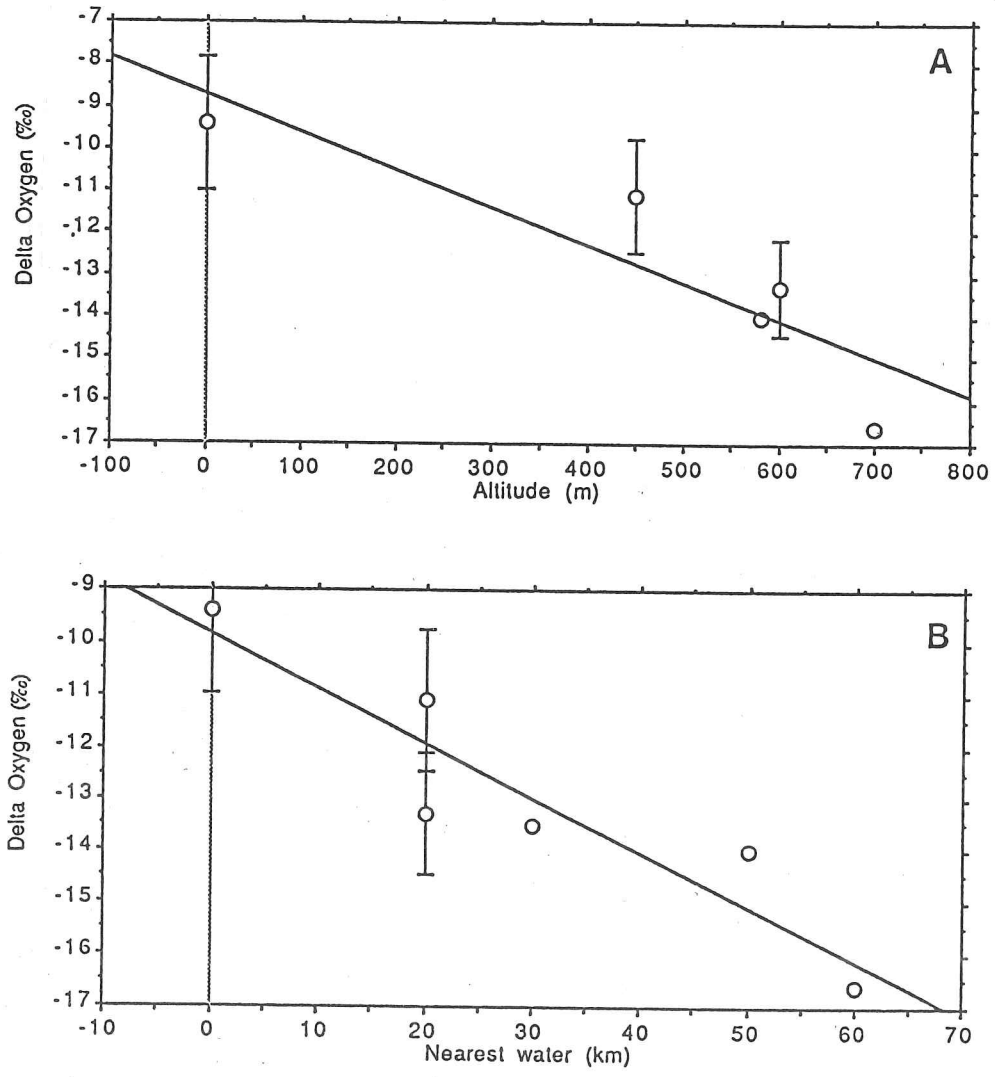

Figure 4.4- Mean values of $\delta^{18}O$ at Svalbard sites during the 1960s as a function of the altitude (A) and distance from the nearest open water (B). Bars represent one standard error in the mean isotopic composition.

Table 4.1- Mean $\delta^{18}O$, 10 m temperatures, and estimated surface temperature for snow- and ice-sampling sites in Svalbard.

Site	Altitude (m)	10 m Temp.	Mean Surface Temp. [b] (°C)	Mean $\delta^{18}O$ [b] (‰)	Accumulation [b] (kg m^{-2} a^{-1})
1. Barentsburg	70	------	-6.0	-10.8	?
2. Isfjord	7	------	-5.8	-9.4	440
3. Grönfjord-Fridtjovbreen	450	0.0	-9.0 [a]	-11.1	570
4. Lomonosov	1120	-1.5	-15.0 [a]	-13.5	828
5. Austfonna	700	-1.0	-14.0 [a]	-16.6	890
6. Vestfonna	580	-3.2	-12.0 [a]	-14.0	810
7. Skobreen	600	-2.8	-11.0 [a]	-13.3	330

Notes:

(a) Long-term weather observations in Svalbard are restricted to the coastal stations. Investigations of the climatic conditions on the ice masses of the Archipelago have been carried out briefly during scientific expeditions, in general in summer. On the other hand, these observations (e.g. Baranowski and Glowicki, 1975, for southern Spitsbergen; Arkhipov et al., 1987, for Austfonna; and Izumi et al., 1988, for Åsgårdfonna) indicate an environmental lapse rate of between 0.5 and 0.9 °C/100 m and an east–west gradient of between 0.6 and 1 °C per 100 km. Temperatures for the other ice-core sites were estimated by applying these values to the weather station nearest to an ice-core site. The given values are the mean of the maximum and minimum estimated temperatures.

(b) All data refer to the decade of 1960. This is because it is the only period for which there are data from all the ice cores. The data from Isfjord station are also from the 1960s, but the Barentsburg data includes samples from the 1970s.

4.2.3- Relationship between δD and $\delta^{18}O$

The relationship between δD and $\delta^{18}O$ can provide further information on the process of condensation. An empirically linear relationship has been established between the deuterium and ^{18}O contents of meteoric water samples (Craig, 1961a). This relationship can be represented by the equation $\delta D = 8\delta^{18}O + 10$ in samples collected around the world. It was confirmed in theory by Dansgaard (1964), who calculated a similar relation, taking into consideration a simple equilibrium process of fractionation. This relationship has been confirmed in samples from different polar snow and ice masses (e.g. Antarctica; Epstein, Sharp and Gow, 1965; Lorius and Merlivat, 1977). The slope of the relationship is thought to be determined by the rain-out process. Slopes significantly different from 8 would indicate that the fractionation process has not taken place at thermodynamic equilibrium (Moser and

Stichler, 1980). Recently, some reservations have been raised about this approach for the case of solid precipitation. Jouzel and Merlivat (1984) demonstrated that a model based on snow formation in isotopic equilibrium would not explain the observed global relationship. On the other hand, the slope of about 8 can be reproduced for the case of solid precipitation when a kinetic effect on vapour deposition is taken into consideration (Jouzel and Merlivat, 1984). The kinetic effect must be taken in consideration because snow fractionation takes place in an environment supersaturated over ice (Jouzel et al., 1987).

Fig. 4.5 compares the δD vs. $\delta^{18}O$ relationship in the Isfjord samples with the linear relationship determined by Craig (1961a). Craig's line was recalculated from the original data for the range of isotope values encountered in Isfjord (i.e. $\delta^{18}O$ from -4‰ to -16‰), resulting in the following equation: $\delta D = (8.1 \pm 0.3)\ \delta^{18}O + (5.2 \pm 3.1)$ ‰. The relationship between δD and $\delta^{18}O$ at **Isfjord** is the following:

$$\delta D = (6.3 \pm 0.2)\ \delta^{18}O - (7.5 \pm 2.4)\ ‰$$

This regression line is clearly different from the global relationship. The low slope may be attributed to non-equilibrium fractionation mainly during the summer, or by in-fall alteration as described above. The isotope-ratio relationship in the winter, when the atmospheric temperature was lower than -5°C, confirms these observations (Figure 4.5D). The relationship obtained, $\delta D = (7.3 \pm 0.4)\ \delta^{18}O + (4.6 \pm 4.5)$ ‰, is not significantly different from Craig's line, as can be seen in Fig. 4.5B and D. The 95% confidence limits for the slope of the regression lines are superimposed.

Examination of the variation in *d* - deuterium excess in the course of the year confirms the above observations on non-equilibrium fractionation in summer. Dansgaard (1964) defined the deuterium excess parameter, $d = \delta D - 8\delta^{18}O$. He showed that the deuterium excess could be used to identify non-equilibrium processes. For example, rapid evaporation would increase both δD and $\delta^{18}O$ but would reduce *d* (Stichler et al., 1982). A more detailed discussion of the processes that alter *d* after deposition is presented in Section 3.2.4, which examines the isotope record from the Skobreen core.

There is a strong seasonality in *d* in Svalbard precipitation (Fig. 4.6A). The deuterium excess falls from 16.2‰ in March to 0.4‰ in July. The low summer values may be attributed to a rapid re-evaporation of the liquid precipitation, or to mixing of the precipitation with re-evaporated lake water (Linnévatnet is situated only 3 km from Isfjord). This hypothesis is reasonable in view of the high summer temperatures in Svalbard. Fig. 4.6B shows that there is a highly significant negative correlation with the mean monthly temperature, where $d = (-0.74 \pm 0.11)\ T(°C) + (5.28 \pm 0.83)$ and $r = 0.91$ at $\alpha < 0.001$.

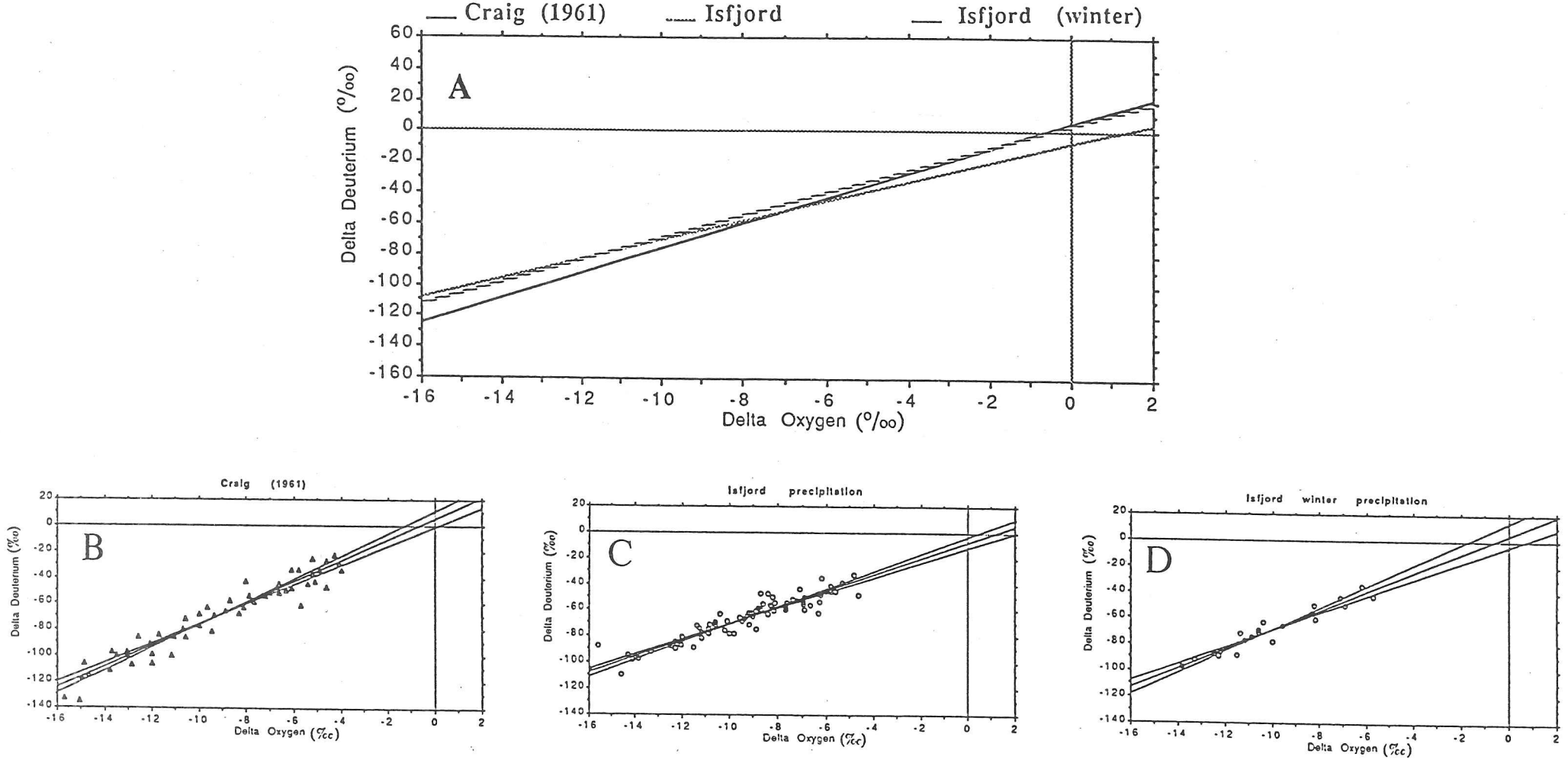

Figure 4.5- Comparison of the δD-$\delta^{18}O$ relationship of samples collected at the IAEA network station at Isfjord and from the meteoric water line (Craig, 1961). Figs. 4.5B-D represent the δD versus $\delta^{18}O$ relationship for each set of samples. The two lines equidistant from the correlation line represent the 95% confidence limits for the slope of the correlation. Note that the confidence limits of the winter precipitation in Isfjord are superimposed on the confidence limit of the meteoric water line. Compare with Fig. 3.7, which plots the same relationship for the Skobreen ice-core samples.

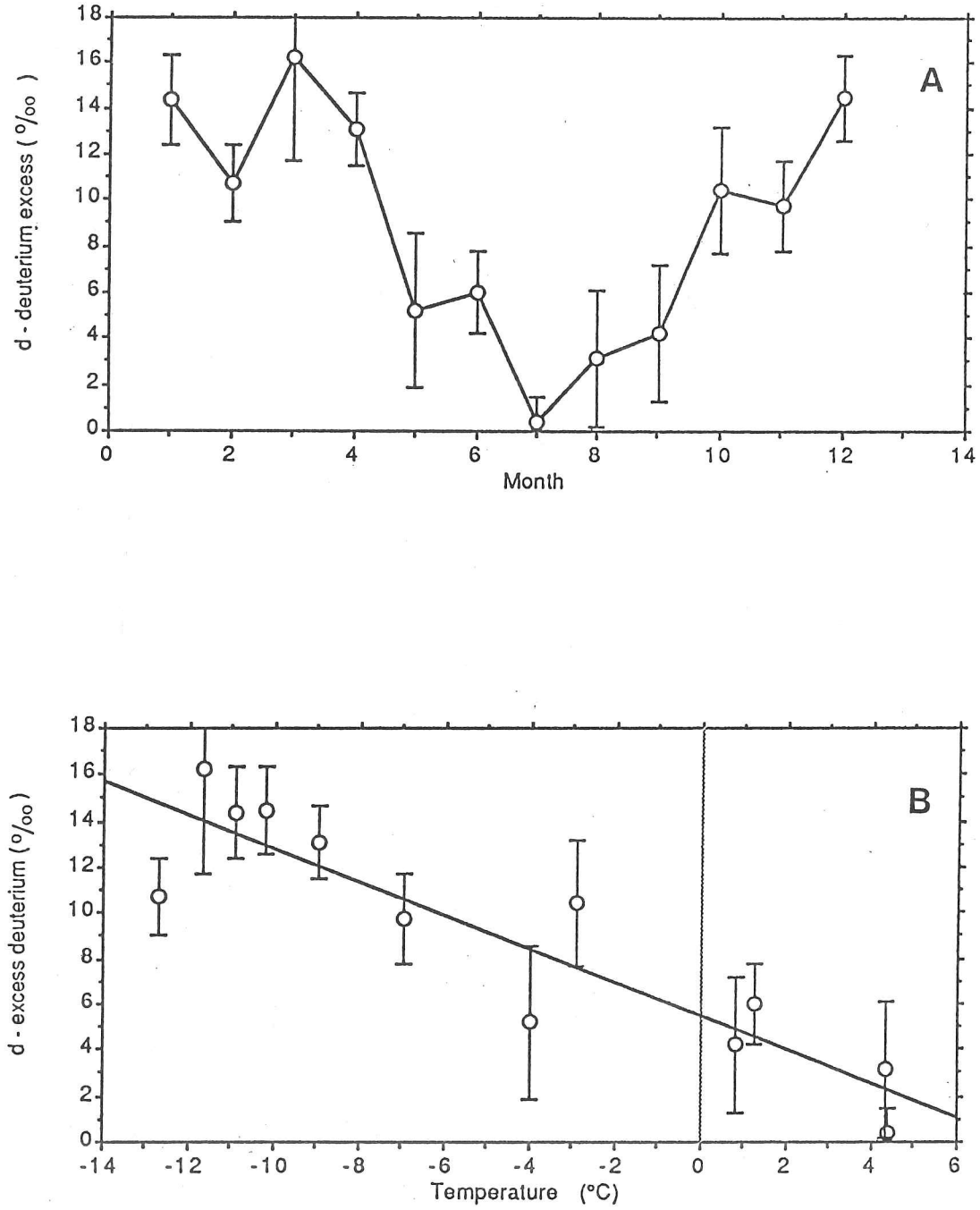

Figure 4.6- Mean monthly deuterium excess - *d* (A) and the relationship of *d* to the temperature of the precipitation (B) in the Isfjord precipitation samples.

This emphasizes the importance of non-equilibrium fractionation at relatively high temperatures.

An explanation is required for the relatively high *d* in winter precipitation in Svalbard. It varies between 11 and 16, whereas worldwide values are in general between 6 and 12. Merlivat and Jouzel (1979) demonstrated that deuterium excess depends mainly on the mean relative humidity of air masses formed above the ocean surface (it also depends on the sea-surface temperature at the source of moisture but this factor is not considered to be so important; ibid.). Past humidity conditions were derived, for example, from the stable-isotope record of the Dome C (East Antarctic) ice core (Jouzel, Merlivat and Lorius, 1982). These observations showed that *d* is negatively correlated with humidity at the moisture source, suggesting that *d* in the winter precipitation of Isfjord reflects a lower relative humidity over the areas that provide moisture (Johnsen, Dansgaard and White, 1989). However, other factors may contribute to this seasonality. For example, below the clouds non-equilibrium fractionation in summer may decrease *d*, creating a 'false' variation. The full explanation would require modelling of the fractionation process, a complex task for precipitation in a low-latitude station, because precipitation may originate from different sources, which arrive by different transport paths, and evaporate and condensate under various conditions of thermodynamic equilibrium (Johnsen, Dansgaard and White, 1989).

For the high values of *d* in samples of the Skobreen ice core there is also another, but frustrating, explanation. Between the analysis for $\delta^{18}O$ and δD enrichment may have occurred, as there was a lapse of five months between the two measurements. This point emphasizes the importance of analysing the samples for stable-isotope studies at the same time and in the same laboratory.

The strong seasonality of *d* may be used as a method of ice-core dating, which will be useful for areas like Svalbard where there is no clear seasonality in the stable-isotope ratios. In addition, it is known that superficial snow affected by melting and evaporation suffers a reduction in deuterium excess (Stichler et al., 1982, and Section 3.2.4 of this dissertation). This would increase even more the difference between *d* in snow precipitated in summer and in that precipitated in winter. There is also the possibility of proper dating of those ice cores recovered from ice masses affected by superficial summer melting. Another point that deserves attention is the use of the variability of *d* to identify past variations in humidity, which may also indicate by proxy changes in atmospheric circulation. This, however, would require a deeper understanding of cloud physics as well as a detailed examination of spatial variations in *d*.

4.2.4- Present spatial distribution of $\delta^{18}O$

Fig. 4.9 plots the spatial distribution of $\delta^{18}O$ in Svalbard since the 14th century. The data for the different maps (**A – E**) are derived from the 10-year means of ice-core profiles calculated by Soviet scientists (Punning, Vaykmyae and Tóugu, 1987). Exceptions are the data for the Isfjord meteorological station and for the Skobreen ice core. The former come from the IAEA isotope survey (IAEA, 1969–79); the latter have been processed by the author and are described elsewhere in this dissertation. The Soviet authors (Punning, Vaykmyae and Tóugu, 1987) do not give precise details about dating, but errors in the identification of annual layers are substantially smoothed out over a 10-year mean. For Skobreen an error of ±1 year has been estimated. Here only map **A**, which shows the $\delta^{18}O$ for the 1960s, is discussed. This period was chosen because it is the only one for which there are data from all the Svalbard ice cores. The examination of spatial distribution over time is discussed in Section 4.4, which describes the long environmental record of the ice cores.

There is a general decrease in $\delta^{18}O$ in both Spitsbergen and Nordaustlandet from the coast to the interior. The depletion of $\delta^{18}O$ in Spitsbergen and Vestfonna was explained above by adiabatic cooling of the air masses due to an orographic effect. Latitude has almost no influence on isotopic depletion. For example, compare Skobreen (-13.3‰ at 600 m) with Vestfonna (-14.0‰ at 580 m), which is situated about 2° farther north. The probable reason for the small difference is the relatively high temperatures on the west coast of Svalbard, caused by the West Spitsbergen Current (a branch of the Norwegian Current), and as a consequence the transport farther north of moisture relatively rich in the heavier isotope. The mean temperature in Ny-Ålesund is only about 1°C less than in Isfjord. If an isobaric cooling of the air masses is assumed, it would be equivalent to a depletion of the $\delta^{18}O$ by 0.97‰ under Rayleigh conditions (Dansgaard, 1964), so some contribution from local sources is likely (as discussed in Section 4.2.2).

The distance from the open water is important for the determination of the stable-isotope composition. The snow/ice isotopic composition is more depleted farther from the open water, as demonstrated in the previous section (cf. Fig. 4.4). This observation raises the question of the 'anomalous' isotopic composition of Lomonosovfonna. The $\delta^{18}O$ at Lomonosovfonna is relatively high for its altitude (i.e. -13.5‰, at 1120 m a.s.l.). As already mentioned, one of the hypotheses which might account for these values would be the scouring of the isotopically lighter winter accumulation. On the other hand, the $\delta^{18}O$ of this site accords with the relationship between stable isotopes and the distance from open water in Svalbard. Another interesting feature is the chemical composition of the upper layers of the ice core recovered from this site. Cl^- and $[SO_4^{2-}]^*$ are anomalously high, to say the least. Chloride concentrations can reach 271 $\mu Eq\ l^{-1}$ and excess sulphate concentrations 310 $\mu Eq\ l^{-1}$. Chloride concentrations are frequently greater than concentrations at the snow surface of glaciers on the western coast (cf. Section 5.4 for a more detailed discussion of the

ionic variations over the Archipelago). The most probable source of the sulphates is the mining town of Pyramiden, where there is a coal-burning power station near the foot of the Lomonosov plateau. The chloride contribution may come from Isfjorden. That said, it is necessary to find a process that would transport these impurities (chloride and sulphates) to the plateau. It is suggested that the air masses coming from the west in summer pass right over Isfjorden without substantial condensation. This appears to be supported by the distribution of precipitation in the fjord. There is a corridor of low accumulation of about 50 km in width (Fig. 2.4). Furthermore, the relatively high temperatures in summer would allow some evaporation, increasing the stable-isotope ratio. The moisture-rich air would meet the mountains of eastern Spitsbergen and would be uplifted and cooled adiabatically, with resulting precipitation. During this process it would collect impurities emitted from Pyramiden at the foot of the mountains.

The isotopic difference between Austfonna and Vestfonna can in general be attributed to two factors: (a) adiabatic cooling due to difference in altitude – the Austfonna site is 120 m higher than the Vestfonna one; (b) radiation cooling of the air masses moving eastward in summer, and therefore even more depleted of the heavier isotope when they reach Austfonna. The latter mechanisms may be not important in some years, as open water north of Austfonna is common (Vinje, 1977). There is a third mechanism: in winter the moisture-laden air masses approach Svalbard mainly from the southeast and east via Scandinavia and the northwestern USSR. The precipitation reaching the Archipelago is more depleted of the heavier isotope as a result of several factors (e.g lower temperatures, greater distance from the source area, condensation over the sea ice and the continent). The stable-isotope composition of Austfonna should therefore be even more depleted than that of Vestfonna.

4.3- The 20th-century stable-isotope record in Svalbard and the climatic time series

4.3.1- Introduction

This section examines the relationship between the stable-isotope composition of ice cores from Lomonosovfonna and the climatic time series. It is hoped that this will allow the derivation of an oxygen-isotope/air-temperature gradient and thus make possible the interpretation of long-term stable-isotope time series for Svalbard (cf. Section 4.4). The initial plans were to examine the relationship between the $\delta^{18}O$ variations in the Skobreen core and the climatic time series. However, this was not possible because the $\delta^{18}O$ variations have been greatly damped (Chapter 3). The study therefore had to be extended to other Svalbard ice cores. The Lomonosovfonna core was chosen because it is the one that has best preserved the $\delta^{18}O$ variations and sufficient data are available to enable the reconstruction of annual

variations. The results of this study indicate that a ratio of 0.57‰/°C is the most appropriate one for estimating shifts in temperature based on changes in delta oxygen.

4.3.2- The $\delta^{18}O$ versus δT relationship in the Lomonosovfonna core

Fig. 4.8 compares the Skobreen core (Fig. 4.8C) and the upper 40 m of the Lomonosovfonna core (Fig. 4.8D) with the variations in MAAT (Fig. 4.8A), precipitation-weighted mean annual temperatures (Fig. 4.8B; PWMAT – see the definition of this parameter in Appendix 1), and sea-ice concentration off the Iceland coast (Fig. 4.8E).

It can readily be appreciated that the Skobreen record does not resemble the variations in other time series. This was not unexpected because, as described elsewhere in this dissertation, the site is subject to intense summer melting. Only the anomalously cool period of 1965–68 is recognizable. The peak in 1952 was most probably created artificially by the great melting and flush-out in the mid-1950s (as demonstrated by the 'warmth' index in Appendix 1). It is thus not possible to derive any useful relationship between the climatic record and the stable-isotope composition of the Skobreen core.

It was decided, therefore, to examine the stable-isotope variations for the 20th century recorded in other ice cores recovered from Svalbard (i.e. Austfonna, Grönfjord-Fridtjovbreen, Lomonosovfonna, and Vestfonna). Two main problems restricted this examination to the Lomonosovfonna record. First, the Austfonna and Vestfonna profiles have not been published in enough detail to allow the reconstruction of the variations in the $\delta^{18}O$ on a seasonal scale. Only the more general variations, considerably smoothed and averaged for 10 or more years, have been published (e.g. Vaykmyae et al., 1985). Secondly, the Grönfjord-Fridtjovbreen record is useless for the studies covered in this section because the site is subject to intense summer melting and so the original $\delta^{18}O$ had been altered considerably. This can be observed in Fig. 4.10: the Grönfjord-Fridtjovbreen profile rarely reflects the changes recorded in all the other Svalbard cores.

The Lomonosovfonna core used here is the one recovered by the Institute of Geography of the USSR Academy of Sciences in 1976 (Gordiyenko et al., 1981). The core is the best preserved in Svalbard, because the site is situated at about 1120 m a.s.l. and so meltwater percolation in summer is restricted to the upper 2–4 m and refreezes *in situ*. The total core comprises 201 m but only the upper 40 m have been sampled with a frequency (each 20–25 cm) that allows the reconstruction of seasonal variations. However, the seasonal differences in $\delta^{18}O$ are small (1.5–2‰) and it is not possible to identify all the annual layers with confidence. The bottom layer of this upper 40 m section was estimated by Soviet scientists to have been deposited in 1927, which gives a mean annual net accumulation rate (a_n) of about 828 kg m^{-2} a^{-1} (Gordiyenko et al., 1981). The determination of a_n was based mainly on the peaks of total β-activity caused by the thermo-nuclear explosions of 1963–64. It can be appreciated from Fig. 4.7A that the Lomonosovfonna profile as dated by the Soviet scientists does not bear any relationship to the MAAT time series. On the other hand, it

appears that the main temperature anomalies for the period (the cool years of 1965–68 and the warm years of 1954 and 1957) are dislocated by 7–8 years. It was decided, therefore, to re-date the core, using the following methodology: (1) the data was read from Fig. 1 of Gordiyenko et al. (1981) with a ruler divided into units of 0.5 mm, which guarantees an accuracy of ±0.2‰, and digitized for statistical examination; (2) the three MAAT anomalies mentioned were used as reference horizons for fixing the stable-isotope variations. This resulted in a mean annual net accumulation rate of about 1030 kg m^{-2} a^{-1} from 1957 to 1976 (i.e. about 24% greater than the one estimated by Gordiyenko et al., 1981); (3) a simple Nye model (described in Section 3.3.4) was run with this accumulation rate. An uncertainty exists in the running of this model because bedrock was not reached on Lomonosovfonna and no returns have been recorded by RES surveys of the plateau. Gordiyenko et al. (1981) estimated a total ice thickness of 220 m at the core site and the model was run with this value, although the authors do not explain how this thickness was obtained. The re-dated Lomonosovfonna $\delta^{18}O$ profile is compared with the MAAT time series in Fig 4.7B. Clearly, the new dating is much more representative of climatic conditions. The only modification made to the stable-isotope record, in order to obtain the best agreement, was the introduction of a gap between the years 1951 and 1953 (Fig. 4.7B). This procedure can be justified because one or two layers may have been obliterated by melting in those years, which were some of the warmest on record (cf. Fig. A1.5). The re-dated profile also agrees better with the PWMAT profile (cf. 4.8B and D), and the lowest $\delta^{18}O$ coincides with the worst sea-ice conditions for the period (cf. Vinje, 1977; and Fig. 4.8E). The bottom layer of the upper part of the core is estimated by the present author to have been deposited in about 1939.

The dating of the core by Gordiyenko et al. (1981) can be explained by either (a) percolation and refreezing of meltwater with high β-activity running-off from higher parts of the plateau; or (b) displacement of annual $\delta^{18}O$ values, due to the percolation downward in summer of the lighter isotope. In the latter case it is possible that the chemical species (e.g. ^{137}Cs) measured by the β-activity method percolate downward for a shorter distance than the ^{16}O, as they are frequently absorbed by crustal impurities that accumulate on the glacier surface in summer (cf. Section 3.2.5).

The $\delta^{18}O$ variations in the Lomonosovfonna core were converted into a time series to allow correlation with the mean annual climatic conditions. The approach used was to average all the samples between two isotopic troughs (in Fig. 1 of Gordiyenko et al., 1981) and to consider these layers as having been deposited in one calendar year, and then to compare the results with those of the Nye model for the determination of the year of deposition. Differences of up to two years were observed, most probably due to variations in mean annual precipitation and the difficulty of identifying seasonal variations because of the occurrence of damped or double peaks; certainly noise has been introduced as a result of the inclusion of ice from an adjacent year or the omission of ice of the sampling year. In any

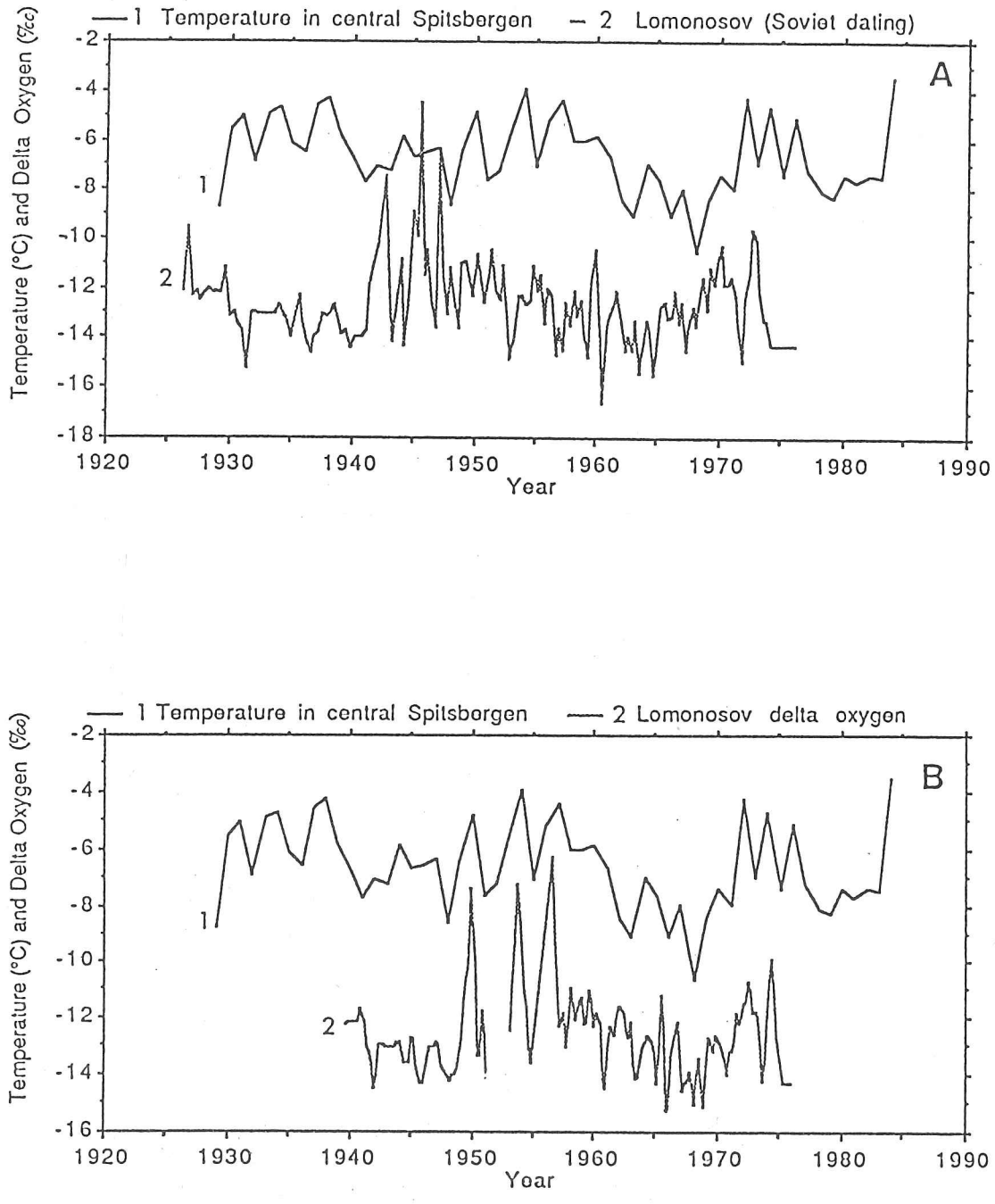

Figure 4.7- Comparison of the stable-isotope record ($\delta^{18}O$) for the upper 40 m of the Lomonosovfonna ice core with the annual mean atmospheric temperature for central Spitsbergen (1). Graph A compares the temperature time series for the Lomonosovfonna core as dated by Soviet scientists (Gordiyenko et al., 1981) and B the series for the same core as dated by the author of this dissertation.

case, 2 years is about the best accuracy that can be expected in dating any layer of this core. This represents about 2–2.5 m of ice, i.e. about the thickness in which the $\delta^{18}O$ variations may have been homogenized or damped by percolation and refreezing in summer.

The annual $\delta^{18}O$ variations in the re-dated Lomonosovfonna core were correlated with the MAAT time series estimated for central-eastern Spitsbergen and corrected for the altitude of Lomonosovfonna by a lapse rate of 0.9°C/100 m. The resulting linear regression for the period 1939–75 is statistically highly significant ($r = 0.64$ at $\alpha < 0.0001$) where $\delta^{18}O = (0.58 \pm 0.12)\ T(°C) - (5.88 \pm 0.82)$. The observed $\delta^{18}O/\delta T$ ratio (0.58‰/°C) is about 67% of the ratio determined from the spatial distribution of stable isotopes in the Archipelago (0.87‰/°C) in Section 4.2.2. Therefore the examination of the relationship between variations in delta oxygen and the MAAT was extended to the comparison of trend lines in both time series, in order to check the above ratio determined by the comparison of inter-annual values. The 1957–68 cooling is well marked in the stable-isotope record of Lomonosovfonna, in the MAAT and PWMAT time series, and appears also to be reflected in the Skobreen core, although displaced by about a year (Fig. 4.8). The gradients derived by this methodology will be less sensitive to local factors than the one determined by comparing the annual variations. The trend lines for the 1957–68 period, plotted in Fig. 4.8, are all significant at the 99% level (Table 4.2). The MAAT decreased from 1957–68 at a rate of 0.410°C a^{-1}, and for the same period the $\delta^{18}O$ at Lomonosovfonna decreased at a rate of 0.233‰ a^{-1}. No other statistically significant trend is recognizable for the period examined in Fig. 4.8 (i.e. 1930–85). Comparison of the isotopic and temperature gradients produces an average stable-isotope/air-temperature ratio of 0.57‰/°C (Table 4.2), confirming the gradient estimated from inter-annual comparisons. Therefore this gradient is used to estimate the amplitude of temperature shifts from the long-term isotope profiles (Section 4.4). A much smaller gradient, i.e. 0.28‰/°C, is obtained by comparing the isotopic trend at Skobreen from 1956 to 1968 with the MAAT trend, but this is not considered to be representative of the real conditions because of the considerable alteration due to melting and associated phenomena.

The $\delta^{18}O/\delta T$ ratio for Lomonosovfonna is similar to the one determined at James Ross Island, Antarctic Peninsula (0.59‰/°C from a $\delta D/\delta T$ of 4.5‰/°C), by Aristarain, Jouzel and Pourchet (1986), and at Devon Island (0.60‰/°C) by Koerner and Russell (1979).

Some explanation is required for the difference between the $\delta^{18}O/\delta T$ determined from analysis of the time series and those determined from spatial variations (i.e. 0.57‰/°C and 0.87‰/°C respectively). Peel, Mulvaney and Davison (1988) suggested several alternatives for a similar discrepancy observed in the Antarctic Peninsula: (1) differences between the MAAT and the temperature regime of the snowfall; (2) differences between the surface and condensation temperatures; (3) irregular seasonal deposition of snow; and (4) the influence of

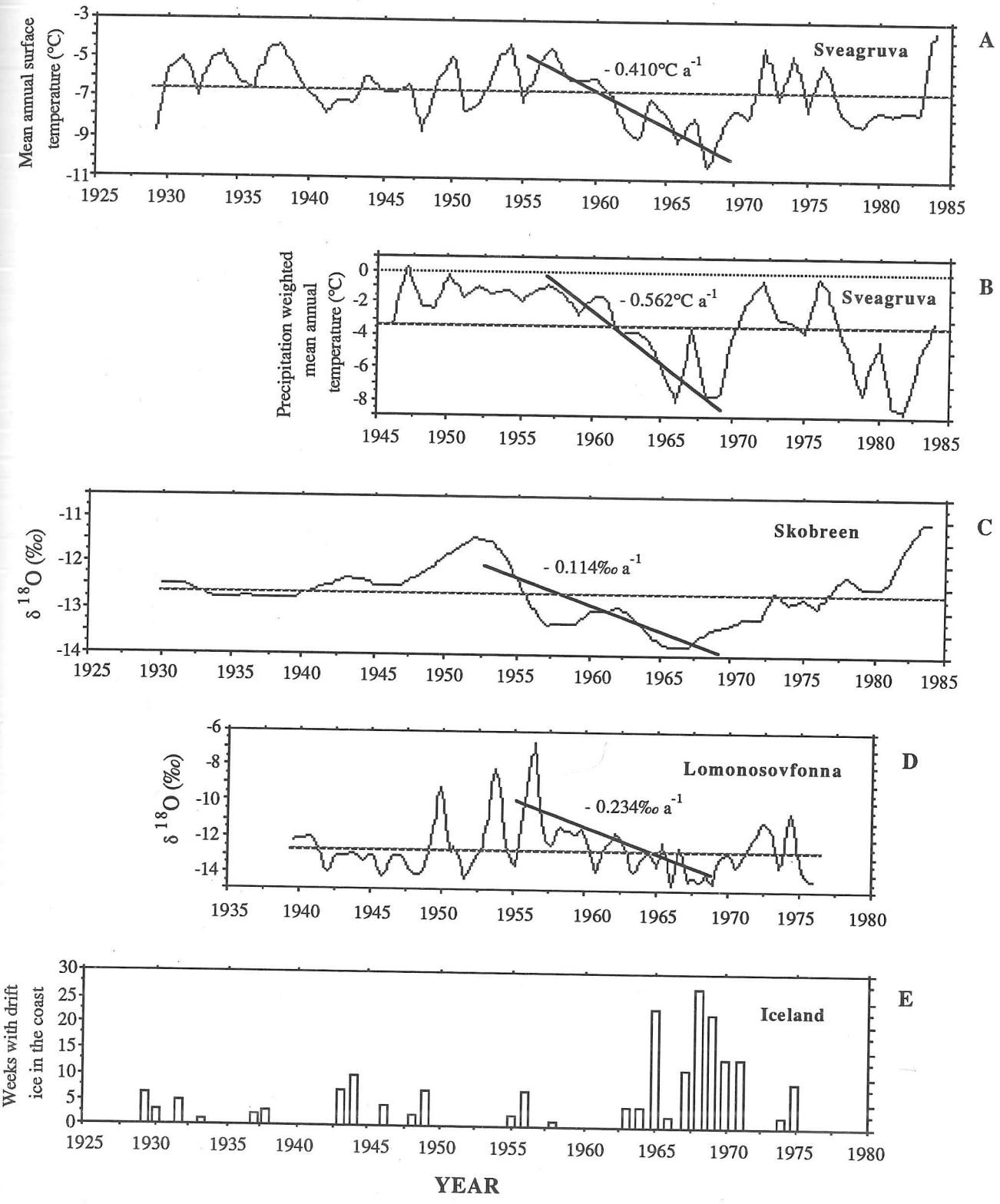

Figure 4.8- Mean annual time series of $\delta^{18}O$ at Skobreen (C) and at Lomonosovfonna (D) compared with the time series of mean annual surface temperature (A), with the precipitation-weighted mean annual temperature (B), and with the concentration of sea ice off the Iceland coast by Lamb, 1977 (E). The two temperature time series refer to values for central Spitsbergen. The thick straight lines and the rates in graphs **a – d** refer to the period between 1957 and 1968, which represent the best-defined trends of both the mean atmospheric temperature and the $\delta^{18}O$. The stippled lines represent the averages for each dataset.

sea-ice fluctuations. To these could be added local noise caused by post-depositional phenomena (e.g. melting, percolation, wind-scouring). Some of these alternatives are examined in the following paragraphs for the case of Svalbard.

Table 4.2- $\delta^{18}O/\delta T$ ratios determined for Svalbard.

Table 4.2A- Ratios determined by comparison of mean annual values for $\delta^{18}O$ at Lomonosovfonna with the MAAT time series estimated for Sveagruva.

Site	Period	$\delta^{18}O/\delta T$ (‰/°C)	r	Significance
Lomonosov	1939-75	0.58 ± 0.12	0.64	<0.001

Table 4.2B- MAAT and $\delta^{18}O$ trend lines for the period 1957–68, and derived oxygen-isotope/air-temperature gradients.

Site	dδ/dt	dT/dt	r	Significance
Lomonosov	0.23	-------	0.87	<0.001
Sveagruva	-------	0.41	0.86	<0.001
Derived $\delta^{18}O/\delta T$	0.57‰/°C			

Variations in the mean annual $\delta^{18}O$ have been used frequently in ice-core research as direct proxy for MAAT variations since Dansgaard (1964) and Dansgaard et al. (1973) demonstrated that there is a strong linear relationship between these two parameters. However, this methodology has in recent years been criticized strongly, not only because the $\delta^{18}O$ or δD depend on other factors besides the temperature of condensation (cf. Section 3.2.4), but also because there is no *a priori* physical reason why the stable-isotope composition of a few days with precipitation should correlate with the mean annual temperature (Bradley and Eischeid, 1985; Peel, Mulvaney and Davison, 1988). Precipitation in polar regions is associated with the passage of moisture-laden cyclones in a relatively small number of days (a mean of about 143 days a^{-1} in Svalbard from 1946 to 1984). Furthermore, the mean temperature of days with precipitation tends to be above the MAAT, and there is a trend towards heavier precipitation in line with the increase in temperature (Peel, Mulvaney and Davidson, 1988). One explanation for the observed relationship between $\delta^{18}O$ and δT at Lomonosovfonna is that the variations in the precipitation temperature co-vary with the MAAT. To test this hypothesis, the precipitation-weighted mean annual temperature (PWMAT) variations from 1946 to 1984 were computed on the basis of the Svalbard meteorological record (cf. Appendix 1). The comparison between the MAAT and PWMAT time series in Fig. 4.8 and a highly significant correlation ($r = 0.63$ and $\alpha < 0.0001$) appear

to confirm the hypothesis of co-variation. The following explanation is suggested to account for this relationship: warm periods will increase the open-water area and reduce the distance from the source of moisture. Furthermore, moisture-laden cyclones will reach the Archipelago more easily because of the retreat of the Arctic Front. As a consequence of these changes, both the precipitation rate and the $\delta^{18}O$ would increase in Svalbard. Thus the coincidence of the MAAT and the stable-isotope record at Lomonosovfonna is a case of indirect correlation, where the $\delta^{18}O$ is controlled by the distance from the source (i.e. the sea-ice extent), which in its turn is determined by the mean atmospheric temperature.

Differences in the surface and condensation temperatures cannot be checked for Svalbard as no simultaneous measurements have been carried out, but it remains a strong possibility that vertical variations in temperature may be great because the precipitation is frequently due to frontal activity.

There is increased evidence that distance from the closest moisture source is one of the most important determinants of the stable-isotope composition of snowfall (Kato, 1978; Koerner, 1979; Koerner and Russell, 1979; Bromwich and Weaver, 1983; Robin, 1983; Fisher and Alt, 1985). Variations in sea-ice extent not only change the distance from the source area, but also restrict the source of local moisture and increase the length of the path in which air masses suffer depletion by isobaric cooling before reaching the area of sampling. The conventional methodology for checking the importance of variations in sea-ice extent for the stable-isotope composition is to cross-correlate the monthly isotope composition and the mean atmospheric temperature at one station. This methodology is based on the observation that sea-ice variations may lag by a month the temperature variations in certain regions and so will the stable-isotope composition (Kato, 1978; Bromwich and Weaver, 1983). A visual examination of the monthly sea-ice variations around Svalbard, determined by satellite passive-microwave observations (Parkinson et al., 1987), and the respective monthly temperature variations shows that this may be the case also for Svalbard. A cross-correlation between the monthly $\delta^{18}O$ and mean temperature values at Isfjord for a period of 12 years (IAEA, 1969–79) resulted in a maximum correlation at one lag (where r increased from 0.73 at 0 lag to 0.80 at 1 lag). This observation appears to reinforce the suggestion that stable-isotope composition in the Svalbard region is controlled mainly by the distance from the moisture source.

4.4- The long-term record in the Svalbard ice cores: the last 700 years from variations in the isotopic ratios

4.4.1- The spatial variation of stable isotopes through time

Fig. 4.9A – E plots the spatial variations in $\delta^{18}O$ over time (cf. comments on the source of these data in Section 4.2.4) and is intended mainly to complement the discussions in the following sections. The periods that each plot represent were chosen for the following reasons: **A**) the stable-isotope composition of the 1960s is used to represent the present delta values as this is the earliest period for which there are data for all the cores; **B**) the period 1920–60 represents the warmest part of the 20th century and one of the warmest periods of recent centuries; **C**) the LIA reached its culmination in Svalbard between the 17th and the end of the 19th century, and this figure plots the mean $\delta^{18}O$ for the whole period; **D**) represents the longest period for which all the deep cores from Svalbard (i.e. Austfonna, Grönfjord-Fridtjovbreen, Lomonosovfonna, and Vestfonna) overlap; E) is the earliest phase of the LIA in Svalbard (cf. Chapter 1 and the following sections).

The west-to-east trend for smaller delta values is observed in all the plots, although there are variations between sites. These oscillations do not appear to bear any relationship to the mean climatic trends, because, for example, the maximum difference between Lomonosovfonna and Vestfonna occurs both in the warmer part of the 20th century and during the LIA. The 20th-century delta values are clearly greater than the long-term mean (i.e. 1600–1970, plot D), and the maximum difference is found at Lomonosovfonna (1.7‰). Minimum values at all the sites were reached during the later phase of the LIA (1600–1910, plot C), when the $\delta^{18}O$ was as low as -18.1‰ in Austfonna (a minimum of -20.0‰ was reached by the 1880s, i.e. the culmination of the LIA; cf. the next section). The mean differences between stations during the period of maximum overlap (i.e. 1600–1970, plot D) were approximately: Grönfjord-Fridtjovbreen – Lomonosovfonna (1.7‰), Lomonosovfonna – Vestfonna (1.4‰), and Vestfonna – Austfonna (2.3‰). Differences of up to 1.9‰ (Vestfonna) are encountered between the mean for the LIA and the present values (i.e. for the 1960s). No other regular differences are observed between these mean values.

4.4.2- The long-term Svalbard ice-core record: the Little Ice Age from the stable-isotope record

4.4.2a- Introduction

In this section the long-term stable-isotope record of the Svalbard ice cores is examined on the basis of the knowledge of the fractionation processes obtained in the previous sections. The period examined extends from A.D. 1300 to the present and therefore permits the study of the evolution of the Little Ice Age in the Archipelago. The discussions

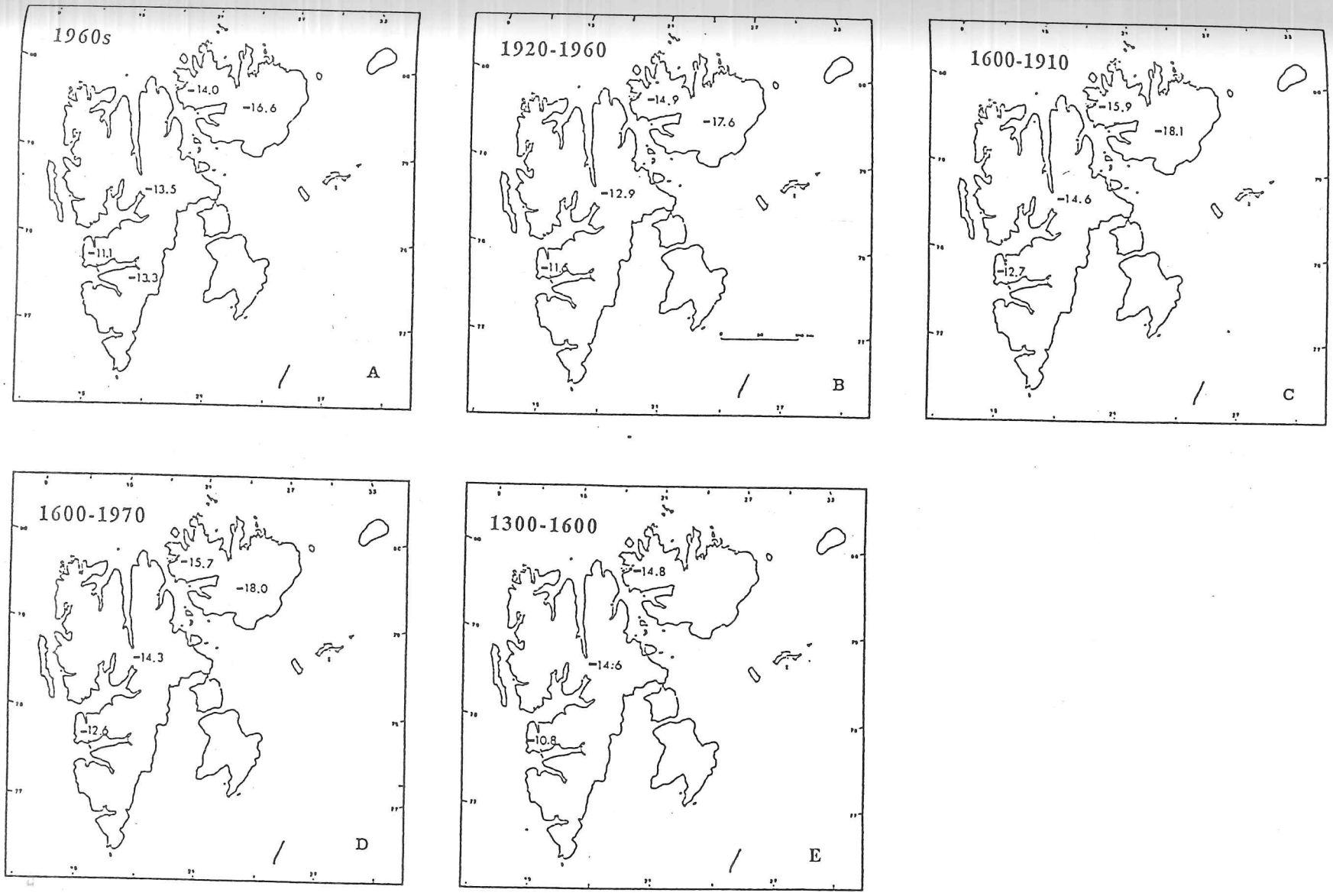

Figure 4.9- The spatial distribution of $\delta^{18}O$ through time at the Svalbard ice-core sites. Values are based on the 10-year mean plotted by Punning, Vaykmyae and Tóugu (1987) for the Austfonna, Grönfjord-Fridtjovbreen, and Vestfonna cores. The 1960s (A) are the earliest period for which there is data for all the cores and are considered to represent their present isotopic composition. Other maps refer to: (B) the relatively warmer period from 1920 to 1960; (C) the later part of the Little Ice Age, from 1600 to 1910; (D) the mean isotopic values for the period for which there is data for all deep cores, 1600-1970; (E) the pre-17th century isotopic composition (1250-1600).

use data derived from deep (i.e. >200 m) ice cores that have been recovered in the Archipelago since 1975 by scientists from the Institute of Geography of the USSR Academy of Sciences (IG – USSR). The records of three ice cores are discussed in detail: Austfonna – 1985 (main reference: Arkhipov et al., 1987), Lomonosovfonna (Gordiyenko et al., 1981), and Vestfonna (Punning, Vaykmyae and Tóugu, 1987). Details of the glaciology of these sites and of the cores are given elsewhere in this dissertation, particularly in Sections 2.3.1, 4.3.2, 5.5.3a, and in Table 2.2. The proportion of percolation ice (i.e. ice formed by melting and refreezing; Arkhipov et al., 1987) shows that the Lomonosovfonna core may be considered the best-preserved core and Vestfonna the worst. The profiles of these cores for the period A.D. 1400–1970 are plotted in Fig. 4.10 for comparison with variations in $\delta^{18}O$ at Crête (Greenland) and with the frequency of sea ice off the Iceland coast. The 10-year mean time series for the Crête core was kindly provided by Dr. H.B. Clausen of the Geophysical Institute, University of Copenhagen. Variations in other properties, such as the ionic concentration and the proportion of ice formed by melting, are used in this section to corroborate the environmental interpretation based on the stable-isotope variations. The $\delta^{18}O$ profile of the Grönfjord-Fridtjovbreen ice core is also plotted in Fig. 4.10, but this core is not considered useful because the original $\delta^{18}O$ values have been greatly altered by summer melting and flush-out.

Although the Austfonna, Lomonosovfonna, and Vestfonna cores represent the best available datasets of environmental changes in the Archipelago, the limitations of these records should be borne in mind. There is great uncertainty in dating and the Soviet scientists have rarely been able to identify seasonal oscillations in $\delta^{18}O$, so the dating of the upper layers was based mainly on the recognition of β-activity peaks caused by thermo-nuclear explosions during the last 35 years. This method has been shown not to be totally reliable in the conditions of high surface melting and percolation encountered in the Svalbard ice masses (cf. Sections 3.2.5 and 4.3.2). Errors in the dating of these upper layers may vary between 2 and 5 years. Furthermore, the mean net annual accumulation rates estimated from these studies are valid only for the second half of the 20th century. In addition, the deep cores were dated by using constant accumulation rates, and no other studies (e.g. identification of volcanic acid peaks and EC) that would allow the identification of reference horizons were carried out to establish variations in the accumulation rate. It is not surprising, therefore, that different accumulation rates have been estimated for each ice-core site at various times (see Sections 4.3.2 and 5.5.3a). Bearing in mind these difficulties in dating, it was decided to examine the stable-isotope variations on the basis of the 10-year averages, an interval that smooths out the low-frequency noise caused by melting and associated phenomena, variations in deposition, and sampling errors. Furthermore, the Austfonna and Lomonosovfonna profiles were re-dated by the author of this dissertation, using the mean annual net accumulation rates (a_n) established in Sections 4.3.2 and 5.5.3a. A simple Nye model (Nye, 1963a; Section 3.3.4) was run, using an a_n of 1030 kg m^{-2} a^{-1} for

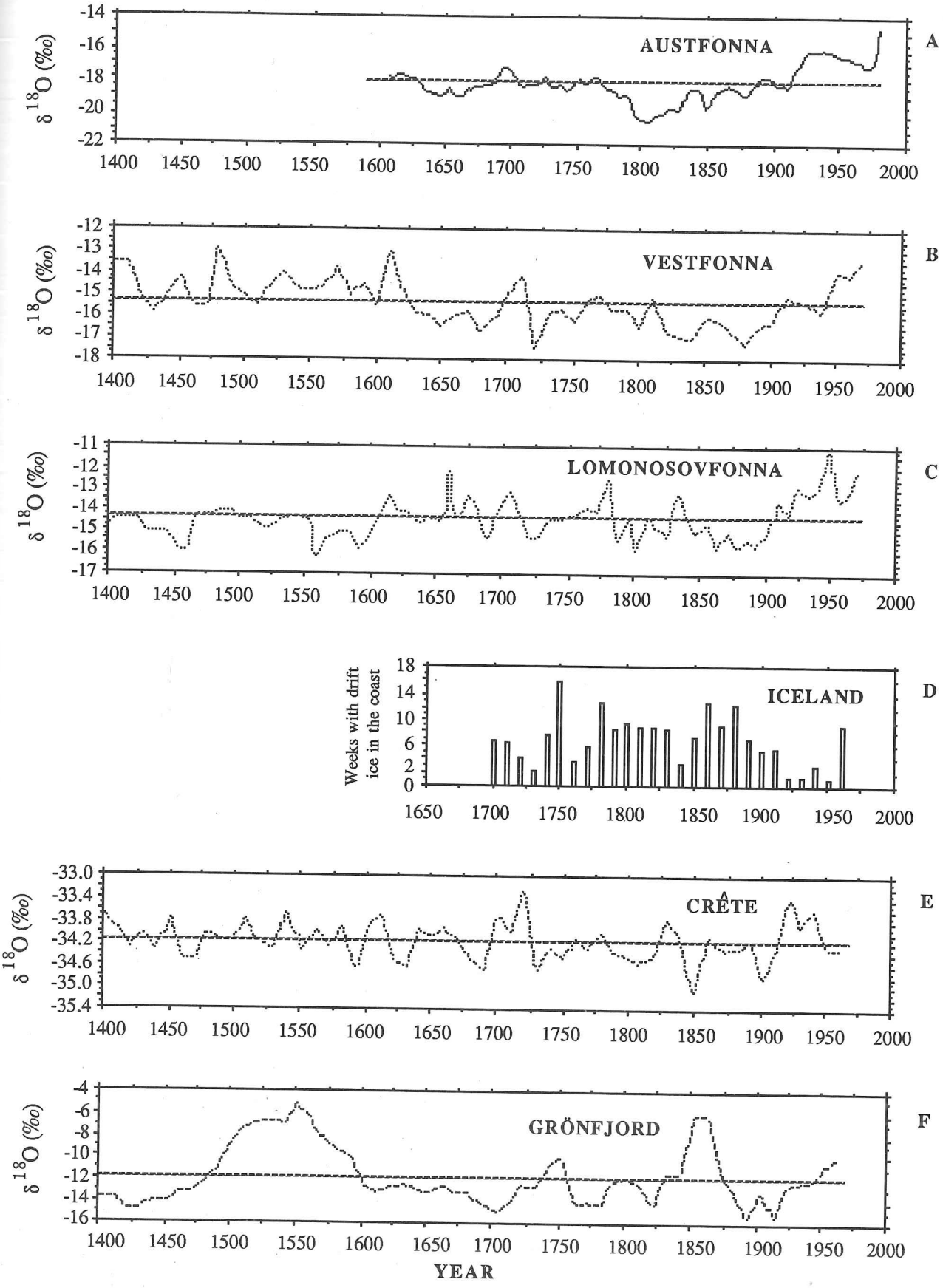

Figure 4.10- Long-term variations in $\delta^{18}O$ in the Svalbard ice cores (i.e. Austfonna, Vestfonna, and Lomonosovfonna) compared with the Crête (Greenland) δ^{18} O variations (courtesy of H.B. Clausen), and the frequency of sea ice around Iceland from the 17th century onwards (source: Lamb, 1977). The Grönfjord-Fridtjovbreen record is plotted to show the degree of alteration at this site due to the intense melting and flush-out of the lighter isotope (^{16}O) during warm periods (e.g. the 16th century). Sources: Austfonna (Arkhipov et al., 1987; re-dated by the author of this dissertation), Lomonosovfonna (Gordiyenko et al., 1981; re-dated by the author of this dissertation); Vestfonna (Punning, Vaykmyae and Tóugu, 1987). The stippled lines represent the averages for each dataset.

Lomonosovfonna (instead of 782 kg m^{-2} a^{-1} as used by Punning, Vaykmyae and Tóugu, 1987) and 460 kg m^{-2} a^{-1} for Austfonna (instead of 890 kg m^{-2} a^{-1}, ibid.). The new a_n for Austfonna is supported by light-transmissivity (which the Soviet scientists call optical-density) studies on the two Austfonna cores (Arkhipov et al., 1987; Zagorodnov and Arkhipov, in preparation), which suggest an a_n ranging from 400 to 500 kg m^{-2} a^{-1} in recent centuries. The two ice cores span the periods 1320–1970 (Lomonosovfonna) and 1590–1980 (Austfonna). The Vestfonna record comprises the period from 1100 to 1980 (Punning, Vaykmyae and Tóugu, 1987).

4.4.2b- The Svalbard stable-isotope record in relation to other paleoclimatic records in the Greenland Sea/Northeastern Atlantic

The 10-year mean $\delta^{18}O$ values for the past 600 years at Austfonna, Lomonosovfonna, and Vestfonna are shown in Fig. 4.10A – C. The period comprises the greater part of the Little Ice Age as defined in Chapter 1, and the $\delta^{18}O$ for all three cores was below the 20th-century levels for most of the time. The stippled lines in Fig. 4.10A – C are the mean $\delta^{18}O$ for the time series since 1400 for Lomonosovfonna (-14.4 ± 0.9‰) and Vestfonna (-15.4 ± 1.0‰), or since 1590 in the case of Austfonna (-18.1 ± 1.0‰). The mean $\delta^{18}O$ at Crête for the period 1400–1970 is -34.17 ± 0.36‰. Some information pre-1400 can be obtained from the Lomonosovfonna and Vestfonna cores, but the errors in dating may be large because the earlier part of the record is from the bottom 20–30 m of the cores, near the bedrock, and so the ice-flow conditions may be complex. Therefore a Nye model of ice flow may not be adequate. The Vestfonna core indicates a relatively cool 12th century †, with the mean $\delta^{18}O$ at about -16‰, followed by a warming by the mid-13th century which reached a maximum in the last decade of the 14th century, when the mean $\delta^{18}O$ was -13.6‰. The warming trend was broken by a cool period by 1330 ($\delta^{18}O$ = -15.5‰). The Lomonosovfonna core record also indicates a warm 14th century ($\delta^{18}O \approx$ -14.4‰), again broken by a cool third decade. By the early 15th century the $\delta^{18}O$ begins to fall, reaching a minimum at Vestfonna by 1430 and at Lomonosovfonna by 1460 (Fig. 4.10). It appears, therefore, in the absence of data from earlier periods, that the Medieval warm period in Svalbard continued until the end of the 14th century, and the onset of the LIA took place about the beginning of the 15th century. This estimate differs by about 50–150 years from the estimates based on moraine studies (Section 1.4.3), but is within of the accuracy of the ^{14}C dating method used for those estimates. The $\delta^{18}O$ record in Svalbard for the 13th–14th century is also at variance with the sea-ice conditions off the Icelandic coast and with the Crête core, which both indicate that the lowest $\delta^{18}O$ values during the LIA had occurred by the end of the 13th century (Section 1.4.3).

† The ice-core data for the early period (i.e. 12th–14th centuries) are not plotted in Fig. 4.10 because they are based on only a few samples. The record of sea ice off the Icelandic coast prior to 1700 is not plotted because it is considered unreliable (cf. Ogilvie, 1984, and Section 1.4.3).

Both the Lomonosovfonna and Vestfonna cores record a relatively cool 15th century. On the other hand, the stable-isotope ratio variations do not correspond in the two cores. Although many anomalies in the $\delta^{18}O$ appear similar in these cores in the period 1400–1700, a cross-correlation between the two time series for this period did not show any statistically significant relationship (at any lag). Most probably this is due to inaccuracies in dating. One of the anomalies recorded all over the the North Atlantic sector of the Arctic is the cool decade of the 1460s. The two Svalbard cores and the Crête core record a $\delta^{18}O$ minimum and are associated with extremely bad sea-ice conditions off the Icelandic coast (Section 1.4.3). One of the characteristics of the $\delta^{18}O$ profiles of these cores is that they show rapid variations on a decadal scale. For example, the cool 1460s was followed by an increase of about 2.5‰ at Vestfonna in the next decade. This would represent an increase in the mean atmospheric temperature of about 4°C in a decade (if a delta oxygen/temperature ratio of 0.57‰/°C is taken into account). But most probably the low delta values in the 1460s resulted from the combination of low temperature and the extension of sea ice to the Icelandic coast.

The record for the 16th century is not clear from the comparison between Vestfonna and Lomonosovfonna. At Vestfonna the century was relatively warm and every year had delta values greater than the average for the period 1400–1970 (i.e. > -15.1‰). However, the Lomonosovfonna core shows a different record, with delta values about the average in the first part of the century, but decreasing in the following cold period, particularly in the decades of 1560 and 1590. The Lomonosovfonna core agrees better with the conditions at Crête, but, then again, the Grönfjord-Fridtjovbreen stable-isotope peak in the middle of the century indicates very warm conditions, most probably with strong melting and flush-out of the lighter isotopes to result in $\delta^{18}O$ as high as -5‰. Without carrying out further studies on the core, it is not possible to give an explanation for these differences. A Cl^- profile for Vestfonna, which might have helped to confirm a warm period in the 16th century, is relatively flat, with concentrations less than half the Cl^- concentration in the warm years of the 20th century (i.e. about 65 $\mu Eq\ l^{-1}$; cf. Punning, Vaykmyae and Tóugu, 1987). It appears, therefore, that the high values were caused by factors other than an increase in the precipitation temperature or a retreat of the sea ice. It may be suggested that the high delta oxygen values in Grönfjord-Fridtjovbreen and Vestfonna resulted from high summer melting. At these two sites the melting would be associated with strong flush-out (naturally with the removal of a considerable proportion of the lighter isotope), but not at Lomonosovfonna because of the high altitude. Finally, a cold end for the century in Svalbard would agree with sea-ice observations off the Icelandic coast.

From the early 1600s the discussions on delta oxygen variations are supported by the Austfonna record. The first thirty years of the century were relatively warm, and in at least one of the sites (Vestfonna) climatic conditions may have been similar to those of the second half of the 20th century as indicated by a high $\delta^{18}O$ (-13.0‰). Soon the conditions

deteriorated towards a minimum between 1660 and 1690. However, the records are not alike in all the cores and the Lomonosovfonna $\delta^{18}O$ profile is interrupted by short warm spells. An anomalous sharp warm peak ($\delta^{18}O$ = -12‰) in the 1660s may have resulted from alteration due to melting during one of the warmest years ever recorded in Europe (i.e. 1665; Lamb and Mörth, 1978). The stable-isotope record indicates that the climatic amelioration which made possible the development of the whaling town of Smeerenburg was short-lived (only 10–20 years) and it is no surprise that the station had to be abandoned by 1660. By then, temperature and sea-ice conditions (Ogilvie, 1984) were deteriorating rapidly towards one of the coldest decades on record (the 1680s and 1690s). By 1695 Iceland was surrounded by sea ice (Lamb, 1977; Section 1.4.3). In that decade $\delta^{18}O$ values were as low as -16.7‰ at Vestfonna, -14.6‰ at Lomonosovfonna, and -19.4‰ in 1670 in Austfonna. All the records examined for the North Atlantic (i.e. the Svalbard cores, the Crête and Dye 3 ice-core record, and the sea-ice concentrations off Iceland; Section 1.4.3) indicate that the climate was relatively mild at the beginning of the 18th century.

Arkhipov et al. (1987) measured the proportion of ice formed by percolation and refreezing, which reflects summer conditions, throughout the depth of the 1985 Austfonna core. The proportion of percolation ice gives an idea of climatic conditions in days without precipitation, whereas the $\delta^{18}O$ depends on the snowfall. The 17th century is shown as having relatively cool summers, as the proportion of percolation ice rarely exceeds 50%. On the other hand, the middle of the 18th century (i.e. 1730–1750) was relatively warm and by 1750 the proportion of percolation ice had increased to 80%.

From 1700 the record of sea ice off the Icelandic coast is reliable enough to allow direct comparison with the stable-isotope record (Ogilvie, 1984; and Section 1.4.3 of this dissertation). Table 4.3 is the matrix of cross-correlation between the three Svalbard cores and the stable-isotope ratios at Crête and the sea-ice time series. The statistical analyses were carried out using the 10-year average of the time series (comprising 28 data points). The significance of the cross-correlation coefficients was assessed by an approximate *t* test given by Davis (1986):

$$t = r_m \sqrt{\frac{n^* - 2}{1 - r^2 m}}$$

where n^* is the number of overlapped positions between two time series at the match position m (i.e. number of lags), and r_m is the correlation at the match position m. The number of degrees of freedom is given by (n^* - 2). The delta oxygen time series of the three Svalbard cores are cross-correlated, but a lag of 10 years between changes in Vestfonna and in the other two cores suggested that the mean net accumulation rate of the former core could still have been overestimated slightly. It is also apparent from Table 4.3 that the $\delta^{18}O$ changes in Svalbard were contemporaneous with changes in Crête. The correlations in

Table 4.3 are significantly improved when the data from the ice cores are smoothed by a 3-cycle moving average model, to take into account the $\delta^{18}O$ of the adjacent samples and so to compensate for errors in dating. For example, the correlation between the Lomonosovfonna $\delta^{18}O$ and the number of weeks with drift ice off the Icelandic coast increases from -0.42 to -0.53. The correlation between Lomonosovfonna and Austfonna increases from 0.57 to 0.67.

Table 4.3- Cross-correlation matrix for the period of maximum overlapping for the time series plotted in Fig. 4.10 (i.e. the 10-year means of $\delta^{18}O$ in the Austfonna, Lomonosovfonna, Vestfonna, and Crête cores, and the frequency of sea ice off Iceland). Only maximum correlations are given, together with the respective lag. All correlations are significant at $\alpha < 0.05$.

	Austfonna	Lomonosovfonna	Vestfonna	Crête
Lomonosov-fonna	0.57 (lag = 0)			
Vestfonna	0.63 (lag = -1)	0.53 (lag = -1)		
Crête	0.53 (lag = 0)	0.41 (lag = 0)	0.43 (lag = -1)	
Sea ice off Iceland	- 0.47 (lag = -1)	- 0.41 (lag = 0)	- 0.43[a] (lag = 0)	- 0.57 (lag = -1)

Note: [(a)] the correlation between the sea-ice extent off Iceland and the delta oxygen variations in Vestfonna is statistically significant only after smoothing the delta oxygen time series by a 2-cycle moving-average model.

The beginning of the 18th century was mild in Svalbard and in the Greenland Sea/NE Atlantic region, as can be observed in Fig. 4.10A–E. In fact, $\delta^{18}O$ at Crête was higher then than in the warmest part of the 20th century, reaching -33.24‰ by 1720. These high delta values were associated with reduced sea-ice cover off Iceland. This warm period was followed by one of the most abrupt changes in the stable-isotope composition in any decade and it is recorded in the four cores (i.e. Austfonna, Vestfonna, Lomonosovfonna, and Crête). At Vestfonna the stable-isotope composition fell by about 3‰ in the 1720s, when the minimum $\delta^{18}O$ for the period 1400–1970 was reached (-17.5‰); the decrease was 2.2‰ at Lomonosovfonna, and only about 1‰ at Austfonna. The rest of the century was relatively cool, except the 1770s, which coincide with a time of relatively low sea-ice concentration off Iceland, and a peak in the proportion of melt features at Dye 3 (Section 1.4.3). Another abrupt cooling is recorded in the Austfonna and Lomonosovfonna cores by the 1780s. At Austfonna the lowest delta values during the LIA were reached by 1800 (-20.3‰). A similar reduction in the $\delta^{18}O$ is observed at Lomonosovfonna, reaching a minimum of -15.9‰ also by 1800. On the other hand, the cooling is not so well marked at Vestfonna and Crête.

All records in Fig. 4.10A – E show that the climax of the LIA was reached in the North Atlantic section of the Arctic during the 19th century, although the minimum $\delta^{18}O$ was not contemporaneous in all the cores. The picture emerging from Lomonosovfonna and Vestfonna is one of constant cooling, with a mean $\delta^{18}O$ of about -14.9‰ and -16.5‰ respectively, broken by a warm spell between 1840 and 1850. This is the only and precise period of restricted sea ice off the coast of Iceland during the century, and the proportion of percolation ice in Austfonna (i.e. >90%) indicates summer conditions similar to those of the 20th century. The climax of the LIA in these two cores, in about 1870–90s, also coincides with a period of maximum sea-ice extent (Section 1.4.3). This period was also the time when small cirque glaciers in Svalbard reached their maximum extent (Werner, 1988; Section 1.4.3 of this dissertation). The warm 1840s are also recorded in the Austfonna and Crête $\delta^{18}O$ profiles, but the decadal variations during the century differ markedly from those in the Vestfonna and Lomonosovfonna records. At Austfonna, after the overall low of the 1800s, the climatic conditions appeared to improve almost linearly towards the 1910s: $\delta^{18}O$ increased at a rate of 0.022‰ a^{-1}, or about 2.4‰. At Crête, on the other hand, the $\delta^{18}O$ is slightly below the average for the last 570 years (-34.17‰) and was interrupted by abrupt cooling in 1850 (a fall of 1.02‰ in the $\delta^{18}O$) and 1900 (a fall 0.75‰).

The results of two chloride profiles (from the Austfonna – 1985 and Vestfonna cores) provide further environmental information, particularly on the sea-ice extent off the coast of Nordaustlandet. The Vestfonna core profile is not very useful for the pre-19th-century period because it is relatively flat at that time, with concentrations at about 42 μEq l^{-1} (cf. Punning, Vaykmyae and Tóugu, 1987). On the other hand, there is a clear increase from the mid-19th-century. The Cl^- concentration at this site increases from 36.7 μEq l^{-1} in the 1870s (a minimum that coincides with the maximum $\delta^{18}O$ in the core, and with the extent of sea ice off the Icelandic coast) to 67.7 μEq l^{-1} in the 1970s (i.e. an increase of 84%). This increase was relatively abrupt initially and by 1900 it had already reached the 60 μEq l^{-1} level. The chloride concentration decreased during the cool 1910s (to about 50 μEq l^{-1}), but by 1930 it had recovered to the 1900 levels. The Austfonna core shows pre-19th-century mean concentrations at about 34 μEq l^{-1}. By the middle of the 18th century there was a rapid decrease towards a minimum in the 1800–1810s of 14 μEq l^{-1}, coinciding with the minimum $\delta^{18}O$ during the LIA. During the whole of the 19th century concentrations were below the ice-core mean for the period 1590–1970 (31.0 μEq l^{-1}), although increasing at a rate of 0.13 μEq l^{-1} a^{-1} ($r = 0.92$, at $\alpha < 0.0001$) towards a maximum in the 1970s of 35.0 μEq l^{-1}. In the period 1860–1979 the variations in chloride concentration in the two cores correlate with the $\delta^{18}O$ variations. In Austfonna r is equal to 0.99 at $\alpha < 0.0001$. A weaker correlation is obtained in the Vestfonna core ($r = 0.71$, at $\alpha < 0.05$), which is most probably due to the stronger superficial summer melting in this ice cap. The results of these

correlations reinforce the idea that the stable-isotope composition of Svalbard is influenced mainly by variations in the distance from the source area.

In agreement with the MAAT time series for the Greenland Sea and NE Atlantic, three of the cores (Austfonna, Lomonosovfonna, and Crête) record a sharp increase in the delta values by the 1920s. There was an increase of 2‰ at Austfonna over a period of about 4 years (Fig. 4.10A in this dissertation; and Fig. 11 in Arkhipov et al., 1987); the same increase is observed in the Lomonosovfonna core. The sharp changes in $\delta^{18}O$ profiles were associated with a great reduction in the number of weeks when there was sea ice off the Icelandic coast (Section 1.4.3). In fact, during this century only the 1960s would have seen sea-ice conditions similar to those prevailing throughout the LIA. The Austfonna and Vestfonna cores also record a rapid increase in Cl^- from the 1870s to the 1970s (from 19.7 to 33.8 $\mu Eq\ l^{-1}$ and from 36.7 to 62.1 $\mu Eq\ l^{-1}$ respectively). Another important change by the end of the 19th century–beginning of the 20th century is observed in the process of snow metamorphism. The proportion of percolation ice increased abruptly in the two Austfonna cores, from about 50% to 90% (Zagorodnov, Arkhipov and Macheret, 1985; Arkhipov and Zagorodnov, in preparation). For the 20th century the proportion of ice formed by percolation and refreezing of the meltwater has remained above 85%, which attests the warm summer conditions this century.

The Austfonna core is the one that best represents the variations in MAAT in the Greenland Sea/NE Atlantic region since 1880 (Fig. 1.7b).The stable-isotope record shows a warm period from about 1920 to 1960, and cooling in the 1960s. From 1870 to the end of the 1950s the $\delta^{18}O$ in the Svalbard cores increased by 2.0‰ (Austfonna), 1.7‰ (Lomonosovfonna), and 2.9‰ (Vestfonna). The warm period from 1920 to 1960 is also recorded in the Lomonosovfonna and Crête cores. However, the maximum $\delta^{18}O$ in the Greenland core was reached in the 1920s, instead of in the 1950s as observed in all the Svalbard cores. By the end of the 1960s the $\delta^{18}O$ began to increase rapidly in all three Svalbard cores, following the extension of sea ice in Svalbardbukta, and in recent years (i.e. the late 1970s and early 1980s) the highest ratios ever measured have been found in the Austfonna and Vestfonna cores, coinciding with the increase in temperature. Measurements of the stable-isotope ratios in the next few years will confirm whether or not this warming is only a short pulse in the natural oscillations or the result perhaps of anthropogenic influence on the environment.

4.4.2c- The abrupt termination of the LIA in Svalbard

In recent years, evidence for abrupt changes in the environmental system has been accumulating from different paleoclimatological studies (Berger and Labeyrie, 1987). Ice cores in particular have provided support for the theory that the onset and termination of many climatic events occurred rapidly (i.e. over only a few decades). This observation is

valid for main climatic events, such as the termination of the Younger Dryas (Dansgaard, White and Johnsen, 1989), and also for shorter ones with the time scale of the LIA (e.g. Thompson and Mosley-Thompson, 1987). It is clear from the Svalbard stable-isotope profiles that the area contains a record of rapid changes in the factors that control the composition of the ice. Variations of 2–3‰ had occurred in periods of less than a decade more than once during the LIA (e.g.the beginning of the 17th century, the end of the 18th century; cf. Figs 4.10B and C). But the most dramatic event in the Archipelago in the last 700 years is without doubt the termination of the LIA by the end of the 19th–beginning of the 20th century. Not only the stable-isotope record, but also the chloride concentration and the proportion of ice formed by percolation of meltwater and refreezing, increased abruptly, over a period of 20–40 years. From 1880 to 1920 the $\delta^{18}O$ increased by 2.5‰ in Austfonna and in Lomonosovfonna, the proportion of percolation ice jumped from 40–50% to 85–90% in Austfonna, and Cl^- increased by about 23 $\mu Eq\ l^{-1}$ (60% when compared with the 1880 level) in Vestfonna. These changes imply abrupt increases in the summer temperature and in the temperature of the snowfall, and a rapid sea-ice retreat. Furthermore, it is known from the instrumental record that the MAAT increased by as much as 7.9°C in a period of few years at the end of the 1910s (Chapter 1).

4.5- Summary and conclusions

The fractionation process of the precipitation falling at Isfjord is complex, as is to be expected at a low-altitude station. Summers in Svalbard are relatively warm, with a great number of days when the temperature is above 0°C at sea-level. It should come as no surprise, therefore, that the stable-isotope variations in the Isfjord precipitation suggest that condensation under non-equilibrium conditions is predominant in summer. This observation is confirmed by a δD vs. $\delta^{18}O$ relationship that does not follow Craig's line for meteoric water (Craig, 1961a) and has a slope lower than 8, by a low $\delta^{18}O/\delta T$ gradient (only 0.15‰/°C), and by a relatively small seasonal variation in the stable-isotope ratios. Furthermore, the area is subject to the frontal type of precipitation, and warm moisture-laden cyclones frequently reach Svalbard in mid-winter, causing abrupt changes in the stable-isotope composition. Dating and interpretation of the Svalbard $\delta^{18}O$ core profiles are complex because of these ill-defined relationships and the lack of marked seasonality.

An interesting observation is that the excess deuterium - *d* of precipitation in Svalbard shows a strong seasonality (i.e. it varies from 0.4‰ in July to 16.2‰). This seasonal variation may be attributed to non-equilibrium fractionation in summer, and perhaps to changes in the source area of the moisture. Although further investigation is needed to clarify this point, this strong seasonality could nevertheless be used in the future as a method for dating cores from Svalbard.

There is a trend to smaller $\delta^{18}O$ values towards the northeast. However, the north–south gradient is negligible, as shown by the small difference (0.7‰) between Skobreen and Vestfonna. This small difference probably reflects the influence on the west coast of the Archipelago of the warm West Spitsbergen Current, which keeps areas of water open even in the middle of winter (Section 1.3.3), and thus provides an important source of local moisture.

The distance from the source area appears to be the most important factor controlling stable-isotope composition over Svalbard. Several observations support this conclusion: (1) there is a strong correlation between the mean $\delta^{18}O$ at the ice-core sites and the distance from the nearest open water; (2) the stable-isotope time series of the three cores studied (Austfonna, Lomonosovfonna, and Vestfonna) correlate significantly with the extent of sea ice in the Greenland Sea/NE Atlantic for the period 1700–1970 (provided by the record of sea ice off the Icelandic coast); (3) variations in $\delta^{18}O$ occurred simultaneously with variations in chloride concentration (at least for the period with reliable chloride data, i.e. post-1860), i.e. the variations in $\delta^{18}O$ correlate with regional variations in the extent of sea ice. A significant correlation exists between the upper part of the Lomonosovfonna $\delta^{18}O$ record and the MAAT temperature for the period 1939–76. This indicates that a $\delta^{18}O/\delta T$ gradient of 0.57‰/°C is the most appropriate one for estimating changes in the atmospheric temperature from the stable-isotope record, but this correlation is most probably the result of an indirect relationship, as no physical relationship is to be expected between the isotopic composition of days with precipitation and the atmospheric temperature of every day of the year. It appears that the $\delta^{18}O$ is controlled by the distance from the source area (i.e. the sea-ice extent) which in its turn is determined mainly by the atmospheric temperature. This conclusion is further reinforced by the lag of one month that exists between the variations in temperature and stable-isotope composition in Isfjord. This lag is approximately the time the sea-ice extent takes to respond to variations in atmospheric temperature in the area.

The long-term ice-core profiles suggest the following development of the LIA in the Svalbard region: after a relatively warm 14th century, climatic conditions began to deteriorate. The onset of the LIA appears to have occurred early in the 15th century, which disagrees by about 50–150 years with the results obtained from moraine studies (cf. Section 1.4.3), but is nevertheless still within the accuracy of the ^{14}C dating used for the moraines. However, further studies are necessary to define the development of these early periods, because the stable-isotope record from the cores disagree substantially among themselves for the years before 1600, and this estimate may be revised when the data from the new Austfonna core are published.

From the 16th century (which was relatively warm, at least in Nordaustlandet) a trend to lower $\delta^{18}O$ is observed in all three cores. For the period post-1700 all three Svalbard cores

(Austfonna, Lomonosovfonna, and Vestfonna) show statistically significant correlations with both the Crête stable-isotope record and the Iceland sea-ice record. This demonstrates not only a fairly uniform pattern for environmental changes throughout the Greenland Sea/NE Atlantic region, but also that the stable-isotope record of Svalbard is representative of these environmental changes, despite great alteration as a result of melting and associated phenomena. The beginning of the 17th century was relatively warm, and on Vestfonna conditions may have been similar to those during the warm years of the second half of the 20th century (the $\delta^{18}O$ reached -13.0). This warm spell allowed the development of a whaling town (Smeerenburg) in the extreme northwest of Spitsbergen, but soon conditions deteriorated again. The period of the 1680s–1690s there, as elsewhere in the Greenland Sea/ NE Atlantic, was one of the coldest of the LIA. The 18th century was relatively mild, but was frequently interrupted by short cold pulses, of which the one in 1720 was the coldest.

Without doubt the climax of the LIA in Svalbard was reached during the 19th century, when the mean $\delta^{18}O$ for the century deviated 0.5‰ (Lomonosovfonna) and 0.9‰ (Vestfonna) from the 1400–1970 mean. These two cores indicate that the coldest period was at about the end of the 19th century (between 1870 and 1890), although the Austfonna core records the minimum at the beginning of the century (i.e. 1800–1810). All three cores show a rapid increase in $\delta^{18}O$ from the end of the 19th century. The $\delta^{18}O$ in the three cores increased by 2‰ (Austfonna), 1.7‰ (Lomonosovfonna), and 2.9‰ (Vestfonna) from 1870 to 1950. The difference between the 20th-century mean and the mean of the three preceding centuries indicates a warming of between 2.3°C (Vestfonna) and 3.3°C (Austfonna), if the $\delta^{18}O/\delta T$ ratio of 0.57‰/°C is used. Even if the more conservative ratio determined from spatial studies (0.87‰/°C; Section 4.2.2) is taken into account, the increase in temperature would be at least 1.5–2.2°C in the Archipelago. Finally, the trend in 100a means (i.e. a cooling from the beginning of the 16th century to the 19th century) disagrees with the data from all the Greenland cores (i.e. Camp Century, Milcent, and Dye 3; Robin, 1983) except Crête, and cores from the Canadian islands. These cores indicate that the climax of the LIA occurred about in the second half of the 17th century. Although the Crête core records the LIA maximum by the end of the 14th century, the 19th was also exceptionally cold. This observation emphasizes the regional character of the timing of events during the LIA. Dansgaard et al. (1975) suggested that this delay in the climax of the LIA may have resulted from the position of the long waves of the circumpolar vortex.

The termination of the LIA was relatively abrupt (from about the 1880s to the 1920s) and was accompanied by rapid changes in the $\delta^{18}O$ (e.g. a change of 2.5‰ in the $\delta^{18}O$ in Austfonna and Lomonosovfonna), in the proportion of percolation ice (which increased from 40–50 to 85–90% in Vestfonna) and by an increase of about 60% in the concentration of chloride when compared to the pre-1860 level.

CHAPTER 5

THE RECORD OF ANTHROPOGENIC POLLUTION IN SNOW AND ICE IN SVALBARD

5.1- Introduction

One of the main objectives of environmental research is to derive information about the anthropogenic impact on the global environmental system. By different techniques, such as the examination of peat, tree rings, lake sediments, and ice cores, researchers have tried to obtain, for example, baseline concentrations of chemical species and historical time series for comparison with the present-day concentrations, determining which of the measured parameters reflect anthropogenic activity and which ones reflect natural phenomena. Only when a reliable data set is available will it be possible to assess and monitor the impact of man's activity. The study of pollution in the Arctic appears to be a case that deserves priority. Not only is there clear evidence from atmospheric studies (Rahn, 1982; Barrie, 1986) that the Arctic environment is heavily loaded with man-made impurities but also the examination of ice cores has demonstrated that they are one of the best historical records of pollution. The chemical composition of ice is formed entirely by atmospheric precipitation, at least in the dry-snow zone.

Svalbard is one the areas most affected by anthropogenic pollution in the Arctic. This is a result of specific conditions of atmospheric circulation and of its proximity to Europe. The first part of this chapter reviews the knowledge of atmospheric, snow, and ice pollution in Svalbard hitherto, and explains why the concentration of artificial impurities is so high in this region that does not have significant local sources of pollution. This is followed by an examination of the acidity and excess-sulphate time series in the Skobreen core that provide an historical record of acid deposition over 54 years. An ice core recovered recently from Austfonna (Zagorodnov and Arkhipov, in preparation) provides baseline values and also an historical record of acidity in precipitation for the whole industrial period, therefore allowing the evolution of acid deposition in the Archipelago to be traced. These two records are compared briefly with the chemistry of other Arctic cores and also with the estimated European emissions of SO_2 in order to establish whether Svalbard reflects the overall European trends.

From the examination of the spatial distribution of pollutants and of the record from the Austfonna and Skobreen cores, it is demonstrated that Svalbard is one of the areas most affected by anthropogenic pollution in the Arctic. This pollution has caused an increase of at least 95% in the acidity of the snow deposited in the Archipelago since the beginning of the industrial revolution. Finally, some brief comments on the implications for the Svalbard biota of the increase in acid deposition are presented.

5.2- Pollution meteorology

Due to the expansion of the Arctic air mass into Eurasia, the mean position of the Arctic front is pushed southward during the winter, so that the main cyclone tracks are deflected and forced over the industrialized areas of central Europe, Scandinavia, and the north-western USSR, passing over areas of intense oil and coal combustion, non-ferrous metal production and other sources of man-made pollutants. As a consequence, there is a band with a high concentration of pollutants in the path of these cyclones. Following their route eastward, the cyclones encounter the semi-permanent Siberian high and are deflected first towards the Kara and Barents seas and then towards the Polar Basin (Fig. 5.1A). Svalbard and the islands of Franz Josef Land are the first land masses in the pathway of these pollutant-laden air masses. Therefore concentrations of pollutants over the atmosphere in Svalbard should be higher than in other parts of the Arctic. Another factor that should contribute to a high concentration of pollutants at the Svalbard sites is the relatively low elevation of the Archipelago: the sampling sites are generally situated between 500 m and 1200 m a.s.l., and are therefore subject to the effect of the atmospheric layers with the highest concentrations of pollutants. This contrasts with the altitude of other sites where attempts have been made to obtain a record of anthropogenic pollution. For example, the Agassiz ice cap in Ellesmere Island is situated at 1.6 km a.s.l. and the Greenland sites at about 2.5 km a.s.l., so that the air arriving at these sites is significantly less polluted.

A different picture emerges during the summer. The cold dry Arctic air mass is restricted to the Polar Basin, and the Arctic front retreats to a more northerly position over Svalbard, or even farther north. The circulation pattern in the Arctic becomes more circumpolar. The moisture-laden cyclones generally come from North America via Iceland. They become loaded with pollutants mainly from the industrial areas of north-eastern North America but arrive much depleted in Svalbard, as most of the precipitation occurs over the ocean. Consequently, not only the Arctic, and in particular the Barents-Kara sea region, is subject to a high influx of man-made pollutants, but this influx also shows a strong seasonal variation, with a maximum in late winter – early spring.

The atmospheric circulation over the Arctic North Atlantic thus not only makes the Barents-Kara sea region extremely sensitive to climatic change and fluctuation

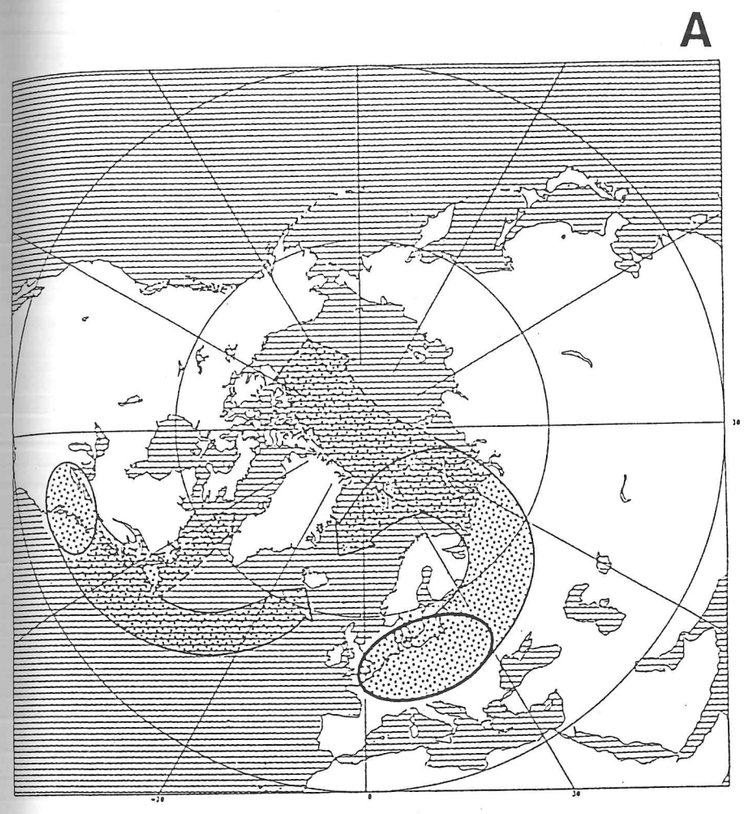

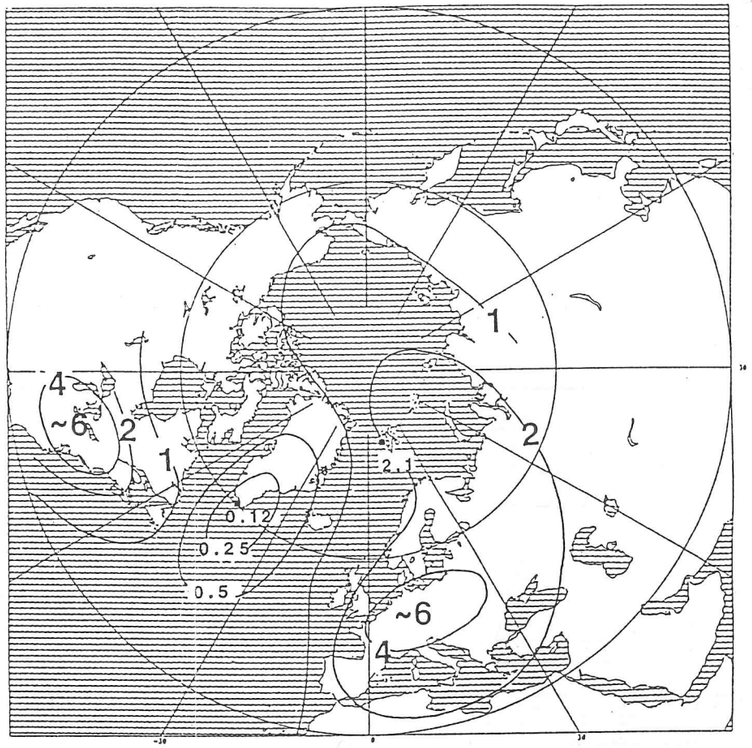

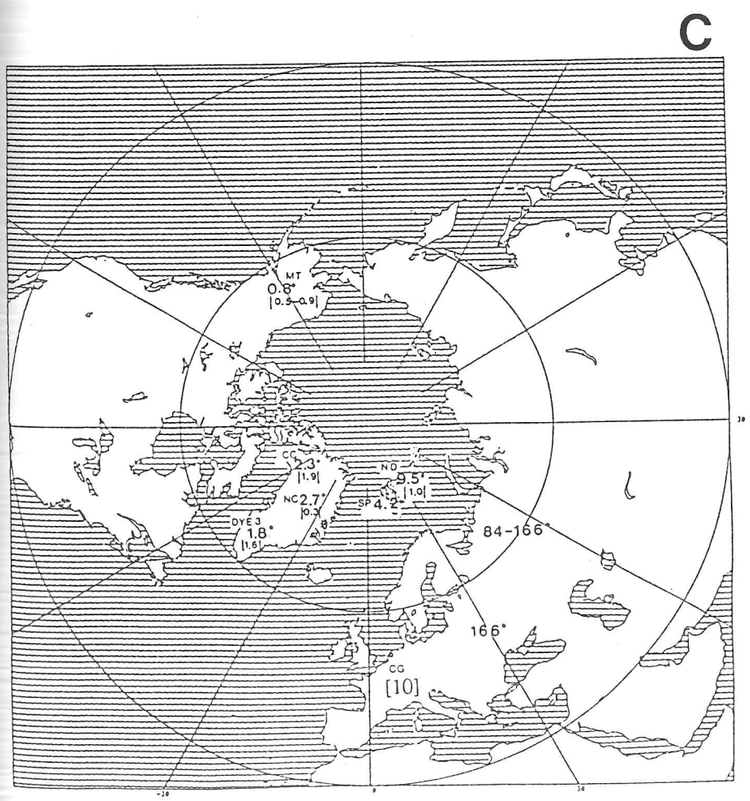

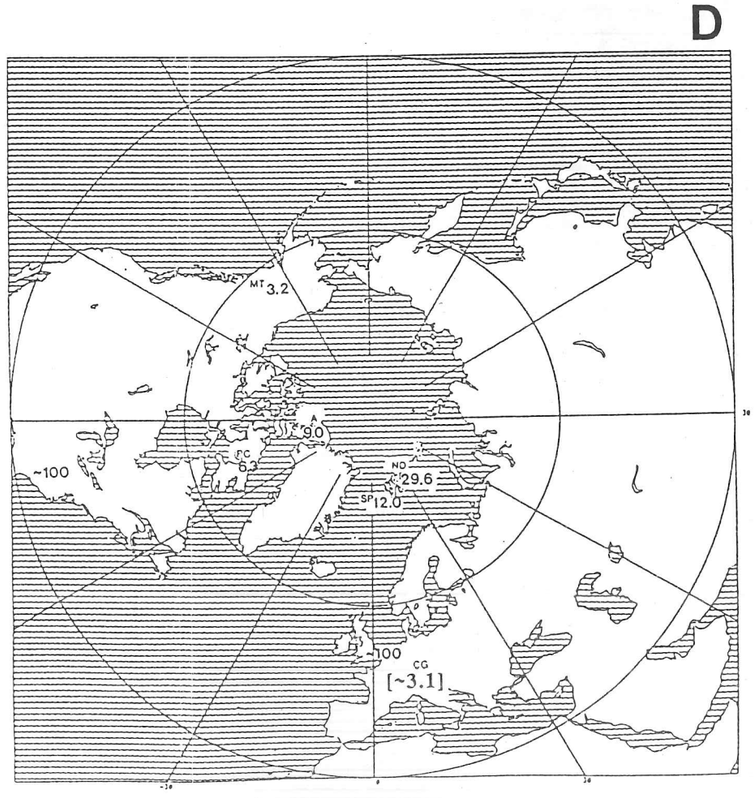

Figure 5.1 – **A**) The main pathway of pollutants to the Arctic and in particular to Svalbard; **B-D**) Ionic concentration in the atmosphere and superficial snow in the Arctic and environs. Fig. 5.1**B** plots the mean winter concentration of excess sulphate in the surface aerosol (after Rahn, 1982). Figs. 5.1**C** and **D**, plot the concentration of H^+ and $[SO_4^{2-}]^*$ in modern snow (i.e. deposited since 1970). Numbers between braces in Fig. 5.1**C** are nitrate concentrations. The atmospheric concentrations are given in $\mu g\ m^{-3}$ and the snow concentrations are given in $\mu Eq\ l^{-1}$. Although there are few snow-surface measurements, it appears that trends at the surface follow the general atmospheric distribution of pollutants. There is a decrease in concentration from Svalbard, where the maximum values are reached towards the west, emphasizing the importance of the Eurasian pathway. The periods covered by the surface values and the sources of the data are the following: **C C** (Camp Century 1976-77; Herron, 1982); **Dye 3** (1970-84; Herron, 1982); **NC** (North Central 1973-77; Langway and Goto-Azuma, 1988); **ND** (Nordaustlandet 1983; Semb et al., 1984); **SP** (Spitsbergen, Skobreen area 1983; Semb et al., 1984); **MT** (Mt. Logan 1979-81; Holdsworth and Peake, 1984); **CG** (Colle Gnifetti 1970-86; Wagenbach et al., 1988); **A** (Agassiz ice cap 1970-80; Barrie, Fisher, and Koerner, 1985); **PC** (Penny ice cap 1977-79; Holdsworth, 1984; data only in graph form).

(cf. Chapter 1) but also results in a great influx of air masses loaded with man-made impurities. This produces what is perhaps the most polluted area of the Arctic, excluding 'anomalously' high local concentrations.

5.3- The record of anthropogenic pollution in the Svalbard atmosphere

For the last 15 years an extensive study of atmospheric chemistry, carried out with a view to explaining the Arctic haze, has shown that the Arctic environment is far from pristine. As a matter of fact, some of the pollutants measured in the Arctic show concentrations higher than or similar to concentrations in parts of Europe. Of all the sites in the Arctic, Svalbard is perhaps the area most affected by anthropogenic pollution transported from industrialized areas.

Since 1977 several studies carried out by the Norwegian Institute for Air Research - NILU (Heintzenberg, Hansson and Lannefors, 1981) at Bjørnøya (75°N, 19°E) and Ny-Ålesund (76°N, 12°E), together with airborne studies over the Archipelago by other institutions, have shown that in winter the Svalbard atmosphere is heavily loaded with a variety of anthropogenic impurities which include: sulphates and sulphur dioxide, and soot (Rahn, 1981); heavy metals (e.g. Pb, Cu, Zn, Ni; Pacyna, Vitols and Hanssen, 1984); pesticides (Oehme and Ottar, 1984); and organic gases (e.g. alkanes; Hov et al., 1984). The presence of the organic compounds supports a mid-latitude origin for these impurities. Another main characteristic is the strong seasonality in the concentration of these impurities in the atmosphere. Although Pacyna and Ottar (1985) have proved that even in the summer some pollutants may arrive in the Archipelago, coming from North America via Iceland and also from Eurasia, the concentrations are one order of magnitude smaller than in winter. On the other hand, they are still one order of magnitude greater than the concentrations in the Antarctic atmosphere (Pacyna and Ottar, 1985). In summer, sea-salt particles (e.g. Cl, K, Ca, S) predominate, as well as crustal elements (e.g. Ti, Al, Si, K, Ca, V). Concentrations are in general also higher than concentrations in Greenland. For example, Table 5.1 compares mean concentrations of some chemical species at two stations in Greenland with concentrations in Ny-Ålesund.

Sulphur dioxide and nitrogen oxides are some of the main pollutants of the Arctic. They are emitted into the atmosphere by incomplete combustion of fossil fuel (i.e. from power stations and car exhausts). Oxidation of these oxides occurs in the clouds, sometimes helped by catalysts such as hydrogen peroxide, ozone, and ammonia. The resulting sulphate and nitrate anions react with H^+ to form the strong acids H_2SO_4 and HNO_3. This is the process of acid-rain formation. Fig. 5.1B shows the mean winter concentration of excess sulphate ($\mu g\ m^{-3}$) at ground-level in the Arctic and environs (after Rahn, 1982). As expected,

the highest concentrations are encountered in the heavily industrialized areas of Europe and north-eastern North America, reflecting a highly reactive atmosphere and marking areas subject to greater acid precipitation. Another important feature emerges from this picture – that there is a broad tongue of relatively high concentration that follows the main pathway of pollutants towards the Arctic through the Barents-Kara sea region. Concentrations in Svalbard during the winter can reach values as high as those for rural areas in Scotland: for example, 2 $\mu g\ m^{-3}$ in Ny-Ålesund, which is four times greater than concentrations in the lower atmosphere in Ellesmere Island, Canada, and up to four times greater than concentrations in southern Greenland (cf. Fig. 5.1B). These great differences demonstrate that the Eurasian pathway is more effective in transporting pollutants to the Arctic than the North American pathway via Davis Strait (Fig.5.1A). Furthermore, daily pulses of up to 6 $\mu g\ m^{-3}$ of SO_2 have been observed in Bjørnøya (Rahn et al., 1980). Table 5.2 compares the mean concentration of SO_2 and SO_4^{2-} in Ny-Ålesund in 1982–83 with concentrations in Scotland (Joranger and Ottar, 1984). A strong seasonality in the concentration of both SO_2 and SO_4^{2-} can be observed. The maximum concentrations are observed in late winter – early spring (Heintzenberg and Larssen, 1983).

Local pollution may be an important contributor to the Svalbard atmosphere, although there is a low scale of human activity, as the source–receptor distance is smaller. Local atmospheric pollution originates from the four mining towns. All these towns (i.e. Barentsburg, Longyearbyen, Pyramiden, and Sveagruva) have either oil-based or coal-based electric power plants, or both. Therefore there is some emission of SO_2, albeit on a small scale. The greatest pollution source in Svalbard appears to be the electric power plant at Longyearbyen, which at its maximum capacity is assumed to burn 30,000 tons of coal annually. Other pollution sources include coal dust from mining production, and fossil-fuel combustion from aircraft and cars, mainly in the Longyearbyen area. The area on the south shore of Isfjorden may contain higher concentrations of anthropogenic pollutants than the rest of Archipelago and these may have affected the chemical composition of the Grönfjord-Fridtjovbreen ice core. Nevertheless, they are not expected to have affected the Austfonna and Skobreen records, as these ice masses are about 230 and 70 km respectively leeward of Longyearbyen. The same may not be true for glaciers and ice caps near the other towns. In fact, as discussed below, the Lomonosovfonna core appears to be heavily contaminated by sulphates, which most probably originated from Pyramiden.

5.4- The glacial record of anthropogenic pollutants: previous pit and ice-core studies

Although a great number of studies have been carried out with a view to explaining the chemistry of the Arctic atmosphere, there have been few attempts to examine the composition of the surface snow. Furthermore, the great majority of the studies were carried

out in Greenland as part of ice-core programmes and few of them quote concentrations for recent years, so it is difficult to reconstruct the spatial distribution of chemical species. Fig. 5.1C plots the known superficial measurements of excess sulphate and nitrates in Arctic glaciers, ice caps, and ice sheets.

In all the discussions in this section the concentration of impurities in the deposited snow, before any post-depositional alteration, is considered to be proportional to atmospheric concentration. Therefore, trends in the cores are assumed to reflect trends in the concentration in the atmosphere. This assumption is rarely justified. For example, the material that is being deposited (both gases and particulates) may undergo alteration during the transport processes, or the rate of deposition may vary greatly over time (Davidson, 1989). Unfortunately, it is still not possible to calculate with reasonable accuracy the atmospheric concentrations on the basis of ice-core concentrations, as the available data on the processes of deposition (both wet and dry) are extremely limited for polar regions (Davidson, 1989). Further, particularly in the case of Svalbard, changes in the concentration of impurities may represent changes in atmospheric circulation, rather than production in source areas. For example, there will be lower concentrations during periods when the Arctic front is retreating, as the transport of material from Eurasia will be less efficient.

Few studies have examined the chemistry of the snow surface of Svalbard. Gorham (1958) reported the first ionic measurements in pits and on exposed crevasse walls in Nordaustlandet. He concluded that some elution and percolation downward of the ionic content also occurs in Austfonna and that the concentration of solid impurities in the ablation area is enough to alter the original pH. The maximum $[SO_4^{2-}]^*$ concentration measured was 14.6 $\mu Eq\ l^{-1}$ (compared with an estimated baseline for excess sulphate in Svalbard of about 2 $\mu Eq\ l^{-1}$; cf. Section 3.2.8), indicating (as expected) that anthropogenic contamination was already substantial. The same is not true for NO_3^-, which showed maximum concentrations of only 0.16 $\mu Eq\ l^{-1}$. The examination by Gjessing (1977) of the ionic concentration in the snow pits in Austfonna demonstrated that the anthropogenic pollutants in the snow pack have marked seasonality, therefore confirming the observations on the chemistry of the atmosphere. Further, the higher concentrations of man-made pollutants were related to precipitation from air masses coming from Scandinavia and the north-western USSR, which are more frequent in winter. Gjessing (1977) concluded that the three main man-made pollutants which had been measured (i.e. NO_3^-, NH_4^+, and $[SO_4^{2-}]^*$) are highly correlated, confirming that they come from the same source. On the other hand, seasonal differences in concentration which vary between 5- and 40-fold are difficult to explain only by variations in atmospheric conditions. The association of high ionic content with melt layers indicates that elution and flush-out downwards to the winter layers may increase the seasonal differences. Mean concentrations in winter layers in 1974/75 were 4.5 $\mu Eq\ l^{-1}$, 0.5 $\mu Eq\ l^{-1}$ for NO_3^-,

associated with a relatively high electrolytic conductivity of 9.8 μS cm^{-1} and a mean pH of 5.2 (minimum of 4.8), which confirms the acidic character of the deposition on Austfonna.

Table 5.1- Comparison of the concentration of some chemical species in the atmosphere at Nord and PCS, Greenland, and in Ny-Ålesund, Svalbard. PCS is one of the SAGA stations (i.e. the Danish programme of Studies of the Aerosol in the Greenland Atmosphere); it is about 60°N 43°W and about 50 km northeast of Cape Farewell. Nord is situated in the north of Greenland and is therefore subject to the influx of pollutants coming from Eurasia; this is not the case for PCS in southern Greenland. Hence concentrations at Nord are more comparable with concentrations in Svalbard. Concentrations are given in μg m^{-3}. 'Episode' denotes a period of air-mass transfer with a high concentration of impurities from Eurasia.

	Nord (1979–80)	PCS (1979–80)	Ny-Ålesund (1983) Winter Episode	Winter Non-episode	Summer Episode	Summer Non-episode
S	178.6	154.6	925	656	556	85
Cu	0.3	0.09	1.4	0.7	0.7	0.4
Zn	3.73	4.95	16.5	6.8	4.3	1.0
Pb	4.98	0.92	14.1	5.0	1.2	0.2

Sources: Greenland (Heidam, 1984), Svalbard (Pacyna and Ottar, 1985).

Table 5.2- Atmospheric concentrations of SO_2 and SO_4^{2-} in the Scotland and Svalbard atmospheres in μg m^{-3}.

	Scotland Winter (1982/83)	Scotland Summer (1982)	Svalbard Winter (1982/83)	Svalbard Summer (1982)
SO_2	1.0–2.0	0.5–2.0	0.67	0.12
SO_4^{2-}	0.5–1	1.0–1.5	0.57	0.12

In the spring of 1983, Semb, Brækkan and Joranger (1984) carried out detailed examination of the spatial distribution of various ions in the Archipelago, including H^+ and SO_4^{2-}. Superficial snow was sampled to the first impenetrable ice crust, which was interpreted as the previous summer layer. The values below refer, therefore, to the period autumn 1982 – spring 1983. This survey confirmed Gjessing's conclusions about the strong seasonality of the ionic concentration, which increases from the ice crust towards the surface. Concentrations increase with altitude on the east side of Svalbard, having an orographic effect on the cyclones reaching the Archipelago. The concentrations here are some of the highest recorded throughout the Arctic. Absolute maxima were recorded on Austfonna, where a maximum acidity of 29.6 μEq l^{-1} (i.e. a pH of 4.53), 9.5 μEq l^{-1} for sulphates, 0.97 μEq l^{-1} for nitrates, and 5.56 μEq l^{-1} for ammonium was measured (Fig. 2.3C and D, and Fig. 5.1C and D).

Recently, Mulvaney (1987) sampled a 5 m pit for Cl^-, NO_3^-, and SO_4^{2-} analysis at Malte Brunfjellet, Sabine Land, Spitsbergen. Both sulphates and nitrates show the high concentrations expected (3.9 and 0.9 $\mu Eq\ l^{-1}$ respectively) and this agrees well with the measurements by Semb, Brækkan and Joranger (1984) for the area. Samples of the snow surface following precipitation events confirmed observations by Pacyna and Ottar (1985) that episodes of high concentration of anthropogenic pollutants (i.e. NO_3^- and SO_4^{2-}) occur also in summer. Values as high as 8.14 $\mu Eq\ l^{-1}$ for excess sulphate and 3.84 $\mu Eq\ l^{-1}$ for nitrates were measured. Although these values are relatively high for summer, they are not unexpected, as sporadic advances of the Arctic front may happen at any time of the year.

There are few other studies on impurities in the snow and ice on Svalbard. All of them have been carried out in association with the Soviet ice-core drilling programmes. No detailed profile is known to the author to have been published, with the exception of one for Lomonosovfonna, and in general only mean values are given. This is regrettable, as these values are useful for determining neither modern concentrations nor baseline values. Yevseyev and Korzun (1985) reported the concentration of some ions along the Vestfonna core. Pb, Cu, Cd, Fe, and Co in layers precipitated since the 1950s are 1.5–2 times greater than the concentration in deeper layers. The high concentrations in heavy metals are associated with high concentrations of sulphates and are attributed by Yevseyev and Korzun to man-made pollutants. No concentrations in the top layers are given and, as the study of heavy metals from ice cores is complicated by the risk of contamination due to the very low concentrations, it is difficult to reach a conclusion about general trends, although an increase in heavy metals is to be expected because they are by-products of fossil-fuel combustion and smelting activity. Jaworowski et al. (1981), in a work that has been much criticized for its sampling techniques (for details see Alderton and Coleman, 1985), reported high concentrations of Pb ($\approx 4.5\ ng\ g^{-1}$) in modern snow; they were richer than in older ice by a factor of 2.3. Unfortunately, due to the shortcomings of the above two papers (i.e. only the briefest details on sampling, dating and age sampling, and possible problems of contamination), no definitive conclusion can be reached on the trends of heavy metals in Svalbard.

A record of sulphate and chloride concentration in the top 40 m of the Lomonosovfonna core has been published (Punning and Vaykmyae, 1985), and makes possible the derivation of an excess-sulphate profile for a period of approximately 40 years (1933–73). Unfortunately, anomalously high concentrations cast doubt on the representativeness of the core. Not only are the mean values for both Cl^- (105 $\mu Eq\ l^{-1}$) and SO_4^{2-} (27 $\mu Eq\ l^{-1}$) 5 – 6.7 times greater than values measured by Semb, Brækkan and Joranger (1984) in the area (for 1982–83), but there are also concentrations of up to 271 $\mu Eq\ l^{-1}$ for Cl^- and up to 310 $\mu Eq\ l^{-1}$ for SO_4^{2-}. Furthermore, it is known that Cl^-

decreases with altitude and continentality in the Archipelago, but the mean concentration in Lomonosovfonna (at 1200 m in central Spitsbergen) is similar to the maximum mean value measured on the western coast of the Archipelago (about 107 $\mu Eq\ l^{-1}$). Concentrations of sulphate are higher than the concentrations in the ice core from Colle Gnifetti, Swiss Alps. It is necessary, therefore, to find a cause for these 'anomalously' high values. Besides the straightforward case of contamination during sampling and analysis, the sulphates could have originated from the nearby mining town of Pyramiden (30 km distant). It is known that this town has a coal-burning electric power plant which may be responsible for the emission of sulphur compounds into the local atmosphere. Examination of the excess-sulphate profile revealed that it began to increase in about the 1940s, coinciding more or less with the opening of Pyramiden in 1947–48. But this cannot be used as conclusive evidence because it was at this time that the emissions of sulphur-rich compounds began to increase in Europe. Furthermore, the high concentration of Cl^- could rarely be explained by coal combustion as on average the amount of Cl^- in power-station emissions tends to be an order of magnitude less than the amount of sulphur dioxide (Brimblecombe, 1986). No matter what the cause of the high values may be, the site is not suitable for historical monitoring of pollutants on a regional or continental scale. An explanation for these 'anomalous' values is given in Section 4.2.

Finally, indirect evidence for the spatial distribution of impurities in Svalbard was provided recently by the examination of radio echo-sounding data from Kvitøyjøkulen, Kvitøya (in the extreme east of Svalbard). Bamber and Dowdeswell (in press) noticed that the dielectric absorption of RES waves in Austfonna and Kvitøyjøkulen is higher than anywhere else in Svalbard. Further, there is an increase of about 40% in the absorption from Austfonna to Kvitøyjøkulen. These two facts appear to contradict the expected thermal conditions of these ice caps. They are supposed to be the coldest in the Archipelago, with Kvitøyajøkulen colder than Austfonna, as they are the farthest north and east, so a smaller dieletric absorption was expected. These unexpectedly high absorption values were explained, at least partially, by an increase in the anthropogenic impurity content in the upper layers of these ice caps (Bamber and Dowdeswell, in press), and represent an eastward trend to a greater concentration of impurities. This distribution of impurities is consistent with the pollution meteorology of Svalbard, which indicates that pollutants come mainly from the east and northeast during the winter (cf. Section 5.2).

How do the above observations on pollutants in Svalbard compare with measurements elsewhere in the Arctic? Do the spatial variations in the pollutant concentration in snow and ice mirror the atmospheric observations and, if so, is there a well-defined tongue of high values from Eurasia via Svalbard to the North American Arctic? To answer these questions, Fig. 5.1C and D plots the known superficial measurements of H^+, NO_3^-, and SO_4^{2-} concentrations in modern snow (i.e. post-1970). Not enough studies have been carried

out for it to be possible to reconstruct the spatial distribution of impurities on the snow surface in the same detail as for the atmosphere in winter (Fig. 5.1B) but the general trends appear to be the same. Acidity and sulphates reach their highest values in Nordaustlandet (H^+ = 29.6 μEq l^{-1}, and SO_4^{2-} = 9.5 μEq l^{-1}) and decrease towards the west. Acidity concentrations in Nordaustlandet are 3 times greater than concentrations at the Agassiz ice-cap site (Ellesmere Island). The sulphates also reach their greatest concentrations in Nordaustlandet, being up to 5 times greater than concentrations at the Greenland sites. Although these differences reflect several geographical factors (such as altitude and the continentality of the site), they are great enough to confirm the importance of the Eurasia pathway. In fact the transport of these impurities to the Arctic appears to be more efficient than the vertical transport at the source region, as demonstrated by the lower concentrations at Colle Gnifetti, 4450 m a.s.l. in the Swiss Alps. The other possible path of transport of anthropogenic pollutants to Svalbard, via the North Atlantic, is not very effective, as demonstrated by the low concentrations at Dye 3 (Greenland) and summer concentrations in Svalbard. Higher concentrations in Ellesmere Island and North Greenland indicate the influx of impurities via the Pole. This distribution of pollutants would agree closely with the best estimate by Rahn (1982) for aerosols in the Eurasian pathway (cf. Fig. 5.1A). Concentrations at Mt. Logan (Yukon, Canada) are low and attest that the site is isolated from the main sources of pollutants. This is to be expected, as the atmospheric circulation is controlled by the Aleutian low rather than by the Arctic circulation (Holdsworth and Peake, 1985). Although it was not possible to obtain measurements of excess sulphate from the USSR, a survey by Belikova (1984) of the total sulphate content of the winter snow cover confirms that the path lies in the direction of the Barents-Kara sea region. The highest values are in the Ukraine (>166 μEq l^{-1}) and are followed by a band of high concentration (84-166 μEq l^{-1}) which extends through central European Russia towards Arkhangel'sk.

From the atmospheric and snow-and-ice observations it can be suggested that the highest concentrations of anthropogenic pollutants in the Arctic are generally to be expected in the Barents-Kara sea region, excepting high local contamination. Sampling of snow east of Nordaustlandet should confirm this observation. Maximum concentration should be found in Novaya Zemlya. A good test case would be Kvitøya because it is the easternmost island in the Svalbard Archipelago. It also appears from these observations that winter precipitation in Svalbard controls mean values. This fact must be attributed to concentration which is higher by up to one order of magnitude in winter, as the accumulation is less at this time of year.

5.5- The record of anthropogenic pollution in the Skobreen and Austfonna cores

Although there are high pollutant concentrations in the atmosphere, few ice-core studies have been carried out in the Arctic to derive an historical record of the anthropogenic

impact (e.g. Barrie, Fisher and Koerner, 1985; Neftel et al., 1985; Mayewski et al., 1986). This is an important task if artificial pollutants are to be separated from the natural ones and anthropogenic influence is to be monitored. For example, it is not known exactly what proportion of the Arctic haze is natural and what is due to anthropogenic pollution. For Svalbard, which has been shown to be a primary area for environmental monitoring because of its sensitivity to anthropogenic contamination, the situation is even worse. Until now, no ice core has been examined for the purpose of deriving an historical record of anthropogenic pollution – a consequence of glaciological conditions that are far from ideal for the ice-core investigators, as stressed elsewhere in this dissertation. Therefore this section aims to examine the acidity and sulphate record of the Skobreen core in order to derive a record of pollution over a period of 54 years (1930–84). This analysis has been partially impaired by high melting and associated problems at the core site, but general trends can still be distinguished. More recently (1987), Austfonna was cored to bedrock by Soviet scientists (Zagorodnov and Arkhipov, in preparation). The pH was measured along all 566.7 m of the core, providing the first long-term record of strong acidity in the Archipelago. This core is examined and interpreted, therefore, in order to provide a historical record of acid precipitation since the beginning of the industrial revolution. The Austfonna core also allows the derivation of a baseline value for strong acidity in the Archipelago, allowing the natural background to be separated from the man-made contribution. This profile was kindly provided for the author by Dr. Zagorodnov (Institute of Geography, USSR Academy of Sciences).

5.5.1- Relationship between acidity and electrolytic conductivity in the Skobreen core

In this section the relationship between acidity and electrolytic conductivity in the Skobreen core is examined. The data for these two parameters have shown that they are not correlated. This observation contrasts with observations elsewhere in the Arctic (e.g. Barrie, Fisher and Koerner, 1985).

Both acidity and EC values appear to vary seasonally (Fig. 3.13B and C). It is tempting to interpret the peaks as winter maxima caused by a higher concentration of anthropogenic pollutants (mainly strong acids). This has been demonstrated for other Arctic cores. For example, Barrie, Fisher and Koerner (1985) found that the EC peaks are positively correlated with the acidic peaks. Higher values occur in winter, when transport of pollutants to the Arctic is easier due to the atmospheric circulation conditions (cf. Section 5.2). The same conditions would be expected to apply to snow and ice masses in Svalbard. However, this good correlation between acidity and EC is observed only if atmospheric aerosol is the main source of impurities, otherwise there will be no correlation, particularly if the contribution from local dust is high.

Fig. 5.2 compares the relationship between acidity and EC (σ) in the Skobreen core with the same relationship as determined for the Agassiz ice-cap core (Barrie, Fisher and Koerner, 1985). There is a significant correlation ($r = 0.92$) between the two parameters in the Agassiz core (Fig. 5.2A). It is obvious that there is no correlation in the Skobreen samples (Fig. 5.2B). This total lack of correlation indicates that other ions, in addition to H^+ and the associated anions (i.e. Cl^-, SO_4^{2-}, NO_3^-), are major contributors to the total EC, which is to be expected in such an environmental setting (i.e. a valley glacier near open water in summer). There is a significant contribution from cations and anions derived from sea salts and crustal weathering.

In the summer, the upper layers of the accumulation zone are intensively affected by melting and percolation. It is known that under these conditions there are some processes that can alter the composition of the percolating water: for example, ionic exchange (Souchez and Lemmens, 1987). The snow and firn may contain clay particles derived from the surrounding outcrops. These particles are usually negatively charged and surrounded by a film of cations (i.e. a Gouey layer) such as Na^+, K^+, Ca^{2+}, and Mg^{2+}, which may be exchanged by the H^+ of the meltwater, decreasing the pH. The high summer concentration of dust layers would be an ideal environment for these process. The examination of the Skobreen layers by SEM (cf. Section 3.2.9) revealed a mineralogical composition not only rich in clay (e.g. chlorite) but also in fragments of immature sandstones and shales. High $CaCO_3$ may be expected in the matrix of this type of sandstone. Reaction of the carbonate and the calcium with the strong acids, particularly HCl and H_2SO_4, is another process that would alter the original pH values. On a smaller scale, the process of carbonation (i.e. chemical weathering, in which a weak carbonic acid solution converts oxides of calcium, potassium, sodium, and magnesium into carbonates and bicarbonates; Drewry, 1986) may also reduce the acidity of the meltwater. Finally, the samples were not filtered immediately on collection, so desorption and dissolution of the particles may have affected the chemical composition (Slatt, 1972). Eyles et al. (1982) observed a great increase in the concentration of carbonates (38%), Na^+ (700%), K^+ (333%), and Ca^{2+} (811%) after 50 days' storage. This was approximately the time that the Skobreen samples were left in the bottles before filtering.

From the discussion in the preceding paragraphs it may be concluded that the peaks in EC and acidity in the Skobreen core have different origins. The highest values of EC are summer peaks due to a higher concentration of local crustal particles and sea salts; the highest values of acidity are winter peaks caused by a high concentration of anthropogenic strong acids (mainly H_2SO_4).

It would be useful to compare the measured EC with the conductivity calculated theoretically from the ionic composition of the melted samples, but this is not possible because the complete ionic composition of the samples was not determined. On the other

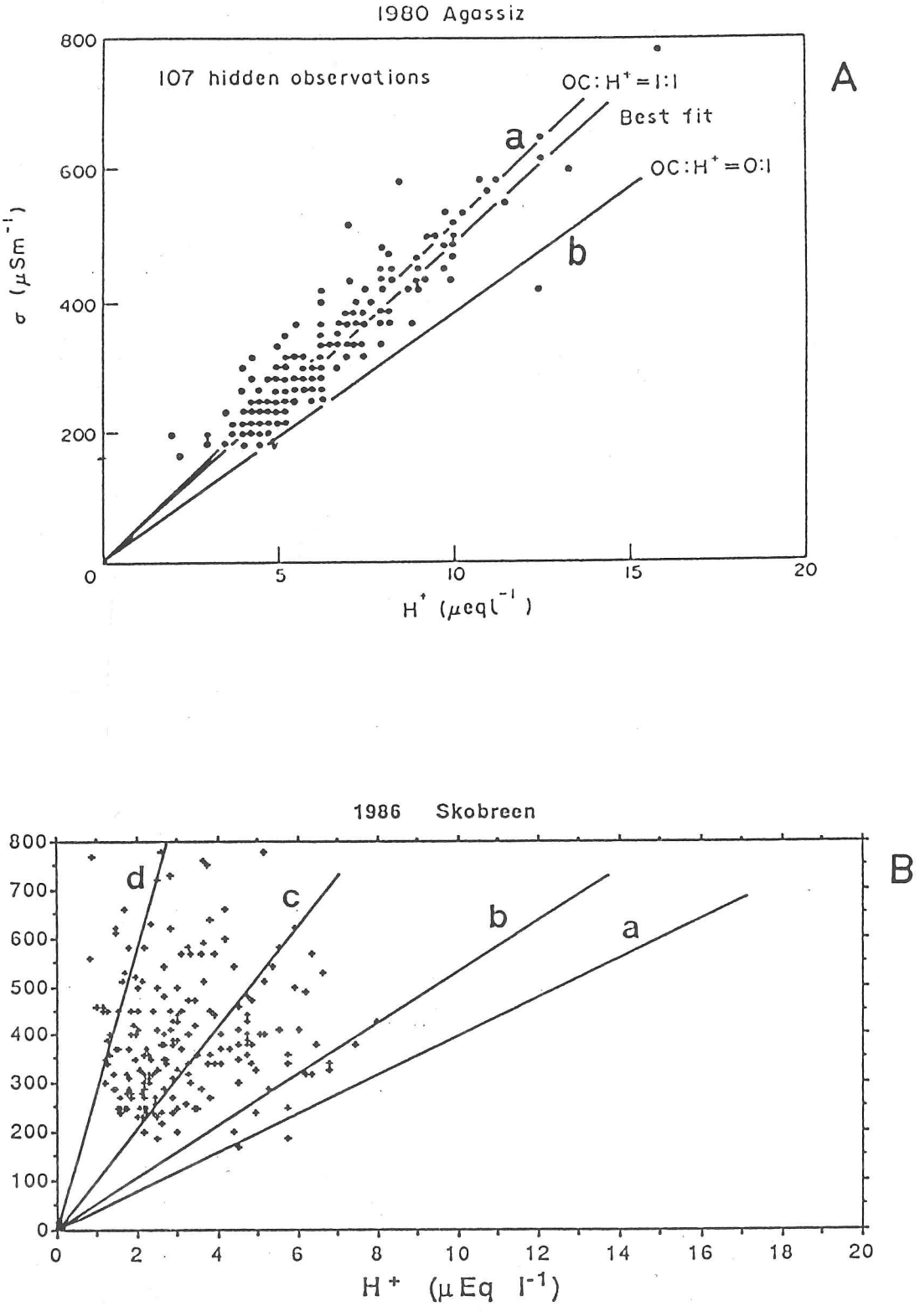

Figure 5.2- Relationship between acidity and electrolytic conductivity in samples from the Agassiz ice core (A) and the Skobreen core (B). Lines a and b in Fig.5.2A and B represent the theoretical cases where the proportion of other cations (OC) to H^+ are 1:1 and 0:1. Lines c and d in Fig. 5.2B represent the case where the OC:H^+ ratios are 5:1 and 20:1 respectively.

hand, an idea of the proportion of H^+ and other cations present in the samples can be obtained if some assumptions are made about the composition of the melted samples. Barrie, Fisher and Koerner (1985) assumed that the major ions in the Agassiz core were H^+, SO_4^{2-}, NO_3^-, Cl^-, NH_4^+, Ca^{2+}, Mg^{2+}, and Na^+. This is reasonable, bearing in mind the location of that core site (i.e. in the central part of an ice cap, relatively distant from local dust sources). The ions would originate mainly from aerosols of marine and anthropogenic origin.

The ions were divided into three groups according their ionic equivalent conductivity, λ_o (i.e. the ionic conductivity at infinite dilution). The three groups are: H^+, which with a λ_o of 315 $cm^2\ \Omega\ mol^{-1}$ far exceeds the other ions; other cations (OC) which differ from each other by less than 45% and can reasonably be represented by the ionic conductivity of NH_4^+ (63.6 $cm^2\ \Omega\ mol^{-1}$); and anions which are represented by the ionic conductivity of SO_4^{2-} (69 $cm^2\ \Omega\ mol^{-1}$). The ionic conductivities at infinite solution are measured at 18°C, the environmental temperature at which the EC was measured. Lines ***a*** and ***b*** in Fig. 5.2A represent the two theoretical cases where the proportion of other cations (OC) to H^+ are 1:1 and 0:1. The best-fit line from the Agassiz core samples is near the line ***a*** , indicating that H^+ is about 50% of the cationic content..

A similar analysis was carried out for the samples from the Skobreen core (Fig. 5.2B). The space between lines ***a*** and ***b*** represents a range of H^+ which varies between 50 and 100% of the total cations. That is rarely the case for the Skobreen samples. It is clear that the proportion of other cations (OC) to H^+ is much greater. Curves ***c*** and ***d*** represent the case where the proportion of cations to H^+ are 5:1 and 20:1 respectively (i.e. H^+ is less than 5% of the total cation equivalent). It can be concluded that the hydrogen concentration varies widely in the Skobreen core. H^+ can represent anything between 100% and an insignificant proportion of the total cations.

The above analysis was carried a step farther by the examination of the total EC and the calculation of the conductivity contribution from H^+ and associated anions (i.e. Cl^-, SO_4^{2-}, NO_3^-) in 27 samples. Melted snow and ice can be considered an infinite diluted solution† (i.e. sufficiently diluted to reduce the importance of ionic interactions). The total conductivity will then be given by the sum of the individual ionic conductivity (Kohlrausch's law; Horvath, 1985). In other words:

$$\sigma = \Sigma_i\ k_i = \Sigma_i\ \lambda_i\ c_i$$

† Even this is idealistic. As already observed in Section 3.1, natural waters are not simple solutions. The current carried by a given ion will depend on several factors, such as the interaction between the ions and ionic mobility. This exercise is intended to give an idea of the composition rather than to determine the individual ionic contribution to the total EC.

where c_i is the concentration of ith ion and λ_i is its molar ionic conductivity (or the ionic equivalent conductivity of individual ions). The latter parameter is tabulated in textbooks about electrolytic solutions (e.g. Horvath, 1985, Table 2.11.2). If the contribution of H^+, Cl^-, SO_4^{2-}, and NO_3^- is compared to the total EC an idea of the importance of the other cations and anions can be obtained.

Fig. 5.3 plots the sum of the ionic conductivity of the four ions against the total EC. It is obvious that the observed conductivity is often higher than the sum of the contribution of the four ions. This difference reflects the high concentration of other anions and cations in solution. It is reasonable to assume, considering the composition of the dust layers and the surrounding lithology, that the ions are mainly Ca^{2+}, Mg^{2+}, Na^+, and CO_3^{2-}. The measured EC is smaller than the calculated contribution of the four ions in six samples (black dots). This would indicate that uncharged or undercharged species are present (Fenn, 1987), perhaps as a result of ion association or ion pairing which produced neutrally charged compounds.

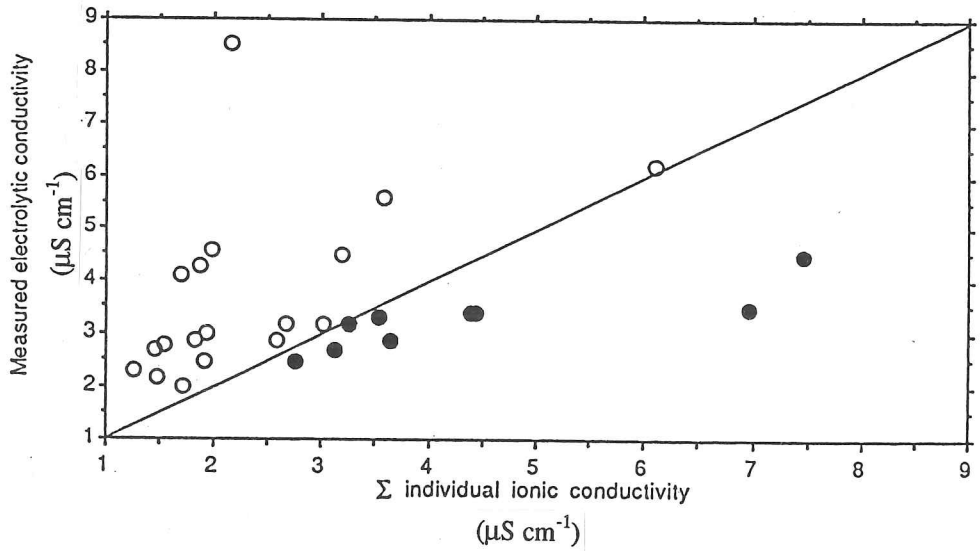

Figure 5.3- Relationship between measured electrolytic conductivity (EC) and the sum of the individual ionic conductivity in samples from the Skobreen core. Black dots mark samples where the measured EC is smaller than the calculated contribution of the four ions for which the concentration was measured.

5.5.2- The record of anthropogenic pollution in the Skobreen core

The annual layers in this core were identified by the processes described in Section 3.3 (Fig. 3.13). Although several of the examined parameters show clear trends of higher values towards the present, there are great fluctuations from year to year (cf. Fig. 3.13) which are caused mainly by two factors: 1) sampling size; the sampling was not only discontinuous but was also restricted to 10 cm sections. As demonstrated in Section 5.3, the concentration of pollutants in the Arctic shows a strong seasonality. It is possible,

therefore, that in some years only snow deposited in summer had been sampled, which would give a false impression of low impurity content; 2) melting and percolation may have been great enough to elute the great majority of some of the ions (e.g. SO_4^{2-}). Only two parameters that could provide information on the quantity of anthropogenic impurities were measured continuously: EC and pH (reported as strong acidity values in this dissertation). As demonstrated in Section 5.5.1, the EC cannot be used to derive information about the load of strong acids, because it has been altered by the high summer dust content.

Fig. 5.4 plots the annual values of both acidity† and $[SO_4^{2-}]^*$, which show statistically significant trends. The excess sulphate has been increasing at a rate of 0.11 μEq l^{-1} over the period 1930–84. On the other hand, this trend is significant only at α <0.06, with r = 0.34. Better results are obtained from the examination of the acidity profile, where the concentration of H^+ has increased at a rate of 0.028 μEq l^{-1} a^{-1} since the 1930s, with r = 0.44 and α <0.001. Maximum values of both excess sulphate and acidity were reached in middle 1970s. The above mean rates of change represent an increase of about 66% in acidity and of 230% in excess sulphate over a period of 54 years (1930–84). However, the excess-sulphate trend is being created artificially by an extremely high value (26.3 μEq l^{-1}) for only one sample in 1977. As the profile is not continuous, it is not possible to know if it represents a winter layer, so the concentration is anomalously high. More probably, it results from enrichment due to the elution and percolation of sulphates from the top layers. If this 'anomalous' layer is disregarded, the rate of increase reduces to 0.068 μEq l^{-1}, which represents an increase of about 150% since 1930.

If the marked seasonality in the transport of pollutants to Svalbard and to the Arctic in general is taken into consideration, it is more representative to examine the trends of the annual maximum and minimum. This examination will give the winter and summer trends respectively. Winter values, which can be 4 times greater than concentrations in summer, and up to 8 μEq l^{-1}, are the ones that should be compared with estimates of emissions from the source area (Eurasia in the case of Svalbard). Fig. 5.5 plots the dated variation in maximum and minimum acidity in the estimated annual cycles for Skobreen. The record was smoothed by a 3-cycle moving average, and the lines represent the linear regression models calculated by least squares. Both time series show greater concentrations towards the surface, although at different levels of significance. This is to be expected, as the winter precipitation is much richer in pollutants (cf. Sections 5.2 and 5.3). The trend of the maximum annual values is highly significant (r = 0.75 at α <0.0001) and it has been increasing at a rate of 0.054 μEq l^{-1} a^{-1}, which represents a total increase of 2.9 μEq l^{-1} over a period of

† pH is a measurement of total acidity. Nevertheless, pH has been converted to H^+ concentrations to facilitate cross-comparison with other acidity time series, and the calculation of the mean and trends. Furthermore, the main contribution to the acidity in polar precipitation is made by the strong acids (e.g. H_2SO_4 and HNO_3), and weak acids (such as organic acids) are in general insignificant in the background precipitation of the polar regions (Legrand and Saigne, 1988).

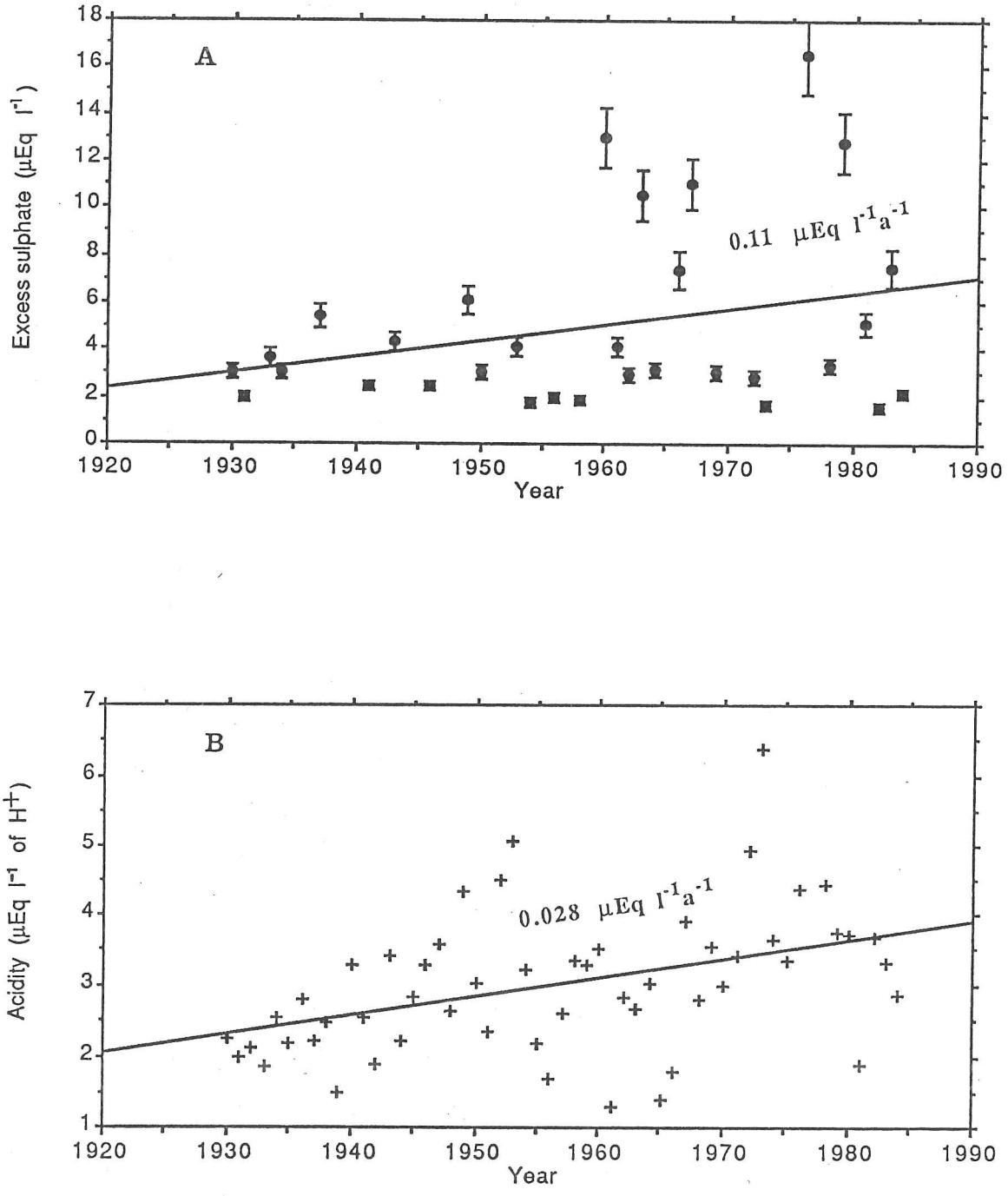

Figure 5.4- Mean annual acidity (A) and excess sulphate (B) in the Skobreen core. Thick lines mark the trend for greater values from 1930 to 1980. Error bars in Fig. 5.4A represent the precision of the measurements (±10% of the concentration).

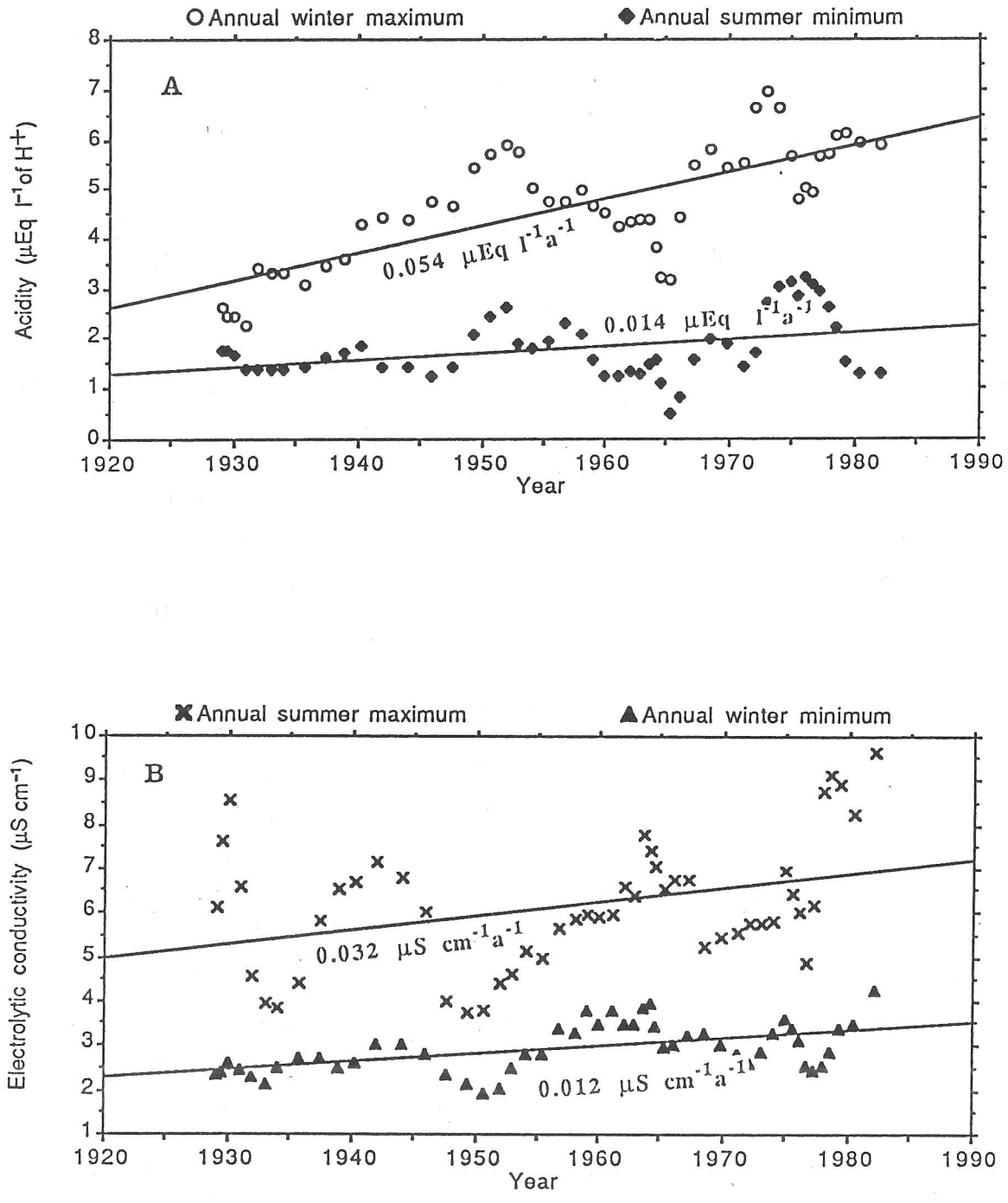

Figure 5.5- Trends in the seasonal maximum and minimum acidity (A) and electrolytic conductivity (B) in the Skobreen core. The values were smoothed by a 3-cycle moving-average model. Note that the acidity maximum is reached in winter, and the electrolytic conductivity maximum in summer (see Section 5.5.1 for explanation).

54 years (1930–84): in other words, an increase of 100% in maximum annual acidity. The annual minimum increase is on a much smaller scale, only 0.014 $\mu Eq\ l^{-1}\ a^{-1}$, and the trend is not well defined ($r = 0.35$, $\alpha < 0.02$). Overall, the minimum values have increased by only 0.8 $\mu Eq\ l^{-1}$ since 1930. It is also important to note that several of the minima are smaller than 2.3 $\mu Eq\ l^{-1}$, which denotes that some neutralization may have occurred, due to the presence of alkaline dust (cf. Section 5.5.1). Although the EC values have been greatly altered by the great concentration of dust, both maxima and minima still show a trend of greater values towards the present, as can been seen from Fig. 5.5B. Unlike the trend of the acidity values, the trend of the minima (0.018 $\mu S\ cm^{-1}\ a^{-1}$) is better defined ($r = 0.54$, $\alpha < 0.0001$) than that of the maxima (0.032 $\mu S\ cm^{-1}\ a^{-1}$ with $r = 0.36$, $\alpha < 0.01$). This is to be expected, because the minima occur, in general, in the winter, when the content of crustal impurities is reduced. The total increase in EC since 1930 is about 30% and 40% for maxima and minima respectively. This increase is also thought to reflect the increasing concentration of strong acids in precipitation, as such a rapid increase in the crustal contribution would be unexpected.

5.5.3- The Austfonna core record

Recently (1987) a new ice core was recovered from Austfonna, Nordaustlandet, by Soviet scientists (Zagorodnov and Arkhipov, in preparation). The core reached bedrock at 566.7 m and is estimated to represent 4000 years of accumulation. One of the studies carried out was the measurement of pH, therefore providing a long-term record of strong acidity for Svalbard and allowing the derivation of a pre-industrial-revolution baseline. The pH profile was kindly provided by Dr. Zagorodnov, but the dating and interpretation of this profile is the work of the author of this dissertation. The main shortcoming of the Austfonna record is the lack of detail in the profile. The acidity values plotted in Fig. 5.6 resulted from the pH graph profile; each data point represents between 5 and 10 m ice equivalent. Unfortunately, it was not possible to isolate all the measurements in more detail.

5.5.3a- Dating and the mean net accumulation rate of the Austfonna core

It is appropriate here to discuss the mean net accumulation rate of Austfonna, as it is important not only for dating the annual layers in order to interpret the acidity time series, but also as a component of models of the ice dynamics and mass-balance conditions (e.g. Dowdeswell and Drewry, 1989). There have been several estimates of the mean net accumulation rate for this ice cap which vary by more than an order of magnitude; that certainly does not inspire great confidence. The first estimate, by Ahlmann (1933c), based on snow-stratigraphy studies, was of only 60-70 $kg\ m^{-2}\ a^{-1}$. This was followed by Schytt (1964), whose measurements indicated an accumulation rate of 530 $kg\ m^{-2}\ a^{-1}$ on the summit of Vestfonna (about 620 m a.s.l.). More recently (1985 and 1987), two ice cores were recovered near the summit of the ice cap and two different estimates have been cited:

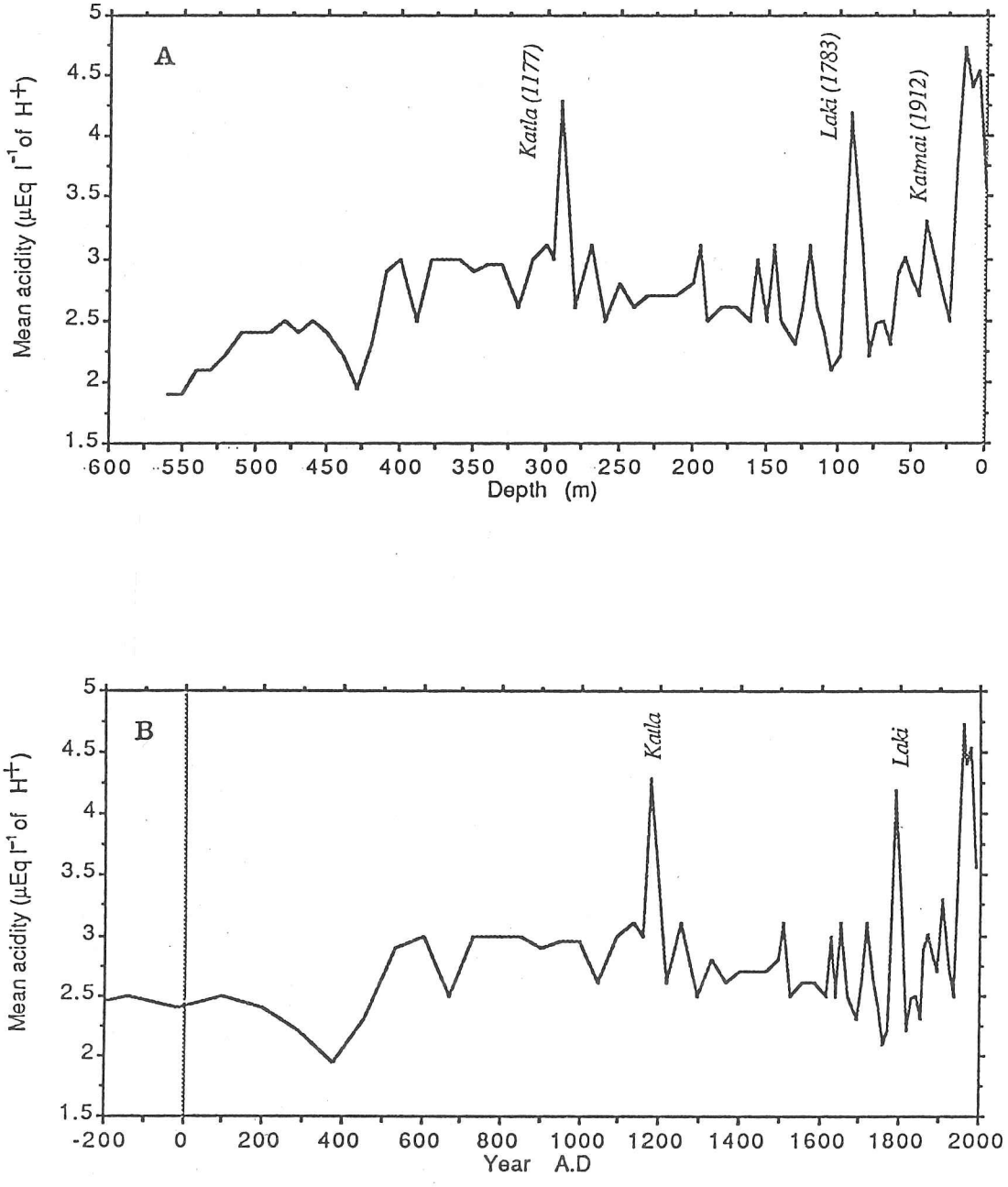

Figure 5.6- Variation in acidity in the Austfonna core. A) acidity plotted against depth; B) acidity plotted against age, calculated by the application of a simple Nye model with a mean annual net accumulation rate of 500 kg m^{-2} a^{-1}. Note the acid peaks, thought to identify major volcanic eruptions.

Punning,Vaykmyae, and Tóugu (1987) estimated a mean net accumulation rate of 890 kg m^{-2} a^{-1} for the 1985 core, and Dowdeswell and Drewry (1989) quoted a personal communication from Zagorodnov citing a different accumulation for the same core (i.e. between 400–500 kg m^{-2} a^{-1}). Zagorodnov and Arkhipov (in preparation) calculated that the 1987 core showed a mean net accumulation rate of 300 kg m^{-2} a^{-1}. This last core is the one used in this chapter to derive the acidity record for Austfonna. As discussed below, the author of this dissertation disagrees with this latter estimate. Finally, Schytt (1964) measured a total winter accumulation of between 800 and 1000 kg m^{-2} a^{-1}, which contrasts with the values measured by Semb, Brækkan and Joranger (1984) of only 350 kg m^{-2} a^{-1}. These disparities bear witness to the complex processes of snow metamorphism on this ice cap, which is subject to intermittent melting. Superimposed ice layers are frequently intercalated with firn layers. Melting and percolation downwards of light isotopes is common, altering the stable-isotope cycles. Therefore none of these estimates appears to be totally reliable.

The methodology adopted for the dating of the 1987 Austfonna core was to set up different runs with a simple Nye model, each time with a different mean net accumulation rate of between 300 and 900 kg m^{-2} a^{-1}. The dated acidity profiles were then cross-compared with the acidity record at Skobreen and with the sum of sulphates and nitrates in the Dye 3 core. The best result was obtained with a mean net accumulation rate of 460 kg m^{-2} a^{-1}, although some uncertainties may exist, because similar variations and trends may occur with some time lag at different ice-core sites. The pre-industrial peaks in strong acidity were tentatively related to the known major volcanic explosions referred to in Simkin et al. (1981), in order to confirm the estimated accumulation rate. 'Major volcanic eruption' in this dissertation means an eruption with a VEI (i.e. Volcanic Explosivity Index; Simkin et al., 1981) greater than 4. Particular attention was given to identifying eruptions of this order of magnitude or greater in Iceland, as the proximity and the air-circulation conditions guarantee rapid transport of impurities to Svalbard (i.e. in the course of few weeks) and it is not necessary for the eruption to eject impurities into the stratosphere. High acidity would reflect the high concentration of H_2SO_4, HCL, and HF which are ejected into the atmosphere at the time of the eruption.

Although confirmation of the volcanic origin of these peaks (Fig. 5.6) would require analysis of excess sulphate, chloride, and fluoride, the estimated age of some of the peaks coincides with major volcanic events. Particularly well marked is a H^+ peak of 4.3 μEq l^{-1} at a depth of 93 m, which is estimated to have been deposited in about 1784. This peak is therefore attributed to the eruption of Laki in 1783 (VEI 4), which is well marked elsewhere in the Arctic (e.g. Clausen and Hammer, 1988). Considering the position of Svalbard, leeward of the air masses passing Iceland, a marked increase in volcanic impurities is to be expected. Although the peak is greater by ≈ 1.8 than the baseline concentration, it is still 3–10 times smaller than concentrations in several of the Greenland ice cores (cf. Clausen and

Hammer, 1988). Further, the strong peak of the Tambora eruption, which had a VEI of 7 (the highest registered in the Holocene), was not found. Another peak occurs at a depth of 290 m (4.3 $\mu Eq\ l^{-1}$) and it is estimated to have been deposited in 1175. It could be due to the eruptions of Hekla in 1158 (VEI 4) and of Katla (VEI 2) in 1177. The peak is probably caused by the sum of the strong acids ejected by these two eruptions, as the difference between the two layers will be less than 5 m, due to vertical strain. Other smaller peaks are recognized at about 35 m ($\approx$ 3.5 $\mu Eq\ l^{-1}$), which may be related to the eruption of Katmai (Alaska Peninsula) in 1912. This eruption has also been detected elsewhere in the Arctic. For example, the Katmai eruption has strongly affected the EC record in the Agassiz ice-cap core (Barrie, Fisher and Koerner, 1985). Another peak of 3 $\mu Eq\ l^{-1}$ at about 1716 may have been caused by the 1721 eruption of Katla (VEI 4). Unfortunately, there are two facts that do not allow total confidence in the identification of these volcanic eruptions, although some of the peaks are dislocated by only one or two years from the date estimated by the Nye model. First, peaks due to major eruptions like Tambora (1815) and Krakatoa (1883) are not recognizable. They have been recorded in Greenland, although these eruptions were in the Southern Hemisphere. Secondly, peaks of the mean concentration of H^+ vary between 8.2 and 31.2 $\mu Eq\ l^{-1}$ in the Greenland cores (Clausen and Hammer, 1988). It appears that peaks in Svalbard are very low, which may be the result of partial elution of the H^+. Bearing in mind these uncertainties, the mean net accumulation rate at the summit of Austfonna can be estimated on the basis of the volcanic peaks and taking the vertical strain on the annual layers into consideration. The mean net accumulation was calculated for periods between the identified eruptions by Nye's model equation, or $e^{-tb/h} = 1 - \frac{y}{h}$, where b is the mean net accumulation rate, t is the time that each layer was deposited, h is the ice thickness at the core site, and y is the depth of the layer at present (in ice equivalents).

5.5.3b- Acidity variations in Austfonna

Fig. 5.7 compares the dated acidity profile from Austfonna with the Skobreen record. The same general trends are observed in both cores between 1930 and 1980. In the two profiles an increase of about 2 $\mu Eq\ l^{-1}$, or about 80%, is observed between 1935 and 1955. After this period the Austfonna core stabilizes, in contrast to the Skobreen core, which tends to have lower values. This latter difference may be only because there is a lack of annual detail for the Austfonna core, rather than because there are any real differences. After the increase between the 1930s and 1950s, the Austfonna core acidity tends to stabilize at 4.5 $\mu Eq\ l^{-1}$. Both cores show a decrease in acidity during the 1980s. Acidity in Austfonna in about 1910 was higher than the baseline value, probably due to the Katmai eruption (VEI 6), as it has been observed elsewhere in the Arctic (e.g. Barrie, Fisher and Koerner, 1985). The record is above the estimated baseline (i.e. 2.3–2.8 $\mu Eq\ l^{-1}$) for the whole industrial period and has been increasing progressively since 1800. Fig. 5.8 shows the record of acidity concentration since 1800: present values are about twice the values at the beginning of

the last century. A linear-regression analysis for the period 1800–1980 shows an increase rate of 0.013 ± 0.002 μEq l^{-1} a^{-1}, with r = 0.80 at a highly significant level (α <0.0001). This means a total increase of about 2.2 μEq l^{-1} over 180 years, or 95%. Three points (in the 1920s–1930s and 1980s) with relatively low values could have been the result of partial elution of H^+ or the presence of alkaline dust, rather than of changes in the precipitation concentration. High summer temperatures in the late 1920s may have caused the great melt and flush-out of part of the H^+.

Table 5.3- Mean net accumulation rate at the summit of Austfonna during different periods. The accumulation was estimated using a Nye flow model and by the identification of acid peaks caused by strong acids originating from major volcanic eruptions (cf. text for details).

Period	Mean net accumulation rate (kg m^{-2} a^{-1})
1930-1987	460
1912-1930	385
1783-1912	467
1716-1783	458
1158-1716	448

Long-term acidity record in Austfonna

Some remarks on the long-term acidity record in Austfonna would be appropriate here. As can been seen in Fig. 5.6, the baseline appears to have oscillated between 2.3 and 2.8 μEq l^{-1} over the last 2000 years. The most probable reason for these long-term changes would be variation in the biogenic production of sulphur compounds (e.g. dimethylsulphide in the surface water of the oceans). This explanation would fit well with the decrease observed at about 1200 BP (before present), reaching a minimum in about 1750, therefore coinciding with part of the Little Ice Age. After 1800, the relatively low background values would be masked by anthropogenic pollution. The bottom part of the core (i.e. below a depth of 400 m) is loaded with insoluble particles (Zagorodnov and Arkhipov, in preparation) and alkaline composition may have been the cause of the reduced pH.

5.5.4- Comparison with the record of other ice cores

How do these trends and concentrations in acidity and sulphates compare with measurements in the rest of the Arctic and also with records recovered from Europe? The excess-sulphate and acidity profiles from Skobreen and the acidity record in Austfonna are compared with the record from Dye 3, Greenland (Neftel et al., 1985; Mayewski et al.,

1986), from Agassiz ice cap, Ellesmere Island (Barrie, Fisher and Koerner, 1985), and from Colle Gnifetti, Monte Rosa, Swiss Alps (Wagenbach et al., 1988) in order to check their representativeness. Table 5.4 summarizes the concentrations and trends for this century in the different ice cores. As discussed in Section 5.5.1, the load of crustal impurities in the Skobreen ice may have been great enough to alter the original trends of acidity variations beyond recognition.

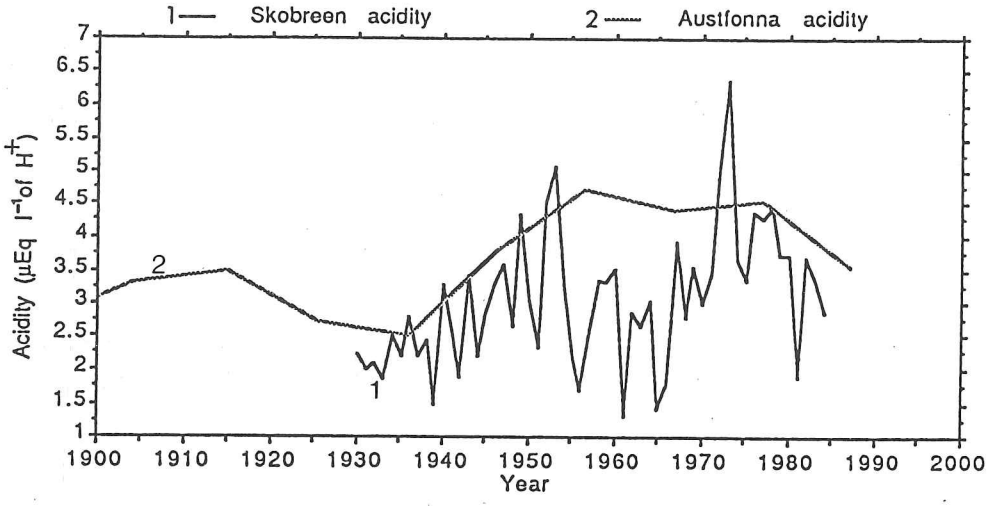

Figure 5.7- Comparison of the acidity record of the Austfonna and Skobreen cores during the 20th century.

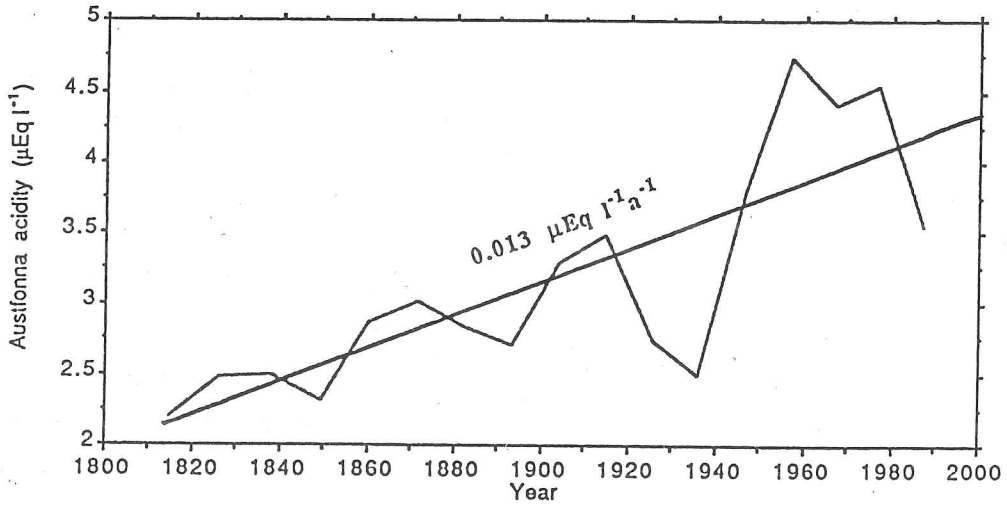

Figure 5.8- Acidity concentration in the Austfonna core since 1800. The thick line marks the trend to greater values from 1800 to 1980.

Acidity

In Fig. 5.9A – C the acidity profiles of Austfonna and Skobreen are compared with the mean H^+ concentration in the Agassiz ice cap, Ellesmere Island, and the SO_4^{2-} plus NO_3^- concentration in the Dye 3 core, Greenland. The latter sum should be a reasonable estimate of the number of equivalents of H^+ at Dye 3, as HNO_3 and H_2SO_4 are the main strong acids due to pollution. Naturally this may not be true for 'anomalous' periods, such as a high incidence of volcanic eruptions which might eject HCl and HF into the atmosphere. In order to confirm the acidity, it would then be necessary to calculate the ionic balance. Although one of the most detailed profiles of ionic concentration at Dye 3 is the one by Neftel et al. (1985), no excess-sulphate concentrations are given. However, it is known from similar work by Mayewski et al. (1986) at Dye 3 that the mean maximum Cl^- is about 0.7 $\mu Eq\ l^{-1}$, which would represent less than 0.1 $\mu Eq\ l^{-1}$ of sea-salt sulphate. It is reasonable, therefore, to assume that the sum of the nitrate and sulphate equivalents is proportional to the H^+ concentration. The H^+ values for Agassiz were inferred from electrolytic conductivity measurements based on an empirical relationship obtained by Barrie, Fisher and Koerner (1985) for the core.

Although the general trend of greater acidity towards the present is recognizable in all the cores, there are marked differences about the timing of the beginning of the main changes. Austfonna, Skobreen, and Dye 3 registered the beginning of the increase in about 1940. This is assumed to be the result of greater emission of anthropogenic sulphur dioxide and nitrogen oxides due to the industrialization process, as there is no evidence for an increase in natural production (such as a period of great volcanic activity). The main features of the Skobreen core acidity profile are observed also at Agassiz and Dye 3. The similarities of the trends at Dye 3 and Skobreen become even more evident when the two time series are smoothed by a 5-year cycle moving-average model. Fig. 5.9C plots the smoothed profiles, which show a correlation of $r = 0.76$ at $\alpha < 0.0001$. The best fit was obtained with a 3-year time lag between Dye 3 and Skobreen. All three profiles show a significant increase in acidity since the 1930s ($0.037 \pm 0.004\ \mu Eq\ l^{-1}\ a^{-1}$ at Dye 3, $0.075 \pm 0.024\ \mu Eq\ l^{-1}\ a^{-1}$ at Agassiz, and $0.028 \pm 0.009\ \mu Eq\ l^{-1}\ a^{-1}$ at Skobreen). But it is more relevant that the ratio between mean concentrations in the 1970s and the 1930s is quite similar at Dye 3 and Skobreen, 1.8 and 1.9 respectively. The ratio at Agassiz is smaller, only 1.5. Concentrations at Skobreen are greater than at Dye 3. On the other hand, they are smaller than concentrations at Agassiz, which contrasts with the spatial distribution of concentrations determined from the superficial layers (Section 5.4 and Fig. 5.1D). This is to be expected, as H^+ has suffered partial elution at Skobreen – something that does not happen at the altitude of Agassiz. In Fig. 5.9B the Austfonna profile is compared with the sum of nitrates and sulphates at Dye 3. The general trends since 1900 are similar and both profiles show a decrease in the mid-1930s. The ratio

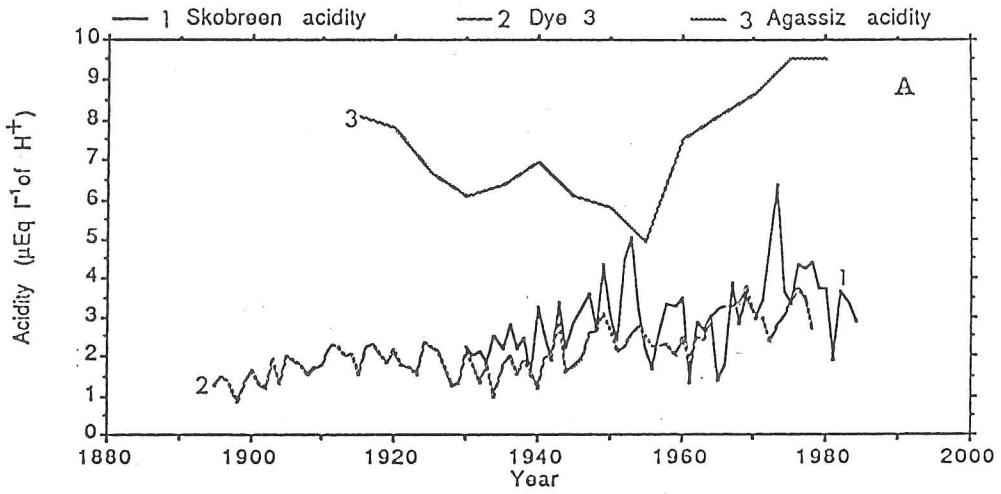

A) Skobreen acidity (1) compared with the Dye 3 sum of SO_4^{2-} and NO_3^- (2) and acidity in Agassiz (3).

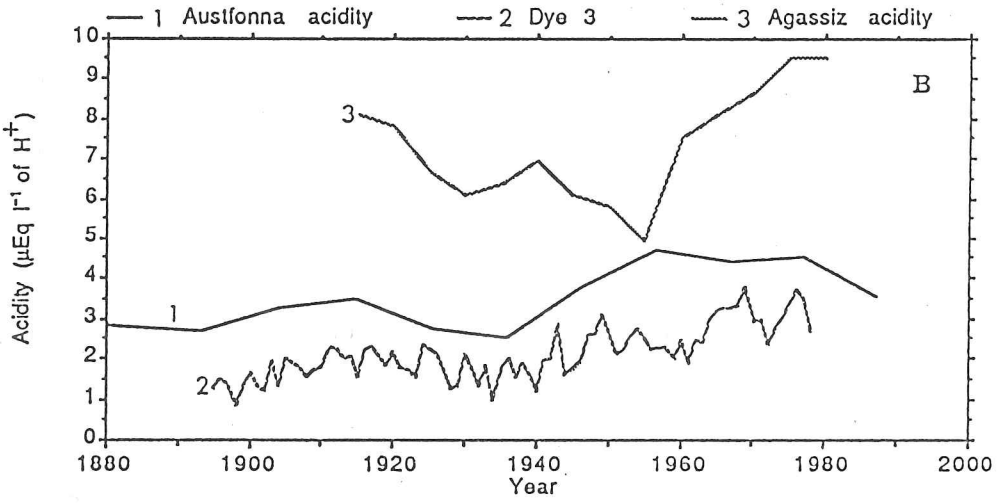

B) Austfonna acidity (1) compared with the acidity at Agassiz (3) and the sum of SO_4^{2-} and NO_3^- in Dye 3 (2).

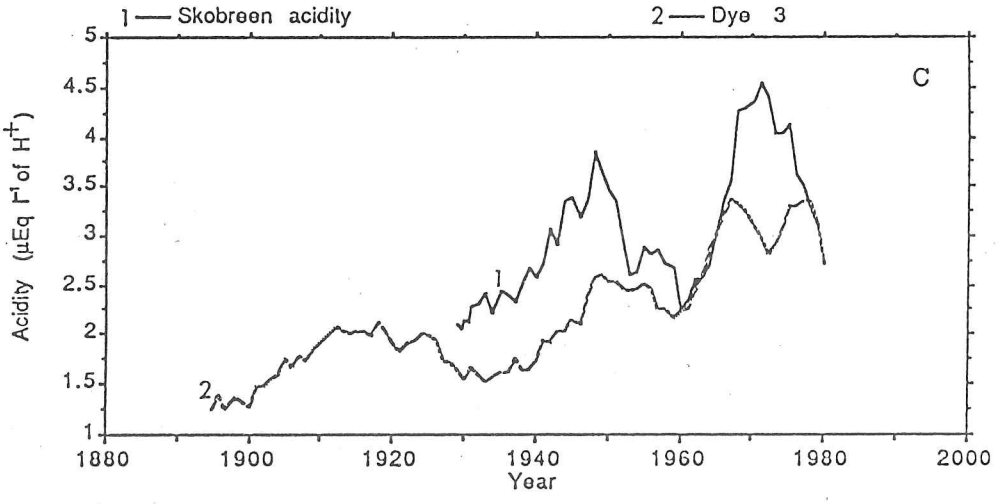

C) Smoothed profiles (by a 5-year cycle moving-average model) of acidity in Skobreen (1) and the sum of SO_4^{2-} and NO_3^- in Dye 3 (2).

Figure 5.9- Comparison of the acidity record of the Austfonna and Skobreen cores with the mean H^+ concentration in the Agassiz ice cap core (Ellsmere Island), and with the sum of sulphates and nitrates at Dye 3 (Greenland).

between concentrations in the 1970s and the 1900s is about 1.5 for Skobreen and 2.8 for Dye 3.

H^+ concentration decreased according to three profiles (i.e. Austfonna, Dye 3, and Skobreen) in the late 1950s, although the minimum at Agassiz is reached earlier than at the three other sites. Three main factors could cause changes in concentration at the receptor (i.e. the original precipitation at the core sites): 1) modifications in the path followed by the air masses transporting impurities from the source to the receptor; 2) the scavenging process; and 3) changes in the strength of the source (Neftel et al., 1985). The production of precursors of strong acids (e.g. SO_2) were in fact increasing rapidly by the 1950s, and the third hypothesis is therefore disregarded. The other two controls remain to explain the decrease in the late 1950s – early 1960s. Two hypotheses are put forward, although more studies would be needed to confirm them: 1) Changes in the precipitation or post-depositional alteration – the decrease would be explained either by elution of the H^+ or by a higher precipitation rate for the period. Any of the two options would agree with meteorological data for Svalbard for the period (i.e. an exceptionally warm period with high precipitation, cf. Appendix 1). For the other sites, it would be necessary to examine the variations in the annual accumulation rate and in summer conditions before reaching any conclusion. 2) Another explanation would be a more zonal air circulation, with a retreated position for the Arctic front, and a less frequent passage of cyclones through the source areas in Eurasia. This would naturally result in a smaller load of anthropogenic impurities in the troposphere.

Sulphates

The examination of the trends of anthropogenic pollutant concentration in Skobreen can be extended by comparing the variations in excess sulphate (SO_4^{2-}) with the record for the Dye 3 and Colle Gnifetti cores. The latter core was recovered from a col 4450 m a.s.l. at the summit of Monte Rosa, Swiss Alps, providing a record of pollutant trends at the source area (i.e. Europe). Dating and the methods for deriving these data are described in Wagenbach et al. (1988). Although the annual accumulation at Colle Gnifetti is affected by wind erosion, the records show a highly significant increase in SO_4^{2-} and nitrates over the last 100 years (Wagenbach et al., 1988; Wagenbach, 1989). These increases are attributed to the increase in anthropogenic emissions (Wagenbach et al., 1988).

Fig. 5.10 compares the three profiles. Note that concentrations at Dye 3 had to be plotted on a different scale to allow comparison with the concentration in Skobreen and the variations from Colle Gnifetti. Furthermore, it was not possible to eliminate the non-sea sulphate from the Dye 3 and Colle Gnifetti records, as no Na^+ or Cl^- record has been published for these cores. Nevertheless, as described above, the sea-salt contribution at Dye 3 is thought to be less than 0.1 $\mu Eq\ l^{-1}$ and no significant trend is observed in the Cl^-

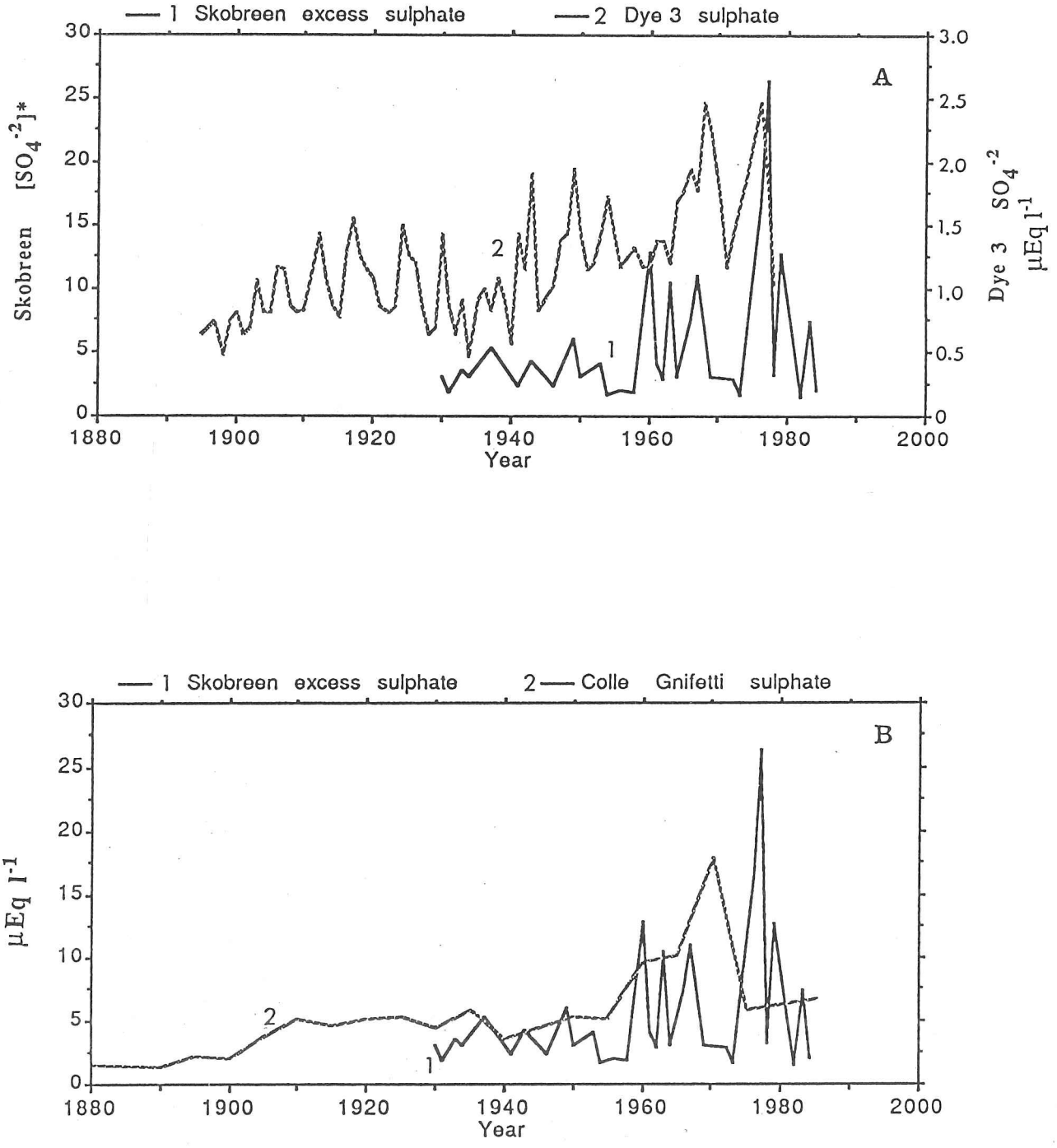

Figure 5.10- Comparison of the excess-sulphate record in the Skobreen core with the sulphate concentration in Dye 3 - Greenland (A) and Colle Gnifetti - Switzerland (B). Note the different scales for Dye 3 (2) and Skobreen (1) in plot A.

concentration at Dye 3. The wider geographical position of Colle Gnifetti guarantees a reduced marine contribution. The three profiles show similar general trends. From 1930 to 1980 the proportional increase in excess sulphate at Skobreen was 120% and the increase in total sulphates at Dye 3 and Colle Gnifetti was 110% and 120% respectively.

Table 5.4- Summary of acidity and sulphate concentrations in the Agassiz (Ellesmere Island, Canada), Austfonna (Nordaustlandet, Svalbard), Colle Gnifetti (Swiss Alps), Dye 3 (Greenland), and Skobreen (central Spitsbergen, Svalbard) cores. Concentrations are given in $\mu Eq\ l^{-1}$ and rates given at $\mu Eq\ l^{-1}\ a^{-1}$. The acidity of these cores was estimated by various procedures: by pH at Austfonna and Skobreen; by electrolytic conductivity from a linear relationship with the H^+ concentration at Agassiz; and from the sum of the number of equivalents of estimated excess sulphate and nitrates at Dye 3.

	Pre-industrial level baseline		1895–1904 concentrations		Modern concentrations		Ratio concentrations 1970s/1900		1970s/1930		Rate of increase 1930–70 [c]	
	Acidity	SO_4^{2-}	Acidity	SO_4^{2-}	Acidity	SO_4^{2-}	Acidity	SO_4^{2-}	Acidity	SO_4^{2-}	Acidity	SO_4^{2-}
Austfonna	2.5	-----	3.0	-----	4.5	-----	1.6	-----	1.8	------	0.046	------
Skobreen	-----	-----	-----	-----	4.2	7.5 [e]	-----	-----	1.7	2.2 [e]	0.028 [d]	0.068 [e]
Agassiz [a]	-----	-----	b	-----	9.3	-----	-----	-----	1.5	-----	0.075	------
Colle Gnifetti	-----	-----	-----	2.3	-----	11.9	-----	4.4	-----	2.2	-----	0.017
Dye 3	1.3	0.5	1.4	0.8	3.1	1.9	2.2	2.5	1.8	2.1	0.037	0.022

Notes:

(a) Source: Herron (1982) for periods 1539–1577 and 1773–1791, obtained from the sum of excess-sulphate and nitrate number of equivalents.

(b) Record extends only to the 1910s, and at that time the acidity of the site was greatly enhanced by by-products of the eruption in 1912 of Katmai (Alaska).

(c) Annual increase rate in $\mu Eq\ l^{-1}$.

(d) One anomalously high concentration ($26.3\ \mu Eq\ l^{-1}$) was disregarded when computing trends.

(e) Excess sulphate. With the exception of the Skobreen core all concentrations are given in total sulphate. As explained in the text, the sea-salt sulphate should be a small proportion of the total sulphate at the continental sites. Naturally this is not true in Svalbard and it is essential to compute the $[SO_4^{2-}]^*$ to separate the anthropogenic from the natural sulphate. It would be better to have the excess sulphate for all the other cores, but unfortunately no Cl^- or Na^+ concentrations were provided by the authors. For Dye 3, an indication of the sea-salt content was obtained from Mayewski et al. (1986).

References: Agassiz (Barrie, Fisher and Koerner, 1985); Austfonna (Zagorodnov and Arkhipov, in preparation; this dissertation); Dye 3 (Neftel et al., 1985); Skobreen (this dissertation).

The concentrations at Skobreen are sometimes greater than the concentrations at Colle Gnifetti, which attest to the efficiency of the transport of pollutants to Svalbard. Low values

of excess sulphate until the 1950s were followed by a sharp increase by the 1960s. Although the rates of increase between the 1930s and the 1980s differ in the cores examined, it is important to note that at the time of maximum concentrations in the late 1970s, all the profiles (i.e. Dye 3, Colle Gnifetti, and Skobreen) had increased by about 2.1 to 2.2 when compared with the levels of the 1930s. It can be concluded that the excess-sulphate profile for Skobreen, despite the non-continuous sampling and the strong elution and flush-out of the sulphates in some years, represents real changes in the sulphate concentration in precipitation.

5.5.5- Comparison with European SO_2 emissions

In this section the acidity and excess sulphate in the Svalbard cores are compared with the anthropogenic pollutant emission in Europe to establish the possibility of a link. As remarked in other parts of this chapter, the increasing emission of sulphur dioxide and nitrogen oxides into the atmosphere since the industrial revolution has resulted in a sharp increase in the acidity of precipitation in Europe and other industrialized areas. Because of specific atmospheric circulation conditions the precipitation chemistry in Svalbard should reflect these trends at least in part. Unfortunately, there is no historical time series of SO_2 and NO_x emissions. On the other hand, there are estimates of global and European sulphur dioxide emissions based on the consumption of sulphur-containing raw materials, taking into consideration mean emission factors. The main sources considered in this estimated time series were: the SO_2 emission due to combustion of fossil fuel (mainly coal); H_2S produced by industrial processes used in oil refineries, paper mills, and natural-gas processing and coal gasification; and the smelting of sulphidic ores, sulphur mining, and production of sulphuric acid (Möller, 1984).

Fig. 5.11 compares the sulphur dioxide emissions† for Europe estimated by Möller (1984) with the acidity and excess-sulphate record from Skobreen and the acidity record in Austfonna. The sulphur dioxide estimates are given in 10^6 tons. Although the excess-sulphate profile for Skobreen appears to reflect the same trends as the SO_2 emissions, it is not possible to estimate the rate of increase by regression analysis as there is a great variability in the excess-sulphate concentrations. The acidity trends are more clear. As already noted on, acidity at both Austfonna and Skobreen has increased by about 80% since 1940 (from 2.5 to 4.5 $\mu Eq\ l^{-1}$). This increase is to be expected from the sulphur dioxide emissions but should have happened 10 years later. Further, the SO_2 emissions increased by about 160% over the period 1950–85 (from 12 to 31.2 Mtons S a^{-1}). The SO_2 estimates were also compared with the time series of maximum annual acidity in Skobreen, since the influx of pollutants is highly seasonal, and similar results were obtained.

† Although other acids (i.e. HNO_3 and HCl) do contribute to the acid precipitation, they are in general less important for the acidification of the precipitation at long distances from the source areas. This is because hydrochloric acid is removed relatively close to the source area, as it is very soluble, and the NO_x is rapidly oxidized to HNO_3 and removed by rainfall in a short time (Brimblecombe, 1986).

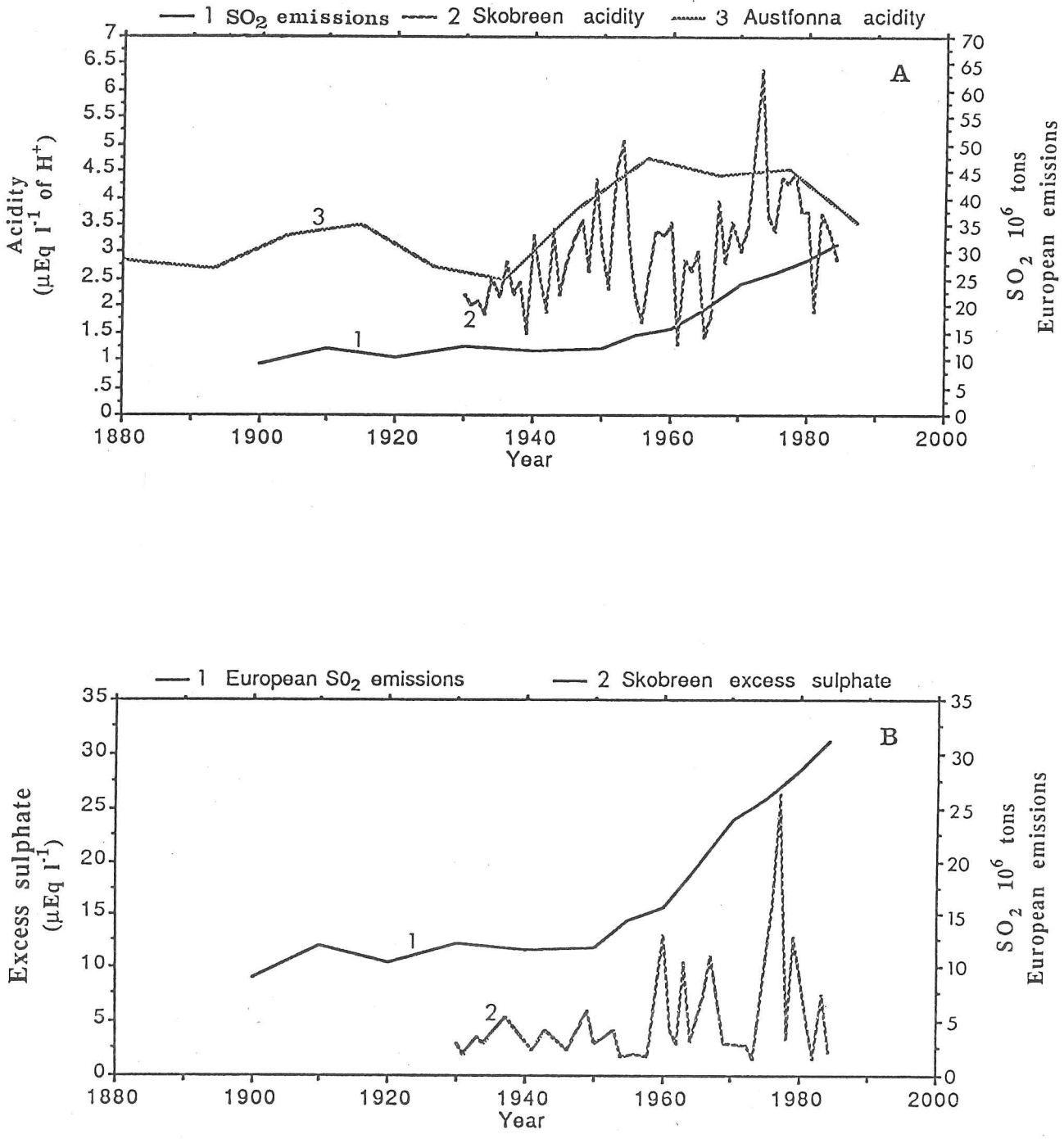

Figure 5.11- A) Comparison of the acidity record in Austfonna (3) and Skobreen (2) with the estimated sulphur dioxide emissions for Europe (1). B) Comparison of the excess-sulphate record in Skobreen (2) with the estimated sulphur dioxide emissions for Europe (1). Source of the estimated SO_2 time series: Möller, 1984.

It can be concluded that the ice cores from Svalbard show substantial increases in acidity and sulphate content since the 1930s, and this increase is most likely to be associated with the increase in anthropogenic emissions from the main source area. Nevertheless, the increase in sulphates and strong acidity in Svalbard is not directly related to the estimated European emissions of SO_2. This contrasts with the results from the Colle Gnifetti core. In Fig. 5.12 the total sulphate profile of this core is also compared with the European emissions of SO_2; the core is a fair representative of the main trends. Many reasons could be cited for this lack of a relationship between European emissions and the Svalbard core records: post-deposition alteration due to melting and percolation processes at the core sites, as discussed elsewhere in this dissertation; changes in atmospheric circulation and so in the quantity of material transported annually to Svalbard; and the chemical behaviour of the pollutants along the trajectory from Europe to Svalbard. A deeper understanding of the processes which affect the source–receptor relationship would be gained by studying the trajectories of the pollutants, by simultaneous sampling of contaminants in the atmosphere, in the precipitation, and in snow recently precipitated; and in studying the chemical behaviour of the pollutants during transport through the atmosphere. This task is beyond the scope of this dissertation.

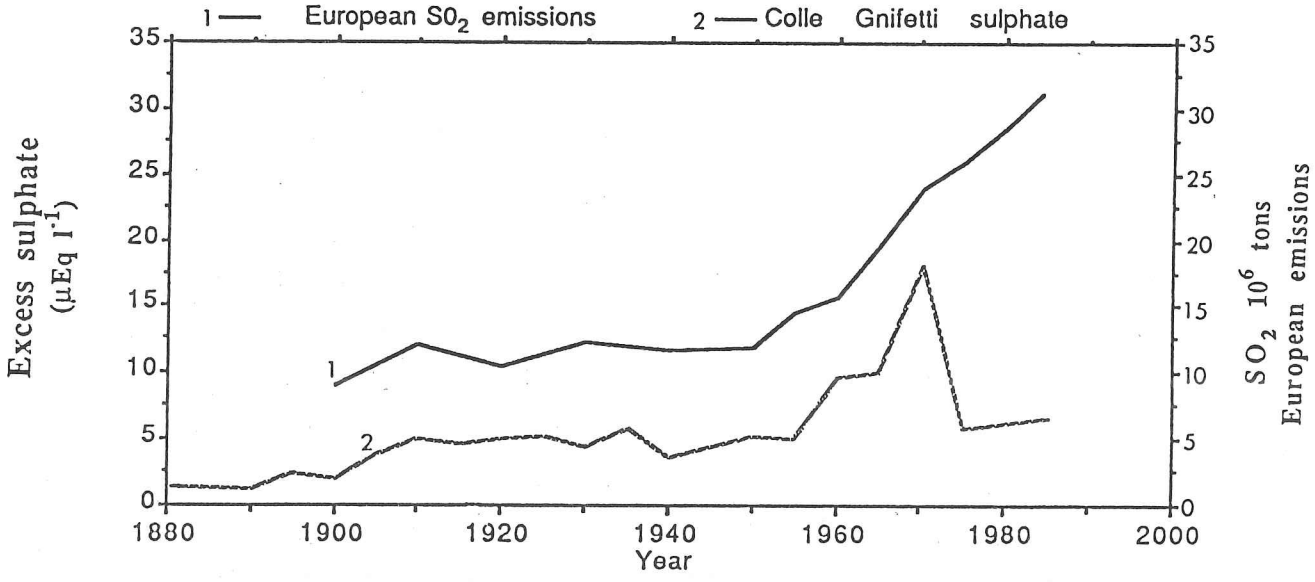

Figure 5.12- Comparison of the total sulphate record (2) in Colle Gnifetti (Switzerland) with the estimated sulphur dioxide emissions for Europe (1). Source of the estimated SO_2 time series: Möller, 1984.

5.6- The impact of snow acidification in the environment of Svalbard

Davies, Vincent and Brimblecombe (1982) demonstrated that ions are eluted from snow differentially in a manner that accentuates the loss of strong acids (i.e. mainly H_2SO_4 and HNO_3). These great losses happen during the first weeks of the thaw and can lead to a three-to-fivefold increase in acidity concentrations (i.e. an 'acid shock'). It is also clear that some of the acids are removed from the snow/firn masses even at an altitude of 600 m in central Spitsbergen, as the examination of the chemistry of the Skobreen core shows. A much more intense release of acids will certainly occur at lower altitudes. This acidic meltwater can cause serious damage to an ecosystem like that of Svalbard, particularly in lakes. A similar process has been observed in Scandinavia (Johannessen and Henriksen, 1978) and the consequences included massive fish kills (Leivestad and Muniz, 1976). Although the impact of the acidification on biota depends on other factors, such as the salinity and inorganic aluminium content (Cresser and Edwards, 1987), similar processes may be taking place in Svalbard or may take place in the future. It is important to remember that the emissions of sulphur dioxide are expected to increase for at least the next 15 years (Möller, 1984). It would be advisable, therefore, to monitor the composition of meltwater, lakes, and fjords in Svalbard to assess the impact of the acidic run-off. This may be carried out by examining the variations in diatomaceous taxa, which are highly sensitive to variations in acidity, in lakes (Battarbee, 1984).

5.7- Summary and conclusions

Specific conditions of atmospheric circulation on a synoptic scale during the winter in the Arctic North Atlantic and Barents-Kara sea regions and the proximity of Europe make Svalbard one of the areas in the Arctic most affected by anthropogenic pollution. The expansion southwards in the winter of the cold dry Arctic air mass forces the main cyclone tracks over the heavily polluted atmosphere of central Europe, Scandinavia, and the north-western USSR, and they are then deflected towards the Arctic. Svalbard is one of the first land masses in the path of these pollutant-laden air masses and as a consequence its atmosphere, snow, and ice have a high content of anthropogenically derived impurities.

Atmospheric concentrations can be as high as 2 $\mu g\ m^{-3}$ of excess sulphate in Ny-Ålesund (Rahn, 1982), and winter concentrations are similar to those in the north of Scotland. Measurements carried out in the snow cover by several authors over the last two decades confirmed the atmospheric observations. Maximum values are reached in Nordaustlandet, where excess sulphate can reach 9.5 $\mu Eq\ l^{-1}$, and the H^+ reaches 29.6 $\mu Eq\ l^{-1}$ (Semb, Brækkan and Joranger, 1984). The examination of an acidity profile for an ice core from Austfonna provides baseline values and trends from the beginning of the

industrial revolution. Pre-industrial acidity oscillated between 2.3 and 2.8 $\mu Eq\ l^{-1}$, tending towards the lower values during the relatively cooler period known as the Little Ice Age (from about A.D 1200). From the beginning of the 19th century a trend towards higher values is observed, most probably due to the increase in production of sulphur compounds in Europe. Since 1800 the H^+ concentration in Austfonna has increased to a total of 2.2 $\mu Eq\ l^{-1}$, which represents an increase of 95% when compared to the baseline concentration. Further evidence of the increase in acidity and excess sulphate is provided by the examination of the Skobreen core. Although interpretation of the core is complex due to melting and associated phenomena, statistically highly significant trends of greater concentrations towards the present were obtained for the acidity and excess-sulphate profiles. In fact, even the electrolytic conductivity values, which have been altered substantially by the influx of local crustal impurities in the summer, show greater values towards the present. Since the 1930s the acidity and the excess-sulphate concentrations have increased by at least 66% and 150% respectively. The annual winter maximum of acidity has increased by 100% since 1930. In short, it can be said that the results from the two ice cores, Austfonna and Skobreen, confirm the atmospheric and superficial snow observations of an environment heavily loaded with anthropogenic impurities. The trends observed in these two cores are approximately similar to trends observed in other cores from the Arctic (i.e. Agassiz and Dye 3) and Europe (i.e. Colle Gnifetti). To confirm these trends it would be interesting to obtain a core from a better site on Svalbard, as both Austfonna and Skobreen undergo summer melting and partial elution of the ionic content to some degree. The high concentrations of H^+, frequently greater than 10 $\mu Eq\ l^{-1}$ (i.e. with pHs lower than 5.0), associated with high concentrations of sulphates, indicate that Svalbard is suffering from the phenomenon of acid precipitation†.

As a by-product of the analysis of the Austfonna core, it was possible to derive the mean net accumulation rate for the last 800 years and also to identify some of the acidic peaks due to impurities ejected into the atmosphere during volcanic eruptions. Accumulation rates have fluctuated between 385 and 467 $kg\ m^{-2}\ a^{-1}$ since 1157. Since 1930 the rate has been about 460 $kg\ m^{-2}\ a^{-1}$. The volcanic eruption of Laki (Iceland) in 1783 appears to have left the most marked acidic peak in the Austfonna core, but further measurements of (for example) excess sulphate are needed to confirm the origin of this peak.

Finally, attention is drawn to the probable impact of acidification of the precipitation on the ecosystem of Svalbard. Preferential elution of strong acids (e.g. H_2SO_4, HNO_3) in early spring may be causing an 'acid shock' to lake biota. A programme for monitoring the impact of acidification on the environment is therefore desirable.

---

† In the case of snow precipitation, which is examined here, the terms 'acid-rain' or 'acid-snow' precipitation are not adequate, as the acidity of the deposited snow may be enhanced by dry deposition. It is more appropriate to talk about a record of acid deposition in snow and ice.

CHAPTER 6

CONCLUSIONS

There is only the fight to recover what has been lost
And found and lost again and again: and now, under conditions
That seem unpropitious. But perhaps neither gain nor loss.
For us, there is only the trying. The rest is not our business.

East Coker, T.S. Eliot

The main conclusions of this dissertation point to (1) the potential of deriving environmental information from ice cores from sites subject to superficial summer melting (but where the original snow/firn stratigraphy has not been altered beyond recognition); (2) the factors that control the stable-isotope composition of precipitation over Svalbard and the record of climatic change in the long-term stable-isotope profiles during the Little Ice Age (LIA) in the Archipelago; (3) the impact of anthropogenic pollution on the chemistry of snow and ice in the region.

6.1- The environmental record in the glaciers and ice caps of Svalbard

The Skobreen site is strongly affected by summer melting, which has altered the original snow/firn stratigraphy. Nevertheless it has still proved possible to derive some environmental information from the Skobreen core (particularly the impact of anthropogenic pollution on the core's chemical composition). The stable-isotope ratios are one of the first variables to be altered by the melting process; however, the examination of the excess deuterium - d has proved to be a useful method for determining annual layers and for helping to date the core. The excess deuterium decreases during the melting process, so the summer layers tend to have lower d values. In the case of Svalbard this seasonality is enhanced by the strong seasonality of d in the precipitation. A full understanding of the seasonality in d in Svalbard precipitation will require modelling of the fractionation process over the Arctic North Atlantic, which may provide insight into the changes in the source area of moisture in the course of the year. Other characteristics of Svalbard precipitation may also help the

identification of annual layers in ice cores. Atmospheric and glaciological studies have shown that the content of anthropogenic impurities is strongly seasonally dependent, with maximum concentrations in winter. Frequently winter concentrations are greater by one order of magnitude than summer concentrations and this seasonality in the concentration of impurities appears to be reflected in the electrolytic conductivity and acidity record. Therefore a multiparameter approach, where acidity, EC, and *d* are measured in detail, may help to define the annual layers. Other studies may also provide an indication of the degree of alteration of layers by melting (e.g. the ratio alkaline metals/earth metals).

The stable-isotope composition of the precipitation reaching Svalbard appears to be mainly a function of the distance from the source area (represented by the distance from open water), but the fractionation process over the Archipelago is most probably due to adiabatic cooling of the air masses moving towards the northeast. Understanding of the fractionation process over the Archipelago would benefit from an examination of the spatial variations in δD and $\delta^{18}O$, and from the comparison on an inter-annual scale of the stable-isotope composition and sea-ice extent (obtained from satellite imagery) in the Greenland Sea/NE Atlantic. The LIA in Svalbard is well marked in the stable-isotope record from about A.D. 1300 to the end of the 19th century. The climax of the LIA was reached in the 19th century and was soon followed by its relatively abrupt termination. Abrupt changes in the stable-isotope record of Svalbard are common and reflect the rapid changes in the elements of the atmosphere–cryosphere–oceanosphere system of the Greenland Sea/NE Atlantic area. The mean stable-isotope ratio for the 20th century indicates that this century has been at least 1.5 to 2.2°C warmer than the average for the three previous centuries. For the early part of the record (i.e. pre-1700) doubts still remain about the development of environmental events, as the stable-isotope record from the Svalbard cores diverges greatly. It is necessary, therefore, to obtain a core from a site where there is thicker ice than at Lomonosovfonna and Vestfonna and which may provide a profile not affected by the complex flow conditions near bedrock. The stable-isotope profile of the new Austfonna core (recovered by Soviet scientists in 1987), coupled with the temperature profile of the borehole, will provide the best record to date for this early period. Nevertheless, difficulties in dating are still expected because of high summer melting and percolation at the summit of this ice cap.

Air, snow, and ice samples from Svalbard indicate that the region is already strongly affected by anthropogenic pollution, and the winter snowfall is frequently acid. The record of acidity in the two ice cores examined (Austfonna and Skobreen) points to a significant increase in the acid content since the industrial revolution. The Austfonna core records an increase of about 95% in the acidity since about 1800. The high concentrations of impurities are thought to result from the episodic transport of anthropogenetic pollutants from Europe by tropospheric circulation (mainly during the winter). The record of pollution in Svalbard, therefore, reflects regional (continental) concentration, contrasting with the record of the

Antarctic and Greenland ice sheets, which are representative primarily of the polar background aerosol on a hemispheric scale (Wagenbach, 1989). Although further studies are necessary to elucidate the source–receptor relationship (e.g. the trajectories of the pollutants, and the chemical behaviour of the pollutants during transport through the atmosphere), a better-preserved core from Svalbard (because both the Austfonna and the Skobreen cores undergo partial elution of the ionic content to some degree) may provide a record which includes inter-annual detail of the history of European pollutant emissions. Complementary studies in Svalbard may include the sampling of snow for analysis of the spatial distribution of other artificial impurities (e.g. heavy metals, pesticides), which are expected to show a trend to high values towards the east, as has been observed in respect of the H^+ concentration. Finally, a programme for monitoring the impact on the Svalbard environment of the increase in impurities appears to be desirable.

In summary, the Svalbard environment has been shown to be highly sensitive to changes over the last 600 years, and some of the greatest variations in the mean annual atmospheric temperature in the world have occurred in this region; the Archipelago is also exposed to anthropogenic pollutants produced in Europe, which are affecting in no small measure the chemistry of the snow and ice. Further studies may include the drilling of a new core and the analysis of the parameters that show strong seasonal variations (e.g. acidity, electrolytic conductivity, and the concentration of pollutants), and may help to date the cores. Comparison with ice-core records from sites situated beneath the mean position of the Arctic front, as happens to be the case for Svalbard, will be interesting because they will establish whether the observed changes were only local or whether they represent a hemispheric phenomenon, associated perhaps with variations in the position of the mean atmospheric front. This analysis could also be extended to the Southern Hemisphere. In this context, it would be interesting to investigate the development of environmental changes in the Archipelago of the South Shetlands (Antarctica). This Archipelago is subject to glacio-meteorological conditions similar to those encountered in Svalbard (i.e. it is situated beneath the mean position of the Antarctic atmospheric front, and its ice masses have a thermal regime which ranges from sub-polar to temperate), and the snow surface is similarly subject to intense summer melting. Thus it may provide a good Southern Hemisphere analogue for Svalbard.

6.2- New Svalbard sites for ice-core studies

The discussions in the previous chapters have shown that the ice cores recovered in Svalbard hitherto are far from ideal for environmental analysis. The main problem is the high superficial summer melting, but other factors (such as contamination by dust from nearby rock outcrops, and incomplete knowledge of the glaciology of the site) make interpretation even more complex. It is no surprise, therefore, that the interpretation of the cores has had to

be based on data averaged over 10 years or more, and there is still great uncertainty in dating. The first way of obtaining a better time series of environmental changes would be, naturally, to drill at a better site. The second option is the development of a methodology which allows the identification of the annual layers even though melting might have altered the original stratigraphy.

For the first option, the following sites are suggested, depending on the main aim of the studies to be carried out: one of the small ice caps in the mountainous Ny-Friesland region may provide a better-preserved core. An examination of the RES profiles for the region indicates that Balderfonna (# 1 in Fig. 1.2), where there is an ice divide at about 1000 m a.s.l. and relatively flat bedrock, could be one of the sites most likely to provide a complete record of the LIA. This ice cap has a maximum measured ice thickness of 256 m, which may represent about 1600 years of deposition (estimate based on an a_n of 500 kg m^{-2} a^{-1}). Nevertheless, melting can be expected even at that altitude (as shown by the Lomonosovfonna core). A shallow ice core from one of the small glaciers in the Chydeniusfjella mountain range (where part of the accumulation area of some of the glaciers is over 1300 m a.s.l.) may provide a better record for the last century or so, and act as a control for the observations at the nearby Balderfonna.

A Balderfonna core would also provide a record of man-made impurities and would be particularly useful for checking the trends observed at both Austfonna and Skobreen, where there is still uncertainty because of the flush-out of some of the impurities. On the other hand, a stronger signal of pollutants might be found in a core from Kvitøya, to the east of Nordaustlandet. High concentrations of artificial impurities there would confirm that the main pathway of the pollutants is via the northwestern USSR and then the Kara–Barents seas. H^+ concentrations in the snow and ice of Kvitøya may well exceed 32 μEq l^{-1} (i.e. pHs <4.5).

The oldest ice may be found in Veteranen (the thickest glacier measured in Svalbard, h = 656 m), which could provide a record for the last 9000 years, and ice from the latter part of the Last Glacial might be compressed in its lower layers. The interpretation of the record in an ice core to bedrock, however, will be complex because the maximum thickness is encountered near the equilibrium line (about 600–700 m a.s.l.). A borehole in this glacier would also allow the investigation of the causes of two kinds of internal reflectors detected by RES, one at about 150 m from the surface, and the other near bedrock.

REFERENCES

Aagaard, K. and Greisman, P. 1975. Toward new mass and heat budgets for the Arctic Ocean. Journal of Geophysical Research, v 80, No. 27, p 3821-3827.

Ahlmann, H.W:son. 1933a. Scientific results of the Swedish-Norwegian Arctic expedition in the summer of 1931. Part III. The inland cartography of North-East Land. Geografiska Annaler, v 15, p 47-68.

Ahlmann, H.W:son. 1933b. Scientific results of the Swedish-Norwegian Arctic expedition in the summer of 1931. Part VIII. Glaciology. Geografiska Annaler, v 15, p 161-216 and p 261-295.

Ahlmann, H.W:son. 1953. Glacier variations and climatic fluctuations. American Geographical Society, New York, USA. Bowman memorial lectures. 51 pp.

Aldaz, L. and Deutsch, S. 1967. On a relationship between air temperature and oxygen isotope ratio of snow and firn in the South Pole region. Earth and Planetary Science Letters, v 3, p 267-274.

Alderton, D.H.M. and Coleman, D.O. 1985. Ice cores and snow. In: Monitoring and Assessment Research Centre (MARC). Historical monitoring. MARC report No. 31, p 97-153.

Ambach, W. et al. 1972. Isotopic oxygen composition of firn, old snow and precipitation in alpine regions. Zeitschrift für Gletscherkunde und Glazialgeologie, v 8, No. 1-2, p 125-135.

Ambach, W. et al. 1987. Radioactive fall-out on alpine glacier from the Chernobyl nuclear accident. Zeitschrift für Gletscherkunde und Glazialgeologie, v 23, No. 2, p 123-129.

André, M.F. 1986. Dating slope deposits and estimating rates of rock wall retreat in northwest Spitsbergen by lichenometry. Geografiska Annaler, v 68A, No. 1-2, p 65-75.

Aristarain, A.J. 1980. Etude glaciologique de la calotte polaire de l'Ile James Ross (Péninsule Antarctique). Université Scientifique et Médicale de Grenoble, Thèse de troisième cycle. 130 pp.

Aristarain, A.J., Jouzel, J. and Pourchet, M. 1986. Past Antarctic Peninsula climate (1850-1980) deduced from an ice core isotope record. Climatic Change, v 8, No. 1, p 69-89.

Aristarain, A.J., Legrand, M.R. and Delmas, R.J. 1982. Acid tritation of polar snow. Analytical Chemistry, v 54, No. 8, p 1336-1339.

Arkhipov, S.M. et al. 1987. Soviet glaciological investigations on Austfonna, Nordaustlandet, Svalbard in 1984-1985. Polar Geography and Geology, v 11, No. 1, p 25-49.

Arnason, B. 1969. Exchange of hydrogen isotopes between ice and water in temperate glaciers. Earth and Planetary Science Letters, v 6, No. 6, p 423-430.

Baker, D. et al. 1985. Comparison of the ^{2}H and ^{18}O content of ice cores from a temperate Alpine glacier (Vernagtferner, Austria) with climatic data. Zeitschrift für Gletscherkunde und Glazialgeologie, v 21, p 389-395.

Bamber, J.L. 1987a. Radio echo sounding studies of Svalbard Glaciers. University of Cambridge, Unpublished Ph.D. thesis. 207 pp.

Bamber, J.L. 1987b. Internal reflecting horizons in Spitsbergen glaciers. Annals of Glaciology, v 9, p 5-10.

Bamber, J.L. 1988. Svalbard radio echo sounding data base. (Unpublished report in the Scott Polar Research Institute).

Bamber, J.L. and Dowdeswell, J.A. In press. Remote sensing of Kvitøyjøkulen: an ice cap on Kvitøya, north east Svalbard. Journal of Glaciology.

Baranowski, S. 1975. Glaciological investigations and glaciomorphological observations made in 1970 on Werenskioldbreen and its forefield. Acta Universitatis Wratislaviensis, No. 251, p 69-94.

Baranowski, S. 1977a. Changes of Spitsbergen glaciation at the end of the Pleistocene and in the Holocene. Questiones Geographicae, No. 4, p 5-27.

Baranowski, S. 1977b. The subpolar glaciers of Spitsbergen seen against the climate of this region. Acta Universitatis Wratislaviensis, No. 410. 111 pp.

Baranowski, S. 1977c. Results of dating of the fossil tundra in the forefield of Werenskioldbreen. Acta Universitatis Wratislaviensis, No. 387, p 31-36.

Baranowski, S. and Glowicki, B. 1975. Meteorological and hydrological investigations in the Hornsund region made in 1970. Acta Universitatis Wratislaviensis, No. 251, p 35-59.

Baranowski, S. and Karlén, W. 1976. Remnants of Viking age tundra in Spitsbergen and Northern Scandinavia. Geografiska Annaler, v 58A, No. 1-2, p 35-40.

Barrie, L.A. 1986. Arctic air pollution: an overview of current knowledge. Atmospheric Environment, v 20, No. 4, p 643-663.

Barrie, L.A., Fisher, D. and Koerner, R.M. 1985. Twentieth century trends in Arctic air pollution revealed by conductivity and acidity in snow and ice in the Canadian high Arctic. Atmospheric Environment, v 19, No. 12, p 2055-2063.

Barry, R.G. 1985. The cryosphere and climate change. In: MacCraken, M.C. and Luther, F.M. (eds.). Detecting the climatic effects of increasing carbon dioxide. Washington, D.C., United States Department of Energy, Office of Basic Energy Sciences, Carbon Dioxide Research Division (DOE/ER - 0235), p 109-148.

Barry, R.G. and Chorley, R.J. 1982. Atmosphere, weather and climate. 4th ed. London, Methuen. 432 pp.

Battarbee, R.W. 1984. Diatomacea analysis and the acidification of lakes. Philosophical Transactions of the Royal Society of London, Series B, v 305, p 451-477.

Belikova, T.V. et al. 1984. Kharakteristiki fonogovo zagryazneniya sul'fatami snezhnogo pokrova na territorii SSSR. [Characteristics of background sulphate pollution of the snow cover in the territory of the USSR]. Meteorologiya i Gidrologiya, No. 9, p 47-56.

Benson, C.S. 1962. Stratigraphic studies in the snow and firn of the Greenland ice sheet. U.S. Snow, Ice, and Permafrost Research Establishment Research Report, No. 70. 93 pp.

Berger, W.H. and Labeyrie, L.D. (eds.). 1987. Abrupt Climatic Change; evidence and implications. Dordrecht, Reidel. 425 pp.

Bergthórsson, P. 1969. An estimate of drift ice and temperature in 1000 years. Jökull, No. 19, p 94-101.

Blindheim, J. and Ljøen, R. 1972. On the hydrographic conditions in the West Spitsbergen Current in relation to ice distribution during the years 1956-1963. In: Karlsson, T. (ed.). Sea ice. Reykjavik, National Research Council of Iceland. p 33-41.

Bradley, R.S. and Eischeid, J. 1985. Aspects of the precipitation climatology of the Canadian high Arctic. In: Bradley, R.S. (ed.). Glacial geologic and glacio-climatic studies in the Canadian high Arctic. Amherst, Massachusetts. (University of Massachusetts, Department of Geology and Geography, Contribution No. 49), p 250-271.

Bradley, R.S. and England, J. 1978. Recent climatic fluctuations of the Canadian high Arctic and their significance for glaciology. Arctic and Alpine Research, v 10, No. 4, p 715-731.

Brázdil, R. and Purkyne, J.E. 1988. Variation of air temperature and atmospheric precipitation in the region of Svalbard and of Jan Mayen. In: Gregory, S. (ed.). Recent climatic change: a regional approach. London, Belhaven. p 53-68.

Brimblecombe, P. 1986. Air composition and chemistry. Cambridge, Cambridge University Press. 224 pp.

Brimblecombe, P. et al. 1985. Relocation and preferential elution of acidic solute through the snowpack of a small, remote, high-altitude Scottish catchment. Annals of Glaciology, v 7, p 141-147.

Bromwich, D.H. and Weaver, C.J. 1983. Latitudinal displacement from main moisture source controls $\delta^{18}O$ of snow in coastal Antarctica. Nature, v 301, No. 5896, p 145-147.

Budd, W.F. and Radok, U. 1971. Glaciers and other large ice masses. Reports on Progress in Physics, v 34, No. 1, p 1-70.

Busenberg, E. and Langway, C.C., Jr. 1979. Levels of ammonium, sulfate, chloride, calcium, and sodium in snow and ice from southern Greenland. Journal of Geophysical Research, v 84, No. C4, p 1705-1709.

Chorley, R.J. and Kennedy, B.A. 1971. Physical geography. London, Prentice Hall. 370 pp.

Clarke, G.K.C. 1976. Thermal regulation of glacier surging. Journal of Glaciology, v 16, No. 74, p 231-250.

Clarke, G.K.C., Collins, S.G. and Thompson, D.E. 1984. Flow, thermal structure, and subglacial conditions of a surge-type glacier. Canadian Journal of Earth Sciences, v 21, No. 2, p 232-240.

Clausen, H.B. and Hammer, C.U. 1988. The Laki and Tambora eruptions as revealed in Greenland ice cores from 11 locations. Annals of Glaciology, v 10, p 16-22.

Clausen, H.B. and Langway, C.C., Jr. 1989. The ionic deposits in polar ice cores. In: Oeschger, H. and Langway, C.C., Jr. (eds.). The environmental record in glaciers and ice sheets. p 225-248.

Craig, H. 1961a. Isotopic variations in meteoric waters. Science, v 133, No. 3465, p 1702-1703.

Craig, H. 1961b. Standard for reporting concentrations of deuterium and oxygen-18 in natural waters. Science, v 133, No. 3467, p 1833-1834.

Cresser, M. and Edwards, A. 1987. Acidification of freshwaters. Cambridge, Cambridge University Press. 136 pp.

Crozaz, G., Langway, C.C., Jr. and Picciotto, E. 1966. Artificial radioactivity reference horizons in Greenland firn. Earth and Planetary Science Letters, v 1, p 42-48.

Dansgaard, W. 1954. The ^{18}O abundance in fresh water. Geochimica et Cosmochimica Acta, v 6, p 241-260.

Dansgaard, W. 1964. Stable isotopes in precipitation. Tellus, v 16, p 436-468.

Dansgaard, W., White, J.W.C. and Johnsen, S.J. 1989. The abrupt termination of Younger Dryas climate event. Nature, v 339, No. , p 532-535.

Dansgaard, W. et al. 1973. Stable isotope glaciology. Meddelelser om Grønland, v 197, No. 2. 53 pp.

Dansgaard, W. et al. 1975. Climatic changes, Norsemen and modern men. Nature, v 255, No. 5503, p 24-28.

Davidson, C.I. 1989. Mechanisms of wet and dry deposition of atmospheric contaminants to snow surface. In: Oeschger, H. and Langway, C.C., Jr. (eds.). The environmental record in glaciers and ice sheets, p 29-51.

Davies, T.D., Vincent, C.E. and Brimblecombe, P. 1982. Preferential elution of strong acids from a Norwegian ice cap. Nature, v 300, No. 5883, p 161-163.

Davis, J.C. 1986. Statistics and data analysis in geology. 2nd ed. Chichester, Wiley. 646 pp.

Delmas, R. and Aristarain, A. 1978. Recent evolution of strong acidity of snow at Mt-Blanc. In: Benerie, M.M. (ed.). Atmospheric Pollution, Proceedings of the 13th International Colloquium, Paris, France, April 25-28.

Delmas, R.J., Ascencio, J. and Legrand, M. 1980. Polar ice evidence that atmospheric CO_2 20,000 BP was 50% of present. Nature, v 284, No. 5752, p 155-157.

Delmas, R.J. et al. 1985. Volcanic deposits in Antarctic snow and ice. Journal of Geophysical Research, v 90, No. D7, p 12901-12920.

Deutsch, S., Ambach, W. and Eisner, H. 1966. Oxygen isotope study of snow and firn on an alpine glacier. Earth and Planetary Science Letters, v 1, p 197-201.

Dowdeswell, J. A. 1984. Remote sensing studies of Svalbard glaciers. University of Cambridge, Unpublished Ph.D. thesis. 250 pp.

Dowdeswell, J. A. 1986. Remote sensing of ice cap outlet glaciers fluctuation on Nordaustlandet, Svalbard. Polar Research, v 4 (new series), p 25-32.

Dowdeswell, J.A. and Drewry, D.J. 1985. Place names on the Nordaustlandet ice caps, Svalbard. Polar Record, v 22 , No. 140, p 519-523.

Dowdeswell, J.A. and Drewry, D.J. 1989. The dynamics of Austfonna, Nordaustlandet, Svalbard: surface velocities, mass balance, and subglacial melt water. Annals of Glaciology, v 12, p 37-45.

Dowdeswell, J.A. et al. 1984a. Airborne radio echo sounding of sub-polar glaciers in Spitsbergen. Norsk Polarinstitutt Skrifter. No. 182. 41 pp.

Dowdeswell, J.A. et al. 1984b. Radio-echo sounding of Spitsbergen glaciers: problems in the interpretation of layers and bottom returns. Journal of Glaciology, v 30, No. 104, p 16-21.

Drewry, D.J. 1985. Ice thickness and other glacial measurements, Bakaninbreen, Paulabreen and Skobreen, Svalbard. Unpublished. BP contract report. 51 pp.

Drewry, D.J. 1986. Glacial geologic processes. London, Edward Arnold. 276 pp.

Drewry, D.J. 1987a. Radar and seismic ice-thickness measurements compared on sub-polar glaciers in Svalbard (Abstract). Annals of Glaciology, v 9, p 246.

Drewry, D.J. (ed.). 1987b. Svalbard glacier study. Unpublished. BP final contract report. v 1 (61 pp) and v 2 (180 pp).

Drewry, D.J. and Liestøl, O. 1985. Glaciological investigations of surging ice caps in Nordaustlandet, Svalbard, 1983. Polar Record, v 22, No. 139, p 359-378.

Drewry, D.J. et al. 1980. Airborne radio echo sounding of glaciers in Svalbard. Polar Record, v 20, No. 126, p 261-266.

Ekman, S.R. 1971. Seismic investigations on the Nordaustlandet ice caps. Geografiska Annaler, v 53A, p 1-13.

Elverhøi, A., Lønne, Ø. and Seland, R. 1983. Glaciomarine sedimentation in a modern fjord environment, Spitsbergen. Polar Research, v 1 (new series), p 127-149.

Epstein, S. 1956. Variations of the $^{18}O/^{16}O$ ratios of fresh water and ice. National Academy of Science, Nuclear Science Series, Report No. 19, p 20-25.

Epstein, S. and Benson, C. 1959. Oxygen isotope studies. Transactions, American Geophysical Union, v 40, No. 1, p 81-84.

Evans, S. and Smith, B.M.E. 1969. A radio echo equipment for depth sounding in polar ice sheets. Journal of Scientific Instruments (Journal of Physics E), ser 2, v 2, p 131-136.

Eyles, N. et al. 1982. Geochemical denudation rates and solute transport mechanisms in a maritime temperate glacier basin. Canadian Journal of Earth Sciences, v 19, No. 8, p 1570-1581.

Fenn, C.R. 1987. Electrical conductivity. In: Gurnell, A.M. and Clark, M.J. (eds.). Glacio-fluvial sediment transfer: an alpine perspective. Chichester, John Wiley, p 377-414.

Finkel, R.C., Langway, C.C., Jr. and Clausen, H.B. 1986. Changes in precipitation chemistry at Dye 3, Greenland. Journal of Geophysical Research, v 91, No. D9, p 9849-9855.

Fisher, D.A. and Alt, B.T. 1985. A global oxygen isotope model – semi-empirical, zonally averaged. Annals of Glaciology, v 7, p 117-124.

Fisher, D.A. and Koerner, R.M. 1981. Some aspects of climatic change in the High Arctic as deduced from ice cores. In: Mahaney, W.C. (ed). Quaternary paleoclimate. Proceedings of the Fourth Colloquium on Quaternary Research held at York University on May 18-20, 1979. Norwich. University of East Anglia, Geoabstracts, p 249-271.

Flood, B. 1971. Geological Map, Svalbard 1:500 000 - Sheet 1G Spitsbergen, Southern part. Norsk Polarinstitutt. Skrifter, No. 154A.

Fujii, Y. 1989. A 5000 year climate record in an ice core from the Høghetta ice cap in northern Spitsbergen. Abstract of a paper presented at the Symposium on snow and ice, Seattle, USA, 21-25 August 1989.

Gat, J.R. 1980. The isotopes of hydrogen and oxygen in precipitation. In: Fritz, P. and Fontes, J.Ch. Handbook of environmental isotope geochemistry. Amsterdam, Elsevier. p 21-48.

* **Gjessing, Y.T.** 1977. Episodic variations of snow contamination of an Arctic snowfield. Atmospheric Environment, v 11, p 643-647.

Glen, A.R. 1941. A sub-arctic glacier cap: the West Ice of North East Land. Geographical Journal, v 98, p 65-76 and p 135-146.

Gokhman, V.V., Troitsky, L.S. and Tyuflin, A.S. 1988. Balans massy lednikov Shpitsbergena v 1984/85 balansovom godu. [Mass balance of Spitsbergen glaciers in the 1984/85 balance year]. Materialy Glyatsiologicheskikh Issledovaniy, v 61, p 89-91.

Goodman, R.H. 1975. Radio echo sounding on temperate glaciers. Journal of Glaciology, v 14, No. 70, p 57-69.

Gordiyenko, F.G. et al. 1981. Study of a 200-m core from the Lomosonov ice plateau on Spitsbergen and the paleoclimatic implications. Polar Geography and Geology, v 5, No. 4, p 242-251.

Gorham, E. 1958. The salt content of some ice samples from Nordaustlandet (North East Land), Svalbard. Journal of Glaciology, v 3, No. 23, p 181-186.

Goudie, A. 1983. Environmental change. 2nd ed. Oxford, Clarendon Press. 258 pp.

Grove, J.M. 1988. The Little Ice Age. London, Methuen. 498 pp.

Guskov, A.S. and Troitsky, L.S. 1987. Vodno-ledovyy balans lednikov Shpitsbergena v 1983/84 balansovom godu [Water-ice balance of the glaciers of Spitsbergen in the 1983/84 balance year]. Materialy Glyatsiologicheskikh Issledovaniy, v 59, p 138-139.

Hacquebord, L. 1981. Smeerenburg: the rise and fall of a Dutch whaling-settlement on the west coast of Spitsbergen. In: van Holk, A.G.F., Jacob, H.K. and Temmingh, A.A.H.J. (eds.). Proceedings of the imternational sumposium Early European Exploitation of the Northern Atlantic 800-1700, February, 1981. Groningen, University of Groningen. p 79-132.

Hacquebord, L. 1984. The history of early Duch whaling. In: Van Marken, A. (ed.). Arctic whaling: a study from the ecological angle. Groningen, University of Groningen. p 135-148.

Haefeli, R. 1963. A numerical and experimental method for determining ice motion in the central parts of the ice sheets. (IAHS. Publication No. 61), p 253-260.

Hambrey, M.J. 1977. Supraglacial drainage and its relationship to structure, with particular reference to Charles Rabots Bre, Okstindan, Norway. Norsk Geografisk Tidsskrift , v 31, No. 2, p 69-77.

Hammer, C.U. 1977. Past volcanism revealed by Greenland Ice Sheet impurities. Nature, v 270, No. 5637, p 482-486.

Hammer, C.U. and Clausen, H.B. 1986. On the d.c. electrical conductivity and acidity of polar ice cores. (Unpublished paper presented at the 7th Symposium on Physics and Chemistry of Ice, Grenoble, France, 1986).

Hammer, C.U., Clausen, H.B. and Dansgaard, W. 1981a. Greenland ice sheet evidence of post-glacial volcanism and its climatic impact. Nature, v 288, No. 5788, p 230-235.

Hammer, C.U., Clausen, H.B. and Dansgaard, W. 1981b. Past volcanism revealed by Greenland ice cores. Journal of Volcanology and Geothermal Research, v 11, No. 1, p 3-10.

Hammer, C.U. et al. 1978. Dating of Greenland ice cores by flow models, isotopes, volcanic debris, and continental dust. Journal of Glaciology, v 20, No. 82, p 3-26.

* Gathaman (1986) see page 218.

Hanson, B. 1987. Reconstructing mass-balance profiles from climate for an Arctic ice cap. The Physical basis of the ice sheets, IAHS. Publication No. 170, p 181-189.

Hare, F.K. 1968. The Arctic. Quarterly Journal of the Royal Meteorological Society, v 94, No. 402, p 439-459.

Harrison, W.D. 1972. Temperature of a temperate glacier. Journal of Glaciology, v 11, No. 61, p.15-29.

Heidam, N.Z. 1984. The components of the Arctic aerosol. Atmospheric Environment, v 18, No. 2, p 329-343.

* **Heintzenberg, J. and Larssen, S.** 1983. SO_2 and $SO_4^=$ in the Arctic: interpretation of observations at three Norwegian arctic-subarctic stations. Tellus, v 35B, No. 4, p 255-265.

Heintzenberg, J., Hansson, H.C. and Lannefors, H. 1981. The chemical composition of Arctic Haze at Ny-Ålesund, Spitsbergen. Tellus, v 33, No. 2, p 162-171.

Heintzenberg, J. et al. 1988. Chemical composition of insoluble particles in an ice cap on Storøya, Svalbard. Annals of Glaciology, v 10, p 204.

Herron, M.M. 1982. Impurity sources of F^-, Cl^-, NO_3^- and SO_4^{2-} in Greenland and Antarctic precipitation. Journal of Geophysical Research, v 87, No. C4, p 3052-3060.

Herron, M.M., Herron, S.L. and Langway, C.C. Jr. 1981. Climatic signal of ice melt features in southern Greenland. Nature, v 293, No. 5831, p 389-391.

Herron, M.M. et al. 1977. Atmospheric trace metals and sulfate in the Greenland Ice Sheet. Geochemica et Cosmochimica Acta, v 41, No. 7, p 915-920.

Hibler, W.D., III and Langway, C.C., Jr. 1977. Ice core stratigraphy as a climatic indicator. In: Dunbar, M.J. (ed.). Polar Oceans. Proceedings of the Polar Oceans conference held at McGill University, Montreal, May 1974. Calgary, Arctic Institute of North America, p 589-601.

Hisdal, V. 1985. Geography of Svalbard. 2nd ed. Norsk Polarinstitutt, Polarhåndbok , No. 2. 84 pp.

Holdsworth, G. 1984. Glaciological reconnaissance of an ice core drilling site, Penny Ice Cap, Baffin Island. Journal of Glaciology, v 30, No. 104, p 3-15.

Holdsworth, G. and Peake, E. 1985. Acid content of snow from a mid-troposphere sampling site on Mt. Logan, Yukon territory. Annals of Glaciology, v 7, p 153-160.

Holdsworth, G. et al. 1984. Radioactivity levels in a firn core from the Yukon Territory, Canada. Atmospheric Environment, v 18, No. 2, p 461-466.

Hollin, J.T. 1956. Oxford University Expedition to Nordaustlandet, 1955. Polar Record, v 8, No. 52, p 26.

Horvath, A.L. 1985. Handbook of aqueous electrolyte solutions - physical properties, estimation and correlation methods. Chichester, Ellis Horwood. 631 pp.

Horvath, E. and Fahn, C. 1975. Glaciers of Svalbard. In: Field, W.O. (ed.). Mountain Glaciers of the Northern Hemisphere, v 2, p 879-932.

Hov, Ø. et al. 1984. Organic gases in the Norwegian Arctic. Geophysical Research Letters, v 11, No. 5, p 425-428.

Husebye, E.S., Sørnes, A. and Wilhelmsen, C.S. 1965. The determination of the thickness of Finsterwalderbreen, Spitsbergen, by gravity measurements. Norsk Polarinstitutt. Årbok, 1963, p 129-136.

International Atomic Energy Agency (IAEA). 1969-79. Environmental isotope data - world survey of isotope concentration in precipitation, No. 1, 1953-63; No. 2, 1964-65; No. 3, 1966-67; No. 4, 1968-69; No. 5, 1970-71; No. 6, 1972-75. Vienna, IAEA.

Izumi, K. et al. 1988. Meteorological observations at Åsgårdfonna, Spitsbergen, 1987. Bulletin of Glacier Research, No. 6, p 51-54.

* Heidam (1986) see page 218.

Jaworowski, Z. et al. 1981. Flow of metals into the global atmosphere. Geochimica et Cosmochimica Acta, v 45, p 2185-2199.

Johannessen, M. and Henriksen, A. 1978. Chemistry of snow meltwater: changes in concentration during melting. Water Resources Research, v 14, No. 4, p 615-619.

Johnsen, S.J., Dansgaard, W. and White, J.W.C. 1989. The origin of Arctic precipitation under present and glacial conditions. Tellus, v 41B, No. 4, p 452-468.

Johnsen, S.J. et al. 1970. Climatic oscillations 1200-2000 A.D. Nature, v 277, No. 5257, p 482-83.

Jones, A.S. 1979. The flow of ice over a till bed. Journal of Glaciology, v 22, No. 87, p 393-395.

Jones, P.D. et al. 1986. Northern Hemisphere surface air temperature variations: 1851-1984. Journal of Climate and Applied Meteorology, v 25, No. 2, p 161-179.

Jonsson, S. 1982. On the present glaciation of Storøya, Svalbard. Geografiska Annaler, v 64A, p 53-79.

Joranger, E. and Ottar, B. 1984. Air pollution studies in the Norwegian Arctic. Geophysical Research Letters, v 11, No. 5, p 365-368.

Jouzel, J. and Merlivat, L. 1984. Deuterium and oxygen 18 in precipitation: modeling of the isotopic effects during snow formation. Journal of Geophysical Research, v 89, No. D7, p 11749-11757.

Jouzel, J., Merlivat, L. and Lorius, C. 1982. Deuterium excess in an East Antarctic ice core suggests higher relative humidity at the oceanic surface during the last glacial maximum. Nature, v 299, No. 588, p 688-691.

Jouzel, J. et al. 1987. Vostok ice core: a continuous isotope temperature record over the last climatic cycle (160,000 years). Nature, v 329, No. 6138, p 403-408.

Kameda, T. et al. 1989. Shapes and distribution of air bubbles in an ice core from Åsgårdfonna, Spitsbergen. Bulletin of Glacier Research, No. 7, p 221-226.

Kato, K. 1978. Factors controlling oxygen isotopic composition of fallen snow in Antarctica. Nature, v 272, No. 5648, p 46-48.

Kellogg, T.B. 1976. Late Quaternary climate change: evidence from deep-sea cores of Norwegian and Greenland Seas. In: Cline, R.M and Hays, J.D. (eds.). Investigation of late Quaternary paleoceanography and paleoclimatology. (Geological Society of America Memoir, v 145), p 77-109.

Kelly, P.M., Goodess, C.M., and Cherry, B.S.G. 1987. The interpretation of the Icelandic sea ice record. Journal of Geophysical Research, v 92, No. C10, p 10835-10843.

Kelly, P.M. et al. 1982. Variations in surface air temperatures: Part 2. Arctic regions, 1881-1980. Monthly Weather Review, v 110, p 71-83.

Klein, W.H. 1957. Principal tracks and mean frequencies of cyclones and anti-cyclones in the Northern Hemisphere. Research Paper No. 40, Weather Bureau, Washington DC. 60 pp.

Koch, L. 1945. The East Greenland ice. Meddelelser om Grønland, v 130, No. 3. 373 pp.

Koci, B.R. 1985. Ice-core drilling at 5700 m powered by a solar voltaic array. Journal of Glaciology, v 31, No. 109, p 360-361.

Koerner, R.M. 1968. Fabric analysis of a core from the Meighen ice cap, Northwest Territories, Canada. Journal of Glaciology, v 7, No. 51, p 421-430.

Koerner, R.M. 1970. The mass balance of the Devon Island Ice Cap, Northwest Territories, Canada, 1961-66. Journal of Glaciology, v 9, No. 57, p 325-336.

Koerner, R.M. 1971. A stratigraphic method of determining the snow accumulation rate at Plateau station, Antarctica, and application to South Pole-Queen Maud Land traverse 2, 1965-66. In: Crary, A.P. (ed). Antarctic snow and ice studies. (American Geophysical Union, v 16), p 225-238.

Koerner, R.M. 1977. Distribution of microparticles in a 299 m core through the Devon Island ice cap, Northwest Territories, Canada. Proceedings of the International Symposium on Isotopes and Impurities in Snow and Ice, Grenoble, 1975. (IAHS. Publication No. 118), p 371-376.

Koerner, R.M. 1979. Accumulation, ablation, and oxygen isotope variations on the Queen Elizabeth Islands ice caps, Canada. Journal of Glaciology, v 22, No. 86, p 25-41.

Koerner, R.M. and Fisher, D.A. 1982. Acid snow in the Canadian high Arctic. Nature, v 295, No. 5845, p 137-140.

Koerner, R.M. and Russell, R.D. 1979. $\delta^{18}O$ variations in the snow on the Devon Island ice cap, Northwest Territories, Canada. Canadian Journal of Earth Sciences, v 16, No. 7, p 1419-1427.

Koerner, R.M., Paterson, W.S.B. and Krouse, H.R. 1973. $\delta^{18}O$ profile of ice formed between the equilibrium and firn lines, ice core, Canadian Arctic. Nature: Physical Science, v 245, No. 148, p 137-140.

Koryakin, V.S. 1974. Izmeneniye razmerov lednikov Shpitsbergena, Sval'bard [Change of dimensions of glaciers of Spitsbergen, Svalbard]. In: Kotlyakov, V.M. (ed.). Materialy issledovaniy oblasti oledeneniya Shpitsbergena, Sval'barda [Materials of investigations of the area of glaciation of Spitsbergen, Svalbard], p 29-44.

Koryakin, V.S. 1985. Kolebaniyya i rezkiye podvizhki lednikov [Fluctuations and surges of glaciers]. In: Kotlyakov, V.M. (ed.). Glyatsiologiya Shpitsbergena [Glaciology of Spitsbergen]. p 80-94.

Kotlyakov, V.M. (ed.). 1985. Glyatsiologiya Shpitsbergena [Glaciology of Spitsbergen]. Moscow, Nauka. 200 pp.

Kotlyakov, V.M., Macheret, Yu.Ya. and Gromyko, A.N. 1982. Soviet studies of mountain glaciers by airborne radio echo sounding. Glaciological Data, Report GD-13, p 49-57.

Kotlyakov, V.M. et al. 1980. Geofizicheskiye i isotopnyye issledovaniya lednikov Shpitsbergena [Geophysical and isotopic investigations of Spitsbergen glaciers]. Vestnik Akademii Nauk SSSR, No. 4, p 132-138.

Krebs, J.S. and Barry, R.G. 1970. The Arctic front and the tundra-taiga boundary in Eurasia. The Geographical Review, v 60, No. 4, p 548-554.

Lagally, M. 1932. Zur Thermodynamik der Gletscher. Zeitschrift für Gletscherkunde, v 20, p 199-214.

Lamb, H.H. 1972. Climate: present, past and future. v 1. Fundamentals and climate now. London, Methuen. 613 pp.

Lamb, H.H. 1977. Climate: present, past and future. v 2. Climatic history and the future. London, Methuen. 835 pp.

Lamb, H.H. 1979. Climatic variation and changes in the wind and ocean circulation: the Little Ice Age in the northeast Atlantic. Quaternary Research, v 11, No. 1, p 1-20.

Lamb, H.H. 1982a. Climate, history and the modern world. London and New York, Methuen. 387 pp.

Lamb, H.H. 1982b. The climatic environment of the Arctic Ocean. In: Rey, L., and Stonehouse, B. (eds.). The Arctic Ocean, The hydrographic environment and the fate of pollutants. London, Macmillan Press, p 135-161.

Lamb, H.H. and Mörth, H.T. 1978. Arctic ice, atmospheric circulation and world climate. Geographical Journal, v 144, Pt1, p 1-22.

Langway, C.C., Jr. 1958. Ice fabrics and the universal stage. U.S. Snow, Ice and Permafrost Research Establishment Technical Report, No. 62. 16 pp.

Langway, C.C., Jr. 1970. Stratigraphic analysis of a deep ice core from Greenland. The Geological Society of America. Special Paper No. 125. 186 pp.

Langway, C.C., Jr. and Goto-Azuma, K. 1988. Temporal variations in the deep ice-core chemistry record from Dye 3, Greenland. Annals of Glaciology, v 10, p 209.

Langway, C.C., Jr., Oeschger, H. and Dansgaard, W. (eds). 1985. Greenland ice core: geophysics, geochemistry, and the environment. Washington, D.C., American Geophysical Union. 118 pp.

Legrand, M. 1980. Mesure de l'acidité et de la conductivité électrique des précipitations antarctiques. Université Scientifique et Médicale de Grenoble, Thèse de troisième cycle (Publication No. 316). 109 pp.

Legrand, M. and Delmas, R.J. 1987. A 220-year continuous record of volcanic H_2SO_4 in the Antarctic ice sheet. Nature, v 327, No. 6124, p 671-676.

Legrand, M. and Saigne, C. 1988. Formate, acetate and methanesulfonate measurements in Antarctic ice: some geochemical implications. Atmospheric Environment, v 22, No. 5, p 1011-1017.

Legrand, M. et al. 1988. Vostok (Antarctica) ice core: atmospheric chemistry changes over the last climatic cycle (160,000 years). Atmospheric Environment, v 22, No. 2, p 317-331.

Leivestad, H. and Muniz, I.P. 1976. Fish kill at low pH in a Norwegian river. Nature, v 259, No. 5539, p 391-392.

Letestu, S. (ed.). 1966. International meteorological tables. Geneva, World Meteorological Organization (WMO - No. 188, TP. 94).

Liestøl, O. 1968. Glasiologiske undersøkelser i 1968 [Glaciological work in 1968]. Norsk Polarinstitutt, Årbok 1968, p 81-89.

Liestøl, O. 1969. Glacier surges in West Spitsbergen. Canadian Journal of Earth Sciences, v 6, No. 4, p 895-897.

Liestøl, O. 1974. Glaciological work in 1972. Norsk Polarinstitutt, Årbok 1972, p 125-135.

Liestøl, O. 1976. Glaciological work in 1974. Norsk Polarinstitutt, Årbok 1974, p 183-194.

Liestøl, O. 1982. Glaciological work in 1981. Norsk Polarinstitutt, Årbok 1981, p 45-52.

Liestøl, O. 1983. Glaciological work in 1982. Norsk Polarinstitutt, Årbok 1982, p 37-43.

Liestøl, O. 1984. Glaciological work in 1983. Norsk Polarinstitutt, Årbok 1983, p 35-45.

Liestøl, O. 1986. Glaciological investigations in the balance years 1983-84. Polar Research, v 4, No. 1, p 97-101.

Liestøl, O. In press (a). Glacier inventory of Svalbard.

Liestøl, O. In press (b). Glaciers of Svalbard, Norway. In: Williams, R.S., Jr. and Ferrigno, J.G. (eds.). Satellite image atlas of glaciers of the world. U.S. Geological Survey Professional Paper, No. 1389.

Lindner, L., Marks, L. and Pekala, K. 1984. Late Quaternary glacial episodes in the Hornsund region of Spitsbergen. Boreas, v 13, No. 1, p 35-47.

Lindner, L., Marks, L. and Pekala, K. 1987. Quaternary chronostratigraphy of south Spitsbergen. Polar Research, v 5, No. 3, p 273-274.

Lindner, L., Marks, L. and Ostaficzvk, S. 1982. Evolution of the marginal zone and the forefield of the Torell, Nann and Tone glaciers in Spitsbergen. Acta Geologica Polonica, v 32, No. 3-4, p 267-278.

List, R.J. 1949. Smithsonian meteorological tables. Sixth revised edition. Smithsonian Miscellaneous Collections, v 114. (Publication 4014).

Lorius, C. and Merlivat, L. 1977. Distribution of mean surface stable isotope values in East Antarctica: observed changes with depth in the coastal area. Proceedings of the International Symposium on Isotopes and Impurities in Snow and Ice, Grenoble, 1975. (IAHS. Publication No. 118), p 127-137.

Macheret, Yu.Ya. 1976. Nekotoryye rezul'taty radiolokatsionnogo zondirovaniya lednikov Zapadnogo Shpitsbergena v 1974 [Some results of radio echo-sounding of the glaciers of Spitsbergen in 1974]. Materialy Glyatsiologicheskikh Issledovaniy. Khronika. Obsuzhdeniya, v 26, p 158-164.

Macheret, Yu.Ya. 1981. Forms of glacial relief of Spitsbergen glaciers. Annals of Glaciology, v 2, p 45-51.

Macheret, Yu.Ya. and Zhuravlev, A.B. 1982. Radio echo-sounding of Svalbard glaciers. Journal of Glaciology, v 28, No. 99, p 295-314.

Macheret, Yu.Ya., Zhuravlev, A.B. and Bobrova, L.I. 1985. Thickness, subglacial relief and volume of Svalbard glaciers based on RES data. Polar Geography and Geology, v 9, No. 3, p 224-243.

Macheret, Yu.Ya. et al. 1984. Radiolokatsionnyy karotazh skvazhiny na lednike Fridt'of, Shpitsbergen [Radio echo logging of the borehole on the Fridtjov Glacier, Spitsbergen]. Materialy Glyatsiologicheskikh Issledovaniy, v 50, p 198-203.

Majoube, M. 1971. Fractionnement en oxygène 18 et en deutérium entre l'eau et sa vapeur. Journal de Chimie Physique et de Physico-Chimie Biologique, v 68, p 1423-1436.

Martinec, J. et al. 1977. Assessment of processes in the snowpack by parallel deuterium, tritium, and oxygen-18 sampling. Proceedings of the International Symposium on Isotopes and Impurities in Snow and Ice, Grenoble, 1975 (IASH. Publication No. 118), p 220-231.

Mayewski, P.A. et al. 1986. Sulfate and nitrate concentrations from a south Greenland ice core. Science, v 232, No. 4753, p 975-977.

McIntyre, A., Ruddiman, W.F. and Jantzen, R. 1972. Southward penetrations of the North Atlantic polar front: faunal and floral evidence of large-scale surface water mass movements over the last 225,000 years. Deep-Sea Research, v 19, No. 1, p 61-77.

Meier, M.F. 1965. Glaciers and climate. In: Wright, H.E. and Frey, D.G. (eds.). The Quaternary of the United States. Princeton, New Jersey, Princeton University Press, p 795-805.

Merlivat, L. and Jouzel, J. 1979. Global climatic interpretation of the deuterium-oxygen 18 relationship for precipitation. Journal of Geophysical Research, v 84, No. C8, p 5029-5033.

Merlivat, L. and Nief, G. 1967. Fractionnement isotopique lors des changements d'états solide-vapeur et liquide-vapeaur de l'eau à des temperatures inferieures à 0°C. Tellus, v 19, No. 1, p 122-127.

Möller, D. 1984. Estimation of the global man-made sulphur emission. Atmospheric Environment, v 18, No. 1, p 19-27.

Moser, H. and Stichler, W. 1980. Environmental isotopes in ice and snow. In: Fritz, P. and Fontes, J.Ch. Handbook of environmental isotope geochemistry. Amsterdam, Elsevier. p 141-176.

Mosley-Thompson, E. 1980. 911 years of microparticle deposition at the South Pole: a climatic interpretation. Institute of Polar Studies Report, No. 73.

Mosley-Thompson, E. et al. 1985. Snow stratigraphic record at South Pole: potential for paleoclimatic reconstruction. Annals of Glaciology, v 7, p 26-33.

Moss, R. 1938. The physics of an ice cap. Geographical Journal, v 93, p 211-231.

Müller, F. 1962. Zonation in the accumulation area of the glaciers of Axel Heiberg Island, N.W.T., Canada. Journal of Glaciology, v 4, No. 23, p 302-313.

Mulvaney, R. 1987. Spitsbergen 1987 Expedition Report. Chesterfield, Polar Exploration Group, p 72-80.

Mulvaney, R. and Peel, D.A. 1988. Anions and cations in ice cores from Dolleman Island and the Palmer Land Plateau, Antarctic Peninsula. Annals of Glaciology, v 10, p 121-125.

Neftel, A. et al. 1982. Ice core sample measurements give atmospheric CO_2 content during the past 40,000 years. Nature, v 295, p 220-223.

Neftel, A. et al. 1985. Sulphate and nitrate concentrations in snow from South Greenland 1895-1978. Nature, v 314, No. 6012, p 611-613.

Nye, J.F. 1961. The influence of climatic variations on glaciers. In: General assembly of Helsinki, Snow and Ice Commission. (IASH publication No. 54), p 397-404.

Nye, J.F. 1963a. Correction factor for accumulation measured by the thickness of the annual layers in an ice sheet. Journal of Glaciology, v 4, No. 36, p 785-788.

Nye, J.F. 1963b. On the theory of the advance and retreat of glaciers. Geophysical Journal of the Royal Astronomical Society, v 7, No. 4, p 431-456.

Nye, J.F. 1965. The flow of a glacier in a channel of rectangular, elliptic or parabolic cross-section. Journal of Glaciology, v 5, No. 41, p 661-690.

Norsk Meteorologisk Institutt. 1947-1979. Norsk Meteorologisk Årbook.

Oehme, M. and Ottar, B. 1984. The long-range transport of polychlorinated hydrocarbons to the Arctic. Geophysical Research Letters, v 11, No. 11, p 1134-1136.

Oerter, H. et al. 1985. Isotope studies of ice cores from a temperate Alpine glacier (Vernagtferner, Austria) with respect to the meltwater flow. Annals of Glaciology, v 7, p 90-93.

Oerter, H. and Rauert, W. 1982. Core drilling on Vernagtferner (Oetztal Alps, Austria) in 1979: tritium content. Zeitschrift für Gletscherkunde und Glazialgeologie, v 18, No. 1, p 13-22.

Oeschger, H. and Langway, C.C., Jr. (ed.). 1989. The environmental record in glaciers and ice sheets. Report of the Dahlem workshop on the environmental record in glaciers and ice sheets. Chichester, Wiley-Interscience. 401 pp.

Ogilvie, A.E.J. 1984. The past climate and sea-ice record from Iceland, part 1: Data to A.D. 1780. Climatic Change, v 6, No. 2, p 135-152.

Orheim, O. 1972. A 200-year record of glacier mass balance at Deception Island, southwest Atlantic Ocean, and its bearing on models of global climatic change. (Institute of Polar Studies Report No. 42). 118 pp.

Orvin, A.K. 1942. The place-names of Svalbard. (Skrifter om Svalbard og Ishavet, No. 80). 539 pp.

Orvin, A.K. 1958. Supplement 1 to 'The place-names of Svalbard'. (Norsk Polarinstitutt, Skrifter, No. 112). 133 pp.

Ottar, N. and Pacyna, J.M. 1986. Origin and characteristics of aerosol in the Norwegian Arctic. In: Stonehouse, B. (ed.). Arctic air pollution. Cambridge, Cambridge University Press, p 53-67.

Ottar, B., Pacyna, J.M. and Berg, T.C. 1986. Aircraft measurements of air pollution in the Norwegian Arctic. Atmospheric Environment , v 20, No. 1, p 87-100.

Pacyna, J.M. and Ottar, B. 1985. Transport and chemical composition of the summer aerosol in the Norwegian Arctic. Atmospheric Environment, v 19, No. 12, p 2109-2120.

Pacyna, J.M., Vitols, V. and Hanssen, J.E. 1984. Size-differentiated composition of the Arctic aerosol at Ny-Ålesund, Spitsbergen. Atmospheric Environment, v 18, No. 11, p 2447-2459.

Palais, J.M. et al. 1984. Liquid conductivity of a 44-meter firn ice-core, McMurdo Ice Shelf. Antarctic Journal of the United States, v 18, No. 5, p 106-107.

Palosuo, E. 1987. A study of snow and ice temperatures on Vestfonna, Svalbard, 1956, 1957, and 1958. Geografiska Annaler, v 69A, No. 3-4, p 431-437.

Paren, J.G. 1970. Dielectric properties of ice. University of Cambridge, Unpublished Ph.D. thesis. 233 pp.

Parkinson, C.L. et al. 1987. Arctic sea ice, 1973-1976: satellite passive-microwave observations. Washington, DC, National Aeronautics and Space Administration. 296 pp.

Paterson, W.S.B. 1981. The physics of glaciers. 2nd ed. Oxford, Pergamon Press. 380 pp.

Paterson, W.S.B. and Clarke, G.K.C. 1978. Comparison of theoretical and observed temperature profiles in Devon Island ice cap, Canada. Geophysical Journal of the Royal Astronomical Society, v 55, p 615-632.

Paterson, W.S.B. et al. 1977. An oxygen isotope climatic record from the Devon Island ice cap, Arctic Canada. Nature, v 266, No. 5602, p 508-511.

Peel, D.A. and Clausen, H.B. 1982. Oxygen-isotope and total beta-radioactivity measurements on a 10 m ice core from the Antarctic Peninsula. Journal of Glaciology, v 28, No. 98, p 43-55.

Peel, D.A., Mulvaney, R. and Davison, B.M. 1988. Stable-isotope/air-temperature relationships in ice cores from Dolleman Island and the Palmer Land Plateau, Antarctic Peninsula. Annals of Glaciology, v 10, p 130-136.

Picciotto, E. and Wilgain, S. 1963. Fission products in Antarctic snow, a reference level for measuring accumulation. Journal of Geophysical Research, v 68, No. 21, p 5965-5972.

Picciotto, E., DeMaire, X. and Friedman, I. 1960. Isotopic composition and temperature of formation of Antarctic snows. Nature, v 187, No. 4740, p 857-859.

Pourchet, M. et al. 1988. Identification of Chernobyl fall-out as a new reference level in Northern Hemisphere glaciers. Journal of Glaciology, v 34, No. 117, p 183-187.

Punning, Ya.-M.K. and Vaykmyae, R.A. 1985. Isotope and chemical composition of glaciers. In: Kotlyakov, V.M. (ed.). Glyatsiologiya Shpitsbergena [Glaciology of Spitsbergen], p 148-159.

Punning, Ya.-M.K., Troitsky, L. and Rajamae, R. 1976. The genesis and age of the Quaternary deposits in the eastern part of Van Mijenfjord, West Spitsbergen, Geologiska Föreningens i Stockholm Förhandlingar, v 98, p 343-347.

Punning, Ya.-M.K.,Vaykmyae, R.A. and Tóugu, K. 1987. Variations of $\delta^{18}O$ and Cl^- in the ice cores of Spitsbergen. Journal de Physique, Colloque C1, Supplément No.3, v 48, p 619-624.

Punning, Ya.-M.K. et al. 1980. Izotopno-kislorodnyye issledovaniya kerna s ledorazdela lednikov Grenf'ord i Frit'of (o. Zapadnyy Shpitsbergen) [Isotope-oxygen investigations of an ice core from the ice divide of Grønfjordbreen-Fridtjovbreen (Island of Spitsbergen)]. Materialy Glyatsiologicheskikh Issledovaniy. Khronika. Obsuzhdeniya, v 37, p 173-177.

Punning, Ya.-M.K. et al. 1986. Stratification in an ice core from Vestfonna, Nordaustlandet. Polar Geography and Geology, v 10, No. 1, p 39-43.

Rahn, K.A. (ed.). 1981. Arctic air chemistry. Atmospheric Environment, No. 15. 171 pp.

Rahn, K.A. 1982. On the causes, characteristics and potential environmental effects of aerosol in the Arctic atmosphere. In: Rey, L., and Stonehouse, B. (eds.). The Arctic Ocean: the hydrographic environment and the fate of pollutants. London, MacMillan. p 163-195.

Rahn, K.A. et al. 1980. High winter concentration of SO_2 in the Norwegian Arctic and transport from Eurasia. Nature, v 287, No. 5785, p 824-826.

Raisbeck, G.M. et al. 1982. Cosmogenic Be^{10} concentrations in Antarctic ice during the past 30,000 years. Nature, v 293, No. 5826, p 825-826.

Rand, J.H. 1976. USA CRREL shallow drill. In: Splettstoesser, J.F. (ed.). Ice core drilling. Proceedings of a symposium, University of Nebraska-Lincoln, 28-30 August 1974. Lincoln, University of Nebraska Press, p 133-138.

Raymond, C.F. 1980. Valley glaciers. In: Colbeck, S.C. (ed). Dynamics of snow and ice masses. New York, Academic Press, p 79-139.

Reeh, N. et al. 1978. Secular trends of accumulation rates at three Greenland stations. Journal of Glaciology, v 20, No. 82, p 27-30.

Rey, L., and Stonehouse, B. (eds.). 1982. The Arctic Ocean: the hydrographic environment and the fate of pollutants. London, MacMillan. 433 pp.

Robin, G. de Q. 1955. Ice movement and temperature distribution in glaciers and ice sheets. Journal of Glaciology, v 2, No. 18, p 523-532.

Robin, G. de Q. 1976. Reconciliation of temperature-depth profiles in polar ice sheets with past surface temperatures deduced from oxygen-isotope profiles. Journal of Glaciology, v 16, No. 74, p 9-22.

Robin, G. de Q. (ed.). 1983. The climatic record in polar ice sheets. Cambridge, Cambridge University Press. 212 pp.

Robin, G. de Q. and Weertman, J. 1973. Cyclic surging of glaciers. Journal of Glaciology, v 12, No. 64, p 3-18.

Robin, G. de Q., Evans, S. and Bailey, J.T. 1969. Interpretation of radio-echo sounding in polar ice sheets. Philosophical Transactions of the Royal Society of London, Series A, v 265, No. 1166, p 437-505.

Rowan, D.E. et al. 1982. Holocene glacial geology of the Svea lowland, Spitsbergen, Svalbard. Geografiska Annaler, No. 64A, p 35-51.

Rufli, H., Stauffer, B. and Oeschger, H. 1976. Lightweight 50-meter core drill for firn and ice. In: Splettstoesser, J.F. (ed.). Ice core drilling. Proceedings of a symposium, University of Nebraska-Lincoln, 28-30 August 1974. Lincoln, University of Nebraska Press, p 150-152.

Schotterer, U. et al. 1977. Isotope measurements on firn and ice cores from alpine glaciers. Proceedings of the International Symposium on Isotopes and Impurities in Snow and Ice, Grenoble, 1975. (IAHS. Publication No. 118), p 232-236.

Schytt, V. 1958. The inner structure of the ice shelf at Maudheim as shown by core drilling (Norwegian-British-Swedish Expedition, 1949-52. Scientific Results, Vol.4, Glaciology 2C), p 357-359.

Schytt, V. 1964. Scientific results of the Swedish Glaciological Expedition to Nordaustlandet, Spitsbergen, 1957 and 1958. Parts I and II. Geografiska Annaler, v 46, p 243-281.

Schytt, V. 1969. Some comments on glacier surges in eastern Svalbard. Canadian Journal of Earth Sciences, v 6, No. 4, p 867-873.

Semb, A., Brækkan, R. and Joranger, E. 1984. Major ions in Spitsbergen snow samples. Geophysical Research Letters, v 11, No. 5, p 445-448.

Siggerud, T. 1972. The volcanic eruption on Jan Mayen in 1970. Norsk Polarinstitutt, Årbok 1970, p 5-18.

Sigtryggsson, H. 1972. An outline of sea ice conditions in the vicinity of Iceland. Jökull, No. 22, p 1-11.

Simkin, T. et al. 1981. Volcanoes of the world. Stroudsburg, Hutchinson Ross. 233 pp.

Slatt, R.M. 1972. Geochemistry of meltwater streams from nine Alaskan glaciers. Geological Society of America Bulletin, v 83, No. 4, p 1125-1132.

Smith, B.M.E. and Evans, S. 1972. Radio echo sounding: absorption and scattering by water inclusion and ice lenses. Journal of Glaciology, v 11, No. 61, p 133-146.

Souchez, R.A. and Lemmens, M.M. 1987. Solutes. In: Gurnell, A.M. and Clark, M.J. (eds.). Glacio-fluvial sediment transfer: an alpine perspective. Chichester, John Wiley, p 285-303.

Splettstoesser, J.F. (ed.). 1976. Ice core drilling. Proceedings of a symposium, University of Nebraska-Lincoln, 28-30 August 1974. Lincoln, University of Nebraska Press. 189 pp.

Steffensen, E.L. 1969. The climate and its recent variations at the Norwegian Arctic stations. Meteorologiske Annaler, v 5, p 215-349.

Steffensen, E.L. 1982. The Climate at Norwegian Arctic Stations. Det Norske Meteorologiske Institutt, Klima. No. 5. 44 pp.

Stichler, W. et al. 1982. Core drilling on Vernagtferner (Oetztal Alps, Austria) in 1979: deuterium and oxygen-18 contents. Zeitschrift für Gletscherkunde und Glazialgeologie. v 18, No. 1, p 23-35.

Sverdrup, H.V. 1935. The temperature of the firn on Isachsen's Plateau and general conclusions regarding the temperatures of the glaciers on West Spitsbergen. Geografiska Annaler, v 17, p 53-58.

Theodórsson, P. 1977. 40-years tritium profiles in a polar and temperate glacier. Annals of Glaciology, v 3, p 393-398.

Thompson, L.G. 1977. Microparticles, ice sheets, and climate. (Institute of Polar Studies Report No. 64). 148 pp.

Thompson, L.G. and Mosley-Thompson, E. 1981a. Microparticle concentration variations linked with climatic change: evidence from polar ice cores. Science, v 212, No. 4496, p 812-815.

Thompson, L.G. and Mosley-Thompson, E. 1981b. Temporal variability of microparticle properties in polar ice sheets. Journal of Volcanology and Geothermal Research, v 11, p 11-27.

Thompson, L.G. and Mosley-Thompson, E. 1987. Evidence of abrupt climatic change during the last 1,500 years recorded in ice cores from the tropical Quelccaya ice cap, Peru. In: Berger, W.H. and Labeyrie, L.D. (eds.). Abrupt climatic change; evidence and implications. Dordrecht, Reidel. p 99-110.

Thompson, L.G. et al. 1986. The Little Ice Age as recorded in the stratigraphy of the tropical Quelccaya ice cap. Science, v 234, No. 4774, p 361-364.

Thórarinsson, S. 1956. The Thousand Year Struggle Against Ice and Fire. Reykjavík, Bókaútgáfa Menningsarsjóds. 52 pp.

Thoroddsen, T. 1916-1917. Arferdi á Islandi í thúsund ár. 1916: p 1-192; 1917: p 193-432. Copenhagen, Hid Islenska Frædafjelag.

Troitsky, L.S. 1988. O balanse massy lednikov raznykh tipov na Shpitsbergene [On the mass balance of different types of glaciers in Spitsbergen]. Materialy Glyatsiologicheskikh Issledovaniy, v 63, p 117-121.

Troitsky, L.S. et al. 1975. Oledeneniye Shpitsbergena (Sval'barda) [The ice cover of Svalbard]. Rezult'taty Issledovaniy po Mezhdunarodnym Geofizicheskim Proyekta. Moscow, Nauka. 276 pp.

Troitsky, L.S. et al. 1981. The history of the glaciation of Svalbard. Polar Geography and Geology, v 5, No. 2, p 57-81.

Troitsky, L.S. et al. 1985. The paleoglaciology of Svalbard during the Holocene. Polar Geography and Geology, v 9, No. 3, p 219-223.

Van der Knaap, W.O. 1985. Human influence on natural arctic vegetation in the 17th century and climatic change since A.D. 1600 in northwest Spitsbergen: a paleobotanical study. Arctic and Alpine Research, v 17, No. 4, p 371-387.

Vaykmyae, R.A. et al. 1977. Iztopnyye, geokhimicheskiye i stratigraficheskiye issledovaniya na ledorazdele lednikov Grenf'ord i Frit'of (o. Zapadnyy Shpitsbergen) [Isotopic, geochemical and stratigraphic studies on the ice divide of Grønfjordbreen and Fridtjovbreen (Spitsbergen)]. Materialy Glyatsiologicheskikh Issledovaniy. Khronika. Obsuzhdeniya, v 30, p 77-87.

Vaykmyae, R.A. et al. 1985. Variations in $\delta^{18}O$ and Cl^- in an ice core from Vestfonna Nordaustlandet. Polar Geography and Geology, v 9, No. 4, p 329-333.

Vinje, T.E. 1977. Sea ice conditions in the European sector of the marginal seas of the Arctic, 1966-1975. Norsk Polarinstitutt. Årbok, 1975, p 163-174.

Wadhams, P. 1981. The ice cover in the Greenland and Norwegian Seas. Reviews of Geophysics and Space Physics, v 19, No. 3, p 345-393.

Wagenbach, D. 1989. Environmental records in alpine glaciers. In: Oeschger, H. and Langway, C.C., Jr. (eds.). The environmental record in glaciers and ice sheets, p 69-83.

Wagenbach, D. et al. 1988. The anthropogenic impact on snow chemistry at Colle Gnifetti, Swiss Alps. Annals of Glaciology, v 10, p 183-187.

Watanabe, O. and Fujii, Y. 1988. Outlines of the Japanese Arctic Glaciological Expedition in 1987. Bulletin of Glacier Research, No. 6, p 47-50.

Welton, J.E. 1984. SEM petrology atlas. Tulsa, Chevron Oil. 237 pp.

Werner, A. 1988. Holocene glaciation and climatic change, Spitsbergen, Svalbard. University of Colorado, Unpublished Ph.D thesis. 297 pp.

Wigley, T.M.L. 1979. Climatic change since 1000 A.D. In: Evolution des atmosphères planetaires et climatologie de la terre, Nice, 16-20 octobre 1978. Toulose, Département des Affaires Universitaires, Centre National d'Etudes Spatiales, p 387-397.

Williams, L.D. and Wigley, T.M.L. 1983. A comparison of evidence for Late Holocene summer temperature variations in the Northern Hemisphere. Quaternary Research, v 20, No. 3, p 286-307.

Wolff, E.W. and Peel, D.A. 1985. The record of global pollution in polar snow and ice. Nature, v 313, No. 6003, p 535-540.

Yevseyev, A.V. and Korzun, A.V. 1985. O khimicheskom sostave lednikovogo pokrova na Severo-Vostochnoy Zemle [On the chemical composition of ice cover on Nordaustlandet]. Materialy Glyatsiologicheskikh Issledovaniy, v 52, p 205-209.

Yurtsever, Y. 1975. World wide survey of stable isotopes in precipitation. IAEA, Report of Sect. Isotope Hydrology. 40 pp.

Zagorodnov, V.Z. 1981. Issledovaniye stroyeniya i temperaturnogo rezhima shpitsbergenskikh lednikov s pomoshch'yu termobureniya. [Investigations of structures and temperature regime of Spitsbergen glaciers with the help of thermal drilling]. Materialy Glyatsiologicheskikh Issledovaniy. Khronika. Obsuzhdeniya, v 41, p 196-199.

Zagorodnov, V.Z. 1988. Recent Soviet activities on ice core drilling and core investigations in the Arctic regions. Bulletin of Glacier Research, No. 6, p 81-84.

Zagorodnov, V.Z. In preparation. Antifreeze-thermal coring of Arctic continental glaciers. Workshop on Ice Core Drilling. Grenoble, France, 10-14 October 1988.

Zagorodnov, V.Z. and Arkhipov, S.M. In preparation. Studies of the structure, composition and temperature regime of sheet glaciers of Svalbard and Severnaya Zemlya: methods and outcomes.

Zagorodnov, V.Z. and Zinger, Ye.M. 1982. Glyatsiologicheskiye raboty na Severo-Vostochnoy Zemle [Glaciological investigations of Nordaustlandet]. Materialy Glyatsiologicheskikh Issledovaniy. Khronika. Obsuzhdeniya, v 43, p 30.

Zagorodnov, V.Z. and Zotikov, I.A. 1981a. Kernovoye bureniye na Shpitsbergene [Ice core drilling on Spitsbergen]. Materialy Glyatsiologicheskikh Issledovaniy. Khronika. Obsuzhdeniya, v 40, p 157-163.

Zagorodnov, V.Z. and Zotikov, I.A. 1981b. Vnutriledikovyye kanaly [Capillary channels in glaciers]. Materialy Glyatsiologicheskikh Issledovaniy. Khronika. Obsuzhdeniya, v 41, p 200-202.

Zagorodnov, V.Z., Arkhipov, S.M. and Macheret, Yu.Ya. 1985. Rekonstruktsiya usloviy l'doobrazovaniya na subpolyarnom lednike po rezul'tatam issledovaniya kerna [Reconstruction of ice formation conditions on a subpolar glacier from the results of core studies]. Materialy Glyatsiologicheskikh Issledovaniy, v 53, p 36-44.

Zagorodnov, V.Z. et al. 1984. Glubinnoye stroyeniye lednikovogo plato Lomonosova na o. Zap. Shpitsbergen [Depth structure of the Lomonosov ice plateau, Spitsbergen]. Materialy Glyatsiologicheskikh Issledovaniy, v 50, p 119-125.

Gathman, S.G. 1986. Climatology. In: Hurdle, B.G.(ed.). The Nordic seas. New York, Springer. p 1-18.

Heidam, N.Z. 1986. The Greenland aerosol: elemental composition, seasonal variations and likely sources. In: Stonehouse, B. (ed.). Arctic air pollution. Cambridge, Cambridge University Press, p 37-52.

APPENDIX 1

CLIMATIC PARAMETERS RELEVANT FOR GLACIOLOGICAL STUDIES IN SVALBARD

A1.1- Introduction

In this appendix some climatological time series useful for glaciological studies are reconstructed. It aims to provide data that could be used for the derivation by proxy of, for example, past mass-balance trends. It also aims to provide information which may explain the environmental record in ice cores recovered from Svalbard, particularly for understanding the factors that have affected the stable-isotope composition of snow, firn and ice (i.e. the relationship between stable isotopes and temperature). It is to be hoped that it will be useful for other environmental studies in the region.

The resulting data set is an estimate for the Sveagruva meteorological station. Therefore it is thought to be representative only for the study area of this dissertation (i.e. central Spitsbergen) and at sea-level. Similar time series for other areas may be obtained from a series of linear correlations (cf. Section A1.3).

There was no continuous record of meteorological observations during the Second World War, so it was decided to calculate all the parameters, except the mean annual temperature (MAAT), only for the post-war period. The calculation of the mean annual temperature uses the data summarized by Steffensen (1982), who estimated the MAAT for the war years (Steffensen, 1969). For other parameters the daily observations were used. The computed parameters include: precipitation-weighted mean annual temperature, mean summer temperature, total number of melting degree days (i.e. the sum of the mean daily temperatures above 0°C), mean maximum temperature in July, length of the summer season, and total precipitation.

A1.2- Sources and input of data

The daily meteorological data are derived from observations at the Svalbard meteorological stations (i.e Isfjord, Longyearbyen, Lufthavn, and Sveagruva). For the period 1946–78 the data have been published in form of tables in the Norsk Meteorologisk Årbok

(Norsk Meteorologisk Institutt, 1947–79). The unpublished data for the period 1979–86 were provided for the author by meteorologist Stein Kristiansen of NMI.

The daily data, including mean temperature, and the quantity and type of precipitation (i.e. whether liquid or solid) were input by the author. The mean daily temperature is calculated from observations at 7, 13, and 19 hours. The resulting data set, about 44.000 entries, may be accessed through the University of Cambridge Phoenix System. The data file and a Fortran program for computing the various parameters are to be found in the Svalbard RES database (Bamber, 1988). The data have also been converted to microcomputer disk format (Apple Macintosh).

A1.3- Methodology

There is no continuous series of daily observations at any one station for the whole period under reconstruction. Furthermore, the nearest meteorological station to the Skobreen ice-core site, Sveagruva, was opened only in 1978. The nearest station with a longer record, Longyearbyen (1957-77), is 65 km distant. Mean daily temperatures at any station in Svalbard are only locally representative (cf. Section 1.3.4). Therefore it was necessary to transfer the climatological observations of Longyearbyen and other meteorological stations to Sveagruva (situated 26 km from Skobreen). The conversion of the temperatures was carried out by a series of linear regressions. The precipitation varies greatly from region to region (cf. Sections 1.3 and 1.4) and so it is impossible to establish any significant relationship between the stations. The total accumulation data are plotted (Fig. A1.8) only for use as a general index for dry and wet periods.

A1.3.1- Mean annual air temperature

The MAAT in central Spitsbergen was estimated by linear regressions from the mean annual temperature at the meteorological stations in the Archipelago for the period 1912–78. For the years 1979–86 the data are the actual observations at the Sveagruva station.

There are five meteorological stations in Svalbard that cover part of the period 1946–86: Isfjord (1912–76), Longyearbyen (1957–77), Lufthavn (1976–), Ny-Ålesund (1969–), and Sveagruva (1978–). A summary of the meteorological conditions at these stations is given by Steffensen (1982). The most appropriate methodology would be the calculation of a transfer function between Sveagruva and another station in the same geographical situation (i.e. situated on the shore and in the inner part of one of the Spitsbergen fjords). The MAATs from the different stations were converted to Sveagruva values in three steps: 1) a linear regression was calculated for the years 1957–75 between Isfjord and Longyearbyen. The MAATs at Isfjord from 1912 to 1957 were converted to Longyearbyen values; 2) there is

only one complete year (1976) of meteorological observations for both Longyearbyen and Lufthavn. It was necessary to use the means of 24 months (August 1975–July 1977) to calculate a linear regression between the two stations. The data for the period 1912–75 were then converted to Lufthavn values; 3) finally, a similar regression from the mean annual temperatures for Lufthavn and Sveagruva was calculated for the period 1978–86 and the mean annual temperature from 1912 to 1978 was estimated for Sveagruva. Fig. A1.1 summarizes the procedure and gives the calculated linear regressions (Equations 1, 2, and 3). Fig. A1.2 shows the resulting mean annual temperature time series for central-eastern Spitsbergen. The same time series is used in Chapter 4 to examine the $\delta^{18}O$ x δT relationship, only the temperature is reduced by 5.4°C to allow for the different altitude (600 m a.s.l.).

The other parameters have been computed from the mean daily observations and were limited to the post-war period. The same procedure described in the last paragraph was adopted in order to transfer the daily temperature observations to Sveagruva values. New linear regressions from the monthly observations were calculated for Isfjord and Longyearbyen (4), and for Lufthavn and Sveagruva (5), and are more significant. Regressions should have been computed from the daily observations. Unfortunately, it was possible to obtain only the 1978 daily observations for Lufthavn. It was therefore decided to use the mean monthly temperatures for the correlations. This process at least allows for the difference in continentality of the stations.

(4) Longyearbyen T(°C) = (1.1.221 ± 0.005) Isfjord T(°C) + (0.142 ± 0.042); r = 0.988 at α <0.0001.
(5) Sveagruva T(°C) = (1.042 ± 0.013) Lufthavn T(°C) - (0.224 ± 0.114); r = 0.979 at α <0.0001.

A1.3.2- Other parameters

After the mean daily temperature had been estimated for Sveagruva a series of climatological parameters relevant to glaciological studies was computed. Table A1.1 describes how the parameters are calculated for each calendar year, and their possible application in glaciology, and some references which give examples of their application are cited. A more detailed discussion of each of these parameters is to be found in the appropriate sections of this dissertation.

It was not possible to obtain a relationship for converting the mean maximum July temperature to Sveagruva, so the series is discontinuous. Further, monthly maximum temperatures only began to be recorded in Longyearbyen in 1957. The plotted data (Fig. A1.7) have therefore been taken from Longyearbyen (1957–76), Lufthavn (1977–78), and Sveagruva (1979–86).

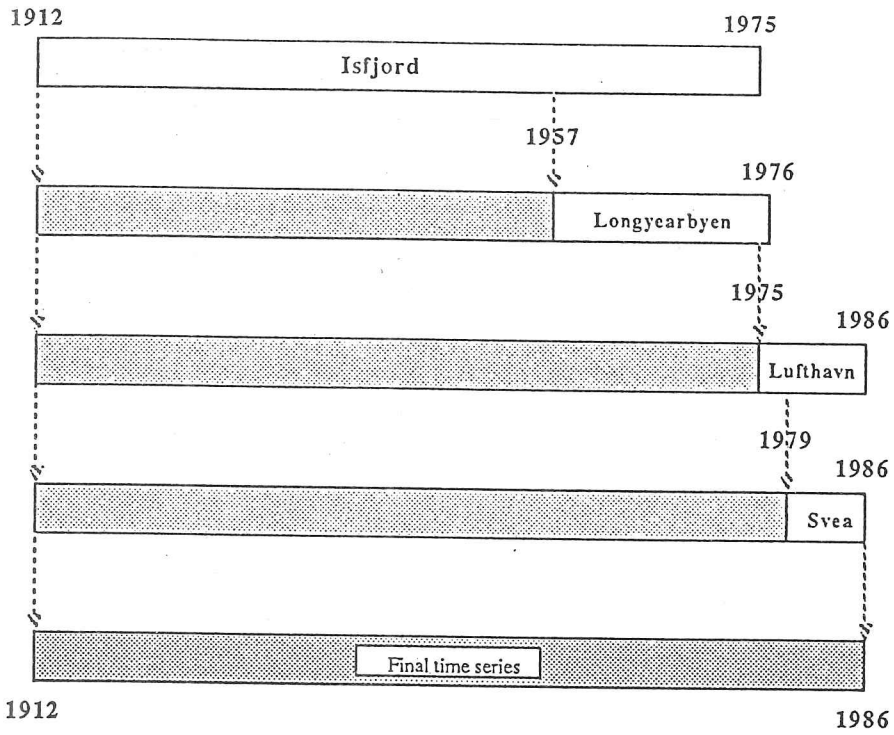

Longyearbyen T(°C) = (1.073±0.040) Isfjord T(°C) - (0.612±0.206)
r = 0.988, α<0.0001, obtained from mean annual (19) data

Lufthavn T(°C) = (1.021±0.011) Longyearbyen T(°C) - (0.589±0.111)
r = 0.999, α <0.0001, obtained from mean monthly (24) data

Sveagruva T(°C) = (0.992±0.108) Lufthavn T(°C) - (0.564±0.682)
r = 0.966, α <0.0001, obtained from mean annual (8) data

Figure A1.1- Summary of the procedure used to estimate the mean annual atmospheric temperature (MAAT) for central-eastern Spitsbergen.

Table A1.1- Climatic parameters calculated for central Spitsbergen

Parameter	How computed	Examples of use in glaciology	References
Mean annual temperature	$\frac{\sum \text{Daily mean T}}{\text{Total no. of days}}$	Examination of the $\delta^{18}O$ and T relationship	
Precipitation-weighted mean annual temperature	$\frac{\sum (\text{Daily mean T} \times \text{Daily precipitation})}{\sum \text{Daily precipitation}}$	Physically more meaningful parameter for the examination of stable isotopes and T relationship	Chapter 4 of this dissertation
Mean summer temperature	$\frac{\sum \text{Daily temperature}}{\text{No. of days}}$, from 1st June to 31st August	Index of summer 'warmth' used to reconstruct ablation-season conditions	Hanson, 1987
Number of melting degree days	$\sum$ Mean daily T when these are > 0 °C	Index of summer melting	Orheim, 1972 Bradley and England, 1978 *
Length of the melt season	No. of days between the first three consecutive days with mean daily T > 0°C in spring and the last three consecutive days with mean daily T > 0 °C in autumn.	Index of summer 'warmth', used to reconstruct past ablation conditions	Bradley and England, 1978

Parameter	How computed	Examples of use in glaciology	References
Mean of the daily maximum temperature in July	Σ Daily maximum T in July	Index of ablation-season conditions	Bradley and England, 1978
Total accumulation	Σ Daily precipitation	Used to differentiate dry from wet periods **	

Observations: * Bradley and England (1978) have reservations about this manner of computing the number of melting degree days. They reason that a day with a mean T < 0 °C may have long periods of T > 0 °C, enough to cause substantial melting. It would be more meaningful to compute the number of melting degree days from the daily minimum and maximum temperatures. This would require the input of more 29.000 figures in the climatic data set.

** Total precipitation is calculated only to determine dry and wet periods. It cannot be used as an index for regional mean accumulation on the Svalbard ice and snow masses: first, because of the great differences in the mean annual accumulation rate from area to area in Svalbard; second, because of the well-known difficulties of measuring accumulation accurately on gauges. The results can differ greatly from actual precipitation.

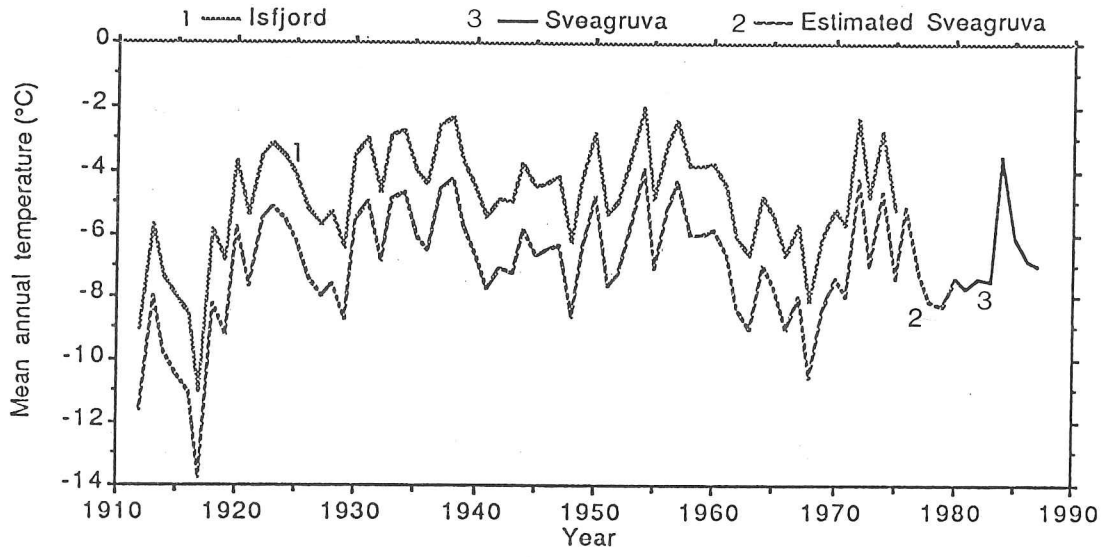

Figure A1.2- Mean annual atmospheric temperature (MAAT) at Isfjord and Sveagruva.

(1) Air temperature at Isfjord from 1912 to 1975 (source: Steffensen, 1982).
(2) Estimated air temperature at Sveagruva from 1912 to 1978 (see text for details).
(3) Air temperature at Sveagruva from 1979 to 1987 (source: S. Kristiansen, personal communication).

A1.4- Graphs

Figures A1.3 – A1.8 show the results of the computations described in Table A1.1, for central-eastern Spitsbergen, i.e. at Sveagruva and at sea-level. The data is valid only on a small local scale. The same collection of data was used for the examination of the environmental record in the Skobreen ice core discussed in Chapters 3 and 4. The data are the same, but they have been corrected for an altitude of 600 m a.s.l. This means a reduction in mean daily temperature of 5.4 °C, if a mean environmental lapse rate of 0.9°C/ 100 m is used. Similar time series may be calculated for other meteorological stations.

As already mentioned, the total precipitation values are not correct for Sveagruva, as there is no correlation between precipitation at different stations. The values are suitable only for general conclusions about dry and wet periods. The arrows in Fig. A1.8 mark the discontinuities where there is a change of station. The values are from Isfjord (up to 1957), Longyearbyen (1958–75), Lufthavn (1976–78), and Sveagruva (1979–86).

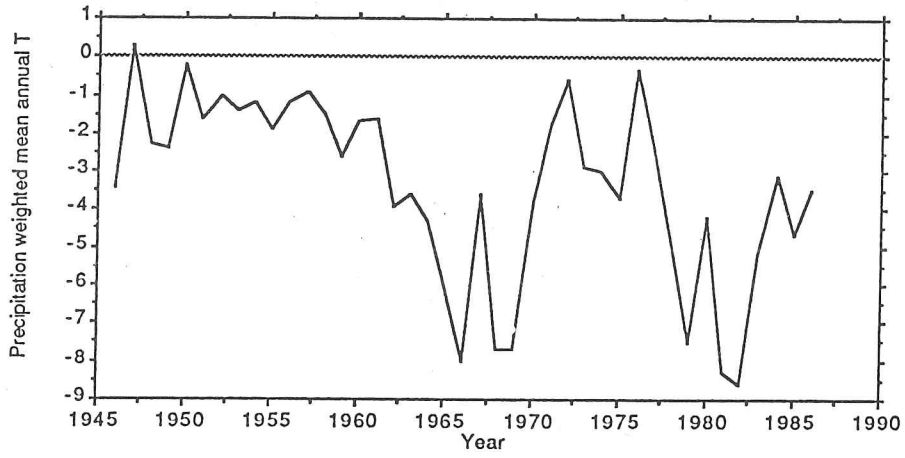

Figure A1.3- Precipitation-weighted mean annual temperature for central-eastern Spitsbergen.

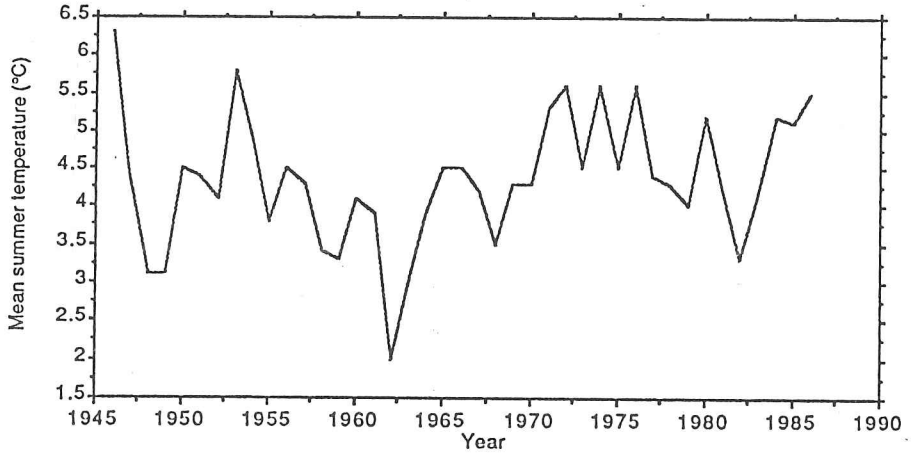

Figure A1.4- Annual mean summer temperature for central-eastern Spitsbergen.

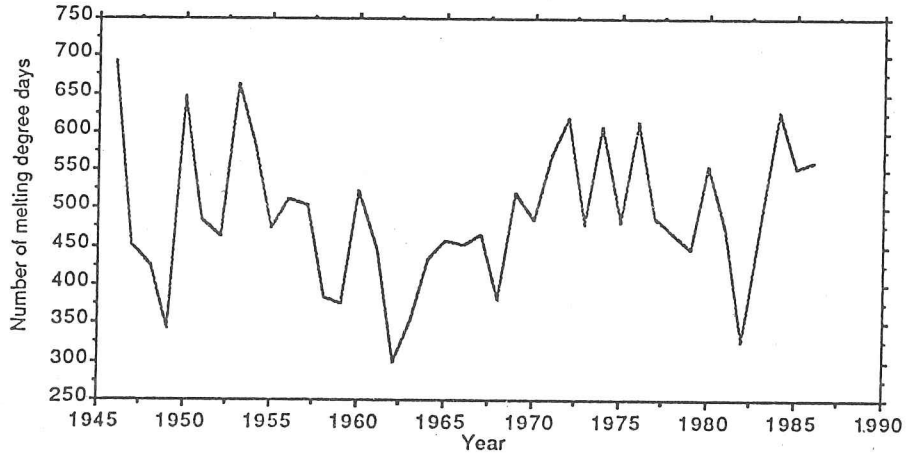

Figure A1.5- Annual number of melting degree days for central-eastern Spitsbergen.

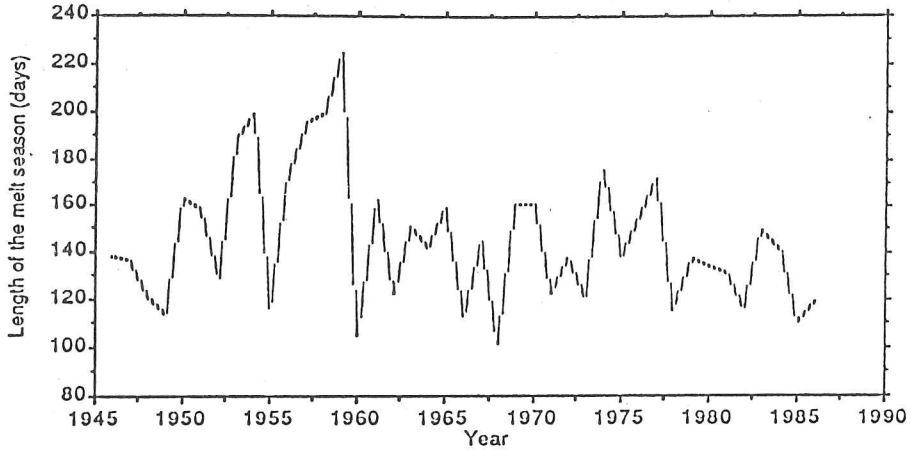

Figure A1.6- Annual length of the melt season for central-eastern Spitsbergen

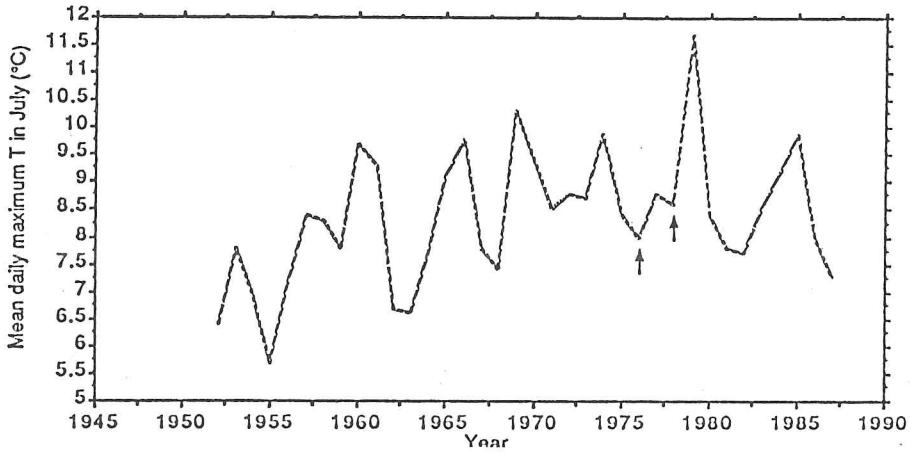

Figure A1.7- Annual mean daily maximum temperature in July for central-eastern Spitsbergen. The arrows mark the discontinuities where there is a change of station. Stations used: Longyearbyen (1957-1976), Lufthavn (1977-1978), and Sveagruva (1979-1986).

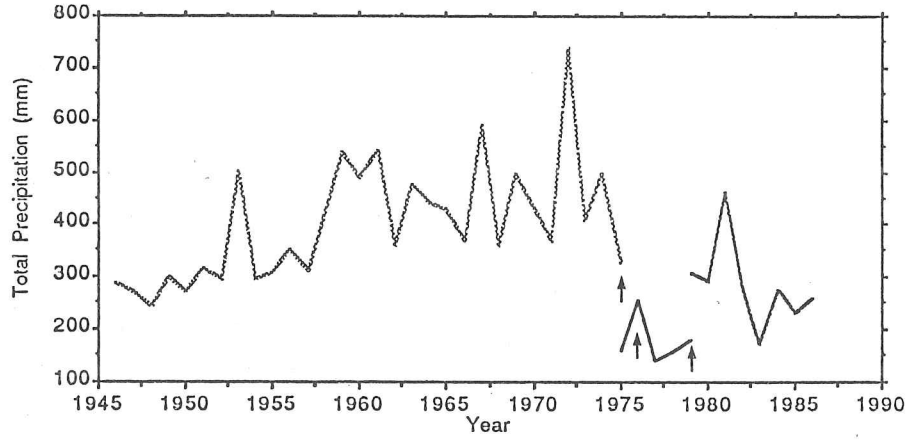

Figure A1.8- Annual amount of precipitation for Spitsbergen. The arrows mark the discontinuities where there is a change of station. Stations used: Isfjord (up to 1975), Longyearbyen (1975-1976), Lufthavn (1977-1979), and Sveagruva (1979-1986).

APPENDIX 2

THE SKOBREEN ICE-CORE DATA

	Sample	Depth (m)	Density (kg/m3)	Depth (m w.eq.)	Delta Oxygen	Delta Deuterium	Excess d	pH	Elec. Conductivity (µS cm-1)	Microparticules	Tritium (TU)	H (µEql-1)	SO (µEq l-1)	Cl (µEq l-1)	NO3 (µEq l-1)
1	1	-2.10	548.42	.85	-11.02	•	•	5.49	36.10	no	•	3.24	•	•	•
2	2	-2.20	551.67	.91	-11.78	•	•	5.68	19.40	no	•	2.09	•	•	•
3	3	-2.30	687.59	.98	-10.81	-73.50	12.98	5.68	5.10	no	•	2.09	•	•	•
4	4	-2.40	567.08	1.04	-11.10	•	•	5.81	9.50	no	•	1.55	•	•	•
5	5	-2.50	498.53	1.09	-11.35	•	•	5.62	4.50	no	•	2.40	9.88	75.12	1.39
6	6	-2.60	498.04	1.14	-11.26	•	•	5.43	7.50	no	•	3.72	•	•	•
7	7	-2.70	513.73	1.19	-9.82	-74.50	4.10	5.26	4.10	no	•	5.50	•	•	•
8	8	-2.80	564.90	1.24	-11.64	•	•	5.39	3.70	no	•	4.07	•	•	•
9	9	-2.90	557.60	1.30	-11.00	•	•	5.95	9.40	no	•	1.12	•	•	•
10	10	-3.00	565.21	1.36	-10.84	•	•	5.35	8.50	no	•	4.47	11.62	40.76	•
11	11	-3.10	512.91	1.41	-10.87	-69.60	17.36	5.91	3.90	no	•	1.23	•	•	•
12	12	-3.20	474.07	1.45	-11.24	•	•	5.38	6.60	no	•	4.17	•	•	•
13	13	-3.30	531.29	1.51	-10.29	•	•	5.46	3.60	no	•	3.47	•	•	•
14	14	-3.40	505.66	1.56	-11.39	•	•	5.26	5.80	no	•	5.50	•	•	•
15	15	-3.50	454.35	1.60	-10.94	•	•	5.59	3.80	no	•	2.57	•	•	•
16	16	-3.60	334.82	1.64	-11.98	•	•	5.33	3.90	no	•	4.68	•	•	•
17	17	-3.70	548.54	1.69	-10.79	•	•	5.68	2.80	no	•	2.09	2.38	7.59	.68
18	18	-3.80	624.21	1.75	-12.22	-85.30	12.46	5.35	4.60	no	•	4.47	•	•	•
19	19	-3.90	536.94	1.81	-12.51	•	•	5.78	5.30	no	•	1.66	•	•	•
20	20	-4.00	550.46	1.86	-12.14	•	•	5.85	11.50	no	•	1.41	•	•	•
21	21	-4.10	641.03	1.93	-11.03	•	•	5.91	4.50	no	•	1.23	7.88	26.83	1.05
22	22	-4.20	895.48	2.02	-13.65	•	•	5.55	7.30	high	•	2.82	•	•	•
23	23	-4.30	895.48	2.11	-14.24	-97.00	16.92	5.32	3.40	high	•	4.79	•	•	•
24	24	-4.40	861.32	2.19	-13.18	•	•	5.18	5.30	very high	•	6.61	•	•	•
25	25	-4.50	861.32	2.28	-11.75	•	•	5.67	3.60	high	•	2.14	•	•	•
26	26	-4.60	889.66	2.37	-12.61	•	•	5.83	10.00	no	•	1.48	•	•	•
27	27	-4.70	584.19	2.43	-12.03	-71.60	24.64	5.54	2.40	no	•	2.88	•	•	•
28	28	-4.80	561.73	2.48	-11.88	•	•	5.24	3.60	no	•	5.75	•	•	•
29	29	-4.90	611.15	2.54	-12.16	•	•	5.72	4.20	no	•	1.91	•	•	•
30	30	-5.00	611.15	2.60	-12.30	•	•	5.47	4.70	no	•	3.39	16.75	38.48	•
31	31	-5.10	568.36	2.66	-11.90	•	•	5.58	4.00	no	•	2.63	•	•	•
32	32	-5.20	568.36	2.72	-12.13	•	•	5.22	4.10	no	•	6.03	•	•	•
33	33	-5.30	676.71	2.79	-12.63	•	•	5.24	1.90	no	•	5.75	•	•	•
34	34	-5.40	607.56	2.85	-12.51	•	•	5.33	4.00	no	•	4.68	•	•	•
35	35	-5.50	605.39	2.91	-12.44	•	•	5.49	3.20	no	•	3.24	5.50	20.76	1.24
36	36	-5.60	613.36	2.97	-12.14	•	•	5.19	3.80	no	•	6.46	•	•	•
37	37	-5.70	659.92	3.03	-12.26	•	•	5.64	3.10	high	•	2.29	•	•	•
38	38	-5.80	659.92	3.10	-12.38	•	•	5.33	3.80	no	•	4.68	•	•	•
39	39	-5.90	659.92	3.17	-12.28	•	•	5.54	3.80	no	•	2.88	•	•	•
40	40	-6.00	659.92	3.23	-12.23	-82.00	15.88	5.23	6.20	no	•	5.89	28.62	22.26	.65
41	41	-6.10	681.03	3.30	-11.86	-84.00	10.88	5.42	2.70	no	•	3.80	•	•	•
42	42	-6.20	898.26	3.39	-12.39	-82.60	16.52	5.38	6.00	no	•	4.17	•	•	•
43	43	-6.30	852.97	3.48	-11.90	-73.10	22.14	5.44	5.10	no	•	3.63	•	•	•
44	44	-6.40	895.61	3.56	-12.93	-86.70	16.78	5.34	8.10	no	•	4.57	•	•	•
45	45	-6.50	873.33	3.65	-13.78	-93.10	17.18	5.35	3.50	high	•	4.47	21.38	47.28	1.26
46	46	-6.60	727.04	3.72	-13.12	-87.20	17.80	5.30	4.00	high	•	5.01	•	•	•
47	47	-6.70	891.86	3.81	-14.16	-93.90	19.42	5.51	4.50	no	•	3.09	•	•	•
48	48	-6.80	875.27	3.90	-13.61	-93.90	14.94	5.29	5.10	no	•	5.13	•	•	•
49	49	-6.90	907.11	3.99	-12.69	-80.90	20.62	5.74	4.00	no	•	1.82	•	•	•
50	50	-7.00	896.52	4.08	-12.27	•	•	5.59	7.80	no	•	2.57	•	•	•
51	51	-7.10	661.48	4.15	-12.85	•	•	5.29	7.80	no	•	5.13	•	•	•
52	52	-7.20	894.95	4.24	-13.27	•	•	5.20	5.70	no	•	6.31	•	•	•
53	53	-7.30	873.79	4.32	-13.11	•	•	5.17	3.30	no	•	6.76	2.88	11.71	.71
54	54	-7.40	881.71	4.41	-13.05	•	•	5.35	4.60	no	•	4.47	•	•	•
55	55	-7.50	871.74	4.50	-12.93	•	•	5.10	4.30	very high	•	7.94	•	•	•
56	56	-7.60	876.48	4.59	-13.70	-92.60	16.96	5.13	3.80	no	•	7.41	•	•	•
57	57	-7.70	887.77	4.68	-12.89	•	•	5.50	2.60	no	•	3.16	•	•	•
58	58	-7.80	895.91	4.77	-12.79	•	•	5.21	4.90	no	•	6.17	•	•	•
59	59	-7.90	867.68	4.85	-13.32	•	•	5.54	2.70	no	•	2.88	5.12	21.64	.68
60	60	-8.00	867.68	4.94	-14.07	•	•	5.37	3.70	no	95	4.27	•	•	•
61	61	-8.10	624.48	5.00	-13.06	•	•	6.07	7.70	no	•	.85	•	•	•
62	62	-8.20	887.49	5.09	-12.79	•	•	5.35	3.80	no	•	4.47	•	•	•
63	63	-8.30	890.33	5.18	-13.64	•	•	5.24	2.50	no	•	5.75	•	•	•
64	64	-8.40	849.95	5.26	-12.73	•	•	5.60	4.10	no	•	2.51	•	•	•
65	65	-8.50	890.21	5.35	-13.03	•	•	5.86	3.20	no	•	1.38	•	•	•
66	66	-8.60	895.17	5.44	-13.90	•	•	5.39	3.40	no	•	4.07	•	•	•

	Sample	Depth (m)	Density (kg/m3)	Depth (m w.eq.)	Delta Oxygen	Delta Deuterium	Excess d	pH	Elec. Conductivity (µS cm-1)	Microparticules	Tritium (TU)	H (µEq l-1)	SO (µEq l-1)	Cl (µEq l-1)	NO3 (µEq l-1)
67	67	-8.70	899.64	5.53	-13.19	.	.	5.70	4.50	no	.	2.00	.	.	.
68	68	-8.80	897.09	5.62	-14.39	.	.	5.33	3.60	no	.	4.68	.	.	.
69	69	-8.90	879.38	5.71	-13.64	-84.80	24.36	5.60	3.30	no	.	2.51	3.88	8.21	.
70	70	-9.00	635.75	5.77	-13.44	.	.	5.60	7.20	no	.	2.51	.	.	.
71	71	-9.10	662.11	5.84	-13.02	.	.	5.69	3.30	no	.	2.04	.	.	.
72	72	-9.20	662.11	5.91	-13.26	.	.	5.23	5.00	no	.	5.89	.	.	.
73	73	-9.30	865.06	5.99	-13.53	-79.20	29.04	5.64	8.50	no	.	2.29	0	17.18	.58
74	74	-9.40	856.15	6.08	-13.60	.	.	5.49	4.00	no	.	3.24	.	.	.
75	75	-9.50	883.35	6.17	-13.74	-91.30	18.66	5.54	3.10	no	183	2.88	.	.	.
76	76	-9.60	879.76	6.26	-14.22	.	.	5.17	3.40	no	.	6.76	12.42	13.71	.45
77	77	-9.70	600.83	6.32	-14.38	.	.	5.81	2.70	no	.	1.55	.	.	.
78	78	-9.80	702.75	6.39	-14.48	.	.	5.42	4.50	no	.	3.80	.	.	.
79	79	-9.90	662.25	6.45	-13.54	.	.	5.61	2.60	no	.	2.45	.	.	.
80	80	-10.00	631.34	6.52	-13.76	.	.	5.53	5.00	no	.	2.95	.	.	.
81	81	-10.10	882.33	6.60	-13.73	.	.	6.10	5.60	no	.	.79	10.62	31.45	.69
82	82	-10.20	631.34	6.67	-13.27	.	.	5.78	6.60	high	.	1.66	.	.	.
83	83	-10.30	861.65	6.75	-13.65	.	.	5.67	3.20	no	.	2.14	.	.	.
84	84	-10.40	876.39	6.84	-13.40	.	.	5.58	5.40	no	.	2.63	.	.	.
85	85	-10.50	887.12	6.93	-13.60	.	.	6.71	54.10	no	.	.19	.	27.62	.
86	86	-10.60	880.13	7.02	-14.22	.	.	5.55	4.50	no	.	2.82	.	.	.
87	87	-10.70	874.70	7.10	-13.86	.	.	5.58	4.80	no	.	2.63	.	.	.
88	88	-10.80	703.85	7.17	-13.61	.	.	5.51	5.70	no	.	3.09	.	.	.
89	89	-10.90	703.67	7.25	-12.87	.	.	5.70	4.10	no	.	2.00	4.00	7.93	.87
90	90	-11.00	725.33	7.32	-12.65	-87.70	13.54	5.41	4.40	high	306	3.89	.	.	.
91	91	-11.10	747.49	7.39	-12.67	-85.50	15.86	5.95	4.60	no	327	1.12	.	.	.
92	92	-11.20	783.51	7.47	-12.74	-87.50	14.38	5.44	7.60	no	262	3.63	.	.	.
93	93	-11.30	868.86	7.56	-12.81	-85.30	17.14	5.35	3.00	no	324	4.47	.	.	.
94	94	-11.40	863.77	7.64	-13.42	-82.40	24.96	5.44	5.90	no	.	3.63	12.00	14.50	.
95	95	-11.50	868.19	7.73	-12.57	-86.40	14.20	5.60	5.00	no	232	2.51	.	.	.
96	96	-11.60	865.02	7.82	-12.21	-87.40	10.28	5.48	5.70	no	275	3.31	.	.	.
97	97	-11.70	865.02	7.90	-12.85	-87.90	14.90	5.91	3.40	no	206	1.23	.	.	.
98	98	-11.80	872.43	7.99	-13.17	-88.50	16.86	5.33	4.80	no	271	4.68	.	.	.
99	99	-11.90	871.06	8.08	-13.24	-88.70	17.26	5.83	6.10	no	231	1.48	.	.	.
100	100	-12.00	883.09	8.17	-12.82	.	.	5.63	6.30	no	.	2.34	.	.	.
101	101	-12.10	888.85	8.26	-12.23	.	.	5.71	4.00	no	.	1.95	.	.	.
102	102	-12.20	882.92	8.34	-13.23	.	.	5.41	5.70	no	.	3.89	.	.	.
103	103	-12.30	871.78	8.43	-12.34	-81.50	17.26	5.88	4.00	no	.	1.32	3.88	8.63	.
104	104	-12.40	877.98	8.52	-12.97	.	.	5.36	5.40	no	.	4.37	.	.	.
105	105	-12.50	848.88	8.60	-13.62	.	.	6.02	4.60	no	.	.95	5.73	15.51	.03
106	106	-12.60	891.41	8.69	-14.01	.	.	5.75	5.80	no	.	1.78	.	.	.
107	107	-12.70	876.13	8.78	-12.77	.	.	5.93	3.50	no	.	1.17	.	.	.
108	108	-12.80	890.31	8.87	-13.91	.	.	5.35	4.10	no	.	4.47	.	.	.
109	109	-12.90	890.19	8.96	-13.09	-84.40	20.28	5.65	2.40	no	263	2.24	.	.	.
110	110	-13.00	884.48	9.05	-12.65	.	.	5.42	6.40	no	115	3.80	14.50	14.44	.
111	111	-13.10	892.61	9.14	-13.60	.	.	5.84	6.20	no	.	1.45	.	.	.
112	112	-13.20	882.85	9.22	-13.91	.	.	5.33	3.80	no	.	4.68	.	.	.
113	113	-13.30	881.32	9.31	-13.22	.	.	5.64	3.00	no	.	2.29	.	.	.
114	114	-13.40	895.68	9.40	-13.66	.	.	5.32	3.80	no	.	4.79	.	.	.
115	115	-13.50	890.58	9.49	-13.81	.	.	5.62	3.20	no	147	2.40	4.25	22.96	1.16
116	116	-13.60	858.15	9.58	-13.23	.	.	5.27	5.40	high	.	5.37	.	.	.
117	117	-13.70	884.72	9.67	-13.11	.	.	5.46	2.50	no	.	3.47	.	.	.
118	118	-13.80	889.39	9.75	-13.26	.	.	5.64	3.60	no	.	2.29	.	.	.
119	119	-13.90	902.25	9.84	-13.43	.	.	5.66	2.90	no	.	2.19	.	.	.
120	120	-14.00	898.95	9.93	-12.97	-88.20	15.52	5.39	4.00	no	154	4.07	.	.	.
121	121	-14.10	905.75	10.03	-12.69	.	.	5.75	3.70	no	60	1.78	.	.	.
122	122	-14.20	896.14	10.11	-12.86	.	.	5.79	5.10	no	.	1.62	.	.	.
123	123	-14.30	904.74	10.21	-12.64	.	.	5.74	2.70	no	69	1.82	2.75	7.22	.77
124	124	-14.40	685.22	10.27	-11.60	.	.	5.82	4.50	no	36	1.51	.	.	.
125	125	-14.50	703.54	10.34	-11.89	.	.	5.94	4.50	no	.	1.15	.	.	.
126	126	-14.60	734.34	10.42	-11.97	.	.	5.53	3.30	no	30	2.95	.	.	.
127	127	-14.70	706.05	10.49	-11.44	.	.	5.64	3.60	no	.	2.29	.	.	.
128	128	-14.80	733.66	10.56	-11.32	.	.	5.67	5.80	no	.	2.14	.	.	.
129	129	-14.90	724.58	10.63	-11.42	.	.	5.53	2.50	no	43	2.95	3.50	16.90	2.21
130	130	-15.00	747.95	10.71	-11.02	-74.70	13.42	5.33	4.30	no	25	4.68	.	.	.
131	131	-15.10	715.58	10.78	-11.35	-74.00	16.80	5.69	2.50	no	43	2.04	.	.	.
132	132	-15.20	722.83	10.85	-11.59	-77.90	14.78	5.21	3.20	no	101	6.17	.	.	.

	Sample	Depth (m)	Density (kg/m^3)	Depth (m w.eq.)	Delta Oxygen	Delta Deuterium	Excess d	pH	Elec. Conductivity (µS cm^{-1})	Microparticules	Tritium (TU)	H (µEq l^{-1})	SO (µEq l^{-1})	Cl (µEq l^{-1})	NO3 (µEq l^{-1})
133	133	-15.30	716.12	10.92	-11.49	-74.60	17.32	5.61	2.70	no	124	2.45	•	•	•
134	134	-15.40	769.71	11.00	-11.53	-75.20	17.08	5.20	3.20	no	48	6.31	5.00	8.07	•
135	135	-15.50	754.74	11.08	-11.56	-77.70	14.78	5.47	2.50	no	58	3.39	•	•	•
136	136	-15.60	759.71	11.15	-11.53	-67.50	24.74	5.31	3.30	high	212	4.90	•	•	•
137	137	-15.70	770.86	11.23	-11.42	-74.20	17.16	5.35	1.70	high	78	4.47	•	•	•
138	138	-15.80	875.00	11.32	-11.38	-74.50	16.50	5.29	4.00	no	50	5.13	•	•	•
139	139	-15.90	894.36	11.41	-11.65	-80.60	12.64	5.60	1.90	no	44	2.51	•	•	•
140	140	-16.00	854.61	11.49	-11.57	•	•	5.54	3.90	no	•	2.88	•	•	•
141	141	-16.10	876.54	11.58	-12.21	•	•	5.84	3.70	no	•	1.45	•	•	•
142	142	-16.20	882.06	11.67	-12.26	•	•	5.58	3.50	no	54	2.63	•	•	•
143	143	-16.30	882.62	11.76	-12.20	•	•	5.59	2.20	no	63	2.57	2.25	4.91	.37
144	144	-16.40	877.40	11.84	-12.16	•	•	5.41	3.40	no	55	3.89	5.00	5.92	•
145	145	-16.50	863.14	11.93	-12.64	•	•	5.28	2.90	no	79	5.25	3.25	19.32	1.08
146	146	-16.60	896.58	12.02	-12.28	•	•	5.24	3.40	no	123	5.75	12.25	17.21	1.11
147	147	-16.70	902.20	12.11	-12.04	•	•	5.68	2.30	no	65	2.09	2.12	4.15	.58
148	148	-16.80	901.75	12.20	-12.43	•	•	5.32	4.70	no	22	4.79	•	•	•
149	149	-16.90	855.53	12.29	-12.14	•	•	5.65	2.50	no	36	2.24	•	•	•
150	150	-17.00	865.58	12.37	-12.26	•	•	5.85	36.00	no	•	1.41	•	•	•
151	151	-17.10	859.33	12.46	-12.30	•	•	5.82	3.70	no	44	1.51	•	•	•
152	152	-17.20	859.13	12.54	-12.43	•	•	5.53	4.30	no	42	2.95	•	•	•
153	153	-17.30	904.02	12.63	-12.66	•	•	5.53	3.90	no	22	2.95	•	•	•
154	154	-17.40	897.51	12.72	-12.55	-82.80	17.60	5.45	5.70	no	80	3.55	•	•	•
155	155	-17.50	902.51	12.81	-12.70	•	•	5.45	2.90	no	44	3.55	•	•	•
156	156	-17.60	900.93	12.90	-12.95	-82.50	21.14	5.53	4.40	no	16	2.95	•	•	•
157	157	-17.70	808.45	12.99	-11.88	•	•	5.45	2.90	no	39	3.55	3.75	12.72	1.00
158	158	-17.80	900.10	13.08	-12.47	•	•	5.49	5.80	no	21	3.24	•	•	•
159	159	-17.90	873.91	13.16	-12.37	•	•	5.67	2.50	no	38	2.14	•	•	•
160	160	-18.00	862.76	13.25	-12.24	•	•	5.98	8.60	no	40	1.05	•	•	•
161	161	-18.10	856.42	13.33	-12.18	•	•	5.31	2.40	no	38	4.90	•	•	•
162	162	-18.20	861.44	13.42	-12.49	•	•	5.71	5.20	no	39	1.95	•	•	•
163	163	-18.30	866.24	13.51	-12.34	•	•	5.61	2.60	no	54	2.45	•	•	•
164	164	-18.40	869.84	13.59	-12.09	•	•	5.57	3.40	no	37	2.69	•	•	•
165	165	-18.50	871.80	13.68	-12.26	•	•	5.73	2.80	no	44	1.86	•	•	•
166	166	-18.60	906.55	13.77	-12.38	•	•	5.42	3.60	no	•	3.80	•	•	•
167	167	-18.70	906.55	13.86	-12.35	•	•	5.75	3.10	no	49	1.78	•	•	•
168	168	-18.80	906.55	13.95	-12.50	-81.00	19.00	5.33	4.40	very high	59	4.68	•	66.26	4.31
169	169	-18.90	906.55	14.04	-12.74	•	•	5.81	2.40	no	•	1.55	•	•	•
170	170	-19.00	878.27	14.13	-12.76	•	•	5.58	3.80	no	66	2.63	•	•	•
171	171	-19.10	890.88	14.22	-12.65	•	•	5.82	2.50	no	69	1.51	•	•	•
172	172	-19.20	889.44	14.31	-12.64	-82.90	18.22	5.71	3.50	no	61	1.95	•	•	•
173	173	-19.30	896.23	14.40	-12.81	•	•	5.76	2.50	no	42	1.74	•	•	•
174	174	-19.40	900.36	14.49	-12.61	•	•	5.43	3.40	no	32	3.72	•	•	•
175	175	-19.50	876.69	14.58	-12.71	-83.30	18.42	5.66	2.00	no	•	2.19	3.25	7.93	1.16
176	176	-19.60	852.14	14.66	-12.83	•	•	5.49	4.00	no	61	3.24	•	•	•
177	177	-19.70	889.66	14.75	-12.69	•	•	5.53	2.00	no	•	2.95	•	•	•
178	178	-19.80	881.58	14.84	-12.66	-84.20	17.08	5.51	3.70	no	•	3.09	•	•	•
179	179	-19.90	894.36	14.93	-12.64	•	•	5.36	2.00	no	65	4.37	•	•	•
180	180	-20.00	905.75	15.02	-12.61	-85.60	15.28	5.55	6.20	no	•	2.82	•	•	•
181	181	-20.10	907.90	15.11	-13.15	-85.80	19.40	5.85	2.90	no	•	1.41	•	•	•
182	182	-20.20	896.71	15.20	-12.90	-87.10	16.06	5.82	9.50	no	42	1.51	•	•	•
183	183	-20.30	889.58	15.29	-12.89	•	•	5.83	2.90	no	•	1.48	•	•	•
184	184	-20.40	906.35	15.38	-13.20	-81.80	23.84	5.57	3.50	no	•	2.69	•	•	•
185	185	-20.50	881.27	15.47	-12.34	-78.40	20.28	5.62	2.40	no	•	2.40	•	•	•
186	186	-20.60	885.37	15.56	-12.53	-81.80	18.44	5.63	3.50	no	74	2.34	•	•	•
187	187	-20.70	913.98	15.65	-12.78	-75.30	26.94	5.93	16.60	high	•	1.17	•	•	•
188	188	-20.80	885.54	15.74	-12.70	-86.00	15.60	5.55	4.10	high	58	2.82	•	•	•
189	189	-20.90	898.12	15.83	-12.62	-83.90	17.10	5.78	2.50	no	•	1.66	6.38	9.68	1.19
190	190	-21.00	895.04	15.92	-12.64	•	•	5.76	3.20	no	•	1.74	•	•	•
191	191	-21.10	903.99	16.01	-12.64	•	•	5.48	3.00	high	51	3.31	•	•	•
192	192	-21.20	898.04	16.10	-12.92	•	•	5.49	3.40	high	•	3.24	•	•	•
193	193	-21.30	892.55	16.19	-12.82	•	•	5.60	2.30	no	53	2.51	•	•	•
194	194	-21.40	906.42	16.28	-12.69	•	•	5.49	4.70	high	•	3.24	•	•	•
195	195	-21.50	885.38	16.36	-12.80	•	•	5.88	3.60	high	•	1.32	•	•	•
196	196	-21.60	912.51	16.46	-12.80	•	•	5.70	5.00	high	72	2.00	•	•	•
197	197	-21.70	900.49	16.55	-12.71	-85.90	15.78	5.54	4.30	no	•	2.88	3.75	6.49	.97
198	198	-21.80	899.29	16.64	-12.75	•	•	5.47	4.20	no	•	3.39	•	•	•

	Sample	Depth (m)	Density (kg/m3)	Depth (m w.eq.)	Delta Oxygen	Delta Deuterium	Excess d	pH	Elec. Conductivity (µS cm-1)	Microparticules	Tritium (TU)	H (µEq l-1)	SO (µEq l-1)	Cl (µEq l-1)	NO3 (µEq l-1)
199	199	-21.90	892.38	16.73	-12.68	.	.	5.70	2.30	no	.	2.00	.	.	.
200	200	-22.00	896.95	16.81	-12.83	.	.	5.73	4.50	no	54	1.86	.	.	.
201	201	-22.10	896.76	16.90	-12.55	-70.50	29.90	5.92	3.00	no	.	1.20	5.00	13.17	1.44
202	202	-22.20	888.75	16.99	-12.68	.	.	5.66	3.00	no	.	2.19	.	.	.
203	203	-22.30	899.01	17.08	-12.51	.	.	5.65	3.70	no	69	2.24	.	.	.
204	204	-22.40	895.14	17.17	-12.50	.	.	5.65	3.70	no	.	2.24	.	.	.
205	205	-22.50	907.91	17.26	-12.59	.	.	5.59	2.40	no	.	2.57	.	.	.
206	206	-22.60	894.64	17.35	-12.16	.	.	5.80	2.50	no	68	1.58	.	.	.
207	207	-22.70	896.22	17.44	-12.29	.	.	5.66	2.70	high	.	2.19	.	.	.
208	208	-22.80	902.94	17.53	-12.53	-75.00	25.28	5.75	2.90	no	.	1.78	3.12	11.48	.97
209	209	-22.90	885.46	17.62	-12.63	.	.	5.64	3.20	no	.	2.29	4.88	17.63	1.71
210	210	-23.00	895.64	17.71	-12.45	.	.	5.58	2.90	high	.	2.63	.	34.25	7.08
211	211	-23.10	903.22	17.80	-12.84	.	.	5.76	2.80	no	.	1.74	.	.	.

APPENDIX 3

ICE-CORE DRILLING OPERATIONS ON SKOBREEN

A3.1- Drilling operations

The ice-core drilling activities on Skobreen were carried out in the spring of 1986, between the 2nd and 8th May. This time of year was considered best for fieldwork because the air temperature is still well below 0°C, an important point to consider in drilling activities on temperate and sub-polar glaciers. The presence of any surface water would increase the chances of sample contamination, as well as being an impediment to drilling.

The field programme was run in cooperation with British Petroleum (BP) and the Physikalisches Institut of the University of Bern, which provided the drill. Operations were based at Longyearbyen airport. From there, the field equipment, including a modified electro-mechanical Rufli drill (described below), a light table and tents, was transported to the site by aircraft, a de Havilland Twin Otter. Later the drilling group, Dr. N. Riley (BP), M. Andree (Bern), and J.C. Simões (SPRI) arrived from Sveagruva on snow-mobiles. Weather conditions were poor throughout the period, with frequent snow storms. The mean temperature, about -10°C, was ideal for drilling.

A3.2- The Rufli drill

A modified version of the electro-mechanical Rufli drill was used in our operations. This lightweight drill is basically the same as the one described in Rufli, Stauffer and Oeschger (1976). The drill unit consists of coring, driving and anti-torque systems, a drilling tower, a winch, and a generator. The drill is suspended by an electro-mechanical cable which is wound on a drum. The main modifications include a control panel, a cable drum with a gear reducer, and a longer cable. These modifications increase the maximum depth of drilling from 50 m to approximately 180 m. Each core section has a diameter of 75 mm and a maximum length of 1 m. The unit is relative easily dis-assembled and packed in several metal containers for transport. This drill produces a dry hole, which is important for chemical studies of the core.

Recent years have seen the development of several drills (e.g. Holdsworth, 1984) based on this and Rand's designs (Rand, 1976). Innovations, such as a geodesic dome to support the drilling tower and to serve as shelter, new cutters, the use of alternative power sources (i.e. solar energy; Koci, 1985), and the use of composites in the design, have made this type of drill very versatile and extended the maximum depth at which it may be used. These drills are ideal for studies of a medium time-scale, being able to recover ice up to 1000 years old from the Antarctic Plateau. Furthermore, the new design allows convenient transportation, which is very important when obtaining ice cores from high-altitude glaciers with difficult access.

The experience at Skobreen demonstrates that electro-mechanical drills are not appropriate for sub-polar ice masses as encountered on Svalbard. The temperature is frequently near the melting point and any friction with the drilling equipment may cause melting. The equipment may stick in a mixture of ice chips and slush. The best results have been obtained with an electro-thermal drill (i.e. electrical resistance heating). Soviet scientists have drilled a total of more than 2500 m in Svalbard by this method (Zagorodnov, 1988) and recently (1987) a 566.7 m core from Austfonna reached bedrock (Zagorodnov, in preparation). The main disadvantage of this type of drill is the contamination of the core either by the melted water or by the antifreeze fluid which fills the hole. It is thus not suitable for providing ice cores for low-concentration (i.e. < ppm) impurity analyses.

A3.3- Core retrieval and transport

During the first day in the field the drill was erected and a 2.10 m deep trench was dug for the study of the stratigraphy of the upper layers and to serve as an operational pit (Frontispiece). Another trench of approximately 5 x 3 x 2 m was excavated in order to function as an ice laboratory and cold-room for the storage of the recovered sections (Fig. A3.1). It was impossible to obtain an adequate roof for the trenches, and coring had to cease frequently, due to snow storms.

The snow stratigraphy of the 2.1 m pit was extremely simple, without internal structures. It was a homogeneous, fine-grained mass of compacted snow. The 2.1 m is thought to be the winter accumulation, as the first ice layer (about 2 cm) was found at this depth. There were no other associated features (for example, a depth-hoar layer that could confirm this ice layer as a summer layer; Koerner, 1971).

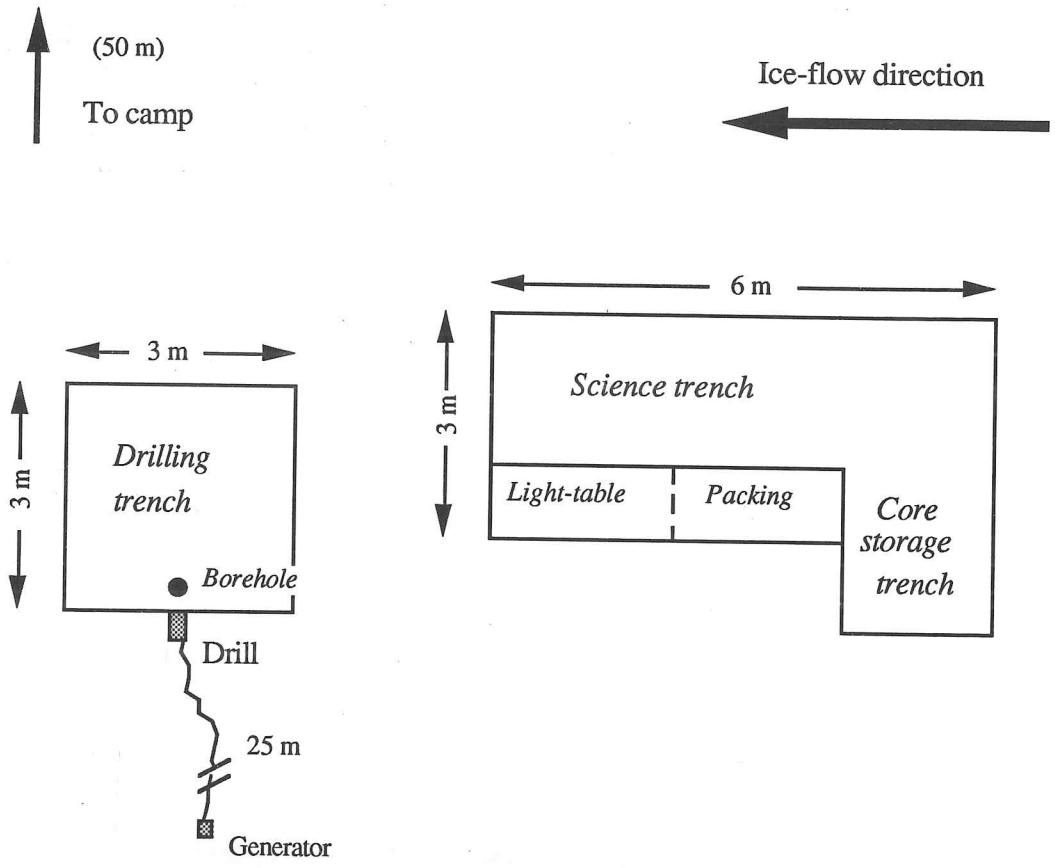

Figure A3.1- Trenches used for drilling operations on Skobreen

The first 13 m were quickly recovered during the second day of drilling. Each section took about 10 minutes to collect. From there onwards penetration was difficult, and drilling stopped, on account of a snow storm. Drilling was resumed after 2 days. At a depth of 23.1 m, the drill jammed. Several hours were spent trying to release the drill by various means (e.g. by increasing and releasing tension over the cables). Unfortunately, as a result of these attempts the control box burnt out. After 5 hours the drill was recovered by hand, but had been damaged beyond repair in the field. The electrical cables were broken and the outside barrel had lost all its screws. It was fortunate that the drill was recovered. Water was not observed in the borehole at any time.

On the sixth day of operations, personnel, equipment, and the 23.1 m core were collected by helicopter and transported to Sveagruva.

A3.4- Core handling and processing

After removal from the core barrel, the ice core was taken straight to the light-table (Fig. A3.2) for observation of the general stratigraphy. To obtain information in a gross way about density in the field, the technique of light transmissivity (Langway, 1970) was used. The stratigraphy and ice-core conditions were logged on paper specially designed for the

task. A wedge was cut in the top part of each section for orientation. Each 1 m section was placed in a cardboard tube. In general it was not necessary to saw any part of the core, as the core quality was good and it had been recovered at full length (i.e. about 1 m). When necessary, a new tenon saw coated with teflon (PTFE) was used to reduce contamination. Precautions were taken to avoid contamination, and these are discussed in the section on sampling (Chapter 3). For example, the core was handled with plastic surgical gloves, worn over the normal cotton gloves. Unfortunately, the ice-core sections were not placed in polyethylene bags and were in contact with the cardboard. However, the temperature remained below -10°C during the greater period of storage, thus diffusion would not have been sufficient to affect the ionic content of the core. Twelve tubes were assembled in an insulated box and kept under 50 cm of ice until they were collected and transported to Sveagruva. There they were stored in a cold-room at -15°C, before being taken to Longyearbyen. Finally, all the tubes were packed in dry ice and transported by air from Svalbard to BP's Cold Regions Laboratory, Sunbury-on-Thames, England. The core was kept there at an average temperature of -20°C. At this Laboratory, two months later, the final stratigraphic studies, determination of density, and the sampling for different analyses were carried out.

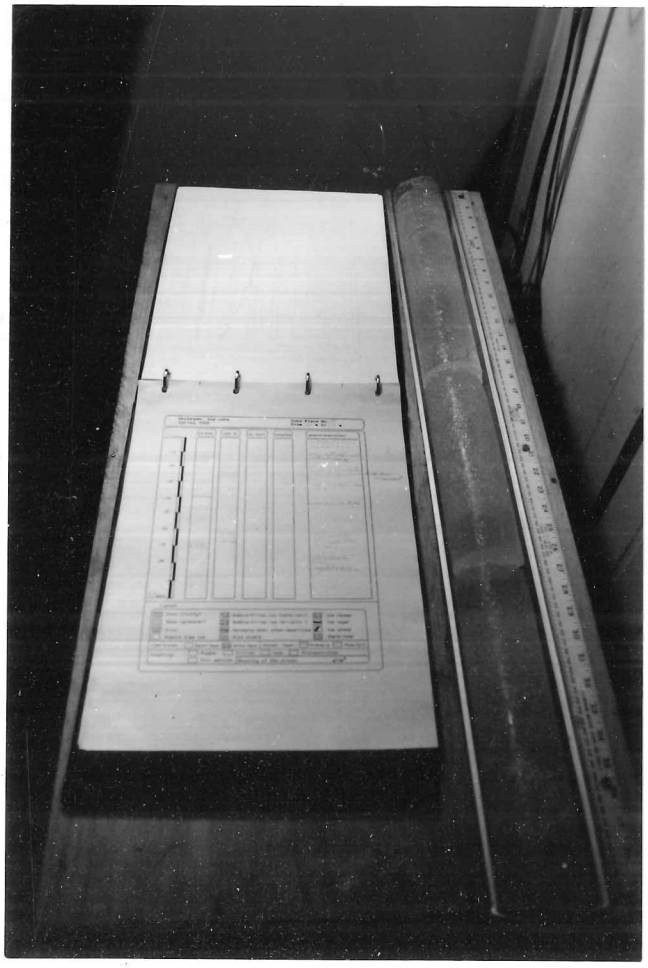

Figure A3.2- Light-table purpose-built for stratigraphic analysis.